Immunomodulatory Innate Defense Regulator (IDR)-1002 Peptide in Airway Inflammation

by

Hadeesha Piyadasa

A Thesis submitted to the Faculty of Graduate Studies of

The University of Manitoba

in partial fulfilment of the requirements for the degree of

Doctor of Philosophy

Department of Immunology

University of Manitoba

Winnipeg, Manitoba

Preface

Thesis Summary

Allergic asthma is a chronic respiratory disease characterized by airway inflammation and airway hyper-responsiveness (AHR) leading to airway obstruction and difficulty breathing. The disease is primarily driven by exposure to inhaled allergens such as house dust mite (HDM). Despite available treatments e.g. inhaled corticosteroids (ICS) and β2-agonists, disease control is complicated due to the heterogeneous nature of asthma, as evident from approximately 20% of asthmatics who are either difficult to treat or have uncontrolled severe asthma. Systemic corticosteroids (SCS), often administered to severe asthmatics, increases the susceptibility to infections and systemic complications e.g. infection and cardiovascular. These challenges highlight the need to identify novel therapeutic targets and to develop alternate strategies to control asthma.

Cationic host defense peptides (CHDP) exhibit a wide range of immunomodulatory functions to resolve both infections and inflammation. Synthetic peptides designed from CHDP are known as innate defense regulator (IDR) peptides. Administration of IDR peptides *in vivo* enhances resolution of infections, contribute to wound healing, regulate cytokine and chemokine production, and overall contribute to the maintenance of immunological homeostasis. As a result, IDR peptides are attractive therapeutic candidates for regulating inflammation. In this thesis, I focus on generating a fundamental understanding of IDR peptides in airway inflammation that could be used in the future to develop a new class of peptide based drugs to treat diseases such as allergic asthma.

To investigate the effects of administration of IDR peptides in allergic asthma, I systematically characterized the inflammatory and physiological changes induced in a 2-week acute HDM-challenged murine model of allergic airway inflammation. I further showed that the administration of IDR-1002 reduces AHR, and eosinophil and neutrophil accumulation in the lungs of HDM-challenged mice. Concomitantly, IDR-1002 suppressed HDM-induced interleukin (IL)-33 in the lungs. In mechanistic studies, I demonstrated that suppression of IL-33 is essential for the immunomodulatory activity of IDR-1002, but not the activity to reduce AHR in HDM-challenged mice.

IL-33 is involved in orchestrating an inflammatory phenotype and tissue damage in the lungs, and is a critical contributor to ICS insensitivity. Although targeting of the IL-33 pathway is being examined as a therapeutic strategy for chronic pulmonary diseases, there are limited studies that have characterized the molecular expression profile of the lungs in response to IL-33 *in vivo*. Therefore, I characterized the immunological, physiological and transcriptomic responses in the lungs of IL-33-challenged mice. I showed that IL-33 administered intranasally induced inflammation, structural changes and AHR, similar to HDM-challenge, in the lungs of mice. In addition, I detailed the global transcriptional changes in the lung tissue of IL-33-challenged mice using RNA-Seq, enabling the identification of novel molecular targets to control downstream effects of IL-33.

To examine the sequence/function association of IDR-1002, I generated a series of IDR-1002 derivatives with single amino acid substitutions to identify the sequence requirement of IDR-1002 in its immunomodulatory function. I demonstrated that disruption of a central tryptophan (W8) in the IDR-1002 sequence selectively mitigated inflammation control, including IL-33 suppression and leukocyte accumulation, without altering the ability to reduce AHR in a murine model of allergic asthma. These results also provide a unique opportunity to use IDR-1002(W8/R) as a probe to identify specific molecular mechanisms involved in AHR independent of airway inflammation.

Together, the findings of this thesis provide the foundation to examine the development of IDR peptides, in particular IDR-1002, as a new drug class for airway inflammation, potentially targeting ICS insensitivity through the suppression of IL-33. Additionally, my findings suggest that IDR-1002-derived peptides can be used as probes to investigate molecular mechanisms contributing to asthma pathogenesis, such as those that differentiate between airway inflammation and AHR, that may result in the identification of novel molecular targets for drug development.

Acknowledgements

This body of work would have not been possible without the tremendous support that I have received from my family, friends and colleagues.

To my supervisor, Dr. Neeloffer Mookherjee, you have been an incredible mentor, who is passionate about training the next generation of scientists. You have given me numerous opportunities and have opened many doors to help me succeed, not only in my PhD but also in my future endeavors. In my first year, you gave me the option to select a project in your lab that interested me the most, gave me the independence to challenge myself and develop the project while continually guiding me and being a pillar of support. You have given countless hours of your time to train me as the scientist I am today. I truly believe I would not have come this far without your generosity and constant encouragement.

To my colleagues, thank you for all the scientific (and non-scientific) discussions, insights, and advice you have given me throughout my graduate degree.

To the Halayko Lab, thank you for always providing the knowledge, support, and training, without which would have been very difficult for me progress in many parts of my project.

To my committee members, Dr. Halayko, Dr. Coombs, and Dr. HayGlass, thank you for all the suggestions, guidance and feedback that helped me throughout my degree.

To my parents, Anoma and Gamini, and my sister, Manaka, thank you for the never-ending support and always believing in me.

Finally, to my loving wife Joanna, your encouragement jump started my research career. Thank you for supporting me throughout this time, from listening to endless practice presentations to editing my documents.

I am also grateful for the financial support from AllerGen NCE, Asthma Canada, Children's Hospital Research Institute of Manitoba, Research Manitoba, Health Sciences Centre Foundation, and Manitoba Medical Services Foundation.

Dedication

For my father and mother, who have provided me with everything they never had.

For my wife, who made me the person I am today.

Table of Contents

List of Figures

List of Tables

List of Abbreviations

AEC	Airway epithelial cells
AHR	Airway hyper-responsiveness
AMP	Antimicrobial peptides
ASM	Airway smooth muscle
BALF	Bronchoalveolar lavage fluid
BCA	Bicinchoninic acid
BLOSUM	Blocks substitution matrices
BSA	Bovine serum albumin
CCL	Chemokine (C-C motif) ligand
CCR	C-c chemokine receptor
CFTR	Cystic fibrosis transmembrane conductance regulator
CHDP	Cationic host defense peptides
CLC	Charcot-leyden crystal
CLR	C-type lectin receptors
CMP	Common myeloid progenitor
COPD	Chronic obstructive pulmonary disease
CX_3CL	Chemokine C-X3-C motif ligand
CXCL	Chemokine C-X-C motif ligand
CXCR	C-X-C motif chemokine receptor
DE	Differentially expressed
DMSO	Dimethylsulfoxide
DNA	Deoxyribonucleic acid
ECP	Eosinophil cationic protein
EDN	Eosinophil derived neurotoxin
ELISA	Enzyme-linked immunosorbent assay
EPO	Eosinophil peroxidase
ERV	Expiratory reserve volume
FEV_1	Forced expiratory volume in the 1^{st} second
FOT	Forced oscillation technique

FRC	Functional residual capacity
FRET	Florescence resonance energy transfer
GAF	Gamma activated factor
GAPDH	Glyceraldehyde 3-phosphate dehydrogenase
GAS	Gamma interferon activation sites
GM-CSF	Granulocyte-macrophage colony-stimulating factor
GO	Gene ontology
GPCR	G protein coupled receptors
H&E	Hematoxylin and eosin
hBD	Human β-defensin
HBEC	Human bronchial epithelial cells
HDM	House dust mite
HI	Hydrophobicity index
HPLC	High performance liquid chromatography
HRP	Horseradish peroxidase
IC	Inspiratory capacity
ICS	Inhaled corticosteroids
IDR	Innate defense regulator
IFN	Interferons
Ig	Immunoglobulin
IL	Interleukin
ILC	Innate lymphoid cells
IPA	Ingenuity® pathway analysis
IRV	Inspiratory reserve volume
JNK	C-jun kinase
kDa	Kilo daltons
KSFM	Keratinocyte serum-free medium
LABA	Long acting β-agonists
LDH	Lactate dehydrogenase
LPS	Lipopolysaccharide
mAChR	Muscarinic acetylcholine receptors

MAPK	Mitogen-activated protein kinases
MBP	Major basic protein
MCP	Monocyte chemoattractant protein
MDC	Macrophage-derived chemokine
MIP	Macrophage inflammatory protein
MMP	Matrix metalloproteinases
MPO	Myeloperoxidase
MSD	Mesoscale discovery
NF-κB	Nuclear factor kappa-light-chain-enhancer of activated b cells
NK	Natural killer
NLR	Nod-like receptors
NO	Nitric oxide
NOS	Nitric oxide synthases
PAMP	Pathogen associated molecular patterns
PAS	Periodic acid schiff
PBEC	Primary bronchial epithelial cells
PBMC	Peripheral blood mononuclear cells
PBS	Phosphate-buffered saline
PC	Provocative concentration
PCA	Principle component analysis
PI3K	Phosphoinositide 3-kinase
PIC	Protease inhibitor cocktail
PMA	Phorbol 12-myristate 13-acetate
PRR	Pattern recognition receptors
qPCR	Quantitative polymerase chair reaction
QSAR	Quantitative structure-activity relationship
RA	Receptor antagonist
RCV	Respiratory syncytial virus
RFU	Relative fluorescence units
RNA	Ribonucleic acid
RORA	Retinoic acid-related orphan receptor α

ROS	Reactive oxygen species
RT	Retention time
RV	Residual volume
SABA	Short acting β-agonists
SCS	Systemic corticosteroids
SEM	Standard error of mean
SLE	Systemic lupus erythematosus
SP	Surfactant proteins
STAT	Signal transducer and activator of transcription
STC	Stanniocalcin
TARC	Thymus and activation regulated chemokine
TFBS	Transcription factor site binding
Th	T-helper
TLC	Total lung capacity
TLR	Toll-like receptors
TMB	3,3',5,5'-tetramethylbenzidine
TNF	Tumor necrosis factor
TSLP	Thymic stromal lymphopoietin
TV	Tidal volume
VC	Vital capacity

Copyright

List of copyright material for which permission was obtained.

Figure I. Illustration summarizing structure and function of the airway epithelium.

Denney, L. and L.P. Ho, The role of respiratory epithelium in host defense against influenza virus infection. Biomed J, 2018. 41(4): p. 219. This figure was modified and reproduced by permission of Elsevier publishing group.

Figure II. Multitude of biological activities displayed by CHDP.

van der Does, A.M., P.S. Hiemstra, and N. Mookherjee, Antimicrobial Host Defense Peptides: Immunomodulatory Functions and Translational Prospects. Adv Exp Med Biol, 2019. 1117: p. 156. This figure was reproduced by permission of Springer Nature.

Figure III. Anatomy of the human lung.

(A) Figure was modified and reproduced from Wikimedia Commons public domain. (B) Figure was modified from the Severe Asthma Toolkit (https://toolkit.severeasthma.org.au), which was developed by the Centre of Excellence in Severe Asthma. The original was developed by Dr. Michael Fricker, University of Newcastle.

Figure IV. Mechanism of allergic sensitivity and challenge.

Lambrecht, B.N. and H. Hammad, The immunology of asthma. Nat Immunol, 2015. 16(1): p. 45-56. This figure was reproduced by permission of Springer Nature by combined 4 figures.

Figure V. Flow-volume loop.

In: UpToDate, Post TW (Ed), UpToDate, Waltham, MA. Copyright © 2019 UpToDate, Inc. (www.uptodate.com). This figure was modified and reproduced with permission from: Irvin CG. Pulmonary function testing in asthma.

Chapter 1: General Introduction

1.1 Immune System

1.1.1 General overview

Inflammation, *rubor et tumor cum calore et dolore* (redness and swelling with heat and pain), was first defined during the 1st century [1]. Illness was considered to be an imbalance between these four pillars of inflammation [1]. The fifth pillar of inflammation, *fucntio laesa* (loss of function) was later added in the late 1800s after investigations into the cellular basis of pathologies [1]. In the 21st century, we now know that inflammation is a biological response of the immune system and is essential for the survival of multicellular animals that are continually exposed to disease causing molecules and pathogens [1, 2]. The immune system is comprised of a collection of cells, tissues and molecules, with a primary function of defending the host against infectious diseases [3, 4]. The central feature of the immune system, seen in organisms ranging from protozoa to highly complex vertebrates, is the ability to correctly identify non-self vs self-molecules [4-6]. In the event of identification of non-self-molecules, an inflammatory response is initiated that is characterized by vascular dilation, increased vascular permeability and blood flow, and leukocyte recruitment to the site of non-self-molecule detection [3, 4]. Although inflammation is essential for the protection against infectious pathogens, failure to resolve inflammation can leads to sustained chronic inflammation, which is a major cause of disease in the 21st century [1, 3, 4]. Therefore, immunological homeostasis or the ability to initiate and resolve inflammation is critical for health [7].

The immune system is broadly categorized into innate and adaptive immunity [5, 8]. Innate immunity acts as a broad first line of defense against foreign molecules and pathogens while also directing and shaping the adaptive immune response that mounts a highly specialized defense

against foreign molecules with antigen-specific receptors [3, 4]. The adaptive immune system will be discussed briefly in chapter 1.3.2 in the context of allergic asthma. The focus of my thesis and of chapter 1.1 will be on the innate immune system.

Innate immunity has several layers of defense mechanisms against microbes. The first layer of defense are physical barriers that separate the body and the external environment [3, 4]. These physical barriers include the skin, lungs, gastrointestinal tract and genitourinary track [3, 4]. These barriers are primarily composed of epithelial cells [3, 4]. To mount an immune response against microbes that may invade through the physical barriers, germline encoded pattern recognition receptors (PRR) are used by the innate immune system to identify a broad range of microbial species by pathogen associated molecular patterns (PAMP) [3, 4]. The four families of PRR are toll-like receptors (TLR), c-type lectin receptors (CLR), retinoic acid-inducible gene (RIG)-I-like receptors (RLR) and nod-like receptors (NLR) [9]. These PRR are expressed on immune (Macrophages, dendritic cells, (natural killer) NK cells, etc.) and non-immune cells (epithelial cells, fibroblasts, etc.) [9, 10]. Upon binding of PAMP, PRR activates pro-inflammatory mediators by recruiting and activating resident and circulating phagocytes e.g. neutrophils [4, 9]. The production of neutrophils is also rapidly increased in the bone marrow in response to an infection and is the first cell type recruited to the site of infection to phagocytose microbes and further produce inflammatory mediators [3, 4]. Monocytes are present at a lower amount relative to neutrophils but are also recruited subsequently to the site of infection to ingest microbes, regulate inflammation and clear dead tissue/neutrophils [11]. Further, there are dendritic cells, innate lymphoid cells (ILC) and natural killer cells that induce additional inflammatory mediators and stimulate adaptive immunity to enhance clearance of infectious pathogens [3, 4]. As the focus of

my thesis is on airway inflammation, the subsequent sections, will be focused on components of the innate immune response in the lungs.

1.1.2 Cytokines

Cytokines are soluble, low molecular weight (6-70 kDa) secreted proteins that serve as cellular messengers and mediate a number of biological functions including an immune response [4, 5, 12]. Interleukins (IL) are the most common type of cytokines [13]. The binding of cytokines to receptor (on the cell that produced the cytokine, autocrine, or on neighboring cells, paracrine) leads to activation of signaling pathways within the target cell [14]. This results in transcriptional activation of specific genes, including additional cytokines [14]. The overall nature of the response therefore depends on the secreted cytokine milieu and cell types present expressing the relevant receptors [12]. Cytokines can be broadly categorized into pro- and anti-inflammatory depending on the nature of response [3, 4].

Some common pro-inflammatory cytokines include IL-1, IL-6 and tumor necrosis factor (TNF) family cytokines [4]. Pro-inflammatory cytokines trigger inflammatory responses including activation, differentiation, and proliferation of immune cells contributing to a pro-inflammatory state [3, 4]. However, as mentioned above resolution of pro-inflammatory responses is critical to prevent chronic (persistent and enhanced) inflammation and subsequent damage to host tissues [14-16]. This includes the active removal of toxic molecules secreted by granulocytes (discussed in chapter 1.1.4), apoptotic cells and the suppression of pro-inflammatory cytokines. The immune resolution phase is highly regulated and involve specialized cells and molecules such as resolvins, lipoxins, protectins and potent anti-inflammatory cytokines [1]. Anti-inflammatory cytokines such as IL-1 receptor antagonist (IL-1RA) and IL-10 limit inflammatory reactions by a

variety of mechanisms [17]. For example, IL-1RA binds the IL-1 receptor preventing IL-1 (pro-inflammatory cytokine) from binding and activating downstream target genes. IL-10 activates a signaling cascade involving signal transducer and activator of transcription (STAT) family of transcription factors, namely STAT3, which results in the suppression of the transcription of pro-inflammatory genes [18]. The essential anti-inflammatory role of IL-10 is highlighted with IL-10-deficient mice infected with pathogens that rapidly die due to the untampered inflammatory response resulting in damage to organs [18]. Therefore, the balance and the kinetics of pro- and anti-inflammatory cytokine production and release is critical for maintaining immunological homeostasis and health.

Chemokines are a subset of cytokines containing three to four conserved cysteine residues that mainly function to influence cell trafficking [19, 20]. Chemokines are grouped in 4 different families (CC, CXC, CX3C and C) depending on the spacing between the conserved cysteine's. Chemokines bind the large family of G protein coupled receptors (GPCR) on target cells [20]. The interplay between chemokines and the receptors are complex as several chemokines can bind to multiple different receptors, and a GPCR can bind multiple chemokines [21]. Each pair of binding configuration may elicit a different response depending on the cell the receptor is expressed on [21].

As discussed above, cytokines and chemokines are essential in regulating an immune response especially in surfaces that are exposed to pathogens and external particles like the lungs. Airways in an average human adult lung have a surface area of approximately $70m^2$, and inhales as much as 8000 liters of air every day [22, 23]. Therefore, it is critical to maintain an effective and balanced immune response in the airways. Cytokines in the lung produced by a variety of cell types mediate responses to injury or infections leading to resolution of the insult and the return to

homeostasis [15]. The major immune cell types that are initially recruited by cytokines and chemokines are granulocytes and monocytes.

1.1.3 Airway granulocytes and monocytes

Immune cells are formed through a process referred to as hematopoiesis. Myeloid cells which include neutrophils, eosinophils and monocytes arise from common myeloid progenitor (CMP) cells [24]. This section will discuss CMP-derived cells in the context of airway inflammation.

1.1.3.1 Neutrophils

Neutrophils are polymorphonuclear granulocytes and are typically the first cell type to respond to the site of infection or injury [25]. The multi-lobe nucleus of neutrophils allows them to move through tight junctions and extracellular matrix, permitting neutrophils to rapidly mobilize into damage tissues [26]. One of the most potent chemokines for recruitment of neutrophils is CXCL8 (KC in mice) which binds to its receptor, C-X-C motif chemokine receptor (CXCR)2 expressed on neutrophils [26]. However other factors such as Chemokine C-X-C motif Ligand (CXCL)1, 2, 5, 7, leukotriene B_4 and IL-33 can also play a role in neutrophil recruitment [27]. Neutrophils are generally short lived and are responsible for phagocytosis, release of granules, formation of extracellular nets and recruiting additional immune cells to the site of injury [27]. The granules of neutrophils contain pro-inflammatory mediators such as cytokines, Matrix metalloproteinases (MMPs), myeloperoxidase (MPO), neutrophil elastase, M-Ficole, proteinase 3, lysozyme, arginase-1, reactive oxygen species (ROS) and many antimicrobial cationic host defense peptides (CHDP) such as cathelicidins and defensins [26, 28]. These mediators are released upon neutrophil activation by local inflammatory signals [26, 28]. Although neutrophils

are pivotal early responders to a site of injury, neutrophils have also been implicated in the development and maintenance of chronic pulmonary diseases such as asthma and chronic obstructive pulmonary disease (COPD) [29]. The critical role of neutrophils in asthma will be discussed in section 1.3.

1.1.3.2 Eosinophils

Eosinophils are granulocytes containing segmented nuclei and are largely characterized due to their large specific granules containing inflammatory and tissue damaging mediators [30]. The granule contents include major basic protein (MBP), eosinophil cationic protein (ECP), eosinophil peroxidase (EPO), eosinophil derived neurotoxin (EDN), charcot-leyden crystal (CLC) Protein and a host of cytokines (IL-12, IFNγ, IL-4, IL-13, TNF, IL-10, GM-CSF, etc.) [30, 31]. Due to the large number of stored mediators in granules and vesicles with varied and contradictory functions, eosinophils are capable of piecemeal degranulation [31]. This unique degranulation method allows eosinophils to differentially release inflammatory mediators in the granules based on activation stimuli and in a context dependent manner [31].

Eosinophil chemoattractants include eotaxin (chemokine (C-C motif) ligand (CCL)11 and CCL24), RANTES (CCL5), monocyte chemoattractant protein (MCP)-3, MCP-4 which bind to the C-C chemokine receptor (CCR)3 receptor expressed on eosinophils [31]. Eosinophils are central to fighting helminth infections by releasing reactive oxygen species and MBP in granules [32]. In contrast to fighting infections, eosinophils are also involved in the pathogenesis of asthma, which is discussed in detail in section 1.3.

1.1.3.3 Macrophages

Macrophages have diverse functions in immunity but are primarily known for their phagocytic function [33]. Macrophages are primarily either monocyte-derived blood macrophages or tissue-resident macrophages [34]. Tissue-resident macrophages are heterogeneous, long lived and display tissue specific functions [35]. For example, tissue resident macrophages in the lung located in alveoli interact with alveolar epithelial cells. Alveolar resident macrophages clear pulmonary surfactants and play a large role in regulating the alveolar microenvironment [34]. However alveolar macrophages in chronic inflammatory disease such as asthma, have been found to be altered and possibly contributing to overall pathogenesis of the disease by producing increased levels of IL-13 and MMPs [34, 36]. In contrast to the tissue-resident macrophages, monocyte-derived macrophages infiltrate into a site of injury during inflammation exerting wide range of inflammatory functions including phagocytosis of short lived neutrophils [33, 34, 37]. Monocytes/Macrophage home to specific sites, a process driven by chemoattractants that including MCP1 (CCL2) and MCP3 (CCL7), which bind to CCR2 on macrophages. Macrophages also express other chemokine receptors, such as CCR1 and CCR5, which bind macrophage inflammatory protein (MIP)1α (CCL3) and CCL5, respectively. Fractalkine, or chemokine C-X3-C motif ligand (CX_3CL)1, is also a chemoattractant that binds to CX_3CR1 receptor on macrophages [37]. Upon activation, macrophages secrete TNF, IL-1, IL1-2, IL-23 and nitric oxide (NO) that further contribute to microbial defense by directing the differentiation and expansion of immune cells including T cells. Therefore, macrophages are an essential cell type that contributes to homeostasis and plays a pivotal role in the defense against pathogens. In addition to neutrophils, eosinophils, and macrophages, airway epithelial cells (AEC) play a critical role in pulmonary host defense and homeostasis.

1.1.4 Airway epithelium

AEC are the most abundant cells in the lungs, providing a first direct line of defense by forming a physical barrier against inhaled microbes, particulates and other molecules [4, 38]. Tight junctions formed between AEC by occludins, tricellulin, cadherins and junction adhesion molecules are essential for establishing a continuous undisrupted layer of AEC [16]. The tight junctions also are involved in regulating proliferation, differentiation of AEC as evident by the presence of cell cycle regulators and signaling molecules localized in the tight junction plaque [39].

Apart from acting as a physical barrier, the role of AEC is increasingly appreciated as an active component in maintaining pulmonary homeostasis (Figure I) [38]. The multifunctional role of AEC is evident when considering that the airway epithelium is composed of various differentiated epithelial cells consisting of ciliated, columnar, basal, goblet, secretory (clara and serous) and undifferentiated cells all with diverse functions (discussed in more detail below) [40]. The structure of the airway epithelium varies from pseudostratified containing mainly ciliated, goblet and basal cells in the large airways to a single layered barrier containing columnar (clara cells) and cuboidal in the small airways. In alveolar sacs the airway is lined mainly with specialized squamous type 1 and cuboidal type II alveolar epithelial cells (Figure I) [40, 41]. AEC have been shown to renew every 30 to 50 days and if injured will re-establish the epithelial layer using stem/progenitor cells [40].

In addition, the airway epithelium has a prominent role in initiating, sustaining and directing an immune response by actively meditating the secretion of immune mediators and recruitment of immune cells (Figure I) [38]. Taken together, the airway epithelium plays a multifunctional role

in pulmonary function and host defense. Consequently, disruption of the AEC layer can result in deleterious effects. For example in asthma patients, altered epithelium composition has been observed where there is an increase in basal and goblet cells while a decrease in ciliated cells [16]. These changes to the AEC composition results in altered mucociliary clearance, heightened inflammatory response and increased airway obstruction which is discussed in more detail below [16, 42].

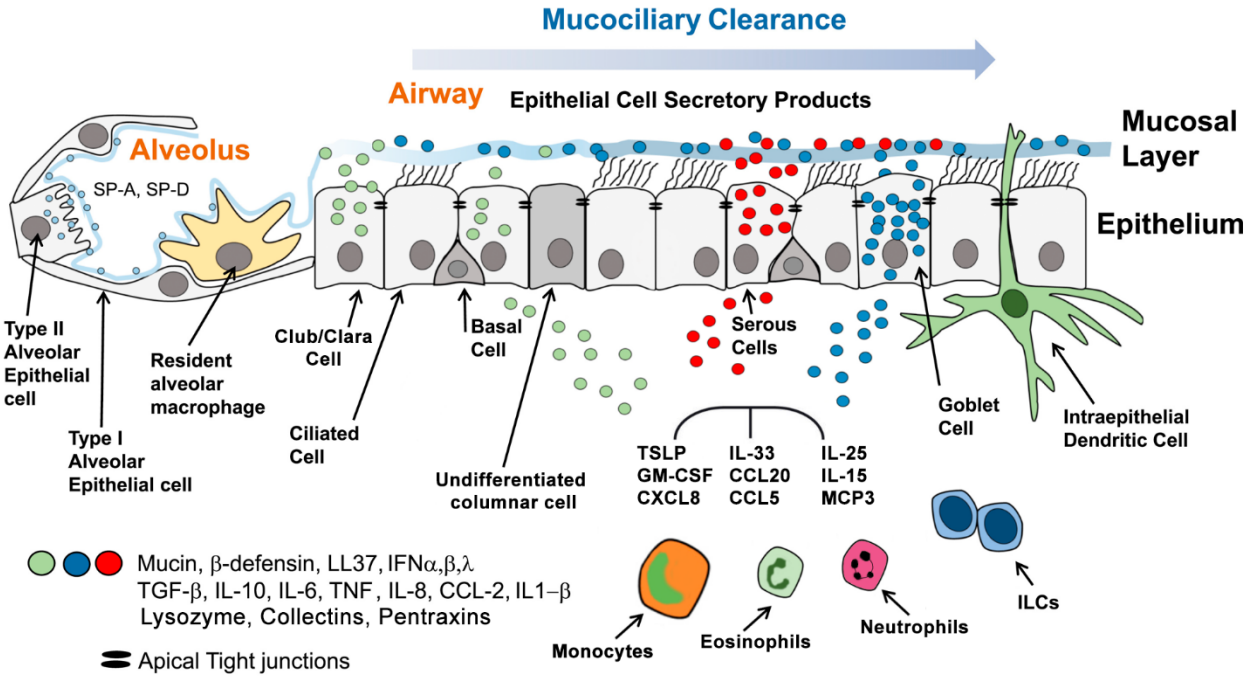

Figure I: Illustration summarizing structure and function of the airway epithelium. *The airway epithelium is differentiated in a pseudostratified layer (right) which transitions into alveolar sac containing specialized type I and II epithelial cells. Mucociliary clearance is also depicted on the apical side of the airway epithelium including secretory products produced by specialized AEC. On the basal side of the AEC, mediators such as CXCL8, CCL5, MCP3 are secreted to recruit immune cells to the airways. This figure was modified from Biomed J, 2018. 41(4): p. 219.*

1.1.4.1 Mucins and mucociliary clearance

Mucins are glycoproteins with large carbohydrate chains attached on a protein backbone and are released by goblet cells in the airways [43]. There are a total of 17 *MUC* genes but *MUC5AC* gene expression is predominantly seen in the airways [43, 44]. Mucin expression is regulated by a variety of factors, including inflammatory cytokines such as IL-13 [45]. Mucins are generally preformed and stored in granules and released upon activation of the goblet cells [44]. Mucins help lubricate the air exposed epithelial layer (apical), moistening the inhaled air, and helps trap particulate matter and pathogens from the environment [44]. Further, the negative charge of mucins facilitate binding of smaller positively charged molecules that display antimicrobial activity such as lysozyme, secretory immunoglobulin (Ig)A and antimicrobial peptides for host defense functions [46-48]. Arguably one of the most critical function of mucins in the airways is the interaction with beating cilia for mucociliary clearance that move bacteria and particles up to the throat from the airways for enhanced clearance [43, 44]. Ciliated cells, defined due to their highly specialized organelle called motile cilia, contain motor proteins that allow cilia protruding on the apical surface to beat in a synchronized fashion to move mucus towards the throat [41, 43]. The importance of mucociliary clearance is illustrated in cystic fibrosis patients where loss of CFTR (cystic fibrosis transmembrane conductance regulator) leads to dehydration of mucus and consequently reduced mucociliary clearance due to increased thickness [49]. This results in increased susceptibility to pulmonary infections [50].

1.1.4.2 AEC-induced cytokines

AEC express PRR which upon binding to infectious pathogens or allergens directs and shapes the subsequent immune responses [29]. The downstream signaling of PRR along with physical injury to AEC leads to excess secretion of cytokines such as TNF, IL-6, IL-25, thymic

stromal lymphopoietin (TSLP), IL-33, interferons (IFN), and a host of chemokines leading to recruitment and activation of immune cells such as granulocytes and monocytes (Figure I) [51]. Although activating AEC are beneficial for an effective immune response to clear infectious pathogens or inhaled particulates, AEC also play a major pathological role by increased secretion of pro-inflammatory mediators resulting in accumulation of immune cells in the lungs leading to chronic inflammation and tissue damage in disease such as asthma and COPD [16].

1.1.4.3 Antimicrobial molecules in AEC

AEC actively participate in host defense mechanisms by secreting a number of proteins and peptides such as lysozymes, lactoferrin, collectins, serum amyloid A, pentraxins, surfactant proteins, and other CHDP with antimicrobial activity (Figure I) [40, 52]. CHDP also known as antimicrobial peptides are peptides that have direct antimicrobial activity against pathogens and are potent regulators of inflammation [53-55]. CHDP are discussed in detail below.

1.2 Cationic Host Defense Peptides

1.2.1 General overview

This section contains text from a collaborative book chapter in: Parnham M. (eds) *Encyclopedia of Inflammatory Diseases*. Birkhäuser, Basel. **Hadeesha Piyadasa,** Ka-Yee Grace Choi and Neeloffer Mookherjee. (2014) Antibacterial Host Defense Peptides. Online ISBN: 978-3-0348-0620-6.

CHDP also known as antimicrobial peptides (AMP) are evolutionary conserved peptides that are integral in the innate immune response [56-59]. CHDP were first discovered as early as 1939 in prokaryotic cells but it was not until 1962 that CHDP were described in animals from an orange

speckled frog *Bombina variegate* [60]. CHDP were initially identified to be directly antimicrobial, able to disrupt bacterial membranes or target intracellular targets in bacteria, similar to an antibiotic [61, 62]. Studies to date have identified more than 2600 CHDP with diverse structures and sequences in a wide variety of organisms, ranging from plants, insects, to mammals with highly complex immune systems [51, 53, 56, 57, 63-66]. In the last two decades, investigations of CHDP under physiological conditions *in vitro* e.g. in the presence of serum, and animal models, have illustrated the wide range of immunomodulatory functions of CHDP which include inducing anti-inflammatory cytokines, controlling endotoxin and pro-inflammatory cytokine mediated inflammation, promoting cell migration, wound healing, and influencing the maturation and differentiation of dendritic cells and T-cells [53, 55-57, 67-71]. Therefore, the term CHDP is now increasingly being used as an accepted nomenclature to encompass both their antimicrobial and immunomodulatory functions.

CHDP are typically 12-50 amino acids in length with a net positive charge ranging from +2 to +7 with ≥ 30 % hydrophobic residues [54]. Based on their structures, CHDP can be categorized into four groups; amphipathic α-helical (e.g. cathelicidins and magainins), β-sheet structures stabilized with two or more disulphide bonds (e.g. α and β defensins), loop-structured peptides with one disulfide bond (e.g. bactenecin), and extended structures (e.g. indolicidin) [65]. The two best charecterized families of CHDP in humans are cathelicidins and defensins [53, 72]. All cathelicidins contain a conserved precursor protein sequence known as the cathelin domain and is basis on which cathelicidins from different species are grouped together. In contrast, defensins are grouped based on their structural similarity [53, 73]. All defensins have a common beta sheet core that is stabilized by three disulfide bonds [53, 73]. The best defined subgroups of defensins are α- and β-defensins in humans and a third subgroup known as θ-defensins, to date found only in rhesus

monkeys [73, 74]. The structure and sequence and activity reltionships of CHDP will be discussed in more detail in chapter 3.4.

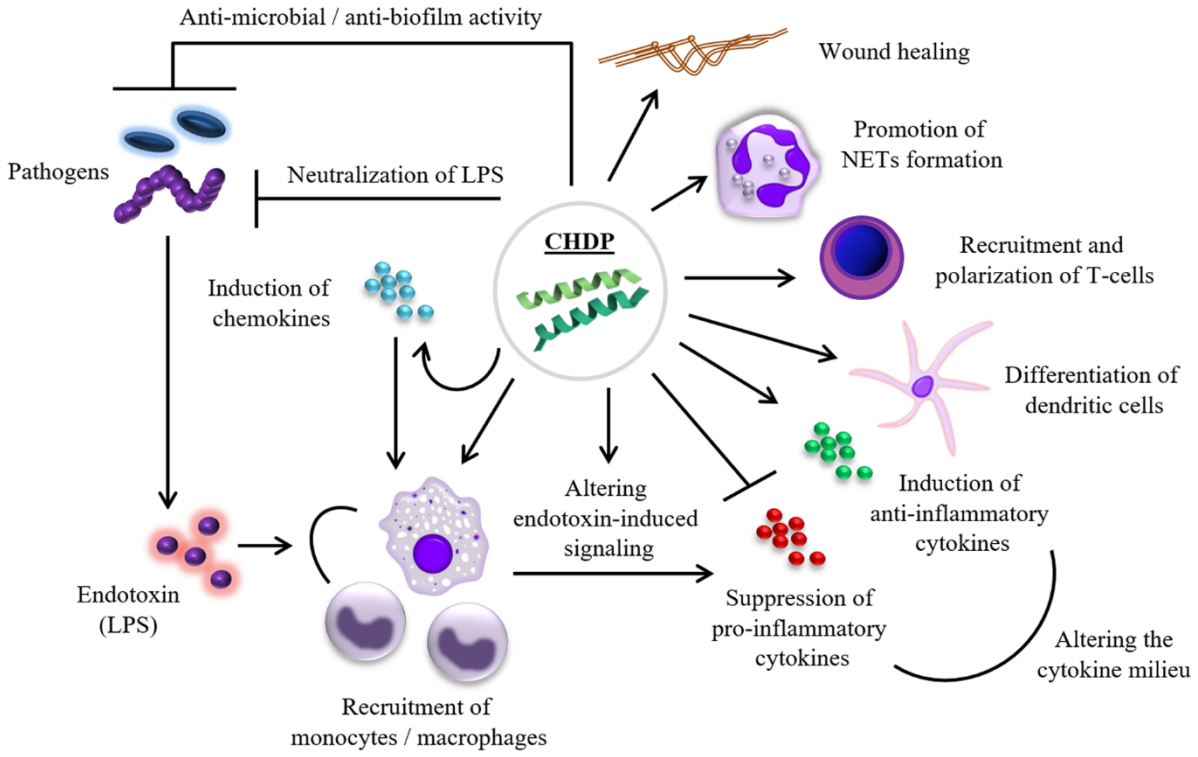

Figure II: Multitude of biological activities displayed by CHDP. *CHDP have wide range of functions including direct anti-microbial and extensive immunomodulatory activities that further enhance clearance of microbes by shaping a more effective immune response against the pathogen. CHDP are* also *involved in maintaining immunological homeostasis. This figure was obtained from Adv Exp Med Biol, 2019. 1117: p. 156.*

1.2.1.1 Biosynthesis and release CHDP

Mammalian CHDP are expressed in a wide variety of cells, including cells of myeloid origin such as neutrophils, lymphocytes, monocytes / macrophages, and in structural cells e.g. keratinocytes and epithelial cells [75, 76]. CHDP are expressed in a wide range of tissues e.g. skin, oral cavity, lungs and cervix, and found in body fluids such as saliva, sweat, breast milk, semen,

and plasma [77]. CHDP are generally synthesized as precursor pre-pro-proteins, which allow for transcriptional and post-transcriptional regulation of the mature biologically active peptides. The precursor proteins are proteolytically cleaved by specific proteases to generate the biologically active mature form of the peptide [76, 78, 79]. For example, the human cathelicidin is expressed as a 18 kDa pre-pro-protein hCAP18, containing a signal sequence, the conserved cathelin domain and the active peptide region [80]. Cell types such as neutrophils, natural killer cells and mast cells constitutively express the inactive hCAP18 precursor protein in their granules, which are released upon cellular degranulation in response to pathogenic or inflammatory stimuli, and proteolytically processed by endogenous proteases such as serine proteinase-3 to generate the biologically active, 37-amino acid, α-helical, amphipathic peptide, LL-37 [81]. Although LL-37 is the most abundant form processed from hCAP18, a few studies have also reported alternative processing of hCAP18. For example, hCAP18 in seminal plasma was demonstrated to be processed by the prostate-derived protease gastricsin to generate a 38 amino acid peptide known as ALL38 [82]. On the skin surface, LL-37 was shown to be further processed to smaller peptides (RK-31, KS-30 and KR-20) by proteases present in human sweat [83]. In addition, mouse cathelicidin CRAMP is remarkably similar in gene sequence, structure and peptide processing to LL-37 [84]. Defensins are also synthesized as precursor proteins, stored in cells such as primary granules of neutrophils, and processed to their mature forms upon activation [85].

Depending on the cell type, tissue and environmental stimuli, the expression of CHDP can be constitutive or inducible [76]. Constitutive expression of CHDP such as LL-37 and defensins in the skin and colon epithelium play an important role in defense against pathogens while expression of specific CHDP are up-regulated or induced in response to pathogens, cytokines, growth factors, and certain nutrients [86, 87]. Recent studies have shown that metabolites, in

particular the biologically active 1,25-dihydroxy vitamin D_3, can induce the expression of LL-37 and β-defensin in human keratinocytes, monocytes, neutrophils and gingival epithelial cells [88]. It has been hypothesized that the induction of CHDP by 1,25 - dihydroxyvitamin D_3 may be mediated by the vitamin D receptor complex, and can contribute to protection against infections and the damaging effect of UVB in the sunlight [88].

In the lungs, CHDP are constitutively secreted by AEC and are a major component of the airway surface liquid (apical side of airway epithelium) [89, 90]. The most abundant airway CHDP are LL-37/hCAP-18, α and β-defensins while lactoferrin, lysozyme, SLPI, elafin, surfactant proteins (SP)-A and D are considered to be host defense proteins [89, 90]. Further the recruited immune cells such as neutrophils, macrophages and T cells also actively produce and secrete CHDP in the lungs [91].

1.2.1.2 Biological activities of CHDP

As described earlier CHDP mediate a multitude of biological activities required for protection against infections and the regulation of the host immune response. The contribution of CHDP to the innate immune system has been clearly demonstrated using knockout models for CHDP [92, 93]. In a study published by Lemaitre *et al*, shows that complete knockout of CHDP in Drosophila melanogaster, with only an innate immune system, results in increased infections and reduced survival [92]. Similarly, in mouse models, blocking S100A8 and A9 inhibits transmigration of neutrophils and macrophages in to the airways [93].

The biological functions of CHDP can be largely classified into two areas; antimicrobial activity and modulation of immune functions (Figure II). Historically, research in the biology of CHDP have been largely focused on the antimicrobial property of these peptides [56]. Animal

models of infections, and *in vitro* studies, have clearly established the role of CHDP in conferring protection against bacterial, fungal, viral and parasitic infections [54, 56]. The mechanism of the antimicrobial action was primarily thought to be mediated by direct interaction of cationic CHDP with negatively charged cell membranes of the pathogen, resulting in damage to the cell membrane [61, 73]. Various models have been suggested for the perturbation of membrane by CHDP, such as the barrel-starve, carpet and toroidal models [94]. Other studies have also suggested that CHDP may target intracellular components resulting in inhibition of synthesis of bacterial components such as the cell wall, nucleic acid and specific proteins, resulting in bacterial death [61, 94]. Thus, the direct antimicrobial action of CHDP results in loss of membrane integrity, perturbation of intracellular pH, and interference of biosynthesis of cellular components such as the cell wall, and inhibition of specific bacterial enzymes [61, 95]. Apart from planktonic cultures, recent studies have also shown that certain CHDP and their synthetic peptide-mimics can also inhibit bacterial biofilm formation [96, 97]. Thus, it is not surprising that translational research in this field has been driven with a focus on the development of alternative therapeutics for infectious diseases. However, the direct antimicrobial activity of certain CHDP e.g. LL-37 and human β-defensin (hBD)-2 antagonizes in physiological salt concentration, in the presence of host factors such as serum and heparin, and microbial polysaccharides [71, 98]. However, in spite of the extensive research and promise of antimicrobial peptides as alternative antibiotics, to date there is no antimicrobial peptide based clinically approved drug [55, 56]. This was elegantly shown in a recent review article by Haney *et al.* where he critically reassessed the CHDP direct antimicrobial landscape [56]. These studies prompted research to define the mechanisms that contribute to the ability of CHDP to resolve infections *in vivo*. It is now well appreciated that CHDP act as immune effector molecules, influencing both innate and adaptive immunity [56]. Thus, the antimicrobial

mechanisms of CHDP are likely influenced by mediating the host immune responses to resolve infections.

Research conducted, primarily since the early 2000s, have established that CHDP are immune effector molecules that influence both innate and adaptive immunity [53, 56, 58, 59, 69, 70, 72, 77, 79, 88, 90, 99-102]. CHDP have been shown to act directly on immune (macrophages, dendritic cells, lymphocytes), as well as on structural cells (airway epithelium and keratinocytes) [58, 72, 77, 99, 103]. One of the prominent functions of CHDP are the promotion of leukocyte recruitment to the site of infection and tissue injury (Figure II) [53, 71]. LL-37 and human defensins such as HNP1 and hBD-2 exhibit direct chemoattractant properties to attract cell types such as neutrophils, dendritic cells and T-cells [53, 77, 78, 103-105]. In addition, at physiological concentrations CHDP such as LL-37, hBD-2 /3 can also induce the production of chemokines (e.g. MCP1, MIP1β, MIP3α, RANTES, Groα and IL-8) to facilitate recruitment of immune cell types such as monocytes, neutrophils, dendritic cells and T-cells, to the site of infection [53, 77, 78, 105]. Recent studies have also shown that CHDP e.g. LL-37 can induce the expression of certain chemokine receptors such as IL-8RB, CXCR4 and CCR2 [53, 77]. The function of CHDP to promote leukocyte movement and recruitment is thought to be a major property that facilitates resolution of infections.

Another immune mechanism mediated by CHDP such as LL-37 and hBD-3 which assists in the clearance of infection, is the promotion of bacterial phagocytosis [105]. For example, a study has shown that LL-37 upregulates the expression of BcL-X_L, an anti-apoptotic protein, and suppresses neutrophil apoptosis by inhibiting caspase-3 activity [104]. Therefore, prolonging the life span of neutrophils allows for increased phagocytosis and aids host mechanisms required for the clearance of bacterial infections. Recently, it has been suggested that CHDP may also play a

role in promoting autophagy, demonstrated to be mediated by the vitamin D-LL-37 axis for protection against tuberculosis [106]. Furthermore, LL-37 exhibits synergistic effects amplifying downstream responses mediated by cytokines such as granulocyte-macrophage colony-stimulating factor (GM-CSF), which also likely facilitate immune mechanisms required for resolution of infections [99].

CHDP also serve as a link between innate and adaptive immune responses by mechanisms that include induction of specific cytokines, upregulate expression of co-stimulatory molecules and promotion of the differentiation of dendritic cells and polarization of T-cells (Figure II) [53, 71, 107]. The functional role of CHDP in adaptive immunity have been further substantiated by recent studies demonstrating that some of these peptides exhibit adjuvant-like properties to enhance production of antigen-specific antibodies [71]. Other immune functions mediated by CHDP include promotion of wound healing and angiogenesis, induction of mast cell degranulation, histamine and prostaglandin D2 release (Figure II) [53, 71].

The immunomodulatory functions described so far for CHDP can be categorized as mechanisms that result in immune activation and are classically defined as 'pro-inflammatory'. However, it has been very well demonstrated that CHDP such as LL-37, hBD-2 and bovine myeloid antimicrobial peptide 28, can also control inflammation in animal models of infection and sepsis [108]. The anti-inflammatory mechanisms of CHDP include induction of specific mediators such as IL-10, IL-1RA and negative regulators of NF-κB e.g. A20 and NFκBIA [53, 56, 58, 109, 110]. Cathelicidin peptides can selectively suppress pathogen-induced inflammation by inhibiting specific pro-inflammatory responses such as production of cytokines TNF-α and IL-1β, activation of NF-κB (p50) and the expression of TNF-α-induced protein-2 (TNFAIP2), without

compromising chemokine production that is required for leukocyte recruitment to the site of infection.

The molecular mechanisms underlying the switch between CHDP-mediated immune activation and control of inflammation are not completely understood. A recent study from Hemshekhar *et al* showed that LL-37-mediated chemoattractant properties were controlled by Cdc42 Rho GTPase via GPCRs while induction of anti-inflammatory IL-1RA was independent of GPCR signaling [111]. However, LL-37 also interacts with intracellular glyceraldehyde 3-phosphate dehydrogenase (GAPDH) to induce chemokines, suggesting the involvement of multiple pathways [101]. Nevertheless, the dual role of CHDP to promote immune effector functions to resolve infections and yet mediate the control of excessive inflammation suggests that CHDP may play a vital role in shaping the innate immune response and help maintain immunological homeostasis [53, 56, 58, 109].

1.2.1.3 Pathophysiological relevance of CHDP activity

Decreased expression of CHDP leads to increase susceptibility to infections. For example, deficiency of LL-37 was demonstrated in patients with repeated periodontal infections, and lack of defensins was associated with severe frequent bacterial infections [112, 113]. Moreover, recent studies have shown that expressions of specific CHDP are either suppressed or elevated, in various autoimmune and/or inflammatory diseases. Therefore, it is uncertain whether CHDP influence disease activity or in fact contributes to the resolution of inflammation. For example, elevated levels of LL-37 have been suggested to play a role in the pathogenesis of systemic lupus erythematosus (SLE) by contributing to the loss of immune tolerance [114], whereas in psoriasis, LL-37 has been proposed to act as both an effector and a regulator [115]. Moreover, a study has demonstrated that LL-37 intervenes in the activation of the inflammasome resulting in the control

of inflammation in psoriasis [116]. Likewise, recent reports are conflicting regarding the role of CHDP in cancers. For example, LL-37 is found to be elevated and associated with the development of ovarian tumors but is downregulated and thought to function as a tumor suppressor in gastric carcinogenesis [117, 118]. Further in chronic pulmonary inflammatory diseases, expression of CHDP is dysregulated in the lungs [90, 119, 120]. For example, β-defensin-1 were elevated in COPD and severe asthma patients but β-defensin-2 expression was decreased in COPD patients [89]. Similarly, LL-37 was highly expressed in COPD during GOLD stage I and II but reduced during GOLD stage III and IV [121]. The contrasting effects of CHDP under inflammatory conditions may be dependent on the concentration of the peptide, tissue type and the stage of the disease [122]. Therefore, the exact functions of CHDP in chronic inflammatory diseases are still not well understood [121]. However, the duality of CHDP function in resolving infections and modulating immunity have garnered interest in using these natural peptides to design synthetic novel peptides as candidate therapeutics.

1.2.2 Innate Defense Regulator (IDR) peptides

The functional diversity of CHDP have propelled interest in the development of these peptides as novel therapeutics for both infectious diseases and inflammatory disorders. Research in the therapeutic potential of CHDP is focused on two general areas (i) as antimicrobial and/or anti-biofilm peptides or (ii) as immunomodulatory agents for inflammatory diseases [110]. The wide range of more than 2600 natural CHDP defined to date provides templates for the design of more active, short, synthetic peptide mimics. IDR peptides are synthetic immunomodulatory peptides designed from internal fragments and/or amino acid substitutions of natural CHDP [110]. Systematic alterations of endogenous CHDP allows for screening for IDR peptides with minimal cytotoxicity, non immunogenic with enhanced activity [110, 123]. For example, IDR-1

(KSRIVPAIPVSLL-NH2) was derived from the bovine cathelicidin Bac2a (RLARIVVIRVAR-NH2) by introduction of two Proline residues in the sequence. This mutation disrupted the direct antimicrobial activity of Bac2a while enhancing activity of chemokine induction and the suppression of lipopolysaccharide (LPS)-induced pro-inflammatory cytokines in peripheral blood mononuclear cells (PMBC) [123]. IDR-1 also has a maximum tolerable dose of 125 mg/kg given intravenously while no toxicity was detected when the same dose was given intraperitoneally, highlighting the minimal toxicity profile of synthetic IDR peptides [123]. Overall, IDR peptides have minimal toxicity in animals, optimized for required function and cheaper to produce compared to the natural CHDP.

The safety of CHDP-based peptide mimics have been established as some of these synthetic peptides are in phase II / III clinical trials [124, 125]. Most of the clinical trials to date are with topical application of peptides primarily for treatment of infectious diseases, whereas pre-clinical studies have established the safe, systemic administration of peptide-based therapeutics [53, 124, 125]. The distinct advantage of developing IDR peptide-based therapeutics is the potential to selectively control inflammation without compromising host's resistance to infections. However, there are several challenges in the development CHDP/IDR peptide-based therapeutics, which include limited stability and bioavailability, and not yet well-defined toxicities in humans. Even though the concept of CHDP/IDR peptide-based immunomodulatory therapeutics is a promising field with tangible translational outcomes, future research needs to be conducted focusing on solving the structure-function relationship of the candidate peptide's immunomodulatory activities, optimization of the pharmacokinetics of the peptide, formulations and targeted delivery methods.

In the last decade, due to the increasing computational capabilities, synthetic CHDP derivatives have been designed based on predicted activities. This method, referred to as structure-activity relationship modelling, though limited, attempts to overlay immunomodulatory functions based on physico-chemical descriptors such as amino acid hydrophobicity, size, charge-related properties and contact energy between neighboring amino acids [126]. Using this method on a Bac2A screen have identified more effective IDR peptides such as IDR-1002 (VQRWLIVWRIRK-NH2) and IDR-1018 (VRLIVAVRIWRR-NH2) [127]. IDR-1018 is significantly capable of inducing chemokines, differentiating macrophages, promotes wound healing and shown to protect against malaria as an adjunctive treatment [128-131]. The focus of this thesis is on IDR-1002 and is discussed in more detail below.

1.2.3.1 IDR-1002

In this thesis I investigate the therapeutic effects of the administration of IDR-1002 in allergic asthma. IDR-1002 is a synthetic peptide derived from the bovine cathelicidin Bac2a using structure-activity relationship modelling methodology as described above [127]. IDR-1002 was initially selected for analysis due to its more potent chemokine induction capability compared to IDR-1, in myeloid cells *in vitro* [132]. Further studies done by Nijnik *et al* comparing IDR-1002 to IDR-1, showed that the potent *in vitro* chemokine induction property of IDR-1002 translated to stronger *in vivo* protection against *Staphylococcus aureus* infection while also reducing the therapeutic dose by more than 5-fold [132]. Additional studies done by Madera *et al* showed that IDR-1002 was capable of directly activating phosphoinositide 3-kinase (PI3K)-akt, p38 mitogen-activated protein kinases (MAPK) pathways and resulting in increased expression of β_1-integrin and CCR5 (Chemokine receptor towards CCL3 and CCL5) on monocyte derived macrophage cell line THP-1 and PBMC [133, 134].

Examining the anti-inflammatory properties of IDR-1002 have revealed that IL-1β induced pro-inflammatory responses were suppressed through regulating nuclear factor kappa-light-chain-enhancer of activated b cells (NF-κB), c-jun kinase (JNK) and p38 MAPK activation in synovial fibroblasts [135]. A study by Wuerth *et al* demonstrated that IDR-1002 is protective against pulmonary inflammation and pathology induced by *Pseudomonas aeruginosa* infection [136]. Further analysis of the Pseudomonas aeruginosa infection using whole lung RNA sequencing revealed that IDR-1002 reduced gene expression of genes related to innate immune responses, lymphocyte activation, metabolism and collagen biosynthesis [137]. In a sterile inflammatory mouse model with phorbol 12-myristate 13-acetate (PMA)-induced ear inflammation, IDR-1002 reduced inflammation by suppressing GPCR, chemokines, histamine and IFN regulatory networks [138].

IDR-1002 has also been used as an adjuvant in novel vaccines for *Bordetella pertussis*, respiratory syncytial virus (RSV) and *Mycoplasma bovis* in animals, generating a more effective protective immune response [139-142]. It is thus evident from these previous studies that IDR-1002 is immunomodulatory in various disease models and applications, and highlights the cell, tissue, and context specific function of IDR-1002 as well as the potential as a novel therapeutic to treat inflammation.

1.3 Asthma

1.3.1 General overview

Asthma is a chronic inflammatory lung disease, affecting over 300 million people worldwide [143, 144]. In Canada, 3.8 million (10%) people are diagnosed with asthma with an estimated $2 billion annual economic burden. Asthma results in impaired quality of life, disability

and sometimes death in children and adults [143]. Women have 20% higher asthma prevalence than men over the age of 35 [145]. However, in children, boys have higher prevalence then girls [145].

Asthma is also a heterogeneous disease with diverse clinical features and underlying mechanisms [146]. The heterogeneity is largely thought to be due to genetic and epigenetic differences superimposed by various environmental exposures [146]. Therefore, there are several approaches present to categorize this heterogeneous population [146]. For example, a genome wide association study has identified four different adult asthma phenotypes that are characterized by disease activity, age of onset and atopic status [147]. Another approach is to classify based on inflammatory signature in the lungs, e.g. level of eosinophilic vs neutrophilic inflammation, cytokines in the sputum or BAL [146]. It is therefore important to understand these differences in asthma phenotype to prescribe effective treatments and prevent disease progression.

Symptoms of asthma are often non-specific and can include shortness of breath, wheezing, cough and tightness in the chest [148, 149]. Asthma is an inflammatory lung disease often associated with airway hyper-responsiveness (AHR), airway remodeling and progressive decline in lung function [143, 150]. Asthmatic patients have difficulty breathing due to airway obstruction as a result of bronchoconstriction, excess mucus production, loss of lung elasticity and airway remodeling [151]. Therefore, before elaborating on asthma further, it is important to first address the lungs.

1.3.2 Lungs

Every cell in your body requires oxygen. The primary role of the lungs is to bring oxygen into the circulatory system while removing the waste product carbon dioxide. The lung is a

complex organ composed of nearly 50 distinct cell types including structural cells such as epithelial, smooth muscle, fibroblasts, endothelial, and infiltrating and resident immune cells including macrophages, eosinophils, neutrophils, and Langerhans cells [152]. Progenitor cells of various cell types including stem cells have not been well characterized in the lung [152].

In the development of the human lungs, early structure is seen starting 26 days after conception [153, 154]. In the next stage during weeks 6^{th} to 16^{th}, 3 lobes on the right and 2 lobes on the left are formed following the development of the airways. The airways in the lungs consist of the trachea which divides into 16 generations of conductive bronchi and bronchioles (Figure III.A). There are cartilaginous rings up until the start of bronchioles that help keep the upper portion of the airways relatively rigid. Alveoli start around the 17^{th} generation of bronchioles and increase in frequency until the 23^{rd} generation where the alveoli ducts end in alveolar sacs [154]. After the 26^{th} week, epithelial cells lining the alveolar ducts differentiate into the alveolar type 1 and type II cells [153] (Figure I). Type II alveolar epithelial cells secrete surfactants that help reduce the surface tension of the fluid and exhibit antibacterial properties [153, 154]. Alveolar spaces continue to develop until ~8 years of age to more than 300 million alveoli with a total surface area of 70 m^2. A cross section of the bronchioles shows that in a healthy human, AECs line in the inner portion open to the air liquid interface sitting on top of the basement membrane that separates the epithelial and the mesenchymal compartment, the lamina propria (Figure III.B) [155]. Below the lamina propria lies layers of airway smooth muscle (ASM) cells [155].

The lungs are enveloped by two thin layers of mesothelial cells known as the pleura [154]. The high concentration of mucopolysaccharides in between the two layers of pleura act as a lubricant allowing the lungs to expand and contract within the chest cavity [154]. Breathing happens when the diaphragm and intercostal muscles contract drawing air into the lungs due to the

increase in lung volume resulting in lower air pressure in the lungs compared to atmosphere [156]. During exhalation, relaxation of the diaphragm and intercostal muscles contract the lung, decreasing volume and increase pressure resulting in air moving out of the lungs [156]. Exhalation is a passive process due to relaxation of muscle and elasticity of the lung tissue causing lung recoil. The amount of air moving in and out of the lungs is also determined by the size of the airways. During forced breathing, other muscles including the neck muscles, obliques, and muscles of the abdomen can further assist diaphragm and the chest cavity to expand and relax [156]. Respiratory volumes as listed in Table I are different terms used to characterize air moved by the lungs at different points in the respiratory cycle. By measuring the different respiratory volumes in the respiratory cycle, using pulmonary function tests, can help diagnose respiratory disease such as asthma [154, 156].

An adult human lung can hold approximately 6L of air at full inhalation and 2.5L remain at the end of expiration [154]. In contrast, a mouse has a total lung capacity of about 1 mL [157]. Similar to human lungs, mice have a total of 5 lobes but are distributed 4 on the right and 1 on the left. Mouse lungs also have fewer bronchioles and airway generations (13-17) compared to humans (17-23) [157]. Mice have rapid resting respiration rate of 150-250 per minute compared to humans at 12-20 per minute [158, 159]. These anatomical and physiological differences between mice and human need to be considered when interpreting the findings in mice models for translating research findings to humans.

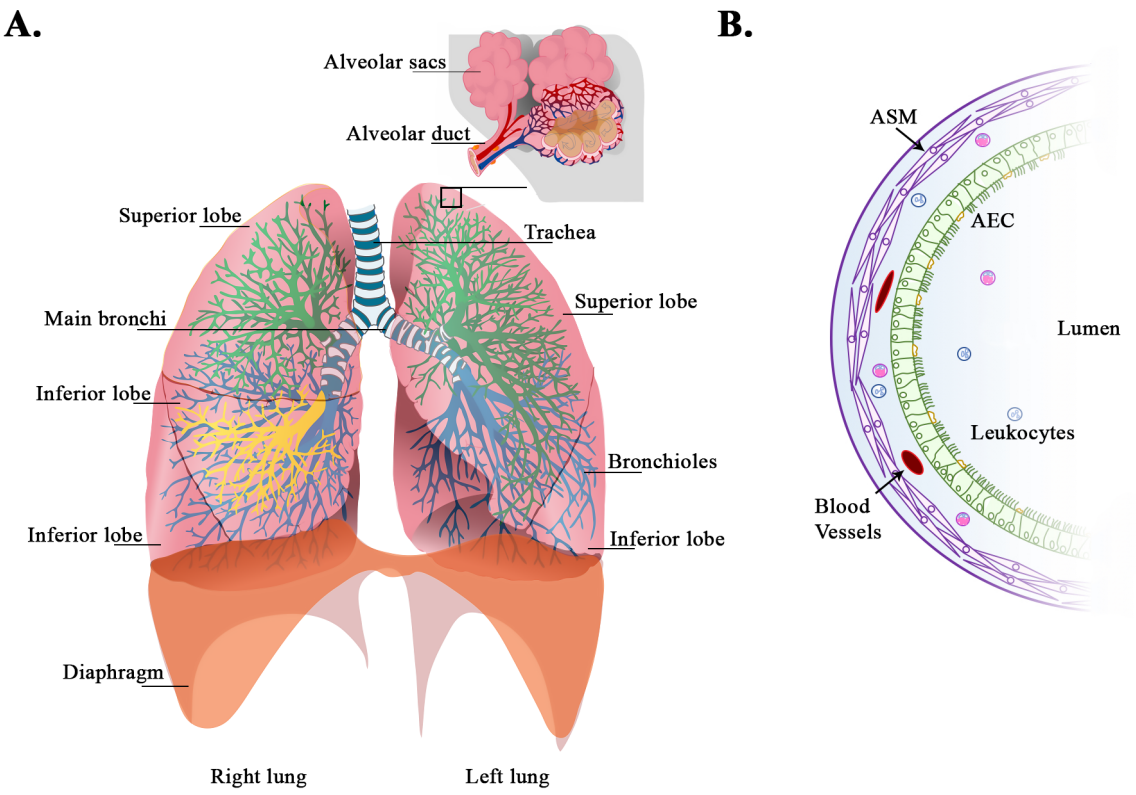

Figure III: Anatomy of the human lung. ***(A)*** *The human lung contains 3 lobes in the right lung and 2 lobes in the left lung. Airways are shown starting from the trachea and down to alveolar sacs.* ***(B)*** *Cross section of a bronchiole showing inner AEC surrounded by ASM cells. This panel was modified from https://toolkit.severeasthma.org.au.*

Table I: Respiratory volumes and capacities. *The volume of air associated with different points in the respiratory cycle (TV, ERV, IRV, RV). The respiratory capacity is the combination of two or more respiratory volumes to further characterize airway functional capacity (TLC, VC, IC, FRC).*

Measures	Function
Tidal volume (TV)	Total volume of air that enters the lung during normal breathing
Expiratory reserve volume (ERV)	The volume of air that can be forcefully exhaled past normal expiration
Inspiratory reserve volume (IRV)	The volume of air entering the lung with forced inspiration past the normal inspiration.
Residual volume (RV)	Total volume of lair left in the lungs after forceful exhalation.
Total lung capacity (TLC)	Sum of TV + ERV + IRV and RV.
Vital capacity (VC)	Total volume of air that can be moved in/out from the lungs (TV + ERV and IRV).
Inspiratory capacity (IC)	Maximum volume of air that can be inhaled past tidal expiration (ERV + RV).
Functional residual capacity (FRC)	Total volume left in the lung after tidal expiration (ERV + RV)

1.3.3 Allergic asthma

The heterogeneity of asthma, discussed earlier, is thought to be due to multiple different causal factors resulting in different molecular phenotypes and inflammatory and pathophysiologic changes. Genome-wide association studies of asthma patients have shown polymorphisms in *IL33, IL1RL1/IL18R1, HLA-DQ, SMAD3, IL2RB, ZPBP2,* and *gasdermin B (GSDMB)* genes are associated with airway epithelial barrier function and immune responses that contribute to asthma pathogenesis [160]. One of the predominant endotypes of asthma is induced by an allergic reaction to inhaled airborne allergens such as pollen, pet dander, mold or dust mites, and this is referred to as allergic asthma. Specific immunological and physiological changes due to allergic asthma in the lungs are discussed below.

1.3.3.1 Immunology

Asthma was thought to be characterized by the presence of T-helper (Th) 2 cytokines, eosinophils in the airways and IgE antibodies [161]. It is now known that there is a spectrum of inflammatory endotypes seen in asthma patients e.g. some patients display predominantly neutrophils in the airways and a mixed Th1/Th17 cytokine milieu [162]. Therefore, it is important to understand that asthma is a heterogeneous disease with different underlying immunological process. For the purpose of this thesis, I will be focusing on allergic asthma with a Th2 predominant inflammatory response.

Allergy is defined as an immune response against an harmless environmental antigen [161]. The first phase of allergic asthma is referred to as the sensitization phase where the inhalation of allergen activates AEC and dendritic cells (DC) primarily through PRR (Figure IV) [151, 161]. DC are professional antigen presenting cells (APC), that process allergen into peptides (antigens)

and display the antigens from the allergen on the surface of the cell through the major histocompatibility complex (MHC) class II [162]. The activated AEC then produce “instructive” cytokines such as IL-25, IL-33 and TSLP that further activate the DC and induce the migration of these DC to the draining mediastinal lymph nodes (Figure IV) [151, 161]. TSLP in particular is able to promote Th2 type phenotype activation in DC resulting in increased expression of OX40L. OX-40L binding to OX-40 on naïve T-cells along with recognition of antigen presented on the MHC II of the DC by the T-cell receptors, result in differentiation of the naïve T-cell into Th2 cells by activating PI3K/AKT and p38 MAPK pathways [163, 164]. Following the interaction with DC, the allergen specific activated Th2 cells will activate B-cells, that also recognize the same antigen, to class switch to IgE, proliferate, and become plasma B-cells capable of secreting the antigen specific IgE antibodies (Figure IV) [165]. The antigen-specific IgE antibodies bind to receptors on immune cells such as mast cells via the constant region of the antibodies (Figure IV). After the sensitization phase, re-exposure to the same allergen results in activation of immune cells, in particular mast cells, through crosslinking of the allergen-specific IgE antibodies coating the mast cells [162]. This results in degranulation of mast cells and release of inflammatory mediators such as prostaglandins, histamine, leukotrienes, platelet activating factor, and a variety of cytokines such as IL-4 and IL-13 that induce vascular dilation, smooth muscle contraction, airway constriction and mucus secretion, eosinophils and neutrophil activation, airway inflammation, and bronchoconstriction [166]. The persistent exposure to allergen results in chronic inflammation, and repeated damage and repair to the lung tissue that generally, but not always, leads to airway remodeling (discussed in section 1.3.3.2) [151].

Eosinophils play a critical role in allergic asthma pathogenesis. Many of the cytokines induced by eosinophil degranulation such as IL-5, eoataxin, GM-CSF further results in recruitment

and activation of more eosinophils from the circulation fueling additional inflammation [167, 168]. Eosinophils also direct T cells by suppressing Th1 responses [30].

Neutrophils that are highly abundant in the lungs of a subset of asthmatics, are potent inflammatory cells that activate Th2 cells, eosinophils, mast cells, macrophages and AEC by producing a variety of cytokines such as IL-9, TNF, IFNγ, IL-6, GMCSF and MIP (macrophage inflammatory proteins) [26, 28, 169]. Neutrophils are elevated after allergen challenge in BALF expressing high affinity IgE receptors [170]. Patients that display predominant neutrophilic asthma are less responsive to the first line of inhaled corticosteroids (ICS) treatment to asthma [169], thus highlighting the prominent role of neutrophils in severe uncontrolled asthma.

In allergic asthma, the resulting airway inflammation discussed above contributes to the development of structural changes and AHR in the lungs. For example, eosinophils are involved in AHR by inhibiting M2 muscarinic receptor with eosinophilic MBP [171]. A study by Halwani *et al* showed that eosinophils were capable of inducing ASM proliferation contributing to airway remodeling [172]. Eosinophil granules also contain MMPs, TGF-β, IL-13 and leukotrienes that further enhance airway remodeling and airway constriction [168]. Similarly, neutrophil granular contents trigger ASM and endothelial cell proliferation, airway remodeling and airway constriction [169].

In addition, it has been proposed that airway inflammation can act as a trigger of AHR [173]. For example, inflammatory cytokine such as IL-4 and IL-13 increases AHR by regulating calcium signaling in ASM cells [174]. Several studies have also shown positive correlation between eosinophil in the sputum with severity of AHR [30, 175, 176]. Therefore, decline in lung function and structural changes to the lungs in asthma are discussed in detail in the following section.

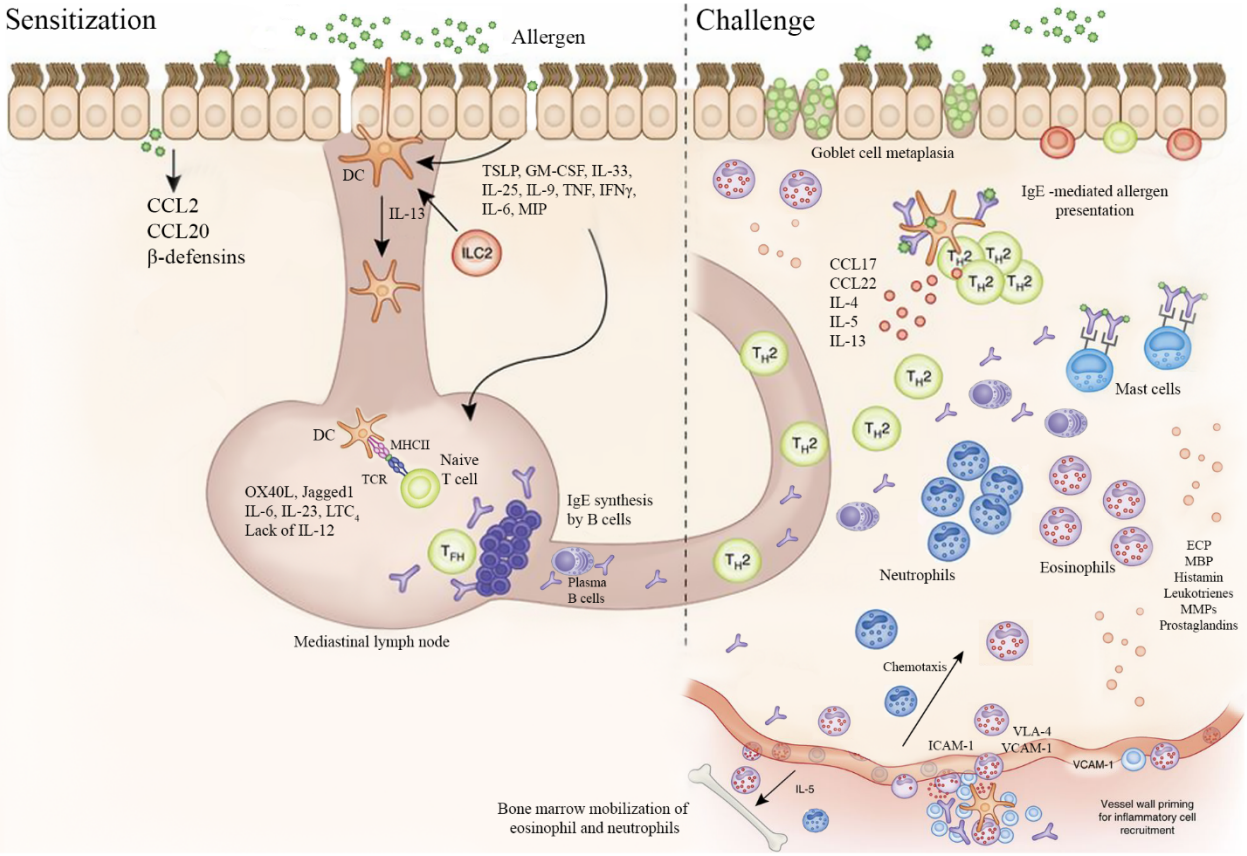

Figure IV: Mechanism of allergic sensitivity and challenge. *Left panel shows sensitization phase where allergens are first encountered. DC uptake allergen and present allergen epitopes to naïve T-cells in the mediastinal lymph nodes. AEC produce instructional cytokines effecting the microenvironment including DCs. Activated T-cells, further induce activation and proliferation of allergen specific B-cells followed by immunoglobulin class switch to IgE. Activated B-cells differentiate into plasma B-cells and secrete allergen-specific IgE antibodies. In the subsequent re-exposure phase (challenge), allergens bind IgE on mast cells and DCs and induce degranulation resulting in recruitment of immune cells from the circulation including neutrophils and eosinophils. This figure was modified from Nat Immunol, 2015. 16(1): p. 45-56.*

1.3.3.2 Physiology and lung function

Allergic asthma results in airway obstruction and increased bronchoconstriction. AHR is a heightened obstructive response of the airways to a variety of exogenous or endogenous stimuli and is considered to be a hallmark of asthma [150]. In humans, pulmonary function testing is done predominantly using a spirometer to determine the degree of airway obstruction [154]. These measurements are usually taken pre- and post-bronchodilator exposure, as airflow limitations in asthma generally show some degree of reversibility after bronchodilator treatment [148]. Increasing dose of bronchoconstrictors such as methacholine, are used to measure sensitivity and reactivity as follows [177]. Spirometry measures forced vital capacity (FVC) and FEV_1 (forced expiratory volume in the first second). As FEV_1 depends on FVC, the ratio between FEV_1/FVC is compared to predicted healthy lung values [154]. Further, more detailed analysis can be done to measure pulmonary function using flow-volume loops. The flow-volume loop is plotted as inspiratory and expiratory flow on the Y-axis against volume of air on the X-axis during forced inspiratory and expiratory maneuvers (Figure V) [178]. Figure V shows an example of asthmatic flow-volume loop (solid line) compared to healthy patients (dotted line) where a large drop in FEV_1 is seen while displaying a characteristic "downward scooping" expiratory curve [148]. This characteristic flow-volume loop represents lower airway obstruction which is typically seen in asthma and COPD patients [148]. Further, RV is increased in asthmatics as more air is trapped in the lungs due to narrowed and occluded airways followed by an increase in TLC, possibly due to compensatory mechanisms of the lung to maintain a functional range of lung volume (Figure V) [148, 178, 179]. To help differentiate between asthma and COPD patients, pre- and post-bronchodilator measurements are generally used as asthmatics are more likely to respond to bronchodilator therapy [180]. However, for complete diagnosis, spirometry tests are interpreted

with other clinical factors such as allergies, family history amount phlegm, chronic cough, and age.

In mice, in contrast to humans, invasive techniques such as tracheal cannulation are widely used due to the lack of sensitivity and reproducibility of the measurements using non-invasive techniques in small animals [177]. Specifically, animals are connected to a small animal ventilator after tracheal cannulation and forced oscillation techniques (FOT) are used to generate complex-frequency perturbations in the volume pushed into the mice while consistently measuring the pressure, flow and volume signals due to the perturbations [177, 181]. These signals are fitted to various well defined mathematical models to calculate outcomes such as Newtonian resistance (resistance of the conducting airways), tissue damping (energy dissipation in the alveoli or the resistance to inflate the peripheral airways) and tissue elastance (energy conservation in the alveoli or the stiffness of the lungs) [181-184]. This allows for detailed lung function measurements that can be used to measure effects of different experimental conditions on different properties of the lungs.

AHR encompasses the sensitivity (amount of bronchoconstrictor required to decrease FEV_1 by 20% in humans) and reactivity (maximum drop in FEV_1 due to highest dose of methacholine used) of airway narrowing [185]. In mice, rather than FEV_1 (as it is difficult to ask a mouse to comply with instructions to forcefully breath out), airway resistance is measured with an increasing dose of methacholine [177]. Although quantitatively, the two measurements, FEV_1 vs airway resistance are not directly comparable, physiological relevance of these have been shown to translate between mice and humans [150, 177]. In recent years, advances in FOT technology have introduced forced expiratory maneuver by using a vacuum to rapidly expose airways of the mouse to a negative pressure [186]. This allows for the measurement of FEV_1 and FVC with the caveat

that the methodology to obtain these parameters in mice is different from humans [186]. Therefore, further validation and comparisons are required before directly comparing mice and human FEV_1 and FVC.

Although extensive progress have been made in humans and mice to dissect AHR, the exact mechanisms of AHR in asthma remain unclear [143]. This is mainly due to the complexity of the disease and the numerous pathophysiological changes, including immune and structural changes, that are associated with increased AHR [187]. Although inflammation may be a trigger, the relationship between airway inflammation and AHR is unclear and is still under investigation. The disparity between inflammation and AHR is becoming increasingly evident as therapies that improve inflammation can do so independent of AHR [188]. Further, many asthmatics have vastly different kinetics of response due to allergen challenge in AHR and inflammation. For example, a study conducted by Kariyawasam *et al* found that allergen-induced eosinophils and neutrophils were resolved while AHR was still persistent in 7 days [189]. This supports the idea that airway inflammation can act as a trigger of AHR in asthma while the persistence of AHR is attributed to the functional changes of effector cells that contribute to the hyperresponsiveness [190]. Primary effector mechanism in AHR that contributes to the bronchoconstriction is due to the contraction of the ASM cells that surround the airways [187]. Airway remodeling results in narrowing of the airways due to thickening of reticular basement membrane and ASM [191]. Therefore, any constriction of the airways due to ASM contraction in AHR would be amplified due to the already narrow radius of the airway, further contributing to the increased AHR. Recent studies have also found that AHR may influence airway remodeling. For example, a clinical study published by Grainge *et al* showed that bronchoconstriction in the absence of additional inflammation can induce airway remodeling [192]. In recent years, due to the complexity of the processes involved,

AHR is being studied more of a cause of airway closure rather than a consequence. Furthermore, as potent anti-inflammatory biologics have minimal effect on AHR, it may be important to develop new therapeutic interventions to directly modulate structural changes and AHR independent of inflammation [193].

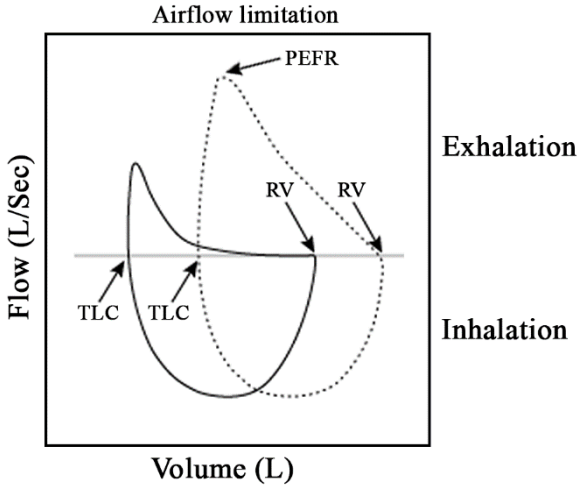

Figure V: Flow-volume loop. *An Example of asthmatic flow-volume loop (solid line) compared to healthy patients (dotted line) where a large drop in FEV_1 is seen while displaying a characteristic "downward scooping" expiratory curve. Increase in RV and TLC is also shown. This figure was modified from https://www.uptodate.com/contents/pulmonary-function-testing-in-asthma.*

1.3.4 Current therapies

There is currently no cure for asthma, and the principal goal of current therapies is to manage the disease by minimizing symptoms to improve quality of life [149]. The major classes of treatments target airway inflammation and ASM contractility (Table II). Despite the available treatments such as ICS and β_2-agonists, symptom control is complicated due to the heterogeneous nature of asthma, evident from nearly 20% of asthmatics that are either difficult to treat or have uncontrolled severe asthma [194-197]. A possible explanation was highlighted in a review by Hall *et al*, that the genes encoding major drug targets in asthma show a high degree of polymorphism within coding regions [198]. Poor adherence to asthma treatments may also contribute to increased asthma exacerbations [199].

Severe asthmatics are often refractory to ICS and are prescribed systemic corticosteroids (SCS) to control airway inflammation [197]. However, a recently published longitudinal observation study in the US evaluating the use of SCS in severe asthma patients showed increased cardiovascular and infection related complications [197]. These patients also had a significant increase in emergency room visits and health care costs associated with SCS related complications. The largest driver of cost associated with acute complications due to OCS were infections, while chronic complications were due to cardiovascular and metabolic related diseases.

Although much progress has been made in dissecting the heterogeneous nature of asthma and development of novel treatments for disease management, 5% to 10% of asthmatics in Canada are still unresponsive to currently available drugs [200]. Therefore, it is important to increase our understanding of the underlying molecular processes related to the pathobiology of asthma, which

will directly help develop effective and targeted treatments to control or reverse asthma pathogenesis.

Table II: Current therapies for asthma. *[149, 201-206].*

Drug class	Examples	Mechanism of Action
Short and long acting β-agonists (SABA and LABA)	Albuterl, Levalbuterol, Salmeterol, Formoterol	Activates β-2 adrenergic receptor resulting in ASM relaxation
ICS	Fluticasone propionate, Beclomethasone, Budesonide	Decreases transcription of inflammatory cytokines and chemokines while increasing anti-inflammatory cytokines and β2 adrenergic
Muscarinic receptor antagonists	Ipratropium, Tiotropium	Binds muscarinic receptors and prevents contraction of ASM
Leukotriene receptor agonists	Montelukast, Zafirlukast	Binds Cysteinyl leukotrienes receptor and prevents activation
Biologic therapies (IL-4, IL-5, IL-13 or IgE)	Omalizumab, Mepolizumab	Monoclonal antibodies against inflammatory mediators

1.5 Thesis overview

1.5.1 Study Rationale

Asthma is a chronic respiratory disease that affects more than 3 million people in Canada, with an annual economic burden of more than $CAD 2 billion [207]. Despite available treatments e.g. ICS and β2-agonists, approximately 20% are difficult to treat or have uncontrolled severe asthma, representing a major burden of asthma and associated healthcare costs [194-197, 208, 209]. SCS, often administered to severe asthmatics does increase susceptibility to infections which often results in exacerbation of asthma [197, 210]. These challenges highlight the need to develop new therapies for asthma with minimal side effects, and with potential to control severe disease without compromising the patients' ability to resolve infections.

CHDP are known to exert a wide range of immunity-related functions. IDR peptides, the synthetic derivatives of CHDP, are also potent immunomodulatory peptides that have been primarily optimized for applications in infectious disease with fewer studies examining its use in the context of inflammatory disorders. Limited studies have shown that a 12-amino acid IDR peptide derived from the bovine CHDP Bactenecin, IDR-1002, can reduce sterile ear inflammation in a murine model and in synovial fibroblasts [135, 138]. However, the use of IDR-1002 in airway inflammatory diseases such as asthma has not yet been explored. Therefore, in this thesis, I examine the effects of IDR-1002 in the context of allergic asthma.

1.5.2 General hypothesis

Administration of IDR-1002 will reduce allergen-induced airway inflammation, AHR, and specific pro-inflammatory cytokines *in vivo* in an acute house dust mite (HDM)-challenged murine model of allergic asthma and *in vitro* in AEC.

1.5.3 Specific aims

This thesis aims to (1) Characterize an acute HDM-challenge murine model of allergic asthma, (2) Investigate effects of IDR-1002 on allergic asthma pathobiology and the downstream molecular mechanisms involved in the HDM-challenged murine model and in AEC, and (3) Identify the critical amino acids within the sequence of IDR-1002 that are essential for biological activity.

Chapter 2: Materials and Methods

2.1 Peptide synthesis: IDR peptides (Table III) were manufactured by CPC Scientific (Sunnyvale, CA, USA). Peptides tagged with a proprietary quencher CPQ2 (N terminus), and fluorescent dye 5FAM (C terminus), were also obtained from CPC Scientific. Non-tagged IDR peptides were reconstituted in E-toxate water (Sigma, St. Louis, MO, USA) for *in vitro* assays. Tagged IDR peptides were reconstituted in dimethylsulfoxide (DMSO) (Sigma) in E-toxate water (Sigma) for a final concentration of 0.01% DMSO for *in vitro* cellular assays [211]. IDR peptides were reconstituted in physiological saline for *in vivo* murine model studies.

Table III: IDR peptide sequences.

Peptide ID	Sequence
IDR-1002	VQRWLIVWRIRK-NH2
IDR-1002:FRET	CPQ2-VQRWLIWRRIR-K(5FAM)-NH2
IDR-1002:5FAM	VQRWLIVWRIR-K(5FAM)-NH2
IDR-1002.1	VRRWLIVWRIRK-NH2
IDR-1002.2	VQRWLIVRRIRK-NH2
IDR-1002.2:FRET	CPQ2-VQRWLIVRRIR-K(5FAM)-NH2
IDR-1002.2:5FAM	VQRWLIVRRIRK-K(5FAM)-NH2
IDR-1002.3	VQRWLIVWVIRK-NH2
IDR-1002.4	VLRWLIVWRIRK-NH2
IDR-1002.5	VQRWLIVWRIWK-NH2
IDR-1002.6	VQRWLIVIRIRK-NH2

2.2 Murine models of allergic asthma and IL-33 challenge: (Figure VI). The murine model protocols used in this thesis were approved by the University of Manitoba Animal Care Ethics Board. Experimental design for the animal studies and reporting of data was compliant with the ARRIVE guidelines in the reporting of *in vivo* animal research [212]. Female BALB/c mice (6-7 weeks) were obtained from the Genetic Modeling of Disease Center at the University of Manitoba for Chapter 3.1 and 3.2, and Charles River Laboratories (Wilmington, MA, USA) for Chapter 3.3 and 3.4. Mice were housed at the central animal care facility at University of Manitoba. Animals,

upon arrival, were randomly sorted into maximum of five mice per cage by the animal care facility staff and acclimatized for a minimum of one week. Female BALB/c mice (7-8 weeks) were challenged with intranasal (i.n) administrations of 35µL (0.7µg/mL saline) of HDM protein extract (Greer laboratories, Wilmington, MA, USA), 5 times a week for two weeks. IDR-1002 (CPC Scientific) dissolved in saline was administered subcutaneously (s.c), 6 mg/Kg per mouse 3 days per week. Recombinant murine IL-33 (BioLegend, San Diego, CA, USA) dissolved in saline was administered i.n. where indicated, at a dose of 1µg/mouse, in the last 5 days in the HDM-challenged mice. In experiments with IL-33 challenge alone, recombinant murine IL-33 was administered i.n, at a dose of 1µg/mouse, for 5 consecutive days [213]. Mice were sedated using isoflurane prior to any i.n. instillation. HDM and IL-33 challenge, as well as peptide administrations were performed in the morning between 9 am and noon. Mice were visually monitored for grooming and activity levels every day. Mice were sacrificed and samples collected 24 hr after the last HDM-challenge, or after the last IL-33 challenge.

2.3 BALF cell differential assessment: Mice were anesthetized with sodium pentobarbital, tracheostomized, and lungs were washed with 1mL of cold saline twice for a total of 2mL. BALF obtained was centrifuged (150 RCF, 10 min) and cell differentials were assessed using a modified Wright-Giemsa staining (Hema 3® Stat Pack, Fisher Scientific, Hampton, NH, USA) using a Carl Zeiss Axio Lab A1 (Carl Zeiss, Oberkochen, Germany) microscope for imaging. Cell differentials were counted blinded by two different personnel in 8-10 image frames at 20X magnification per slide.

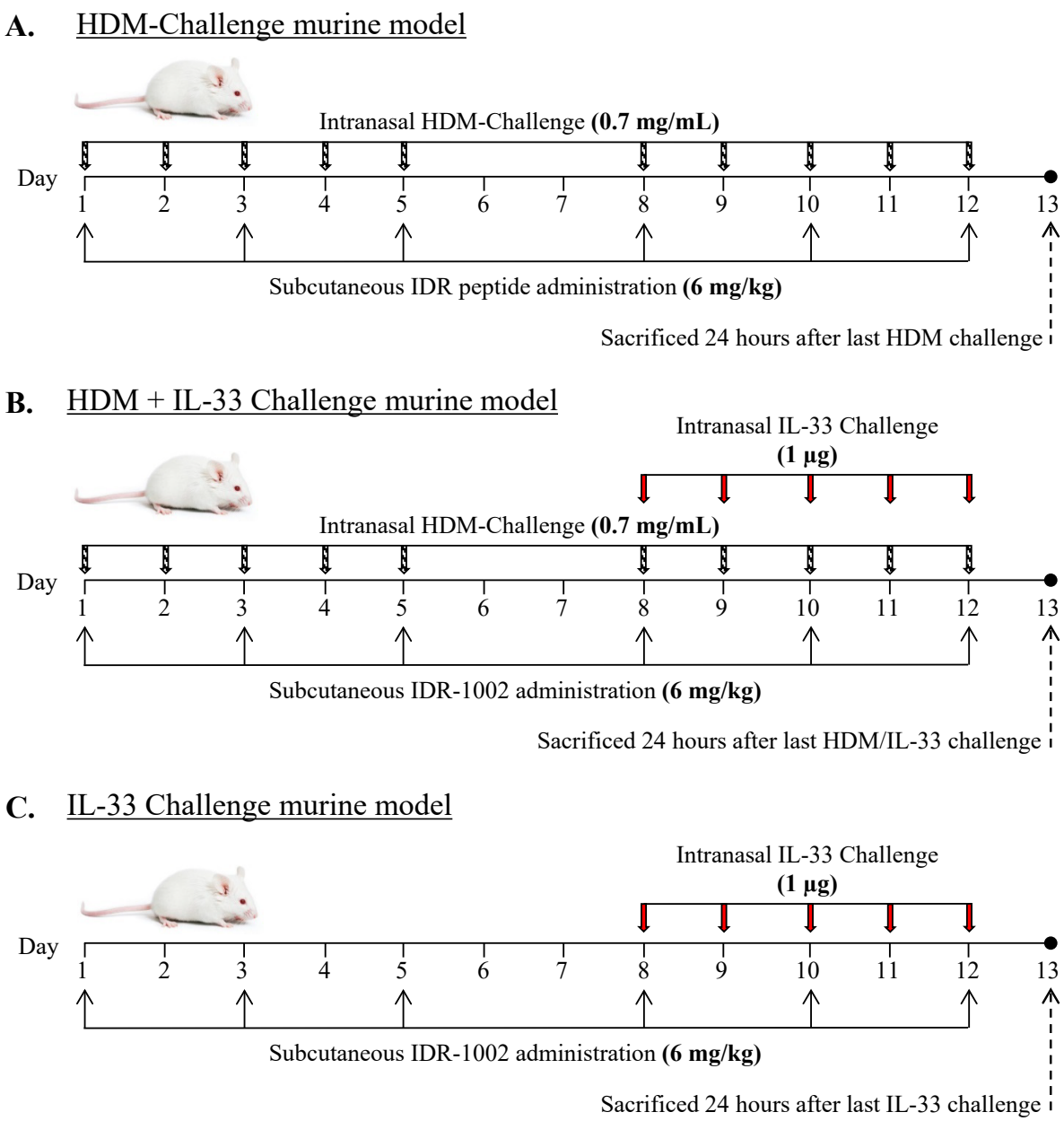

Figure VI: Murine models. *Female BALB/c mice, 7-8 weeks of age (**A**) HDM model; Mice were challenged with 35 µl of whole HDM extract (0.7 mg/mL) in saline i.n., for 2 weeks. IDR-1002 was administered s.c. (6 mg/kg) 3 times a week. **(B)** HDM + IL-33 co-challenge model; Mice were challenged with 35 µl of whole HDM extract (0.7 mg/mL) in saline i.n., for 2 weeks. 1 µg of IL-33 was administered i.n. on days 8-12. IDR-1002 was administered s.c. 3 times a week at 6 mg/kg. (**C**) IL-33 model; Mice received IDR-1002 administered s.c. (6 mg/kg) 3 times a week for 2 weeks, recombinant IL-33 (1 µg per mouse) was administered i.n. on days 8-12.*

2.4 AHR measurements: Mice were anesthetized with sodium pentobarbital, tracheostomized and lung function was measured using a *flexi*Vent™ small animal ventilator (SCIREQ Inc, Montreal, QC, Canada) for quantitative assessment of airway constriction and stiffness of the lung, as previously described [214, 215]. Briefly, high frequency forced oscillation with positive end-expiratory pressure of 3 cmH_2O to assess Newtonian resistance (Rn) to monitor central airway constriction, tissue damping (G) as an index of alveolar tissue restriction, and tissue elastance (H) to determine alveolar tissue stiffness were used. A muscle paralytic agent was not used in this method. Data were collected using flexiWare Software and transferred to Microsoft Excel and GraphPad Prism software for further analysis. Changes in Rn, G and H were monitored in response to nebulized saline (baseline measures), followed by increasing concentrations of nebulized methacholine (3-50mg/mL), using Quick Prime-3 and Snapshot perturbations. Provocative concentration (PC)100 and 50 were calculated by multiplying baseline Rn values by 2 or 1.5 respectively and employed TREND function on Microsoft Excel.

2.5 Histology: As previously described [214, 216], lungs were inflated in situ through a tracheal cannula with ~1ml (20 cmH_2O) of 10% v/v formalin and the trachea were sealed. Whole lungs were removed, transferred into formalin for 24 hours (room temperature) and subsequently transferred into phosphate-buffered saline (PBS) (Thermo Scientific, Waltham, MA, USA). Whole lungs were dehydrated using ethanol and xylene, embedded in paraffin and 6 μm sections were obtained. Paraffin-embedded lung sections (6μm) were stained with Hematoxylin and Eosin (H&E) to enumerate inflammatory cell accumulation and epithelial thickening. Using the Carl Zeiss Zen software, basement membrane of airways was outlined and area inside the contoured space (A μm^2) and perimeter of the outline was measured. A second contour was drawn around the outer edge of the epithelium and area inside was recorded as airway space (B μm^2). The

difference between the two areas (A-B μm^2) and length of basement membrane (perimeter μm) was determined as mean epithelial thickness (μm) per 1 μm of basement membrane. Periodic acid schiff (PAS) stain was used to assess airway epithelial goblet cell abundance. Trichrome and picrosirius red staining were used to assess collagen deposition. A Carl Zeiss Axio Lab.A1 microscope was used for imaging along with Zen software for analysis. Histological assessment was performed blinded by two different personnel.

2.6 Detection of total and HDM-specific antibodies: Serum concentrations of total IgE and IgG were assessed by Ready-Set-Go® kits (eBioscience, Santa Clara, CA, USA) as per the manufacturer's instructions. Serum samples were diluted 1:50 for total IgE and 1:50,000 for total IgG, in PBS containing 1% Bovine serum albumin (BSA) (w/v). An indirect enzyme-linked immunosorbent assay (ELISA) method was used to assess the HDM-specific IgE and IgG1 levels in serum samples. Briefly, 100 μl per well of 10 μg/ml of HDM extract (Greer laboratories) in PBS was used to coat Costar™ 96-well flat-well high-binding plates (Thermo Scientific) overnight at 4°C. The plates were blocked with 3% BSA (w/v) in PBS overnight at 4°C. Serum samples used for detection of HDM-specific IgE were precleared by incubating 1:1 with Protein G Sepharose beads (Amersham, Little Chalfont, UK) overnight at 4°C. Serum samples (50 μl per well) were incubated overnight at 4°C. Biotin conjugated goat anti-mouse IgE or goat anti-mouse IgG1 (Southern Biotech, Birmingham, AL, USA) were used as secondary detection antibodies (1:5000 dilution in PBS containing 1% BSA). Avidin-horseradish peroxidase (HRP) (eBioscience) and 3,3',5,5'-tetramethylbenzidine (TMB) (Thermo Scientific) were used to yield a colorimetric reaction. Reaction was stopped with 2N H_2SO_4, and absorbance recorded using a BioTek Synergy 4 Microplate reader.

2.7 Gene expression profiling using a qPCR array: Lung tissues collected from naïve and HDM-challenged mice, 24 hr after the final HDM-challenge, were homogenized in RNA lysis buffer using the LabGEN 125 homogenizer (Cole-Parmer, Vernon Hills, IL, USA). Total ribonucleic acid (RNA) was isolated using the RNeasy kit (Qiagen, Hilden, Germany). A quantitative polymerase chair reaction (qPCR) Array (RT^2 Profiler™) (Qiagen) was employed using ABI 7300 Quantitative Real time PCR system to profile the expression of 84 targeted genes related to in allergy and asthma (RT^2 Profiler™ PCR Array Mouse Allergy & Asthma, Catalog No. PAMM-067ZA), as specified by the manufacturer. Data quality control and analyses to calculate fold changes were performed using the PCR Array data analysis software as per the manufacturer's instructions. Briefly, data analysis was based on the $\Delta\Delta C_T$ method with normalization using three housekeeping genes (β-actin, β-glucuronidase and Hsp90ab1). Network and pathway analyses were performed using the Ingenuity® Pathway analysis (IPA) tool (Qiagen).

2.8 Assessment of cytokine levels: Serum, BALF and lung tissue lysates were monitored for the production of a panel of murine cytokines and chemokines. Bottom right lobe of murine lungs were collected in Total Protein Extraction Reagent T-Per (Thermo Scientific) containing protease inhibitor cocktail (Sigma) and homogenized on ice using the LabGEN 125 homogenizer (Cole-Parmer). Lungs were collected after AHR assessment and BALF collection. Homogenates were centrifuged at 10,000xg to obtain tissue lysates. Total protein concentration was determined using a bicinchoninic acid (BCA) assay (Thermo Scientific). Production of a panel of cytokines (IFNγ, IL-10, IL-12p70, IL-15, IL-16, IL-17A, IL-17A/F, IL-17C, IL-17E/IL-25, IL-17F, IL-1β, IL-2, IL-21, IL-22, IL-23, IL-27p28/IL-30, IL-31, IL-33, IL-4, IL-5, IL-6, IL-9, IP-10, KC/GRO, MCP1, MIP1α, MIP2, MIP3α, TNF) was monitored using V-PLEX mouse cytokine mesoscale discovery (MSD) assays, according to manufacturer's instructions. Cytokines IL-33, IL-25, TSLP,

macrophage-derived chemokine (MDC) and thymus and activation regulated chemokine (TARC) were measured by individual ELISA assays (R&D Systems, Minneapolis, MN, USA). Serum and BALF samples were diluted 1:2 for MSD analysis. BALF samples were used undiluted for ELISA. Lung tissue samples were normalized to 50 mg of total protein for cytokine evaluation. Secretion of MCP1, IL-1RA, and stanniocalcin (STC)1 was evaluated in supernatants collected from human bronchial epithelial cells (HBEC)-3KT cells were stimulated ± IDR peptides for 24 hr using specific sandwich ELISA assays (R&D Systems) according to the manufacture instructions.

2.9 Cell culture: Human PBEC were isolated from resected lung tissue from four anonymized donors (n=4) undergoing surgery at the Leiden University Medical Center, and cultured as previously described [217]. Demographics of the donors are shown in Table IV. Briefly, bronchial rings were enzymatically digested with 1X Proteinase XIV (Sigma) at 37ºC. Epithelial cells isolated were cultured in keratinocyte serum-free medium (KSFM) (Gibco) supplemented with epithelial growth factor, bovine pituitary extract and isoproterenol, and an antibiotic mix containing penicillin, streptomycin and ciprofloxacin until ~90% confluent. Cells were trypsinized and stored in liquid nitrogen until further use. Cells were seeded at a density of 5000 cells/cm^2 in tissue culture plates pre-coated with 30µg/mL PureCol (Advanced BioMatrix, CA, USA), 10µg/mL fibronectin (Sanbio, NLD) and 10µg/mL BSA (Sigma) containing 1:1 mixture of Dulbecco's modified Eagle's medium (Gibco) and bronchial epithelial growth medium (Sanbio, NLD), supplemented with 1mg/mL BSA (Sigma), 15ng/mL retinoic acid (Tocris, UK) and 100µg/mL penicillin/streptomycin (Lonza). Cells were cultured until ~80% confluent, and medium replaced every 48 hr.

HBEC-3KT cell line (ATCC® CRL-4051™, Manassas, VA, USA) was grown according to manufacture specifications. Briefly, cells were plated in airway epithelial cell basal medium (ATCC PCS-300-030) supplemented with bronchial epithelial cell growth kit (ATCC PCS-300-040) and incubated at 37^0C at 5% CO_2. Cells were growth factor starved for 24 hr prior to stimulation. Cells were cultured to a maximum confluency of 80%.

PBEC and HBEC-3KT cells were starved in medium with no growth factors for 24 hr before stimulation. IDR peptides were added 30 min prior to stimulation with 20 ng/mL TNF (PeproTech, NJ, USA) and/or 30 ng/mL IFNγ (R&D Systems, MN, USA). Cell lysates were collected to assess protein abundance by Western blots after 24 hr stimulation.

Table IV: Demographics of donors of human PBEC used in this study.

Donor #	Sex	Age	Height	Weight	BMI	Current smoker	Ex-Smoker	Oral Steroids	Inhaled Steroids
BR384	Female	55	168	90	31.9	No	Yes	Yes	No
BR390	Female	68	162	61	23.24	No	Yes	No	No
BR421	Male	56	181	83	25.3	No	Yes	unknown	unknown
BR448	Male	74	160	68	27	No	No	No	No

2.10 Western Blots: Human PBEC and HBEC-3KT cells were scraped, collected in PBS containing protease inhibitor cocktail (PIC) (Cell Signaling, Danvers, MA, USA), and centrifuged at 300xg for 7 min. The cell pellets were lysed in PBS containing PIC and 0.5% NP40 (Sigma). Samples were subjected to one freeze thaw cycle prior to centrifuging at 10,000xg for 10 min to obtain cell-free lysates. Total protein concentration was determined using a microBCA assay (Thermo Scientific). Protein was extracted and quantified from murine lung tissue lysates as described above. Equal amounts of protein were resolved on 4–20% Mini-PROTEAN TGX Precast Protein gels (Bio-Rad, Hercules, CA, USA) or 4-12% Bis-Tris Protein gels (Invitrogen,

Carlsbad, CA, USA), followed by transfer to nitrocellulose membranes (Burlington, Millipore, MA, USA). Membranes were blocked with TBST (20mM Tris–HCl pH 7·5, 150mM NaCl, 0·1% Tween-20) containing 5% milk powder. The membranes were probed with antibodies for IL-33, STAT4, STAT6, HMGB1 and CARM1 (Abcam, Cambridge, UK), IRF1 (Cell Signaling), IP10 (Cell Signaling), and β-Actin (Cell Signaling), in TBST containing 2.5% w/v milk powder. Affinity purified HRP-linked secondary antibodies (Cell Signaling) were used for detection. Membranes were developed using Pico and Femto Electrochemiluminescence detection system (Thermo Scientific) or Amersham Electrochemiluminescence Prime (GE Healthcare, Chicago, IL, USA) according to the manufacturer's instructions. Densitometry for band intensity was determined using an Bio-Rad ChemiDoc or Alpha Innotech Imager (San Leandro, CA, USA) with ImageLab or AlphaView software respectively.

2.11 RNA sequencing: Total RNA was extracted from the bottom left lobe of lungs preserved in RNALater using the RNeasy Plus Mini kit (Qiagen) following the manufacturer's protocol. Quantification and quality assessment of total RNA was performed using an Agilent 2100 Bioanalyzer (Santa Clara, CA, USA), and only samples with RNA integrity number greater than 8 were used for mRNA enrichment with the poly(dT) beads (NEB; Ipswich, MA, USA). Strand-specific cDNA libraries were generated from poly-adenylated RNA using the KAPA Stranded RNA-Seq Library Preparation Kit (Roche, Basel, Switzerland). After 3′-adenylation, adapters (Bio Scientific, Austin, TX, USA) for multiplexing were ligated, followed by amplification and then purification using Agencourt Ampure XP beads (Beckman Coulter, Brea, CA, USA). The quality of the library was checked using a high-sensitivity Deoxyribonucleic Acid (DNA) chip (Agilent) on an Agilent 2100 Bioanalyzer. All cDNA libraries were prepared at the same time and all sequenced on a HiSeq 2500 high output run.

After demultiplexing, FASTQ sequence quality was assessed using FastQC v0.11.6 and MultiQC v1.6. The FASTQ sequence reads were aligned to the Ensembl murine reference genome GRCm38 (build 91) using STAR v2.5.4b and mapped to Ensembl release 91 transcripts. Read-counts were generated using htseq-count (HTSeq v0.9.1). All data processing and subsequent differential gene expression analyses were performed using R version v3.4.4 and DESeq2 v1.18.1 [218]. Differentially expressed genes were identified with the Wald statistics test and filtering for any genes that showed 2-fold change and adjusted p-value < 0.05 (cut-off at 5% FDR) as the threshold. Functional discovery of pathway enrichment, network analyses and transcription factor site binding (TFBS) analysis was performed using IPA, and InnateDB [219].

2.12 Peptide retention time: Agilent 1100 series HPLC system with UV detection at 214 nm and manual 50 µL injector was employed to determine the retention time of peptides using C18 reverse-phase High Performance Liquid Chromatography (HPLC) column. Peptides (2µg each) were injected in to the Luna C18(2) 5 µm, Phenomenex (Torrance, CA, USA), 1x100 mm column and separated using binary 2% water:acetonitrile gradient per minute (0.1% trifluoroacetic acid as ion-pairing modifier) at a flow rate of 0.2 mL/min.

2.13 *In silico* determination of secondary structures and hydrophobicity index: The *in silico* predictions of the secondary structures were performed using PEP-FOLD services (http://bioserv.rpbs.univ-paris-diderot.fr/services/PEP-FOLD/). PEP-FOLD is a *de novo* approach (on-line version) available for external users for predicting structural characteristics/secondary structures of peptides or protein fragments from amino acid sequences [220, 221]. The hydrophobicity index (HI) for the peptides was determined using Sequence Specific Retention Calculator (SSRCalc), (http://hs2.proteome.ca/SSRCalc/SSRCalcQ.html; Version Q point oh©2015 MB Centre for Proteomics & Systems Biology [222]).

2.14 Cytotoxicity assay: Lactate dehydrogenase (LDH) release assay was performed to assess cytotoxicity using a commercially available kit (Roche, Basel, Switzerland) according to manufacture specifications. Briefly 2% triton X100 (Sigma) was added to a well containing HBEC-3KT cells and incubated at 37^0C for 30 min (as 100% lysis positive control). Media alone, without any cells, incubated at 37^0C was used as negative control. 50uL of supernatant from positive/negative control and from wells stimulated with IDR peptides were collected and transferred to a 96-well plate (Corning Inc. Corning, NY, USA) in triplicates. 50uL of cytotoxicity substrate mix were added to each well and incubated at room temperature for 30 min. Plates were read at 490nm and % cytotoxicity was calculated based on positive control at 100%.

2.15 Florescence resonance energy transfer (FRET) assay: IDR-1002 and IDR-1002.2(W8/R) FRET peptides (Table. III) were added at 10uM into 24-well plates containing either media only or HBEC-3KT cells. Fluorescence measurements (492/518nm) were taken every 10 min for total of 16 hr using the BioTek synergy 4 plate reader (Winooski, VE, USA). 1:50 ratio of Trypsin (Promega, Madison, WI, USA) was added to peptides in PBS to determine 100% degradation.

2.16 Live cell Imaging: HBEC-3KT cells were plated on chamber slides (Nunc, Roskilde, Denmark) and stimulated with 5FAM-tagged IDR-1002 or IDR-1002.2(W8/R). Zeiss Observer.Z1 microscope with Zeiss ZEN software was used to capture 12 hr post exposure. 1:50 ratio of Trypsin (Promega) was added to peptides and neutralized with soy bean trypsin inhibitor as negative control.

2.17 Kinome analysis: Kinome peptide array analysis was performed as previously described [223, 224]. Briefly, three independent replicates of HBEC-3KT cells in the presence or absence of peptide simulation, either IDR-1002 or IDR-1002.2(W8/R) were lysed after 15 min

using cell lysis buffer (Cell signalling) containing phenylmethylsulfonyl fluoride and PIC. Total protein concentration was determined using microBCA assay (Thermo Scientific). Activation mix (50% glycerol, 50 μM ATP, 60 mM MgCl2, 0.05% Brij 35, 0.25 mg/mL bovine serum albumin) was added to the equivalent amounts of total protein (150 μg) for each sample, and total sample volumes were matched by the addition of kinome lysis buffer. Each sample was spotted onto a kinome peptide array (JPT Peptide Technologies GmbH, Berlin, Germany) and incubated for 2 hr at 37°C at 5% CO_2. Following incubation, arrays were washed once with PBS containing 1% Triton X-100, followed by a single wash in deionized H_2O. Arrays were stained with PRO-Q Diamond phosphoprotein stain (Invitrogen) for 1 hr with gentle agitation. Arrays were subsequently destained (20% acetonitrile, 50 mM sodium acetate, pH 4.0) 3 times, 10 min each with the addition of fresh destain each time. A final 10 min wash was performed with deionized H2O. Arrays were dried by gentle centrifugation. Array images were acquired using a PowerScanner microarray scanner (Tecan, Morrisville, NC, USA) with a 580-nm filter to detect dye fluorescence. Signal intensity values were collected using Array-Pro Analyzer version 6.3 software (Media Cybernetics, Rockville, MD, USA). Background corrected values above were transformed to log2 scale for differential analysis using Welch's T-test.

2.18 Statistical analyses: Specific statistical analysis used are detailed in each figure legend. Briefly, two-way repeated measures ANOVA with Tukey's multiple comparisons test was used to compare the means between multiple groups for lung function analyses to examine changes in Newtonian resistance (Rn), tissue damping (G) and tissue elastance (H) with increasing concentrations of methacholine. Mann-Whitney U test was used to compare provocative concentration (PC)50 or PC100 values between the HDM-treated and naïve groups, and between HDM-treated mice and HDM-challenged mice treated with IDR-1002. In animal studies, for

immune cell accumulation, cytokine levels and goblet cell counts, one-way ANOVA with Tukey's and Dunnett's multiple comparisons test was used for statistical analyses. Repeated measures one-way ANOVA with Fisher's Least Significant Difference was used for statistical analysis of western blot densitometry for IL-33, IP10 and IRF1 using human PBEC. One-way ANOVA with Dunnett's and Tukey multiple corrections was used for ELISA and MSD assay. One-way repeated measured ANOVA with Tukey's multiple comparisons test was used to compare differences in peptide stability over time. Welch's t-test was used to analyze kinome array results. GraphPad PRISM 6 and R was used for statistical analyses. Differences at a value of $p<0.05$ or $p<0.01$ were considered to be statistically significant.

Chapter 3: Results

3.1 HDM-challenged murine model of allergic asthma induces airway inflammation and AHR

This section contains text and figures from a collaborative work published as an original article in *Biology Open* 2016. 5(2): p. 112-21. **Hadeesha Piyadasa**, Anthony Altieri, Sujata Basu, Jacquie Schwartz, Andrew J. Halayko, Neeloffer Mookherjee.

H.P. performed large portion of the animal experiments and most of the data analyses, contributed to the development of the scientific concepts and wrote the text. A.A. performed the quantitative real-time PCR assay. S.B. performed the lung function measurements. J.S. was involved in the histological assessment. A.J.H. provided significant intellectual input in the development of this study and edited the text. N.M. conceived and directly supervised the study, performed the bioinformatics analyses and edited the text.

3.1.1 Abstract

Background: HDM-challenge is commonly used in murine models of allergic asthma for preclinical pathophysiological studies. However, few studies define objective readouts or biomarkers in this model.

Objective: To characterise immune responses and define molecular markers of AHR and airway inflammation induced by repeated HDM-challenge.

Methods: BALB/c mice were challenged with HDM for two weeks. Lung function analysis was performed with increasing dose of methacholine by *flexi*Vent™ small animal ventilator, cell differentials in bronchoalveolar lavage performed by modified Wright-Giemsa staining, and

cytokines monitored by MSD assay. Differential gene expression was detected in lung tissues by quantitative real-time PCR array from SA Biosciences.

Results: I demonstrated using kinetic studies that 24 hr after last HDM-challenge results in significant AHR along with eosinophil accumulation in the lungs. Histologic assessment of lung revealed increase in epithelial thickness and goblet cell hyperplasia, in the absence of airway wall collagen deposition, suggesting ongoing tissue repair concomitant with acute allergic lung inflammation. These results suggest that the two week HDM-challenge acute model may be suitable to delineate airway inflammation processes that precede airway remodeling and development of fixed airway obstruction. I further demonstrated that a panel of inflammatory cytokines e.g. IFNγ, IL-1β, IL-4, IL-5, IL-6, KC, TNF, IL-13, IL-33, MDC and TARC are elevated in lung tissue and bronchoalveolar fluid, indicating local lung inflammation, after two weeks of HDM challenge. However, levels of these cytokines remain unchanged in serum, reflecting lack of systemic inflammation in this model. Based on these findings, I further monitored the expression of 84 selected genes in lung tissues by quantitative real-time PCR array, and identified 31 mRNAs that were significantly up-regulated and non downregulated >2 fold in lung tissue from HDM-challenged mice. These include genes associated with human asthma (e.g. *Clca3*, *Ear11*, *Il-13, Il-13ra2, Il-10, Il-21*, *Arg1* and *Chia1*) and leukocyte recruitment in the lungs (e.g. *Ccl11, Ccl12* and *Ccl24*).

Conclusion: This chapter describes a biosignature to enable broad and systematic interrogation of molecular mechanisms and intervention strategies for airway inflammation pertinent to allergic asthma, in an allergen-challenged murine model that precedes and possibly potentiates airway remodeling and fibrosis.

3.1.2 Rationale and Introduction

Allergic asthma as described in detail in chapter 1.3, is a common chronic inflammatory lung disease, affecting nearly 300 million people worldwide, with significant health, health service and economic burden (www.publichealth.gc.ca). Animal models of human asthma have not been extensively characterized using a systems biology approach, which has created a knowledge gap that has greatly limited success in promoting development of new therapies.

HDM, *Dermatophagoides sp*., is associated with allergic response in up to 85% of asthma patients worldwide [225, 226]. Thus, HDM-challenged murine models have been used to dissect different aspects of the pathogenesis and to define some of the molecular mechanisms that may be important in the disease process of allergic asthma [227]. These models involve the sensitization of the animal to HDM by repeated i.n. challenge which results in a Th2-polarized bronchial inflammation, airway remodeling and epithelial damage similar to that seen in human asthma [228-230]. The advantage of this model, in contrast to the commonly used ovalbumin-exposure murine models, is that HDM is a natural inhaled antigen and repeated exposure to HDM is not associated with the development of tolerance [229]. Previous studies have shown that repeated HDM exposure of 2 to 3 weeks, considered to be acute exposure, induces markedly mixed (eosinophilic and neutrophilic) airway inflammation and AHR to methacholine challenge [229]. Whereas mice subjected to repeated HDM exposure for 5 to 8 weeks (the chronic HDM-challenge model) results in airway inflammation along with significant airway wall remodeling, including airway smooth muscle, epithelial and goblet cell hyperplasia, accumulation of collagen, fibronectin and other extracellular matrix proteins that manifest as airway wall fibrosis and thickening [231].

A major challenge in using the HDM-challenged murine model is that the immune responses and physiological outcomes vary depending on the sensitization protocol and the time point at which the animals are sacrificed after the last HDM-challenge. For example, neutrophils are detected relatively early [232, 233] with peak numbers evident in the BALF 6-12 hr post HDM exposure [234]. In contrast, peak numbers of lung eosinophils occurs beyond 24 hr and observed at 48 hr after last HDM challenge [234]. Moreover, studies that use systematic appraisal of how individual pathways, biological mediators and cells contribute in an integrated manner to specific aspects of the disease phenotype are lacking. Despite the use of the HDM-challenge in mice as a preclinical model for asthma, very few studies have comprehensively characterized the immune responses and identified specific biomarkers that can be objectively used to monitor disease progression or predict responses to candidate therapeutics [235, 236].

In this study, I used the acute (2-week) HDM-challenge model murine model to characterize changes in the expression of 84 genes associated with allergy and asthma, using a qPCR array. I also employed a multiplex cytokine profiling platform to define specific cytokine responses in the lung tissues, BALF and serum, in the HDM-challenged mice. I analyzed the data in the context of my observations that AHR develops only after an initial burst of inflammation (up to 8 hr). Thus, I focused on examining the physiological outcomes and defining a biosignature of transcripts 24 hr after the last HDM-challenge, a time point between peak neutrophilic and eosinophilic inflammation. The acute model of HDM-challenge described in this study generated airway inflammation and AHR, preceding airway remodeling and fibrosis. Therefore, I speculate that the panel of quantitated protein and mRNA endpoints described in this study will be surrogates for the human disease, and can be used to interrogate molecular mechanisms and intervention strategies in airway inflammation that precedes and possibly potentiates airway remodeling and fibrosis.

3.1.3 Results

3.1.3.1 Kinetics of cellular accumulation in the BALF following HDM-challenge: To assess the kinetics of lung inflammation, BALF samples collected 8, 24, 48 and 72 hr after the last HDM-challenge were used for cell differential analyses. Peak neutrophil accumulation was at 8 hr after the last HDM-challenge, which subsequently rapidly declined (Figure 1.1A). However, eosinophil and macrophage accumulation was observed beyond 8 hr, and steadily increased peaking at 48 hr after the last HDM-challenge (Figure 1.1A). There was a steady increase of total lymphocyte population beyond 8 hr to 48 hr after last HDM-challenge (Figure 1.1A). All the cell types significantly increased in the BALF 24 hr after the last HDM-challenge, in the HDM-challenged mice compared to allergen-naïve mice (Figure 1.1B).

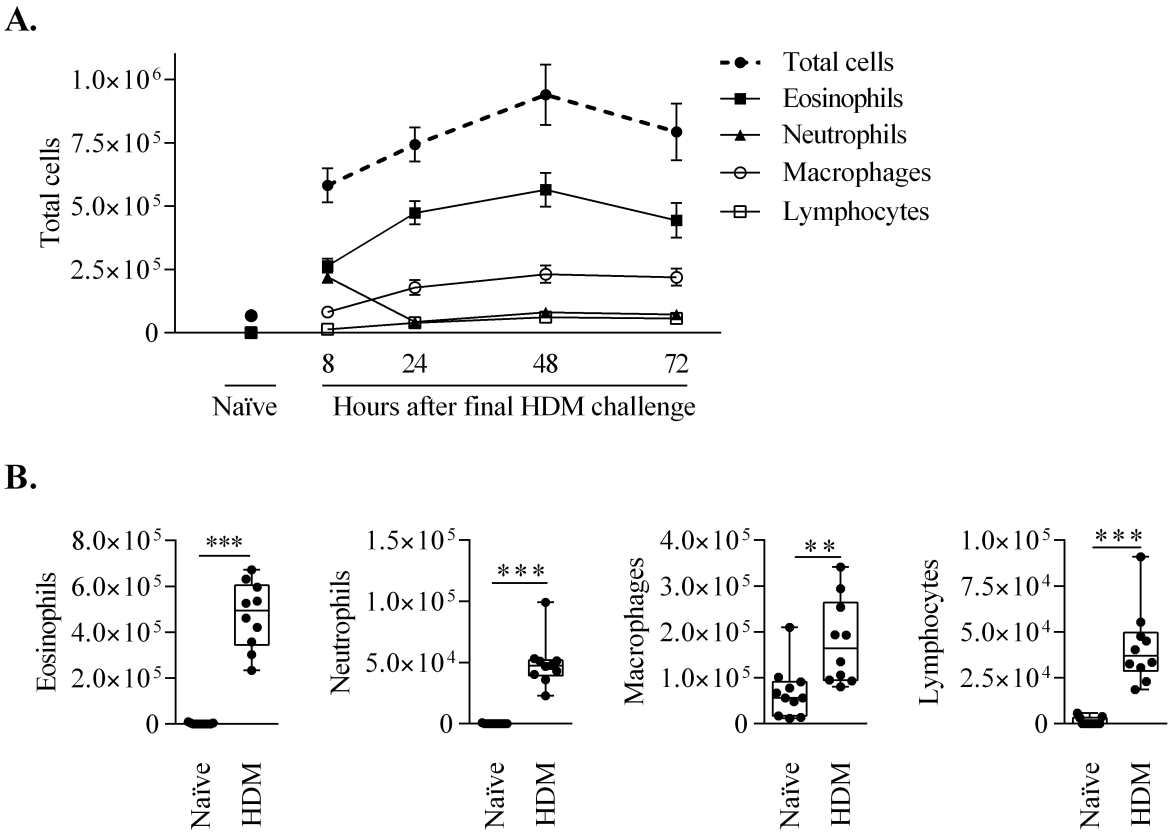

Figure 1.1: HDM-challenge increases immune cell accumulation to lungs. *Mice (n = 10 per group) were challenged by i.n. administration of whole HDM extract in saline, for 2 weeks (Figure VI). BALF was collected 8, 24, 48 and 72 hr after last HDM-challenge, and the supernatant and cell fractions were separated by cytospin. Individual cell populations were normalized to 1mL of BALF. (A) Kinetics of accumulation of eosinophil, neutrophil, macrophage and lymphocyte population in the BALF. (B) Individual cell populations in BALF assessed 24 hr after last HDM-challenge. Mann-Whitney U test was used to assess statistical significance (*p ≤ 0.05, **p ≤ 0.01, ***p ≤ 0.001). Error bar shown represent standard error of mean (SEM).*

3.1.3.2 HDM-challenged mice exhibit AHR: Previous studies show that HDM-challenge significantly induces AHR using various HDM-sensitization protocols and monitored at various time points [237-239]. In this study, I monitored lung function at 8 and 24 hr after last HDM-challenge to confirm that the sensitization protocol induced AHR in the specified 2-week acute model. To that end, lung function was measured using the *flexi*Vent™ small animal ventilator in response to increasing dose of inhaled methacholine (0 to 50 mg/mL). HDM-challenge results in a significant increase in maximum Newtonian resistance (Figure 1.2A), tissue damping (Figure 1.2B) and tissue elastance (Figure 1.2C) at 24 hr after the last HDM-challenge compared to allergen-naïve mice. These responses though significant are not robust when measured 8 hr after last HDM-challenge (Supplementary Figure 1.1). Furthermore, hypersensitivity to inhaled methacholine is elevated for Newtonian resistance after HDM-challenge, as shown by a significantly reduction in methacholine required to double the baseline resistance (PC100), 24 hr after the last HDM-challenge (Figure 1.2D).

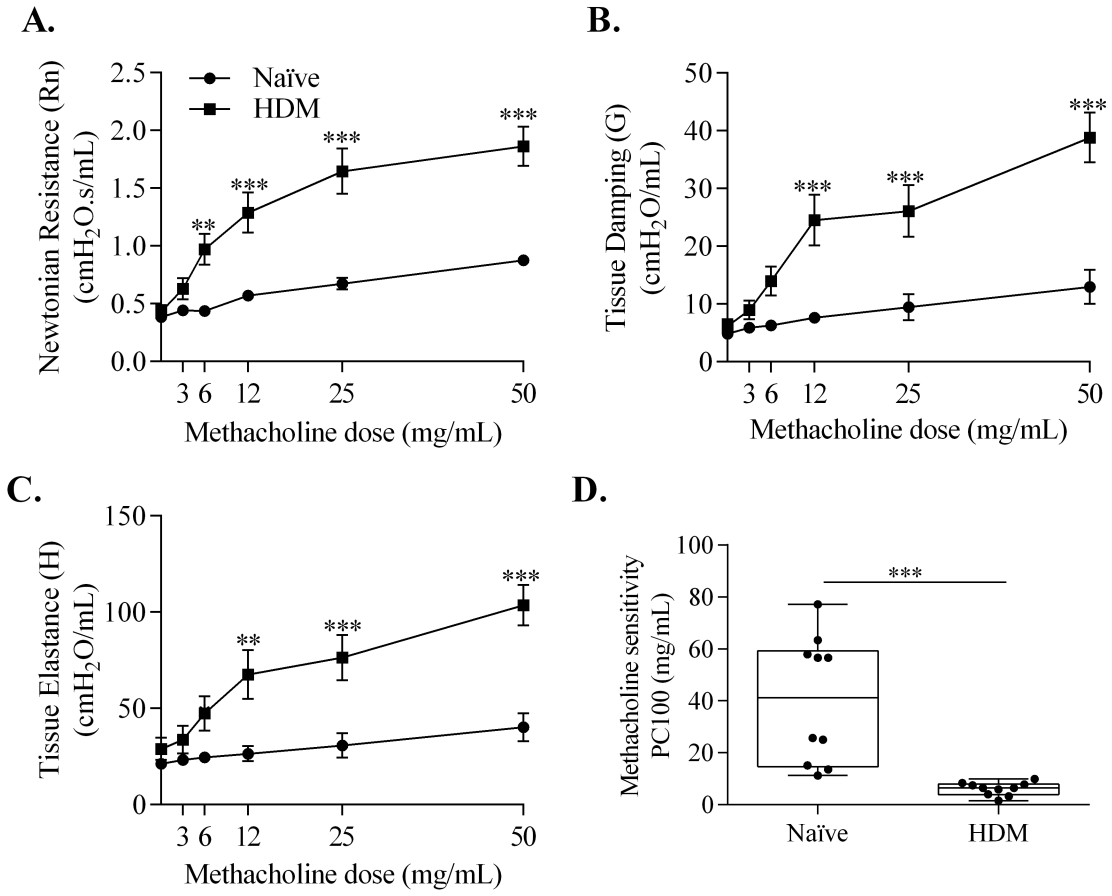

Figure 1.2: HDM-challenge increases AHR. *Mice were challenged by i.n. administration of whole HDM extract in saline, for 2 weeks (Figure VI). Lung mechanics of naïve (n=10) and HDM-challenged (n=10) were monitored, 24 hr after the last HDM-challenge. Baseline airway and tissue damping and tissue elastance was calculated using saline. Mice were exposed to increasing dose of methacholine (3-50 mg/mL) and the change in* ***(A)*** *Newtonian resistance,* ***(B)*** *tissue damping and* ***(C)*** *tissue elastance was monitored.* ***(D)*** *Central airway sensitivity to methacholine was measured by calculating concentration of methacholine required to double baseline Newtonian resistance (PC100). Mann-Whitney U test was used for statistical analyses (*$p \leq 0.05$, **$p \leq 0.01$, ***$p \leq 0.001$). Error bar shown represent SEM.*

3.1.3.3 Two weeks of HDM-challenge results in early signs of airway tissue remodeling, without collagen deposition: To correlate changes in lung inflammation (Figure 1.1) and lung function (Figure 1.2) with the status of tissue repair, I performed complementary assessment of cell accumulation into tissues surrounding the airways using histology. Consistent with the cell differential (Figure 1.1B), H&E staining of the lung sections of HDM-challenged mice showed significant cellular accumulation to the peribronchial and perivascular area. Semi-quantitative analysis showed that there was significant increase in epithelial thickness in the HDM-challenge compared to allergen-naïve mice (Figure 1.3A). PAS stain showed HDM-challenge significantly increases the number of goblet cells compared to the allergen-naïve mice (Figure 1.3B). Finally, to determine whether the HDM-challenge protocol induced structural airway remodeling, I performed picrosirius staining to assess collagen deposition, which is a hallmark of airway remodeling in asthma [240]. Picrosirius staining revealed that there was no marked change in collagen deposition and evidence of subepithelial fibrosis after two week of HDM-challenge (Figure 1.3C and 1.3D).

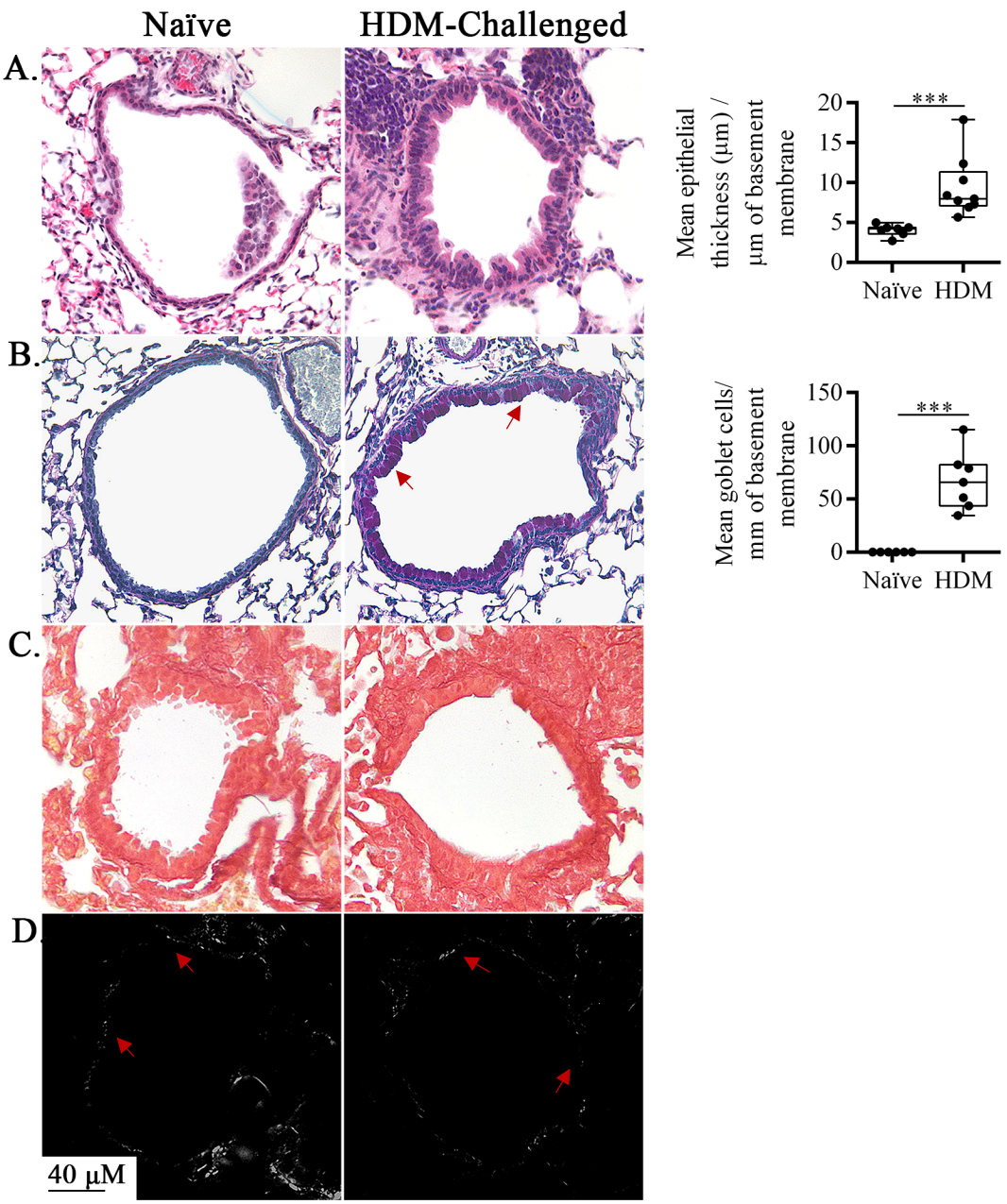

Figure 1.3: Histological assessment of lung sections. *Mice (n = 10 per group) were challenged by i.n. administration of whole HDM extract in saline, for 2 weeks (Figure VI). Paraffin embedded lung sections (6 µm) were stained with* ***(A)*** *hematoxylin and eosin (H&E) to enumerate cell accumulation and epithelial thickening,* ***(B)*** *PAS to assess goblet cells, in HDM-challenged compared to allergen-naïve mice. Picrosirius Red stain was used to enumerate collagen deposition viewed using* ***(C)*** *bright or* ***(D)*** *polarized contrast, in light microscopy. Mann-Whitney U test was used for statistical analyses (*p ≤ 0.05, **p ≤ 0.01, ***p ≤ 0.001). Error bar shown represent SEM.*

3.1.3.4 Serum levels of total and HDM-specific IgE and IgG are significantly elevated in the HDM-challenged mice: Allergen specific antibodies are a hallmark of allergic asthma [241]. HDM-challenged mice showed significantly higher serum levels of total IgE (Figure 1.4A) and IgG (Figure 1.4B), as well as HDM-specific IgE (Figure 1.4C) and IgG1 (Figure 1.4D), compared to allergen-naïve mice consistent with literature [242].

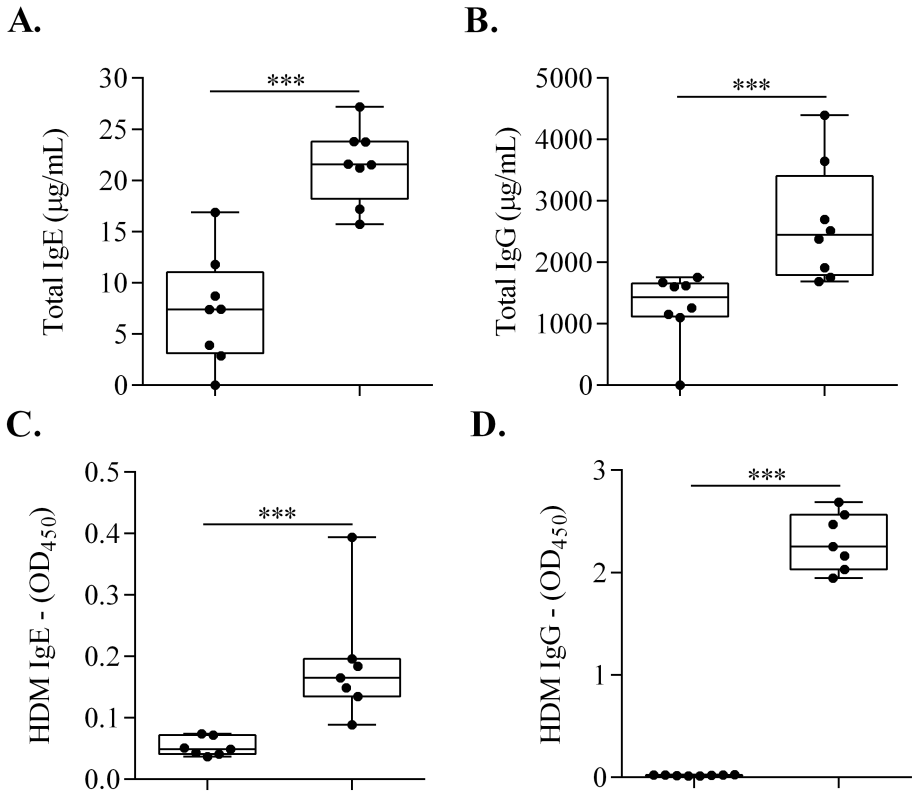

Figure 1.4: HDM-challenge increases immunoglobulin levels. *Mice (n = 8) were challenged by i.n. administration of whole HDM extract in saline, for 2 weeks (Figure VI). Immunoglobulin levels were monitored in serum from naïve and HDM-challenged mice, 24 hr after the last HDM-challenge, by ELISA. Mann-Whitney U test was used for statistical analyses (*p ≤ 0.05, **p ≤ 0.01, ***p ≤ 0.001). Error bar shown represent SEM.*

3.1.3.5 HDM-challenge significantly alters gene expression in the lungs: There are limited studies that include comprehensive analyses of transcriptional responses from murine lung following HDM-challenge. In order to provide objective readouts in this model, I used a disease-focused qPCR array to monitor the expression of selected 84 genes related to allergy and asthma in HDM-challenged (n=3) compared to allergen naïve (n=3) mice. Differentially Expressed (DE) genes were defined as those that were either up- or down-regulated by ≥ 2-fold with associated p≤0.05, in HDM-challenged compared to naïve mice. My analyses revealed marked changes in the gene expression profile of lungs in the HDM-challenged compared to allergen-naïve mice (Supplementary Figure 1.2). HDM-challenge altered the abundance of transcripts for 54% of genes (45 out of 84 genes) monitored (Supplementary Table 1.1). Of the differentially expressed genes, 31 were increased by > 2-fold, whereas only 5 transcripts were down-regulated after HDM-challenge (Supplementary Table 1.1). Among the transcripts that were increased after HDM-challenge, most markedly induced were those for the chloride channel calcium activated member 3(*clca3*), Eosinophil associated ribonuclease A family 11 (*Ear11*) and Mucin-5AC (*Muc5ac*), each of these have been previously identified as potential biomarkers in asthma [243-246]. As expected, Th2-driven cytokines and related receptors (*Il13, Il13ra2, Il4*), chemokines (C*cl11, Ccl12 and Ccl24*), and genes associated with allergic diseases arginase 1 (*Arg1*) and chitinase (*Chia1*) [245, 247, 248] were also significantly up-regulated in the HDM-challenged compared to allergen-naïve lungs (Supplementary Table 1.1).

I further interrogated the DE genes using IPA tool to assess biological processes, interactions and upstream regulators in the data set. Of the 45 DE genes, 33 genes were connected by network analyses employing both direct and indirect relationship (Figure 1.5). The IPA upstream regulator analytic identified 12 upstream transcriptional regulators known to activate the DE genes, and 9

regulators known to inhibit the DE genes (Supplementary Table 1.2 and Supplementary Figure 1.3A). Furthermore, the mRNA expressions of some of the predicted upstream regulators notably *Il33, Il13* and *Il4* were also upregulated in the lungs of HDM-challenged compared to allergen-naïve mice (Supplementary Table 1.1. Supplementary Figure 1.3). Predominant biological processes predicted to be activated by IPA with high confidence as a consequence of the DE genes were AHR, leukocyte migration, granulocyte adhesion and diapedesis, differentiation of leukocytes, T-cell helper differentiation, cytokines and chemokines signaling, flux of calcium, and secretion of mucus, all known to be involved in inflammation and AHR.

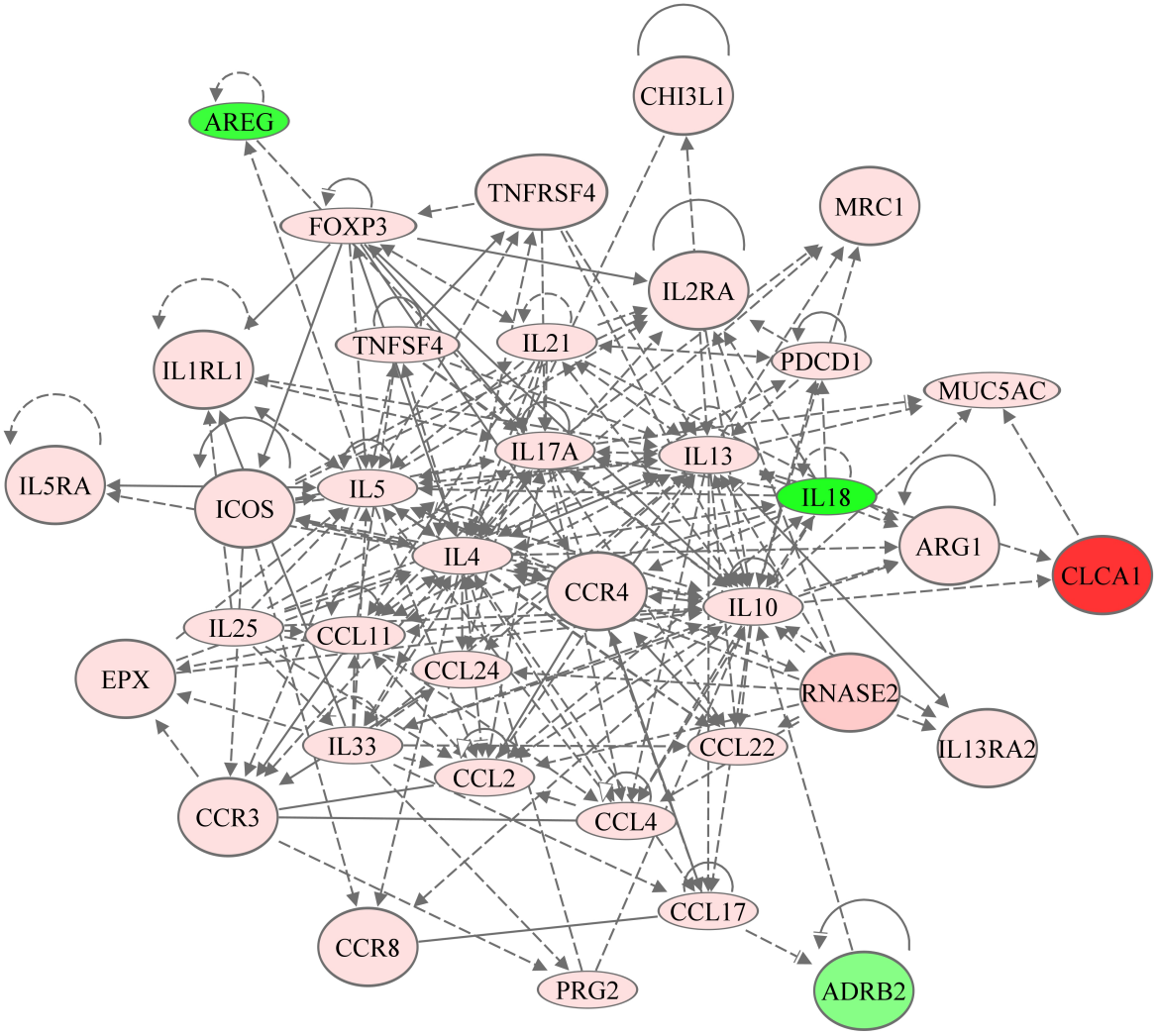

Figure 1.5: Interaction between the genes differentially expressed in response to HDM. *Network diagram showing that of the 45 DE genes in HDM-challenged lung tissues (Supplementary Table 1.1), 33 connected in an interaction network using the Ingenuity® Pathway Analysis tool. Red nodes represent upregulated and green nodes represent downregulated genes. The intensity of color corresponds to the magnitude of fold change in HDM-challenged lungs relative to that in allergen-naïve mice. Solid lines correspond to direct interactions and dotted lines correspond to indirect interactions.*

3.1.3.6 HDM-challenge selectively alters cytokine and chemokine profile in the lungs: I monitored the production of a panel of pro-inflammatory cytokines (IFNγ, IL-1β, IL-10, IL-12 p70, IL-2, IL-4, IL-5, IL-6, KC, and TNF) using a multiplex MSD platform in serum, BALF and lung tissue lysates. I further expanded the analyses to monitor the production of additional cytokines (IL-13, IL-33, MDC and TARC), transcripts of which were upregulated after HDM-challenge in lung tissue lysates (Supplementary Table 1.1) using ELISA. There was a significant increase in the production of cytokines IL-13, IL-10, TNF, IL-4, IL-33, IFNγ, IL-1β, IL-5 and IL-6, and chemokines CCL17 (TARC), CCL22 (MDC) and KC, in lung tissues lysates of the HDM-challenged compared to allergen-naïve mice (Table 1.1). Whereas, the abundance of cytokines IL-2 and IL-12p70 were similar in the lung tissue lysates obtained from HDM-challenged and allergen-naïve mice (Table 1.1). To correlate the cytokine abundance observed in the lung tissue lysates in response to HDM-challenge with that of those secreted in the airway milieu, I also measured cytokine and chemokine levels in BALF. Concentration of IFNγ, IL-1β, IL-2, IL-4, IL-5, IL-6, IL-10 and TNF and chemokine KC, were significantly higher in BALF of HDM-challenged compared to allergen-naïve mice (Table 1.1). In contrast, there was no change in abundance of cytokines and chemokines in serum of HDM-challenged mice compared to allergen-naïve mice (Supplementary Table 1.3). These results suggested that the inflammatory response was localized to the lung tissue compartment in the HDM-challenge protocol.

Table 1.1: HDM-induced cytokine profile in lung tissue lysates. *Mice were challenged by i.n. administration of whole HDM extract in saline, for 2 weeks (Figure VI). Lung tissue lysates (50 mg) and BALF obtained from naïve (n = 9) and HDM-challenged (n = 10) mice were monitored for production of a panel of cytokines, 24 hr after the last HDM-challenge. IFNγ, IL-1β, IL-10, IL-12 p70, IL-2, IL-4, IL-5, IL-6, KC and TNF were monitored using the multiplex MSD platform, and, IL-33, MDC and TARC were monitored by ELISA. Median values shown. Statistical analyses were performed using the Mann-Whitney U test (*p ≤ 0.05, **p ≤ 0.01, ***p ≤ 0.001).*

Cytokine	Lung Tissue Lysates				BALF			
	Naïve (pg/mL)	HDM (pg/mL)	Fold Change	P value	Naïve (pg/mL)	HDM (pg/mL)	Fold Change	P value
IFNγ	0.32	0.89	2.78	**0.003****	0.00	0.10	NA	**0.0001*****
IL-1β	4.69	25.24	5.39	**0.0001*****	0.35	1.29	3.73	**0.0006*****
IL-2	0.87	1.74	1.99	0.069	0.27	1.39	NA	**0.0001*****
IL-4	0.62	10.02	16.08	**0.0001*****	0.07	6.93	92.52	**0.0001*****
IL-5	0.22	4.19	19.33	**0.0001*****	0.00	8.06	NA	**0.0001*****
IL-6	12.11	50.08	4.14	**0.0001*****	0.00	5.91	NA	**0.0002*****
KC	14.37	93.48	6.51	**0.0001*****	10.28	62.42	6.07	**0.0001*****
IL-10	2.69	8.61	3.20	0.028*	0.41	8.46	20.68	**0.001****
IL-12	37.12	79.76	2.15	0.208	0.89	5.51	NA	**0.0002*****
TNF	2.93	5.61	1.91	**0.0021****	5.91	6.27	1.06	0.99
MDC	46.50	89.83	1.93	**0.0041****				
TARC	13.35	47.40	3.55	**0.0003*****				
TSLP	6.98	7.40	1.06	0.413				
IL-33	282.20	1574.00	5.58	**0.0001*****				
IL-13	171.80	333.00	1.94	**0.0006*****				

3.1.4 Discussion and Conclusion

In this study, I characterized various immune responses in the lung tissues, BALF and serum, and monitored differential expression of a panel of 84 genes in the lung tissue known to be associated with the disease process of allergy and asthma. I used an acute allergen challenge model featuring daily i.n. HDM-challenge for 5 days per week for two weeks in female mice. Previous studies have compared the difference in responses to HDM-challenge in female and male BALB/C mice. These studies indicate that female mice exposed to HDM showed higher levels of AHR, infiltration of immune cells to the lung, and also inflammatory mediators such as IL-4, IL-6, and allergen specific IgE antibodies [249-251]. The robust response of female BALB/C mice compared to male, make them ideal sex to be used in an allergic asthma model. In addition, according to Statistics Canada, in the human population a higher percentage of females suffering from asthma compared to males have been observed [252]. Therefore, I focused this study on female BALB/C mice.

Monitoring kinetics of cell accumulation in the lungs, I showed that neutrophil accumulation is most prominent 8 hr after the last HDM-challenge and subsequently declines. However, eosinophils and macrophage accumulation is seen beyond 8 hr and steadily peaks 24 and 48 hr after the last HDM-challenge in this model. The kinetics of neutrophil and eosinophil accumulation observed in this study was consistent with previous studies using the acute model of HDM-challenge [234]. I further demonstrate that it requires at least 24 hr after the last HDM-challenge to observe a significant increase in all cell types (eosinophils, neutrophils and macrophages) in the HDM-challenged mice compared to allergen-naïve mice, albeit with decline in neutrophilic accumulation. These results suggested that 24 hr after the last HDM-challenge is the most favorable time point to characterize molecular processes aligned with airway inflammation in this

model. Therefore, in this study I characterized immune and transcriptional responses 24 hr after the final HDM-challenge. The analyses of lung function, inflammation, and tissue changes demonstrate that the two-week acute model of HDM-challenge results in AHR, increased circulating levels of allergen-specific immunoglobulins, and early signs of airway remodeling without sub epithelial deposition of collagen. Thus, the model used in this study could be used to delineate the underlying mechanisms of airway inflammation that may be either independent or most likely preceding the process of airway remodeling.

Murine models play a key role in dissecting the pathogenesis of human diseases, yet the potential to assess such models using Systems Biology approaches have not been fully exploited. The HDM-challenged murine model of asthma invokes Th2-polarized bronchial inflammation, airway remodeling and epithelial damage similar to that seen in human asthma [228-230]. It is a pathophysiologically relevant model as HDM is the most prevalent allergen associated with asthma worldwide, up to 85% of asthmatics are HDM allergic [226]. A distinct advantage of the HDM-challenged murine model is that it does not induce tolerance, which is a problem associated with the murine models that employ an ovalbumin sensitization and repeated challenge protocol. However, previous studies have shown that outcomes measured using the HDM-challenged murine model can be variable, likely related to details of the HDM exposure protocol used (e.g. HDM concentration, timing and number of HDM exposure per week, and the time after the last HDM-challenge when the outcomes are monitored) [232-234]. There are few studies that report objective biomarkers in HDM-challenged murine model that fully reveal the character of inflammation and its association with tissue repair and pathophysiological parameter of lung function [235, 236]. Notably, a study by Koyama et al performed [236] transcriptomics (RNA sequencing) on lung tissues from a similar HDM-challenged murine model. However, they

focused on the expression and function of only one biomarker from the transcripts upregulated in the HDM mice. This study adds significantly to the previously published studies, as I have characterized a panel of distinct endpoints (biosignature) in lung tissue (the expression of 84 targeted genes) and BAL (a panel of inflammatory cytokines) from a HDM-challenged acute murine model. I have further performed a comprehensive network and pathways bioinformatics analyses to predict transcriptional regulators that may be contributing to the airway inflammation that characterizes this model. I speculate that the biosignature defined in this study will be useful endpoint surrogates for the human disease, especially to delineate molecular mechanisms underlying the progression from airway inflammation to tissue remodeling.

Airway inflammation and AHR are the hallmarks of allergic asthma. The acute model described in this study results in significant increase in maximum Newtonian and tissue damping, and tissue elastance to methacholine challenge, indicating AHR in HDM-challenged mice compared to allergen-naïve mice. These results were consistent with previous studies employing sensitization with HDM in animal models [229]. However, the measurement of lung mechanics in this study shows significant robust increase in AHR to methacholine challenge when monitored 24 hr as oppose to 8hr, after the last HDM-challenge. These data corroborated the selection of 24 hr after the last HDM-challenge to evaluate immune responses and transcriptional profile in this study. Furthermore, as eosinophil accumulation in the lung was seen after 8 hr and beyond 24 hr after the last HDM-challenge, the lung mechanics data also suggest that AHR may be related to eosinophil accumulation in the lungs. Furthermore, the bioinformatics analyses with IPA tool in this study reveals that 5 out of the 6 chemokines, and all three chemokine receptors upregulated in HDM lungs are associated with eosinophil migration, recruitment and eosinophilia. This is consistent with a previous study [253] demonstrating that negative regulation of eosinophil

chemotaxis decreases lung inflammation and the development of AHR in asthma. However, the role of eosinophils remain poorly understood in the pathogenesis of human asthma, as clinical trials targeting eosinophil differentiation and survival produced equivocal results and failed to suppress AHR [254]. Nevertheless, in the murine model discussed in this study, there appears to be a correlation between the kinetics of eosinophil accumulation in the lungs and the development of AHR following HDM-challenge.

Similarly, there are conflicting data on the correlation of AHR with presence of circulating HDM-specific IgE antibodies in animal models. It has been previously demonstrated that AHR is not related to the presence of serum HDM-specific IgE [255]. In contrast, other studies have demonstrated HDM-specific IgE and IgG1 plasma antibodies correlates with AHR [229, 256], however these were in recall murine models of HDM-challenge. In the acute model discussed in this study, I show significant increase in HDM-specific IgE and IgG1, as well as significant increase in total IgG and IgE, in the serum of HDM-challenged mice compared to allergen-naïve mice. These results are in line with the immune response seen in the human disease where elevated levels of total IgE and presence of allergen-specific IgE have been correlated with allergic asthma [257].

In this study, I show that despite significant cellular accumulation and increase in mucous producing goblet cells, there is no significant sub-epithelial collagen deposition in the airways of the HDM-challenged compared to allergen-naïve mice. These results suggest that after two weeks of repeated HDM exposure the airways show early signs of tissue remodeling with increase in epithelial thickness and goblet cell hyperplasia, without fibrosis. This is consistent with previous studies suggesting that two week exposure to HDM in murine models predominantly exhibit airway inflammation [229, 231]. However, the relationship between biological processes that

contribute to airway inflammation and structural tissue changes have not been completely delineated [258]. Previous studies have argued that the process of chronic inflammation in asthma may be partly distinct from those that result in tissue remodeling [259]. Consequently, there is a need to explore therapeutics and alternate drug targets that can separately control the processes of airway inflammation and remodeling. The animal model described in this study may be thus beneficial to define the underlying mechanisms of airway inflammation that may be either independent of, or preceding the process of airway tissue remodeling in allergic asthma.

An impediment in defining the underlying mechanisms of allergic asthma have been limited in part due to the availability of specific biomarkers in animal models relevant to human asthma. Therefore, in this study a qPCR array was used to profile the expression of a panel of 84 genes known to contribute to the pathogenesis of allergy and asthma, primarily curated from human data. The most abundant and significantly upregulated mRNA in the differentially expressed (DE) genes from HDM lungs are molecules that have been previous shown to be induced in human asthma [246, 260-262] such as chloride channel calcium activated member-3 (*Clca3*), eosinophil associated ribonuclease A family 11 (*Ear11*) and *Muc5ac*, those associated with allergic diseases (*Il13, Il13ra2, Il10* and *Il21*), and chemokines involved in cellular recruitment to the lungs (*Ccl11, Ccl12* and *Ccl24*). The biological processes that are predicted to be significantly activated as a consequence of the DE genes are predominantly those associated with leukocyte recruitment especially eosinophils, AHR, secretion of mucus and cytokine signaling, all relevant to the pathophysiology of human allergic asthma. The DE genes identified to be upregulated following HDM-challenge in this study confirms the relevance for the use of this model in delineating the pathophysiology and underlying mechanisms associated with human allergic asthma.

Bioinformatics analyses in this study defined upstream regulators predicted to be activated based on the DE genes. Notably, among the predicted upstream regulators are IL-33 and the transcription factor retinoic acid-related orphan receptor α (RORA), both shown to significantly contribute to the pathogenesis of asthma in a recent genome-wide association study [263]. IL-33 drives airway inflammation by engaging ILC2 and inducing the expression of cytokines IL-13 and IL-5. RORA is known to mediate the differentiation of ILC2, the primary cell targets of IL-33 [264]. In this study, the mRNA transcripts and protein production of both IL-13 and IL-5 are significantly higher in the lungs of HDM-challenged mice compared to allergen-naïve mice. In addition, mRNA of IL1R1, which is a part of the IL-33 receptor complex expressed on ILC2, is also upregulated after HDM-challenge. These results suggest that the IL-33-RORA-ILC2 axis which prominently drives the production of IL-13 is activated in the model used in this study.

Among the upstream regulators predicted to be activated are also GATA-3 and IL-4. The transcription factor GATA-3 promotes the secretion of IL-4 from Th2 cells [265]. In this study, both mRNA and protein production of IL-4 is induced in response to HDM-challenged. Taken together, these results demonstrate that the IL-4-mediated canonical pathway driving Th2-inflammation and synthesis of IgE is also activated in this model. Recent studies have clearly defined the differential roles of IL-4 and IL-13 in allergic inflammation; IL-4 preferentially regulates Th2 cell function and IgE synthesis, whereas IL-13 mediates the pathophysiological processes that control mucus production, eosinophilia and AHR [266]. Consistent with this, the HDM-challenged mice in this model have increased AHR, eosinophil accumulation, goblet cells, as well as increased Th2-cytokines and total and allergen-specific IgE. Taken together, these results indicate that both IL-4- and IL-13-mediated distinct downstream responses are induced in this model. However, IL-13 also contribute to tissue remodeling [266] or fibrosis, which was not

seen in this study. This is likely due to the duration of HDM exposure in this model, suggesting that further extending the duration of this model for a total of 5 to 8 weeks to incorporate prolonged exposure to HDM will likely result in airway remodeling and fibrosis. Nevertheless, as described, this model demonstrates the hallmarks of airway inflammation associated with human asthma, employing the critical processes driven by both the cytokines IL-4 and IL-13.

In summary, this study defines a panel of biomolecules associated with human airway inflammation in a HDM-challenged murine model. I have systematically characterized immune responses, and provided a panel of objective endpoint biosignature that will be valuable to study disease progression in asthma / airway inflammation using this murine model. The biosignature defined in this study will notably be valuable to define underlying molecular mechanisms of airway inflammation that precedes tissue remodeling in allergic asthma. Furthermore, as some of the defined biomolecules in this study do not yet have known functions in asthma, these will be useful to explore as novel candidates in the context of the pathophysiology of asthma.

The analyses of physiological and immunological responses in this study help define certain similarities between the murine model described in this study and the human disease, thus establishing the relevance of this model for preclinical studies in allergic asthma.

Animal models, such as the one used in this study, are powerful and critical for dissecting underlying mechanisms of disease pathogenesis and have provided the foundation for the development of safe and cost effective treatments [267]. However, the limitation is that responses in animal models do not predict responses in humans but help understand and generate a hypotheses of what may happen in humans [268]. This is particular relevant in murine models of asthma as mice do not develop asthma spontaneously. Therefore, the disease is artificially induced,

as in the model used in this study, with HDM. It is therefore important that we understand the limitations of animal research and data should be interpreted in the correct context.

I have discussed above in detail the involvement of the immune system and the physiological changes involved in the pathogenesis of allergen challenge in the HDM-challenged murine model of allergic asthma. In the next section, I describe the effects of a synthetic IDR peptide in the HDM-challenged murine model. CHDP as discussed in chapter 1.2 exhibit a wide range of immunomodulatory functions which include induction of anti-inflammatory cytokines, control of endotoxin and pro-inflammatory cytokine-mediated inflammation, influencing the maturation and differentiation of immune cells [53, 67-70]. Synthetic derivative peptides of CHDP, IDR peptides, are beneficial in controlling infections and inflammation, but the therapeutic potential of these have primarily been explored in various infection models [132, 269, 270]. IDR-1002 as discussed in detail in chapter 1.2 is an immunomodulatory peptide described previously primarily in models of infectious disease and show the potential as a novel therapeutic to treat inflammation. In the following chapter, I discuss the potential therapeutic effects of administration of IDR-1002, in the 2 week HDM-challenged murine model that I characterized in this study. I also detail the effects of the peptide in an IL-33-challenged mice in the next chapter.

3.2 Immunomodulatory peptide IDR-1002 alleviates airway inflammation and AHR

This section contains text and figures from a collaborative work published as an original article in *Thorax* 2018. 73(10): p. 908-917. **Hadeesha Piyadasa**, Mahadevappa Hemshekhar, Anthony Altieri, Sujata Basu, Anna M van der Does, Andrew J Halayko, Pieter S Hiemstra, Neeloffer Mookherjee.

H.P. performed majority of the experiments and data analyses, contributed to the development of the scientific concepts and wrote the manuscript. M.H. and A.A. assisted in endpoint sample collection and quantification of cell differentials. S.B. performed the lung function measurements. A.J.H. provided significant intellectual input in the development of this study and extensively edited the text. A.M.vdD. provided intellectual support in the design of the experiments using human primary cells. P.S.H. provided significant intellectual input and directly supervised the experiments using primary human cells. N.M. conceived and directly supervised the study and extensively edited the manuscript.

3.2.1 Abstract

Background: CHDP and IDR peptides are potent immunomodulatory molecules and have been extensively characterized in host defense responses against pathogens. I examined the effects of a synthetic derivative of CHDP Bactenecin, IDR-1002, in the 2-week HDM-challenged murine model of asthma, in IL-33-challenged mice, and in human primary bronchial epithelial cells (PBEC).

Methods: IDR-1002 (6 mg/Kg per mouse) was administered (s.c.) in HDM-challenged and/or IL-33-challenged BALB/c mice. Lung function analysis was performed with increasing dose of methacholine by *flexi*Vent™ small animal ventilator, cell differentials in bronchoalveolar lavage performed by modified Wright-Giemsa staining, and cytokines monitored by MSD assay and ELISA. PBEC stimulated with TNF and IFNγ, with or without IDR-1002, were analyzed by western blots.

Results: IDR-1002 blunted HDM-challenged induced AHR, and lung leukocyte accumulation; eosinophils and neutrophils, in HDM-challenged mice. Concomitantly, IDR-1002 suppressed HDM-induced IL-33 in the lungs. IFNγ/TNF-induced IL-33 production was abrogated by IDR-1002 in human PBEC. Administration of IL-33 in HDM-challenged mice, or challenge with IL-33 alone, mitigated the ability of IDR-1002 to control leukocyte accumulation in the lungs, suggesting that the suppression of IL-33 is essential for the anti-inflammatory activity of IDR-1002. However, the peptide significantly reduced either HDM-, IL-33- or HDM + IL-33-co-challenge-induced AHR *in vivo*.

Conclusion: This study demonstrates that an immunomodulatory IDR peptide controls the pathophysiology of allergic airway inflammation, applicable to asthma, in a murine model. As IL-33 is implicated in steroid-refractory severe asthma, the results of this study suggest that the effects of IDR-1002 may contribute to the development of novel therapies for steroid-refractory severe asthma.

3.2.2 Rationale and Introduction

Asthma is a chronic respiratory disease as discussed in chapter 1.3. The available therapies for severe asthmatics including OCS may contribute to an increased risk for infections and other complications [210, 271-273]. These challenges highlight the need for the development of alternate strategies that can control asthma, especially the steroid-unresponsiveness disease. Synthetic IDR peptides, as discussed in chapter 1.2, are beneficial in controlling infections and inflammation, but the therapeutic potential of these have primarily been explored in various infection models [132, 269, 270]. In this study, I examined the effects of administration of an IDR peptide, IDR-1002, in the 2-week HDM-challenged murine model of allergic airway inflammation detailed in chapter 3.1, and further interrogated the peptide activity in PBEC.

IDR-1002 as discussed in detail in chapter 1.2, is a 12 amino acid cationic peptide derived from a bovine cathelicidin CHDP, Bac2A [132]. IDR-1002 attenuates inflammatory cytokine production in cystic fibrosis airway cells, exhibits anti-biofilm activity and controls multi drug-resistant bacterial infections [96, 274]. In this study, I provide the first evidence to show that s.c. administration of IDR-1002 significantly reduces AHR and leukocyte accumulation in the lungs of HDM-challenged mice. In mechanistic studies I show that the peptide suppresses the production of the cytokine IL-33 in murine lungs and human PBEC. I further demonstrate that inhibition of IL-33 by IDR-1002 is essential to control airway inflammation, and that the peptide reduces both HDM- and IL-33-induced AHR *in vivo.* As IL-33 is a critical steroid-resistance mediator [275-278], my finding on the effects of IDR-1002 may contribute to the development of new therapies for steroid-refractory asthma.

3.2.3 Results

3.2.3.1 IDR-1002 reduces AHR in HDM-challenged mice: Previous studies, including ours, have shown that HDM-challenge (i.n) for two weeks in mice results in AHR and airway inflammation [279, 280]. Therefore, I used this model to examine the effects of administration (s.c) of IDR-1002. The route and dose of administration of IDR-1002 was based on previous studies [132, 269]. Assessment of lung mechanics showed that administration of IDR-1002 significantly reduced both maximum methacholine (50 mg/ml)-induced Newtonian resistance (Rn) by 56 ± 31% (Figure 2.1A), and decreased sensitivity to methacholine (amount required to increase the baseline Newtonian resistance by 50% (PC50)) by 2-fold ± 0.47-fold (Figure 2.1D), compared to HDM-challenged mice. IDR-1002 restored methacholine PC50 in HDM-challenged mice to levels similar to that in allergen-naïve mice (Figure 2.1D). I observed concomitant inhibition of HDM-challenge-induced maximum tissue damping (G) by 49 ± 34% and tissue elastance (H) by 50 ± 37% with IDR-1002 treatment (Figures 2.1B and 2.1C respectively), at maximal methacholine concentration. Notably, at lower concentrations of methacholine (6 – 12 mg/ml) in HDM-challenged mice, IDR-1002 fully abrogated increased Rn, G and H to similar levels seen in allergen naïve animals. Taken together, these results indicate that the peptide exhibits the ability to decrease overall resistance of the airway tree (Rn), tissue resistance in the alveoli (G) and tissue elastance (H), indicating that the peptide have significant functional impact on airflow conductance of central, small and terminal bronchioles. Administration of IDR-1002 alone had no effect of indices of Newtonian resistance and lung function in allergen-naïve mice (Figure 2.1). These results demonstrate that administration of IDR-1002 significantly reduces AHR in allergen-challenged mice.

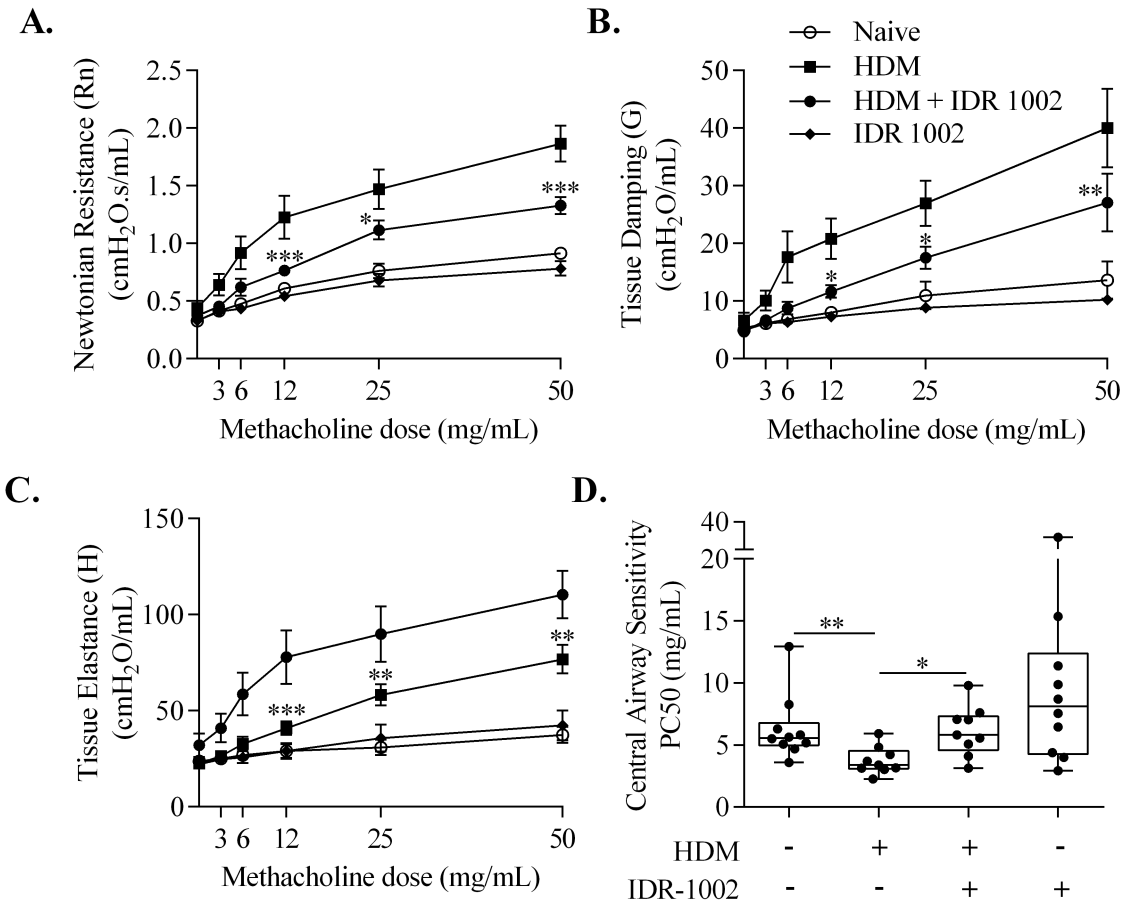

Figure 2.1: IDR-1002 reduces HDM-challenge-induced AHR in mice. *Mice (n = 9 per group) were challenged by i.n. administration of whole HDM extract in saline, for 2 weeks (Figure VI). IDR-1002 was administered s.c. 3 times a week (Figure VI). Lung mechanics were monitored, 24 hr after the last HDM-challenge. Mice were exposed to nebulized saline (baseline measures) followed by increasing concentrations of nebulized methacholine (3-50 mg/mL) and changes in* ***(A)*** *Newtonian resistance (Rn),* ***(B)*** *tissue damping (G),* ***(C)*** *tissue elastance (H) were monitored.* ***(D)*** *Central airway sensitivity determined by calculating PC50. Statistical significance was determined for (A, B, C) using two-way repeated measures ANOVA with Tukey's multiple comparisons test, and (D) using Mann Whitney U test (*p ≤ 0.05, **p ≤ 0.01, ***p ≤ 0.001). Asterisks in A, B, C represent comparison between HDM and HDM + IDR-1002 group.*

3.2.3.2 IDR-1002 suppresses leukocyte accumulation in HDM-challenged mice: As detailed in chapter 3.1, HDM-challenge for two weeks induces airway inflammation that precedes airway remodeling in the murine model [280]. Administration of IDR-1002 significantly reduced immune cell numbers by 35 ± 31% in BALF from HDM-challenged mice (Figure 2.2A). Cell differential analyses revealed that eosinophil numbers were significantly suppressed 51 ± 29% (Figure 2.2B) and neutrophils by 29 ± 22% and lymphocytes by 49 ± 42% (Figure 2.2C), whereas macrophages were not affected by the peptide treatment (Figures 2.2D and 2.2E respectively). However, IDR-1002 treatment did not bring the cell numbers down to baseline, as immune cell numbers in BALF of HDM-challenged groups treated with IDR-1002 were higher compared to that in allergen-naïve mice, and these differences were statistically significant. Administration of IDR-1002 alone did not alter leukocyte accumulation compared to allergen-naïve animals (Figure 2.2). PAS staining of lung specimens revealed a significant increase in mucin-producing goblet cell numbers in airways of HDM-challenged mice, which was reduced by the administration IDR-1002 by ~34% (Supplementary Figure 2.1). These findings demonstrate that administration of IDR-1002 significantly reduces accumulation of eosinophils and neutrophils in the lungs of allergen-challenged mice.

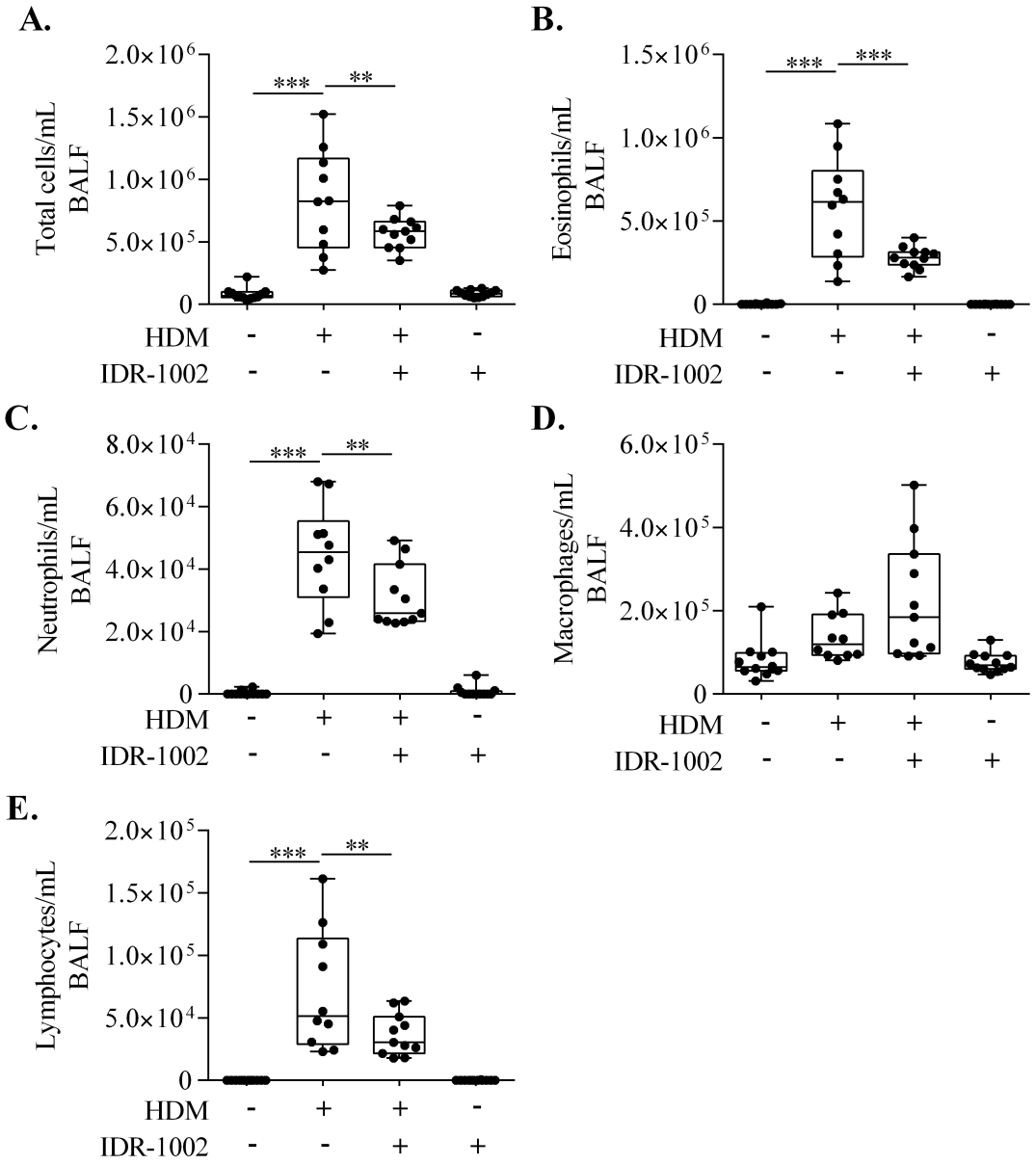

Figure 2.2: Administration of IDR-1002 significantly suppresses HDM-induced eosinophil and neutrophil accumulation and IL-33 production in the lungs. *Mice were challenged by i.n. administration of whole HDM extract in saline, for 2 weeks (Figure VI). IDR-1002 was administered s.c. 3 times a week (Figure VI). Broncheoalveolar lavage fluid (BALF) was collected from naïve (n=12), HDM-challenged (n=10), HDM + IDR-1002 (n=11), and IDR-1002 alone (12) mice, 24 hr after the last HDM-challenge and* ***(A)*** *Total cell,* ***(B)*** *eosinophil,* ***(C)*** *neutrophil,* ***(D)*** *macrophage, and* ***(E)*** *lymphocyte numbers were assessed. Bar's show median and interquartile range, whiskers show min and max points. Statistical significance was determined by one-way ANOVA with Tukey's multiple comparisons test (**p ≤ 0.01, ***p ≤ 0.001).*

3.2.3.3 IDR-1002 suppresses production of IL-33 in HDM-challenged mice: I monitored lung tissue lysates for the production of a panel of cytokines known to increase in this HDM-model, selected based on my previous work [280]. Administration of IDR-1002 significantly suppressed the production of the pro-inflammatory cytokine IL-33 by 62 ± 30% in the HDM-challenged mice (Figure 2.3). However, no other HDM-induced cytokine or chemokine monitored exhibited a statistically significant change in abundance following peptide administration in this model (Supplementary Table 2.1). These results suggest that IDR-1002 regulates the biosynthesis and/or secretion of the cytokine IL-33.

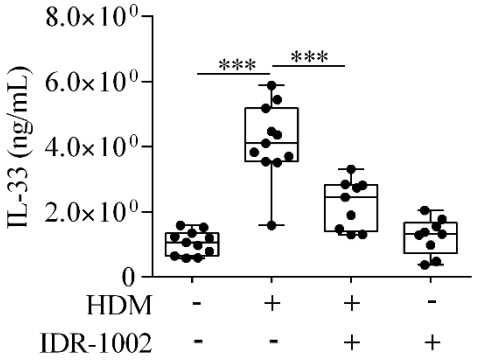

Figure 2.3: Administration of IDR-1002 significantly suppresses HDM-induced IL-33 in the lungs. *Mice were challenged by i.n. administration of whole HDM extract in saline, for 2 weeks (Figure VI). IDR-1002 was administered s.c. 3 times a week (Figure VI). Lung tissue was collected from naïve (n=11), HDM-challenged (n=11), HDM + IDR-1002 (n=9), and IDR-1002 alone (n=9) groups 24 hr after the last HDM-challenge. IL-33 protein abundance was monitored in the lung tissue lysates by ELISA. Bar's shows median and interquartile range, whiskers show min and max points. One-way ANOVA with Tukey's multiple comparisons test was used to assess statistical significance (***$p \leq 0.001$).*

3.2.3.4 IDR-1002 reduces HDM + IL-33 co-challenge-induced AHR, but not leukocyte accumulation in the lungs: I have shown that IDR-1002 administration significantly suppresses IL-33 abundance in the lungs of HDM-challenged mice (Figure 2.3). Therefore, to determine whether IDR-1002 activity is mediated by targeting IL-33, I performed a rescue experiment; recombinant murine IL-33 (1µg/mouse) was administered (i.n) on the last 5 days of HDM-challenge (Figure VI). Administration of IL-33 in the HDM-challenged mice significantly enhanced leukocyte accumulation, including that of eosinophils and neutrophils, compared to naïve mice (Figure 2.4). Administration of IDR-1002 did not reduce HDM + IL-33 co-challenge-induced accumulation of total cell numbers, eosinophils and neutrophils in the BALF (Figure 2.4). As exogenous (additional) administration of IL-33 in HDM-challenged mice mitigated the ability of the peptide to reduce HDM-induced leukocyte accumulation in BALF, these results suggest that IDR-1002 reduces leukocyte accumulation and airway inflammation by suppressing IL-33 in the lungs of allergen-challenged mice. However, IDR-1002 maintained the ability to reduce AHR in IL-33 and HDM co-challenged mice; Rn by 73 ± 30%, G by 57 ± 24% and H by 67 ± 24% (Figure 2.5), suggesting that IDR-1002 lowers AHR by mechanisms either downstream or independent of IL-33.

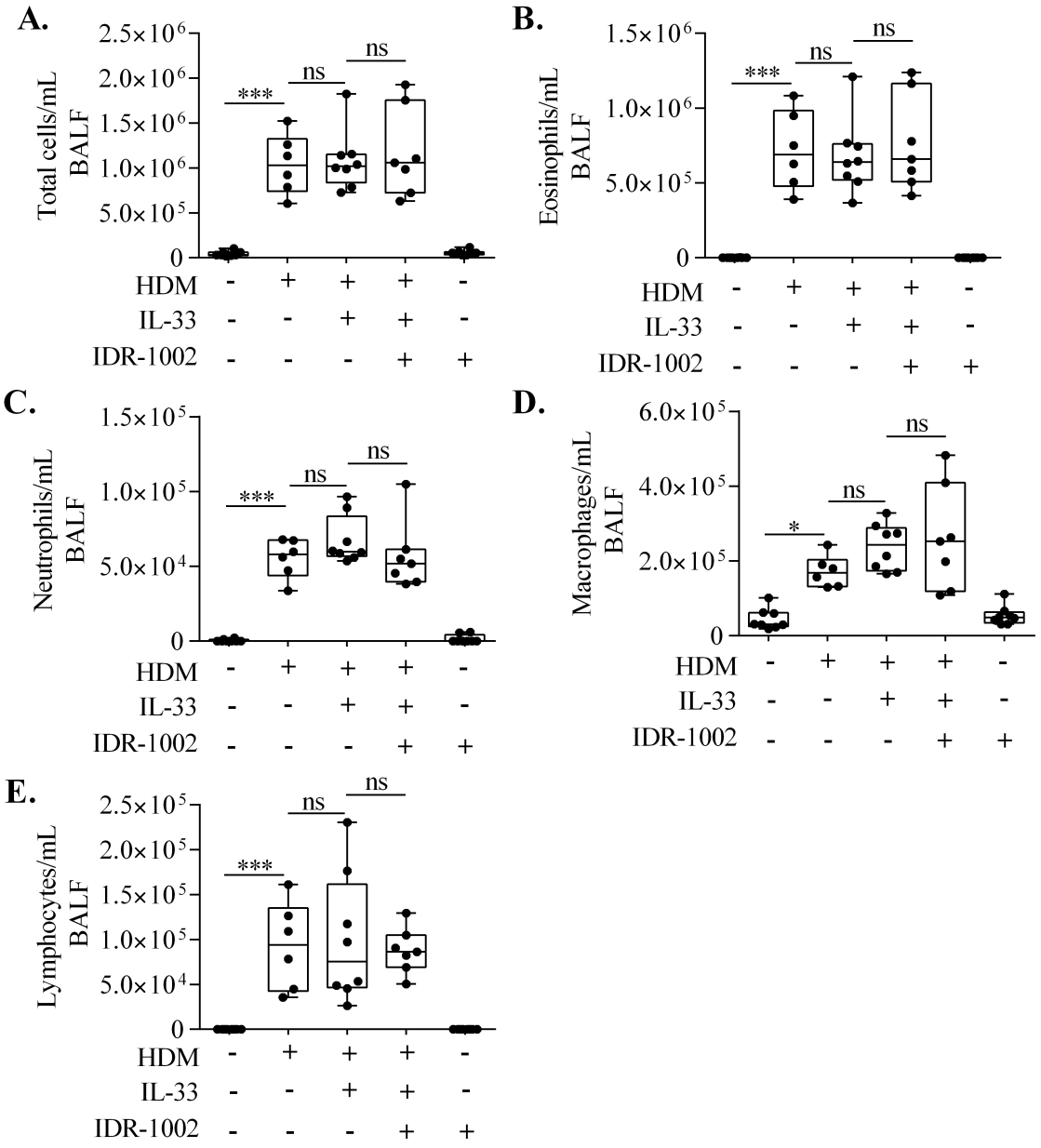

Figure 2.4: Exogenous administration of IL-33 mitigates the ability of the peptide to suppress immune cell accumulation to the lung of HDM-challenged mice. *Mice were challenged by i.n. administration of whole HDM extract in saline, for 2 weeks and IL-33 was administered i.n. on days 8-12 (Figure VI). IDR-1002 was administered s.c. 3 times a week (Figure VI). BALF was collected from naïve (n=8), HDM-challenged (n=6), HDM + IL-33 co-challenged (n=8), HDM + IL-33 co-challenged + IDR-1002 (n=7), and IDR-1002 alone (n=8) groups, 24 hr after last HDM-challenge and* ***(A)*** *Total cells,* ***(B)*** *eosinophil,* ***(C)*** *neutrophil,* ***(D)*** *macrophage, and* ***(E)*** *lymphocyte numbers were assessed. Bar's shows median and interquartile range, whiskers show min and max points. One-way ANOVA with Tukey's multiple comparisons test was used for statistical analyses (*$p \leq 0.05$, **$p \leq 0.01$, ***$p \leq 0.001$, and ns=non-significant).*

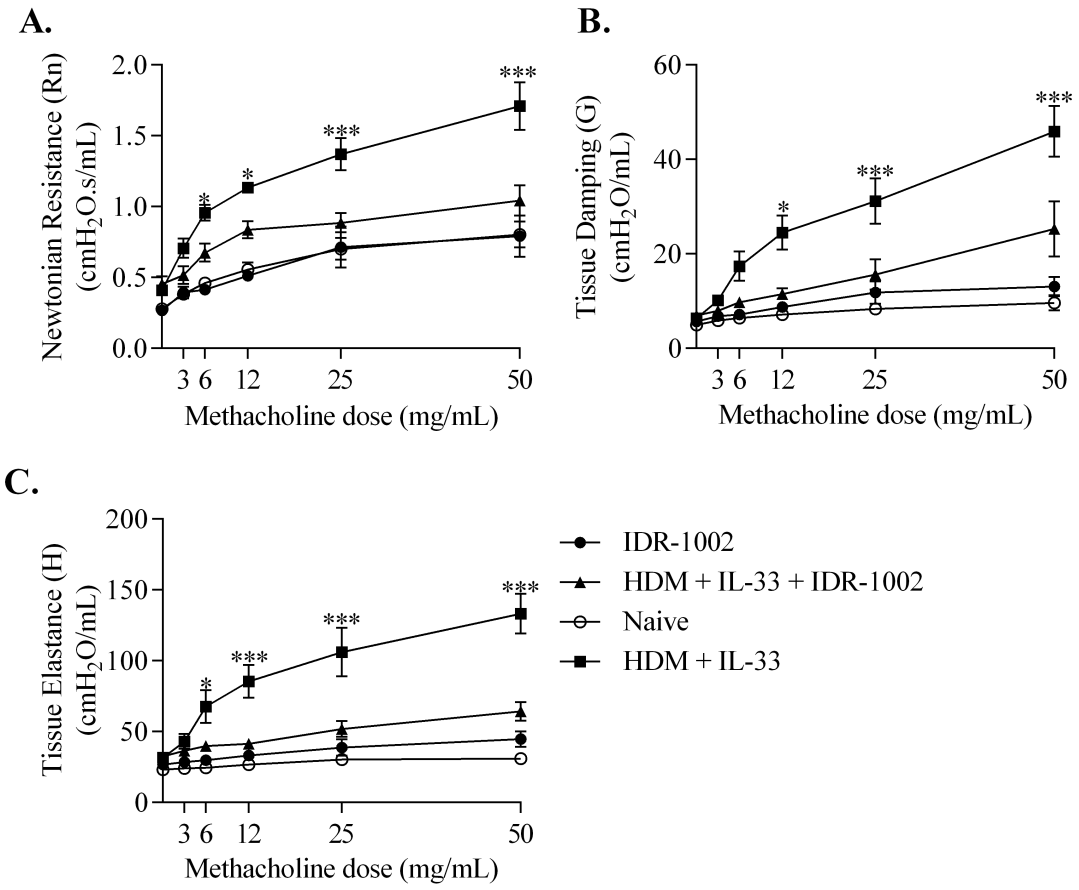

Figure 2.5: IDR-1002 reduces HDM + IL-33 co-challenge-induced AHR in mice. *Mice were challenged by i.n. administration of whole HDM extract in saline, for 2 weeks and IL-33 was administered i.n. on days 8-12 (Figure VI). IDR-1002 was administered s.c. 3 times a week (Figure VI). Lung mechanics were monitored in naïve (n=8), HDM + IL-33 co-challenged (n=8), HDM + IL-33 co-challenged + IDR-1002 (n=7), and IDR-1002 alone (n=4) groups, 24 hr after the last HDM-challenge. Mice were exposed to nebulized saline (baseline measures) followed by increasing concentrations of nebulized methacholine (3-50 mg/mL) and changes in* ***(A)*** *Newtonian resistance (Rn),* ***(B)*** *tissue damping (G), and* ***(C)*** *tissue elastance (H) was monitored. Data shown represents the mean ± standard error of the mean. Statistical significance was determined using two-way repeated measures ANOVA with Tukey's multiple comparisons test (*$p \leq 0.05$, **$p \leq 0.01$, ***$p \leq 0.001$). Asterisks in the figure represent comparison between HDM + IL-33 and HDM + IL-33 + IDR-1002 group.*

3.2.3.5 IDR-1002 reduces IL-33-induced AHR: I showed that IDR-1002 retained its ability to reduce AHR induced by IL-33 and HDM co-challenge in mice (Figure 2.5). Therefore, I further examined the effects of the peptide in responses induced by IL-33 alone. IL-33 by itself induced AHR and accumulation of eosinophils and neutrophils to the lungs (Figure 2.6 and 2.7). IL-33-induced AHR was significantly blunted by IDR-1002 administration; Rn by 56 ± 36%, G by 56 ± 23% and H by 64 ± 22% (Figure 2.6). However, the peptide did not suppress IL-33-mediated leukocyte accumulation in BALF (Figure 2.7). These results suggest that IDR-1002 intervenes in IL-33-induced downstream responses to reduce AHR, but not airway inflammation.

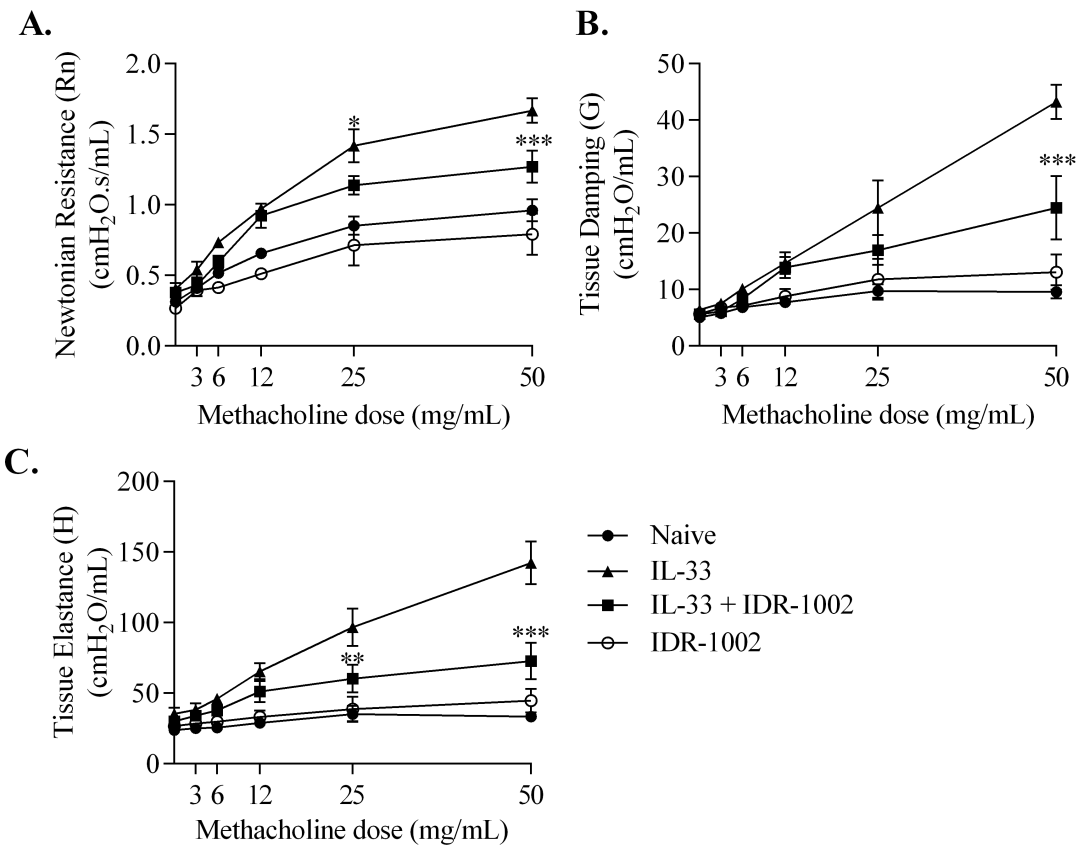

Figure 2.6: IDR-1002 reduces IL-33 alone-induced AHR, but not immune cell accumulation in the lungs. *Mice (n = 4 per group) were administered s.c. with IDR-1002 3 times a week, for 2 weeks. Recombinant IL-33 was administered i.n. on days 8-12. Lung mechanics was monitored, 24 hr after the last IL-33 challenge. Mice were exposed to nebulized saline (baseline measures) followed by increasing concentrations of nebulized methacholine (3-50 mg/mL) and changes in* ***(A)*** *Newtonian resistance (Rn),* ***(B)*** *Tissue damping (G), and* ***(C)*** *Tissue elastance (H) was monitored. Data shown represents the mean ± standard error of the mean. Statistical significance was determined using two-way repeated measures ANOVA with Tukey's multiple comparisons test. Asterisks in the figure represent comparison between IL-33 and IL-33 + IDR-1002 groups. (*p ≤ 0.05, **p ≤ 0.01, ***p ≤ 0.001, and ns=non-significant).*

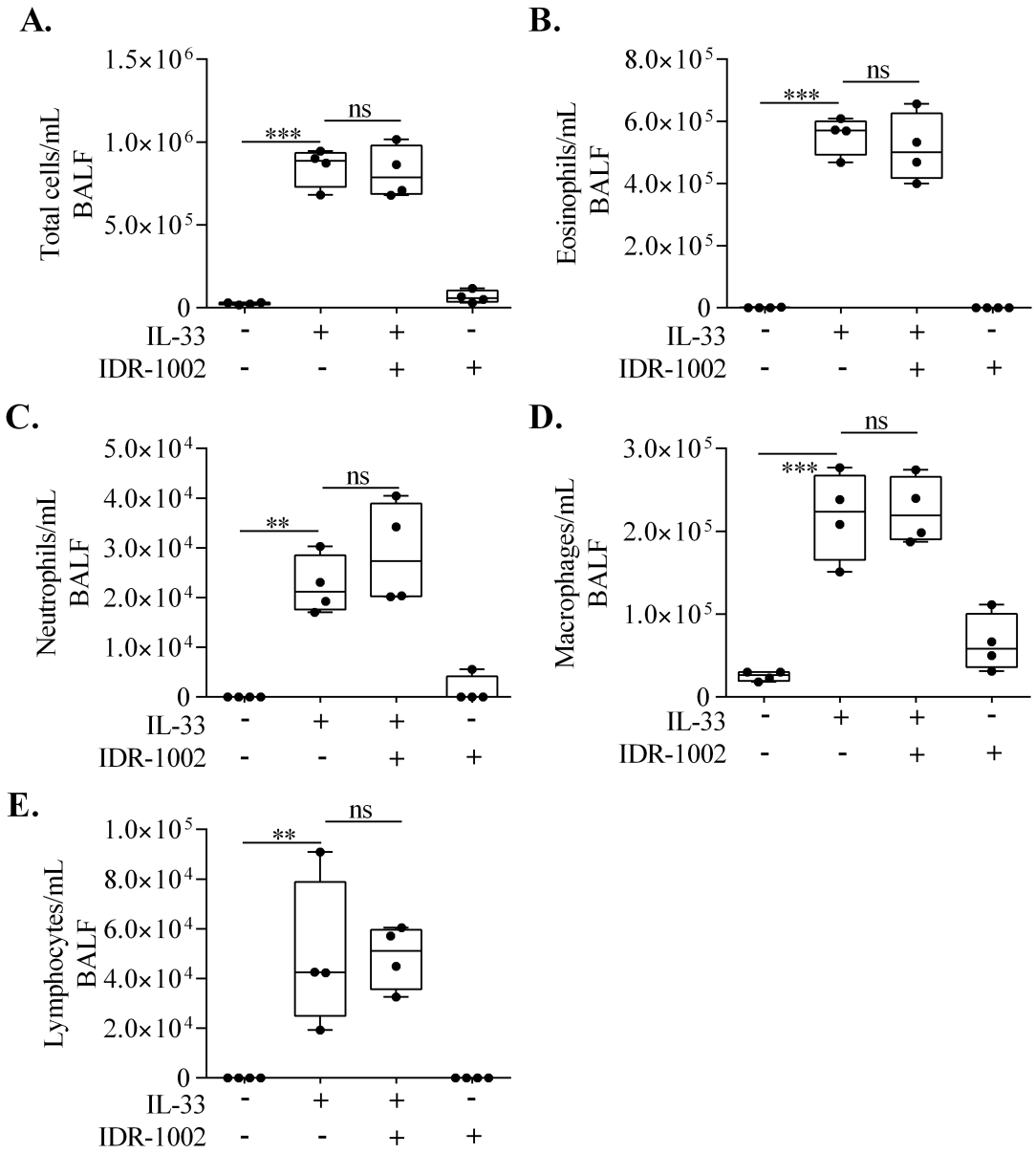

Figure 2.7: IDR-1002 reduces IL-33 alone-induced AHR, but not immune cell accumulation in the lungs. *Mice (n = 4 per group) were administered s.c. with IDR-1002 3 times a week, for 2 weeks. Recombinant IL-33 was administered i.n. on days 8-12. Lung mechanics was monitored, 24 hr after the last IL-33 challenge. BALF was collected 24 hr after the last IL-33 challenge and* ***(A)*** *Total cells,* ***(B)*** *eosinophil,* ***(C)*** *neutrophil,* ***(D)*** *macrophage and* ***(E)*** *lymphocyte cell numbers was assessed. Bar's shows median and interquartile range, whiskers show min and max points. One-way ANOVA with Tukey's multiple comparisons test was used for statistical analyses. (*p ≤ 0.05, **p ≤ 0.01, ***p ≤ 0.001, and ns=non-significant).*

3.2.3.5 IDR-1002 abrogates IL-33 production in human PBEC: As IL-33 is predominantly produced by epithelial and endothelial cells, I further validated the activity of IDR-1002 in mitigating the production of IL-33 in human PBEC. Previous studies have shown that a cytomix of IFNγ and TNF induces the production of IL-33 [281-283]. Therefore, I stimulated human PBEC isolated from four independent human donors (n = 4), with recombinant human IFNγ (30ng/mL) and/or TNF (20ng/mL), in the presence and absence of IDR-1002 (20 or 40μM). The concentration range of IDR-1002 was selected from previous *in vitro* studies [135]. IL-33 abundance was significantly increased in response to either IFNγ or the cytomix (IFNγ + TNF), but not TNF alone (Figures 2.8A and 2.8B), suggesting that IFNγ drives IL-33 production in human PBEC. IDR-1002 abrogated cytomix-induced IL-33 protein abundance in human PBEC (Figures 2.8A and 2.8B).

To further evaluate the specificity of IDR-1002 activity, I repeated these experiments using a related peptide IDR-1 (KSRIVPAIPVSLL-NH_2). Similar to IDR-1002, IDR-1 is also derived from the bovine cathelicidin Bac2A. However, in contrast to IDR-1002, IDR-1 does not suppress inflammatory cytokine-mediated signaling and downstream responses in human cells [135]. IDR-1 did not suppress IL-33 production in PBEC (Supplementary Figure 2.2).

As IL-33 production was primarily driven by IFNγ-mediated response (Figures 2.8A and 2.8B), I further examined the effect of IDR-1002 on expression of response elements induced by the IFNγ canonical signaling, namely transcription factor interferon response factor 1 (IRF1) and downstream IFN-inducible protein 10 (IP10) [284]. Production of IFNγ-induced IP10 and IRF1 was not suppressed by IDR-1002 (Figures 2.8C and 2.8D respectively).

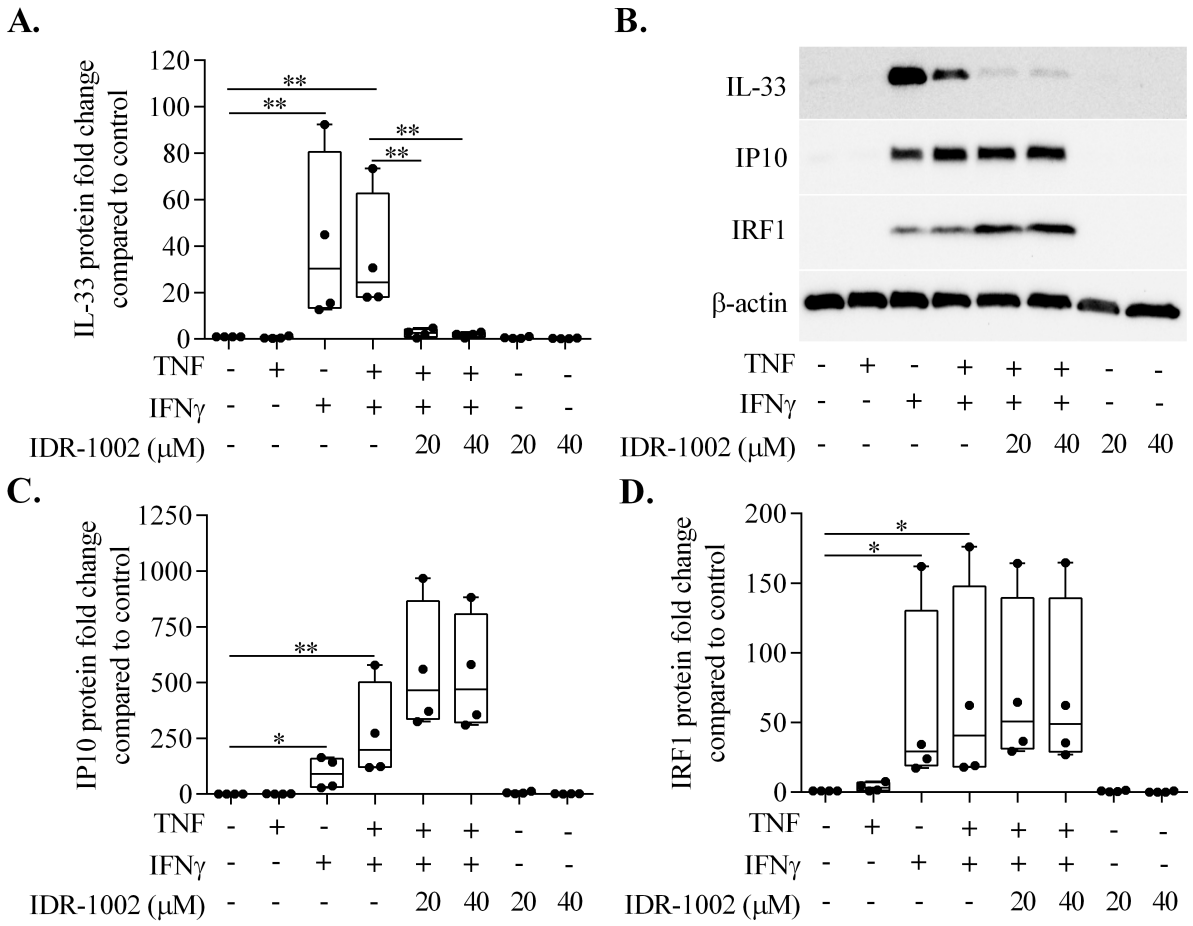

Figure 2.8: IDR-1002 significantly reduces IL-33 production in human PBEC. *Human PBEC obtained from four independent donors (n=4) were stimulated with TNF (20 ng/mL) and/or IFNγ (30 ng/mL), in the presence and absence of IDR-1002 (20 and 40 μM). Cytoplasmic fraction of cells isolated 24 hr post-stimulation was probed in immunoblots to assess the abundance of IL-33, IRF1 and IP10. Protein abundance was quantified by densitometry.* ***(A)*** *A representative immunoblot, and densitometry analysis for* ***(B)*** *IL-33,* ***(C)*** *IRF1 and* ***(D)*** *IP10 is shown. Y-axis represents relative band intensity compared to that in unstimulated cells normalized to 1, after normalization with β-actin for protein input. Each dot represents an individual donor, and bars show the median and interquartile range. RM one-way ANOVA with Fisher's LSD test was used for statistical analyses (*$p \leq 0.05$, **$p \leq 0.01$).*

3.2.4 Discussion and Conclusion

In this study, I demonstrate that an immunomodulatory IDR peptide, IDR-1002, reduces AHR, leukocyte accumulation (eosinophils, neutrophils, and leukocytes) in the lungs, and prevents epithelial goblet cell hyperplasia, which is otherwise induced by repeated allergen challenge, in a murine model of allergic asthma. I also demonstrate that the peptide suppresses IL-33 production in murine lungs and in human PBEC. I show that the ability of the peptide to suppress accumulation of eosinophils and neutrophils in the lungs of HDM-challenged mice is abrogated by additional administration of the IL-33, thus suggesting that suppression of IL-33 production is essential for IDR-1002 to reduce airway inflammation. I also show that IDR-1002 exhibits the ability to reduce AHR induced by either HDM, IL-33 or HDM + IL-33 co-challenge *in vivo*. Taken together, my findings suggest that the peptide engages different mechanisms that do not entirely overlap to control AHR and airway inflammation. Overall, in this study I demonstrate the potential of a synthetic immunomodulatory IDR peptide to alleviate airway inflammation and AHR, and intervene in the pathobiology of allergic asthma.

IDR peptides have been demonstrated to modulate immune responses to control infections and limit excessive inflammation in various models [123, 128, 132, 135, 269, 285-287]. Some IDR peptides are currently in phase II/III clinical trials primarily for infectious diseases [125, 288, 289]. The use of IDR peptides for chronic inflammatory diseases such as asthma have not yet been fully explored. This is the first study to demonstrate the beneficial use of a synthetic IDR peptide in an *in vivo* HDM-challenged model of allergic asthma. A recent study demonstrated that administration of natural cathelicidin CHDP such as the human LL-37 and murine CRAMP leads to an increased inflammatory response in ovalbumin-challenged mice [290]. A critical distinction of this study is the use a synthetic IDR peptide (IDR-1002) that is designed to optimize

immunomodulatory functions without the associated cytotoxic and pro-inflammatory effects of natural CHDP at mucosal surfaces [123]. Synthetic IDR peptides selectively reduce exacerbated inflammatory responses while maintaining the natural functions of endogenous CHDP to resolve infections [123, 125]. The increased inflammatory response reported by Jiao *et al* [290] may also be due to the mode of peptide delivery, as they administered cathelicidin CHDP i.n., whereas, I employed s.c. administration of the synthetic IDR peptide in this study. It is thus possible that the modulation of inflammatory responses in the lung may be dependent on the route of delivery of immunomodulatory peptides.

In this study, I demonstrate that IDR-1002 abrogates IL-33 production in a murine model of allergic asthma and in human PBEC, and inhibits IL-33-induced AHR *in vivo*. The cytokine IL-33 is a member of the IL-1 family of cytokines, and acts as an early cytokine inducer of allergic airway inflammation and asthma by promoting eosinophil and neutrophil recruitment and activation [291]. The IL-33/ST2 receptor axis plays a central role in mediating Th2-biased and glucocorticoid-resistant airway inflammation [292, 293]. Recent studies show that IL-33 is significantly increased in severe asthmatics and is a key mediator of steroid-refractory responses in humans [275-277]. In line with this, studies in multiple animal models demonstrate that corticosteroid therapy have no effect on IL-33 lung levels [275, 278]. Consequently, IL-33 is an attractive therapeutic target for chronic airway inflammatory diseases such as severe asthma. Therefore, my findings on the effects of the IDR peptide on IL-33 production and action, and in the processes of allergic airway inflammation and AHR, may contribute to the development of novel therapies for steroid-refractory severe asthma.

IL-33 is known to increase the expression of the KC receptor CXCR2, which can regulate migration of neutrophils [294]. However, the role of IL-33 to increase neutrophil migration is only

partially dependent on the KC-CXCR2 axis [295], as IL-33 by itself is also capable of directly increasing neutrophil migration [290]. Consistent with this, I demonstrate that IL-33 alone increases leukocyte accumulation, including neutrophils, in the lungs. This suggests that IL-33 may play a role as a driver of neutrophilia in the HDM-challenged murine model. As IDR-1002 did not suppress HDM-induced KC expression in the lungs, the peptide may reduce HDM-induced neutrophil lung influx by suppressing IL-33 production. This is supported by my results demonstrating that exogenous administration of IL-33 mitigates the capacity of the peptide to blunt HDM-induced neutrophil accumulation in the lungs, and that IL-33 alone induced neutrophil accumulation in BALF is not reduced by the peptide. Taken together, these results suggest that the suppression of IL-33 production is an essential underpinning for the ability of the peptide to control leukocyte accumulation in the lungs.

Despite the observations that IDR-1002 prevents goblet cell hyperplasia that can be promoted by IL-5 and IL-13, I did not observe any effects of IDR-1002 on IL-5 or IL-13 production in response to allergen challenge in this murine model. This suggests that the peptide may prevent goblet cell hyperplasia by engaging alternate mechanisms, or that it alters the kinetics of responses to IL-5 or IL-13, and thus may not be captured at the time point used to assess outcomes in this study. Nevertheless, I have established the feasibility of exploring an IDR peptide-based immunomodulatory therapy for reducing airway inflammation in allergic asthma, the core mechanism of which appears to be linked to pathways that regulate IL-33 production.

IL-33 is expressed by human epithelial cells [275, 278], and acute inflammatory cytokines TNF and IFNγ can induce IL-33 production in epithelial cells [281, 282]. Recent studies corroborate an association of TNF and IFNγ with severe steroid-resistant asthma [276, 296]. Aligned with these studies, I demonstrate a significant increase in IL-33 production in response to

cytomix (TNF + IFNγ) in human PBEC, and show that this is primarily driven by IFNγ . I conclusively demonstrate that IDR-1002 abrogates IL-33 abundance that is enhanced in response to IFNγ and TNF cytomix in human PBEC. Interestingly, the mechanistic studies show that IDR-1002 does not mitigate response elements of the IFNγ-induced pathway such as IRF1 or IP10, suggesting that the peptide targets signaling intermediates independent of the IFNγ-induced canonical pathway to suppress IL-33 production. Considering that the IFNγ-mediated canonical pathway plays a major role in the ability to fight infections [297], and as IDR peptides are known to protect against infections [128, 132, 269, 270], it is not surprising that IDR-1002 activity does not intervene in the IFNγ-canonical pathway. Unfortunately, upstream pathways responsible for the production of IL-33 are not well known. Therefore, future studies using broad omics-based approaches will be required to delineate the full repertoire of signalling mechanisms that underlie the ability of IDR-1002 to suppress IFNγ-induced IL-33 production.

As airway inflammation is often correlated with AHR [275], I initially speculated that the suppression of IL-33 by IDR-1002 might be essential for preventing allergen-induced lung dysfunction. However, I show that the protective effects of IDR-1002 on allergen-induced AHR are maintained even after exogenous (additional) administration of IL-33. Therefore, I examined whether the peptide intervenes in AHR and/or airway inflammation induced by IL-33 alone challenge. I show conclusively that IDR-1002 significantly reduces IL-33-induced AHR, but not airway inflammation. These results suggest that the ability of IDR-1002 to reduce AHR is not only explained by a reduction of IL-33 production, but also involves mechanisms downstream or independent from IL-33. My findings align with recent studies using multiple antigens in mouse models that show airway inflammation and AHR are mediated by a complex network of biological pathways which do not fully overlap [298, 299]. Furthermore, in humans there are disparate cause-

effect relationships between airway inflammation and AHR [300]. Taken together, the results of this study suggest that the activity of IDR-1002 to mitigate airway inflammation and AHR likely engages different signaling pathways, and offers the opportunity to use IDR peptides in future studies as a probe to delineate unique molecular mechanisms that link airway inflammation and AHR.

A distinct advantage of developing an IDR peptide based immunomodulatory therapy for asthma is the additional benefit of these peptides in resolving infections. IDR peptides can control pulmonary infections including multidrug resistant tuberculosis and biofilm infections recalcitrant to antibiotics [269, 270]. Specifically, IDR-1002 protects against multiple bacterial infections including tuberculosis, and exhibits potent anti-biofilm activity against *Pseudomonas aeruginosa* which is a major problem in chronic pulmonary disease [96, 132, 269]. Recent studies have demonstrated that IL-33 is a key mechanistic link in viral infection-induced synergistic exacerbation of allergic asthma [301]. This is consistent with previous reports demonstrating that patients with severe asthma are more susceptible to pulmonary infections [302]. Therefore, the finding on the ability of IDR-1002 to alleviate allergic airway inflammation and AHR, taken together with previous studies demonstrating its potent antibacterial and anti-biofilm activity, suggests that IDR-1002-based new therapies may be beneficial for asthma without compromising the patients' ability to resolve infections. However, a limitation in this study is that I only utilized a murine model of allergic asthma. As described in the previous chapter, mice do not spontaneously develop asthma and therefore the findings in this study provide a starting point to further investigate the therapeutic potential of IDR peptides in allergic asthma.

In conclusion, in this study I establish the therapeutic potential of an immunomodulatory IDR peptide, IDR-1002, and provide the foundation to develop IDR peptides as an

immunomodulatory therapy for allergic asthma. The mechanisms underlying the activity of IDR-1002 involve suppression of the steroid-resistant mediator IL-33, thus suggesting the potential of IDR-1002-based development of new therapies to be beneficial for severe asthma. Preclinical studies in mice, similar to the 5-day challenge model used in this study, have shown that targeting the IL-33 pathway may be beneficial in treating airway inflammation [213, 303, 304].

However, there are limited studies that comprehensively characterize the inflammatory and physiological responses to IL-33 in the murine airways. Moreover, the global molecular network induced in response to IL-33 has not yet been defined in the lungs *in vivo*. Therefore, in the following chapter, I used the IL-33-challenged mice (5-day challenge) to systematically delineate the changes in inflammation, structural phenotype, and the transcriptome in the lungs of mice in response to IL-33 challenge.

3.3 Comprehensive analyses of IL-33-mediated responses and the lung transcriptome in a murine model

This section contains text and figures from a collaborative project by **Hadeesha Piyadasa** in the Mookherjee research group, with research groups of Drs. Andrew Halayko and Robert E.W. Hancock. H.P. was the lead in this study, performed majority of the experiments and data analyses, contributed to the development of the scientific concepts and wrote the text. RNA-Seq reported in this chapter was performed by Dr. Hancock's research group at University of British Columbia. HP did the data analyses of RNA-Seq with intellectual input from Hancock research group.

3.3.1 Abstract

Background: IL-33 is an inducer of airway inflammation and AHR in respiratory disease such as asthma and COPD. Despite being defined as a therapeutic target, there are limited studies that comprehensively define IL-33-mediated responses in the lungs *in vivo*.

Objective: To characterise global responses induced by IL-33 in the lungs in a murine model.

Methods: IL-33 (1 μg) was administered in female BALB/c mice (i.n.) for 5 days. Lung mechanics was monitored using a flexiVent© ventilator and cell differentials measured using modified Wright-Giemsa staining. Inflammatory mediators were measured using the Mesoscale platform. Transcriptomic profiling of lungs tissues was performed using RNA-Seq and analysed using DESeq2 package in R, with functional enrichment performed using IPA and InnateDB.

Results: IL-33-challenge increased leukocyte accumulation in the bronchoalveolar lavage, AHR and goblet cell hyperplasia, compared to naïve mice. RNA-Seq identified 2279 transcripts up-

regulated and 1378 genes downregulated (≥ 2-fold, $p < 0.01$) in the lungs of IL-33-challenged mice. Bioinformatic interrogation of the RNA-Seq data identified an enrichment of Th2-skewed inflammation and leukocyte migration as top biological pathways, and airway inflammation in asthma as a top upregulated network while PU.1, E1AF, E2F family, TEL-2A and NRF-2 were predicted to be activated transcription factors induced by IL-33. STAT4, a predicted upstream regulator of IL-33 responses based on IPA, was validated to be upregulated in response to IL-33 in the lungs. IL-33-challenge also increased the expression of many cytokines including IL-4, IL-5, IL-6, IL-10, MIP1α and IP10, at both the transcript and protein level.

Conclusion: This study comprehensively defined IL-33-induced responses in the lungs *in vivo* demonstrating a major Th2-skewed inflammatory response. The specific IL-33-induced molecular targets and hubs defined in this study can be used to assess outcomes in a murine model, for example in studies examining novel interventions to target the downstream effects of IL-33.

3.3.2 Rationale and Introduction

IL-33 is an important cytokine involved in orchestrating the inflammatory phenotype and tissue damage in the lungs. IL-33 contributes to the pathogenesis and progression of various chronic inflammatory diseases, including idiopathic pulmonary fibrosis [303, 305], asthma and COPD [303]. Even though targeting of the IL-33 pathway is being examined as a therapeutic strategy for chronic pulmonary diseases, there are limited studies that have characterized the network of molecular expressions in response to IL-33 *in vivo* [306, 307]. This study provides an assessment of the cellular, immunological, physiological and transcriptomic responses in an IL-33-challenged mice.

IL-33 is primarily expressed by non-hematopoietic cells such as epithelial, endothelial and fibroblast-like cells [308]. It is a chromatin-associated cytokine released after cell injury as an alarmin and/or in response to inflammation [309]. IL-33 in the lungs is released in response to environmental insults such as allergens, respiratory pathogens and air pollution [310-313]. IL-33 mediates its function by binding to the receptor ST2, a member of the IL-1 receptor family and co-receptor IL-1-receptor accessory protein (IL-1RAcP) [309, 314]. ST2 is expressed on various leukocytes such as Th2 cells, ILC2, eosinophils and neutrophils [310, 311]. In the lungs, ST2 is highly expressed on lung resident immune cells, ILC2, mast cells and tissue-resident regulatory T-cells (Tregs) [310]. The central role of IL-33 in airway inflammation have been shown in various studies using IL-33/ST2 deficient mice or anti-IL-33 antibodies [311, 315-320]. Previous studies have demonstrated that airway inflammation induced in response to allergens such as *Alternaria spp*, HDM, and ovalbumin is significantly attenuated in models deficient of either IL-33 or its receptor ST2 [311, 315-317]. Similarly, IL-13, mucins and bleomycin-induced lung fibrosis is also attenuated in the absence of IL-33 or ST2 [318, 319]. Aligned with this, an elevated level of

IL-33 has been reported in allergic asthma in human airway samples, including sputum, BALF, and airway epithelial cells, and levels correlated with the clinical severity of disease and chronic inflammation [277, 305, 320]. Moreover, genome wide associated studies have demonstrated an association of *IL33* and *ST2* gene variants with asthma [321]. Recent studies have also shown that the IL-33-ST2 pathway is a mediator of the steroid-resistant phenotype in airway and nasal inflammation [275, 322]. Consequently, targeting IL-33 is being examined as a therapeutic option for chronic airway disease, especially for steroid-refractory severe asthma.

Preclinical studies have shown that targeting the IL-33 pathway may be beneficial in treating airway inflammation [303]. Mice are commonly used as preclinical models to study the mechanistic impact of IL-33 on inflammatory airway disease [213, 304]. However, there are limited studies that comprehensively characterize the inflammatory and physiological responses to IL-33 in the murine airways. Moreover, the global molecular network induced in response to IL-33 has not yet been defined in the lungs *in vivo*. Therefore, in this study I used a murine model to systematically delineate the changes in lung mechanics, immune cell accumulation, inflammation and the transcriptome in response to IL-33 challenge. In chapter 3.2, I showed that IL-33 administration results in decreased lung function and increased accumulation of leukocytes in the lungs of mice. In this study, I further demonstrate that IL-33 administration alters the profile of inflammatory cytokines in the lung tissue and in the BALF in mice, and causes significant goblet cell hyperplasia and airway epithelial cell thickening. A comprehensive transcriptomic analysis of IL-33-induced alterations of the gene expression network in the lungs identified key mechanisms, and signaling intermediates predicted to be upstream regulators of IL-33-induced transcriptomic changes in the lungs. The objective molecular readouts provided in this study can be used to further

interrogate molecular mechanisms associated with IL-33-induced processes, and to predict new targets for intervention in chronic inflammatory airway diseases.

3.3.3 Results

3.3.3.1 IL-33 administration induces AHR in mice: In this study, recombinant murine IL-33 (1 μg) was administered i.n. for five consecutive days. Previous studies [316], including mine [312], have shown that IL-33 challenge induces significant AHR. Therefore, in this study lung mechanics was assessed using increasing dose of methacholine challenge and a flexiVent™ small animal ventilator, 24 hr after the last IL-33 challenge. IL-33 administration significantly increased Newtonian resistance (Figure 3.1A), tissue damping (Figure 3.1B) and tissue elastance (Figure 3.1C). The increases in all three parameters after IL-33 challenge were statistically significant at doses as low as 12 mg/mL methacholine, when compared to naïve mice. IL-33 administration resulted in a more than 5-fold increase in Rn at the 50 mg/mL methacholine dose, when compared to naïve mice (Figure 3.1A). IL-33 administration also increased tissue damping by 15-fold, and tissue elastance by 10-fold at the maximum methacholine dose of 50 mg/mL, compared to naïve mice (Figure 3.1B and 3.1C respectively). Further, IL-33 administration increased sensitivity to methacholine by 4.7-fold (Figure 3.1D). These results showed that exogenous administration of IL-33 induced resistance in the main airways (Rn), resistance in the alveoli (G) and tissue elastance (H), thereby contributing to decline in lung function. These results are consistent with previous studies [312, 316], thus support the IL-33 administration murine protocol used in this study.

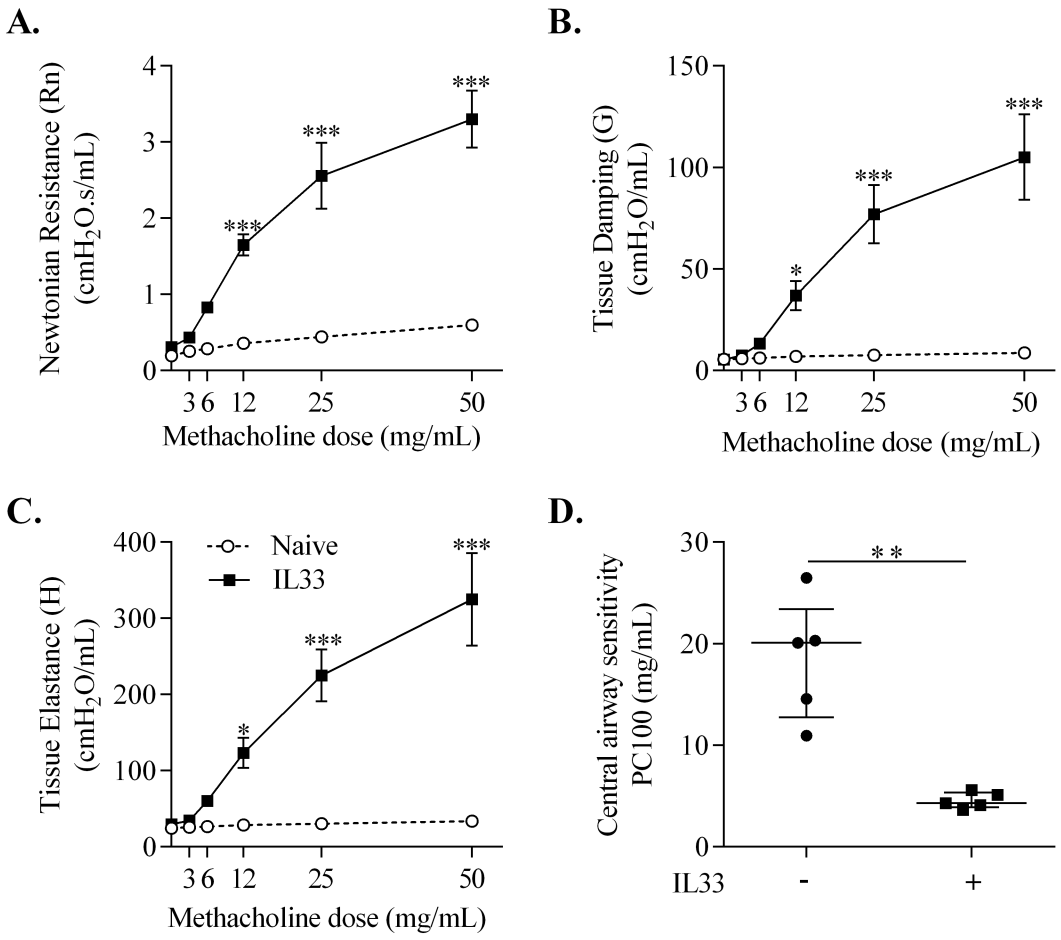

Figure 3.1: IL-33 induces AHR in mice. *Mice (n = 5 per group) were challenged with murine IL-33 in saline i.n., for five consecutive days. Lung mechanics were monitored, 24 hr after the last IL-33 challenge. Mice were exposed to nebulized saline (baseline measures) followed by increasing concentrations of nebulized methacholine (3-50 mg/mL) and changes in* ***(A)*** *Newtonian resistance (Rn),* ***(B)*** *tissue damping* ***(G)****,* ***(C)*** *tissue elastance* ***(H)*** *was monitored.* ***(D)*** *Central airway sensitivity determined by calculating PC100 (amount of methacholine required to increase the baseline Newtonian resistance by 100%). Statistical significance was determined for (A, B, C) using two-way repeated measures ANOVA with Bonferroni correction, and (D) using Mann Whitney U test (*p ≤ 0.05, **p ≤ 0.01, ***p ≤ 0.001).*

3.3.3.2 Administration of IL-33 increases leukocyte accumulation in the lung: Previous studies have shown that IL-33 enhances the production of chemokines such as CCL3 (MIP1α) and CCL7 (MCP3), as well as the expression of chemokine receptors, e.g. CCR3, to induce migration of immune cells [290, 323-325]. To more broadly assess the effect of IL-33 administration on leukocyte accumulation into the murine lungs, BALF samples were collected 24 hr after the last IL-33 challenge. There was a significant increase in total immune cells (by 17.9 ± 1.8-fold) in the BALF of IL-33-challenged mice when compared to naïve mice (Figure 3.2A). Differential cell analysis using H&E staining showed that eosinophils and neutrophils were significantly increased following IL-33 challenge, when compared to the negligible amounts in naïve mice (Figure 3.2B and 3.2C respectively). Similarly, macrophages were increased (by 5-fold) and lymphocytes (by 16.8 ± 2.8-fold) in the BALF of IL-33-challenged mice, compared to naïve (Figure 3.2D and 3.2E respectively). These results demonstrated that exogenous administration of IL-33 significantly increased leukocytes in the lungs of the murine model, which is also consistent with previous studies [317] [316], further validating the IL-33 challenge model used in this study.

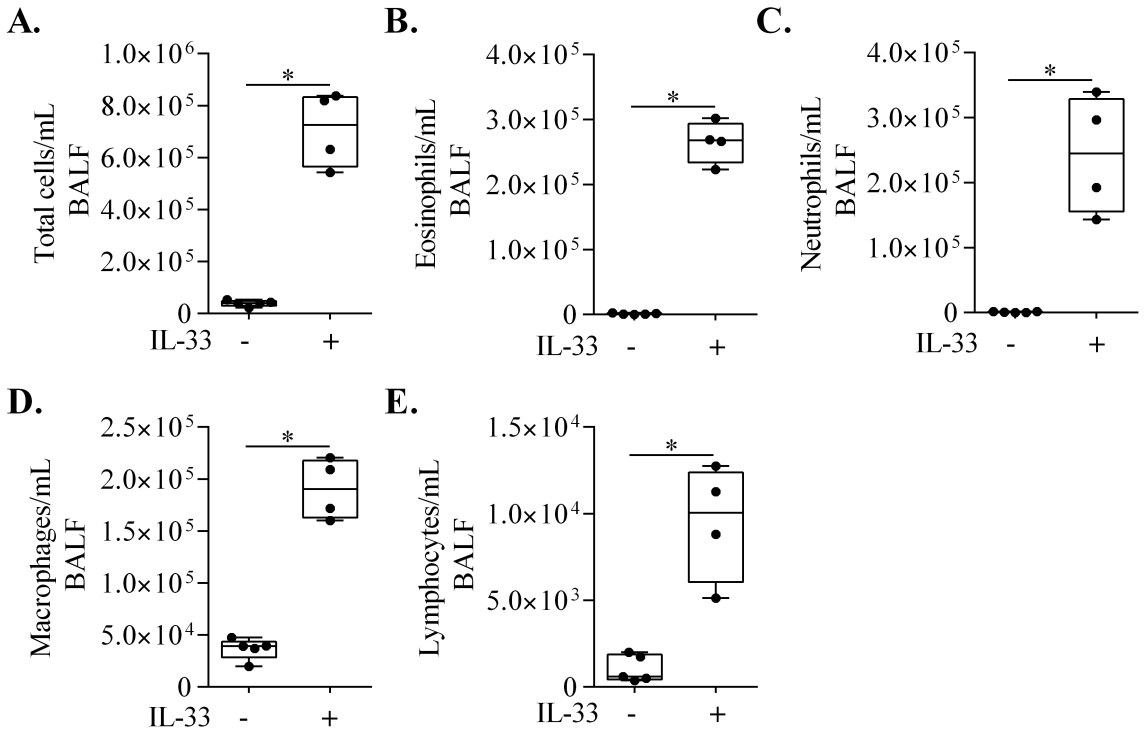

Figure 3.2: IL-33 challenge induces cellular accumulation in the lungs. *Mice were challenged with murine IL-33 in saline i.n., for five consecutive days. BALF was collected from naïve (n=5), and IL-33 challenged (n=4), 24 hr after the last IL-33 challenge and* ***(A)*** *Total cell,* ***(B)*** *eosinophil,* ***(C)*** *neutrophil,* ***(D)*** *macrophage, and* ***(E)*** *lymphocyte numbers were assessed. Bar's show median and interquartile range. Statistical significance was determined by Mann Whitney U test (*p ≤ 0.05).*

3.3.3.3 IL-33 challenge induces goblet cell hyperplasia and increases epithelial layer thickening in airways: IL-33 has been previously shown to induce airway remodeling including epithelial thickening and goblet cell hyperplasia [213, 275, 325-327]. To confirm these structural changes in the airways in the murine model following IL-33 administration, I assessed alterations in airway epithelial thickness and goblet cell numbers by histological analyses. Consistent with the observed cell differentials in BALF (Figure 3.2), H&E staining demonstrated an increased accumulation of cells in the peribronchial and perivascular spaces in IL-33-challenged mice, when compared to naïve mice (Figure 3.3A). H&E staining further showed an increase in epithelial cell thickness in the airways of IL-33 challenged mice when compared to naïve mice (Figure 3.3B). PAS staining showed a significant and large number of goblet cells in large airways in response to IL-33 challenge, when compared to the background levels observed in naïve mice (Figure 3.3C and 3.3D). Taken together, these results (Figures 3.1-3.3) demonstrated that the exogenous administration of IL-33 resulted in cellular and structural changes in the murine lung consistent with previous observations [213, 275, 325-327].

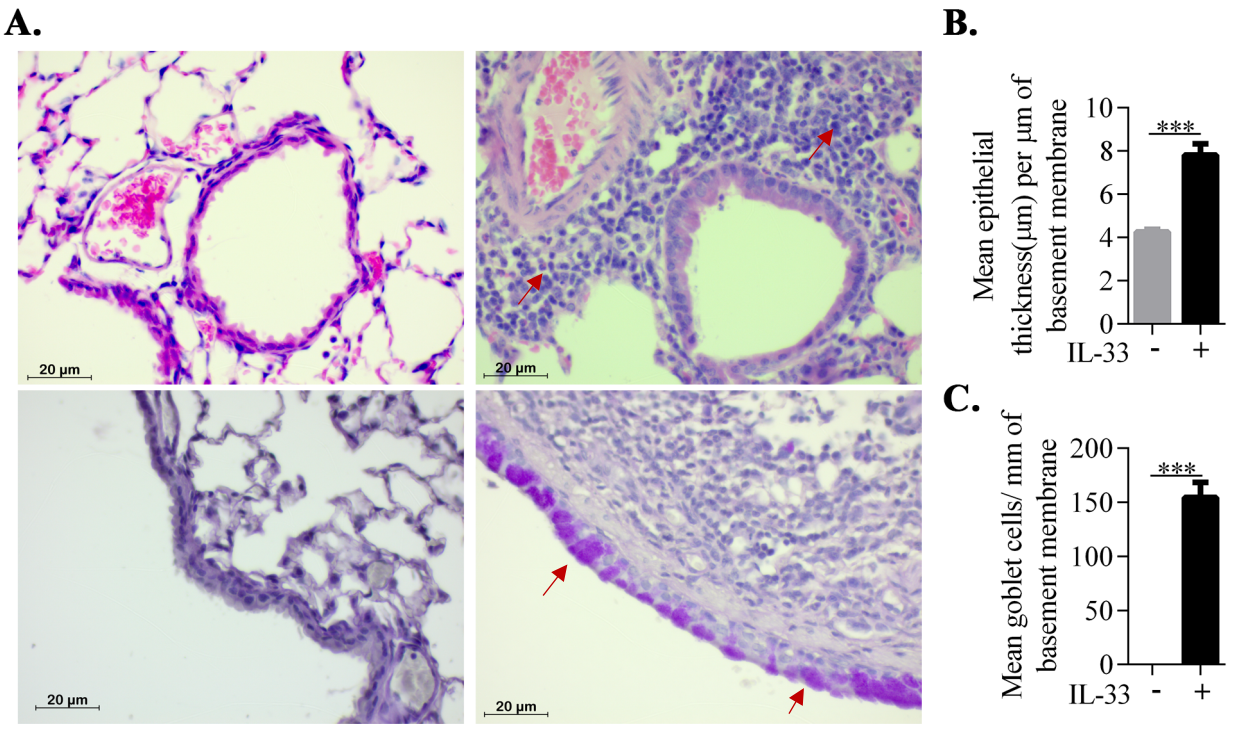

Figure 3.3: Histological assessment of lung sections. *Mice (n = 4 per group) were challenged with murine IL-33 in saline i.n., for five consecutive days. Paraffin-embedded lung sections (6 µm) from naïve and IL-33 challenged mice were stained with* ***(A)*** *hematoxylin and eosin (H&E) to enumerate cell accumulation (Red arrows point to accumulated cells) and* ***(B)*** *epithelial thickening,* ***(C, D)*** *PAS to assess goblet cells (Red arrows point to goblet cells). Statistical significance was determined by unpaired t test (***p ≤ 0.001).*

3.3.3.4 Cytokine profile in lung tissue lysates and BALF: Previous studies have shown that IL-33 plays a key role in airway inflammatory diseases by altering local cytokines, such as IL-13 and IL-4 [309, 311]. Therefore, to broadly monitor cytokines in the murine lung tissue and the BALF, the multiplex MSD platform was used to measure the abundance of 27 different cytokines (detailed in Table 3.1). There was a significant increase in the abundance of 15 analytes, which included cytokines IL-1β, IL-2, IL-4, IL-5, IL-6, IL-9, IL-10, IL-17A and TNF, and chemokines KC, MCP1, MIP1a, MIP2, MIP3a and CXCL10 (IP-10), in both the lung tissue homogenates and BALF (Table 3.1) obtained from IL-33-challenged mice compared to naïve mice. IL-30 abundance was uniquely increased in the lung tissue but not in the BALF (Table 3.1), and in contrast IL-16 and IFNγ were significantly increased in the BALF but not in the lung tissue lysates following IL-33 challenge (Table 3.1). Conversely IL-12p70 and IL-30 abundance were not altered in the BALF in response to IL-33 treatment (Table 3.1). Similarly, IFNγ, IL-12p70, IL-17C, IL-17F, IL-17AF, IL-15, IL-21, IL-22, IL-23, IL-25 and IL-31 were not altered, in lung tissue lysates, by IL-33 challenge (Table 3.1). Several cytokines such as IL-15, IL-17C, IL-17AF, IL-17F, IL-21, IL-22, IL-23, IL-25 and IL-31 were not detected in the BALF (Table 3.1). Taken together, these results demonstrated that IL-33 administration alters the inflammatory cytokine and chemokine profiles in the murine lungs.

Table 3.1: IL-33 induced cytokine profile in lungs. *Mice (n = 5 per group) were challenged with murine IL-33 in saline i.n., for five consecutive days. Lung tissue lysates and BALF obtained from naïve and IL-33-challenged mice were monitored for levels of a panel of cytokines, 24 hr after the last IL-33 challenge. Median values are reported for each cytokine. Statistical analyses were performed using the Mann-Whitney U test (*p ≤ 0.05, **p ≤ 0.01).*

Cytokine	Lung Tissue Lysates				BALF			
	Naïve (pg/mL)	IL-33 (pg/mL)	Fold Change	P value	Naïve (pg/mL)	IL-33 (pg/mL)	Fold Change	P value
IFNγ	0.6	0.9	1.4	0.413	0.0	0.1	NA	**0.048***
IL-1β	81.9	699.9	8.5	**0.008****	0.2	8.7	57.7	**0.008****
IL-2	1.9	3.5	1.9	**0.008****	0.0	1.2	NA	**0.008****
IL-4	0.6	125.7	199.5	**0.008****	0.1	19.5	390.0	**0.016***
IL-5	2.4	685.9	283.4	**0.008****	0.2	1220.4	6101.8	**0.016***
IL-6	54.7	852.2	15.6	**0.008****	0.0	114.6	NA	**0.016***
KC	127.9	1164.5	9.1	**0.008****	19.8	131.1	6.6	**0.016***
IL-10	2.0	24.3	12.0	**0.008****	0.2	5.7	38.0	**0.016***
IL-12	82.6	101.9	1.2	0.95	0.0	20.0	NA	0.246
TNF	28.9	116.6	4.0	**0.008****	6.6	22.9	3.5	**0.016***
MIP3α	522.3	2299.2	4.4	**0.008****	85.0	237.3	2.8	**0.016***
IL-22	1.0	1.8	1.8	0.667	0.0	0.0	NA	1
IL-23	5.0	8.5	1.7	0.667	0.0	0.0	NA	1
IL-17C	21.1	12.4	0.6	0.151	0.0	0.0	NA	1
IL-31	130.1	174.7	1.3	0.667	0.0	0.0	NA	1
IL-21	168.8	242.2	1.4	0.802	0.0	0.0	NA	1
IL-17F	1285.8	2784.6	2.2	0.151	0.0	0.0	NA	1
IL-16	NA	NA	NA	0.31	53.6	2827.5	52.8	**0.016***
IL-17A	1.0	7.6	7.7	**0.008****	0.0	0.7	NA	**0.048***
IL-25	0.4	23.8	56.7	0.087	0.0	0.0	NA	1
IL-9	0.0	7.6	NA	**0.008****	0.5	48.7	108.2	**0.016***
MCP1	188.1	922.6	4.9	**0.008****	0.0	29.7	NA	**0.008****
IL-30	6.5	22.4	3.4	**0.008****	0.3	0.0	0.0	0.683
IL-15	40.9	76.5	1.9	0.31	0.0	0.0	NA	1
IL-17A/F	3.2	5.6	1.7	0.222	0.0	0.0	0.0	0.444
MIP1α	87.0	2062.5	23.7	**0.008****	3.2	61.7	19.3	**0.016***
IP10	144.3	350.0	2.4	**0.008****	1.5	17.9	12.3	**0.016***
MIP2	63.6	686.8	10.8	**0.008****	10.8	29.6	2.7	**0.016***

3.3.3.5 IL-33-mediated lung transcriptome in mice: To obtain a comprehensive understanding of the effects of IL-33 on the lungs, I performed RNA-Seq on mouse lung tissue samples (n = 5 each of naïve and IL-33-challenged mice). Differential gene expression analysis was performed using the DESeq2 package in R where genes altered by ≥ 2-fold with adjusted $p \leq 0.01$ were considered to be DE (Figure 3.4A). RNA-Seq analysis showed that 2279 genes were upregulated and 1378 genes were downregulated in the murine lungs in response to IL-33 challenge (after removal of low count poorly expressed genes with less than 10 counts in at least 5 samples), compared to naïve mice (Figure 3.4A and 3.4B). Principal Component Analysis (PCA) clustered all of the naïve mice separately from IL-33-challenged mice on the first principal component which accounted for 93% of variance (Supplementary Figure 3.1). IL-33 administration resulted in the increased expression of genes encoding for cytokines known to be involved in airway inflammation primarily *Il13* (>600- fold), *Il5* (89-fold) and *Il4* (18-fold), in addition to IL-33 receptor S*t2* (30-fold), Treg-related gene *foxp3* (7-fold) and the mucin genes M*uc5ac* (35-fold) and M*uc5b* (3-fold) (Figure 3.4B). Genes related to eosinophil activation including *Epx*, *Ear2*, *Prg2* and *Prg3* were among the top 50 genes significantly upregulated in response to IL-33 compared to naïve mice (Supplementary Table 3.1). Similarly, neutrophil activation markers L*y6g, Itgm* and *Cd63* were also significantly upregulated in IL-33-challenged mice compared to naïve. Moreover, gene encoding for *Arg1*, a known marker of lung diseases such as cystic fibrosis and asthma, was upregulated by more than 250-fold fold following IL-33 administration (Figure 3.4B). IL-33 challenge also increased gene expression of the CC family of chemokine receptors and ligands (Table 3.2).

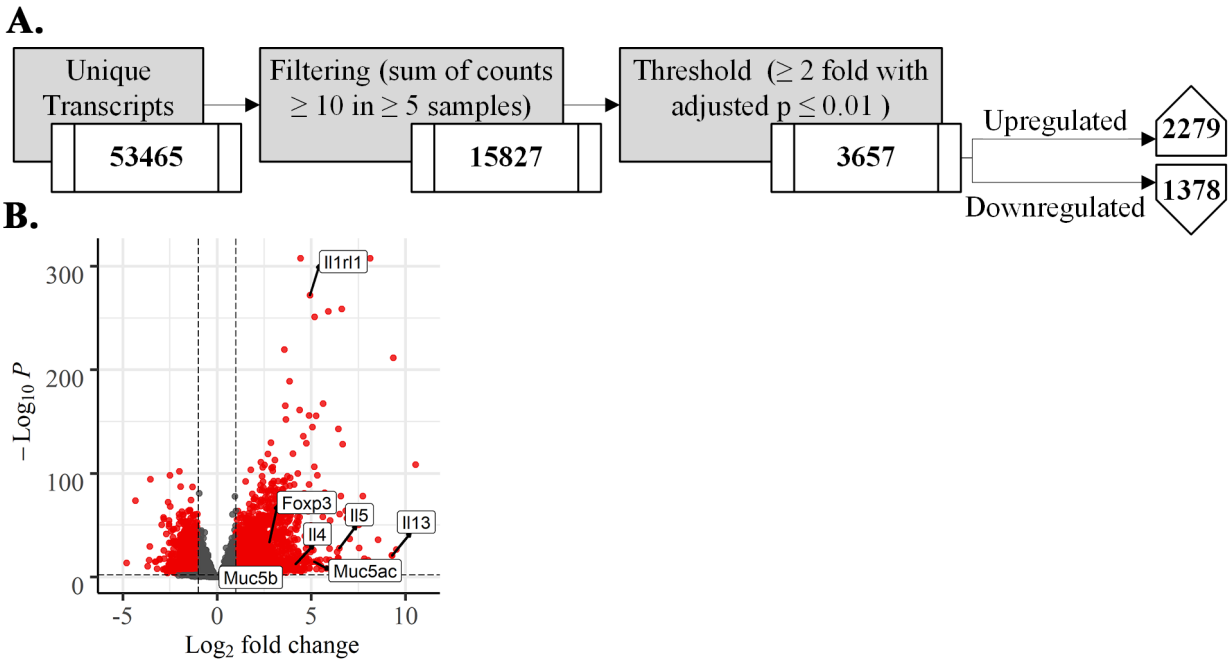

Figure 3.4: Administration of IL-33 significantly alters gene expression in the lungs of mice. *Mice (n = 5 per group) were challenged with murine IL-33 in saline i.n., for five consecutive days. RNA was extracted from lung tissues of saline and IL-33 challenged mice.* ***(A)*** *RNA-Seq data analysis pipeline.* ***(B)*** *Volcano plot representation of differentially expressed genes due to IL-33 administration.*

Interrogation of the IL-33-mediated DE genes for Gene Ontology terms (GO) using the PANTHER Overrepresentation tool showed enrichment of 9 leukocyte migration and chemokine-mediated signaling pathways among the top 15 biological processes sorted by fold enrichment in response to IL-33 (Supplementary Table 3.2). IPA bioinformatics tool predicted that the top 3 biological pathways activated in response to IL-33 challenge were EIF2 signalling, Th2 activation and leukocyte extravasation pathways (Supplementary Table 3.3). 21 of the top 50 upregulated genes were contained in a single biological network (Supplementary Figure 3.2). Upstream regulators predicted by to be involved in the regulation of IL-33-induced genes were namely STAT4, STAT6, HMGB1 and CARM1 (Figure 3.5), all of which are known to be involved in airway disease and asthma. TFBS over-representation analysis of the upregulated genes using

InnateDB biomolecular analysis tool (Hypergeometric algorithm and Benjamini Hochberg correction method) predicted over-representation of transcription factors PU.1, E1AF, E2F family, TEL-2A and NRF-2 in response to IL-33 [219].

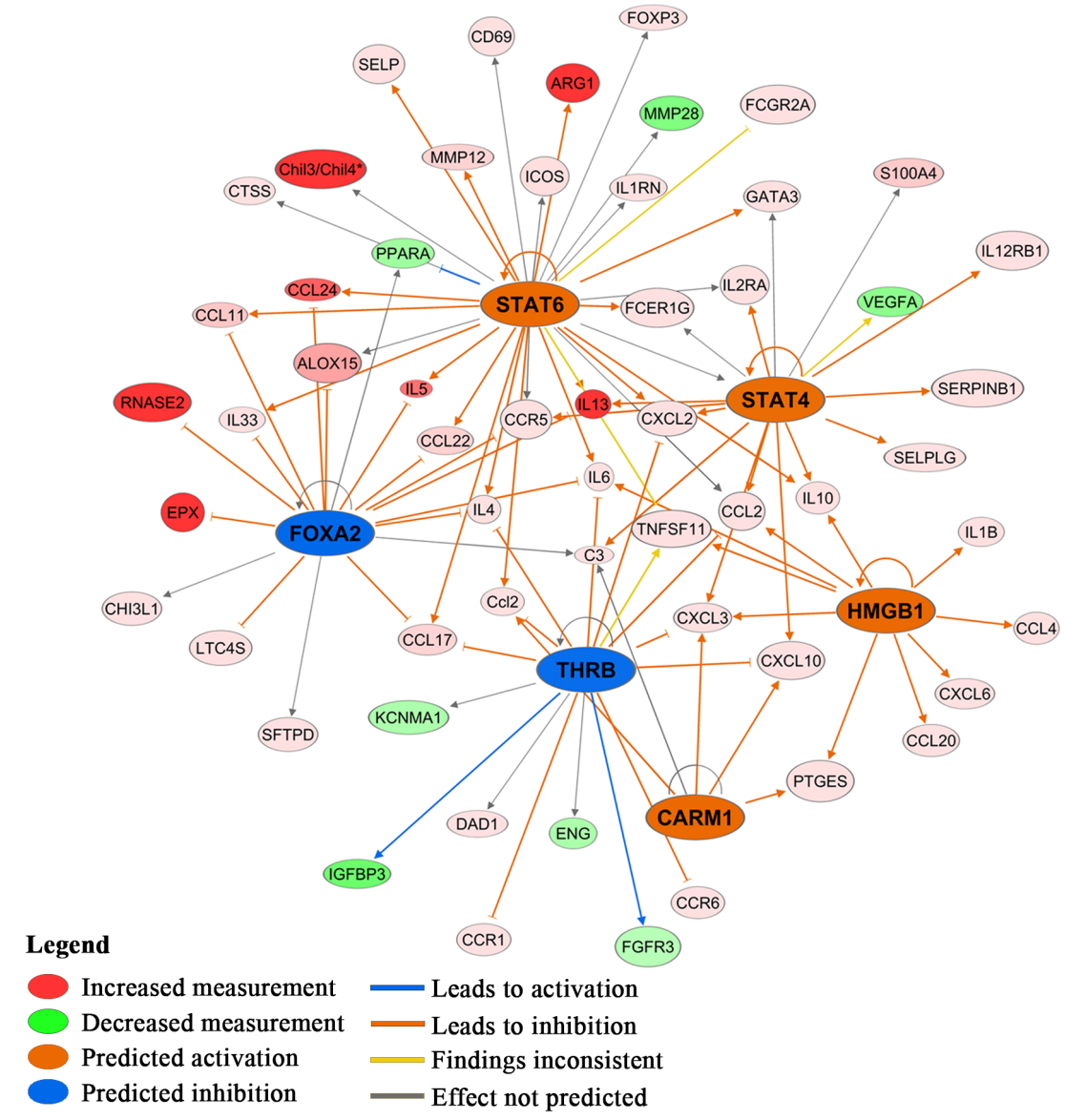

Figure 3.5: Predicted upstream regulators by IPA in response to IL33. *Biological network of predicted upstream regulators in response to IL-33. Red nodes are upregulated genes, and green nodes are downregulated genes, in response to IL-33 compared to naïve mice. The intensity of the colour depicts the degree of regulation (darker = higher magnitude change). Different coloured lines depict different predicted activation states as indicated in the legend.*

Table 3.2: CC family chemokines and receptors differentially regulated in RNA-Seq dataset response to IL-33 compared to naïve mice. *Detected ligands overlapped for multiple receptors [328-332].*

Chemokines	Fold Change	Adjusted P value	Associated Chemokine Receptor	Fold Change	Adjusted P value	Receptor Distribution
CCL3	3.0	1.6E-06	CCR1	3.1	3.9E-21	Neutrophils, Macrophages, Lymphocytes
CCL6	3.9	8.5E-76				
CCL7	19.2	2.2E-23				
CCL8	86.9	1.5E-143				
CCL2	8.2	4.9E-19	CCR2	3.8	5.9E-45	Macrophages, Lymphocytes
CCL7	19.2	2.2E-23				
CCL8	86.9	1.5E-143				
CCL12	5.6	3.0E-11				
CCL7	19.2	2.2E-23	CCR3	31.4	1.8E-50	Eosinophils, Lymphocytes
CCL11	35.9	6.4E-252				
CC24	101.5	7.6E-129				
CCL17	27.5	4.7E-32	CCR4	17.9	2.0E-52	Macrophages, Lymphocytes
CCL22	29.4	1.0E-156				
CCL3	3.0	1.6E-06	CCR5	6.4	1.4E-119	Macrophages, Lymphocytes
CCL4	4.9	2.9E-08				
CCL8	86.9	1.5E-143				
CCL11	35.9	6.4E-252				
CCL20	5.4	2.1E-06	CCR6	2.1	1.2E-03	Lymphocytes
CCL8	86.9	1.5E-143	CCR8	34.9	3.2E-77	Macrophages, Lymphocytes
No ligands detected			CCR9	4.6	8.0E-15	Lymphocytes

3.3.3.6 Validation of transcriptomics data: As discussed above, bioinformatics interrogation of the top 50 DE genes predicted the involvement of four upstream regulators, STAT4, STAT6, HMGB1 and CARM1, in inducing IL-33-mediated alteration of the lung transcriptome. Therefore, I performed independent western blot analysis to examine the expression of these four predicted upstream regulators in the lung tissue homogenates. Abundance of STAT4 was significantly increased in response to IL-33 challenge compared to naïve mice (Figure 3.6, Supplementary Figure 3.3). HMGB1 and CARM1 levels were not detected in the lung tissue homogenates using western blots, and the expression of STAT6 total protein did not significantly change in the lung tissues obtained from IL-33-challenged mice compared to naïve in independent validation

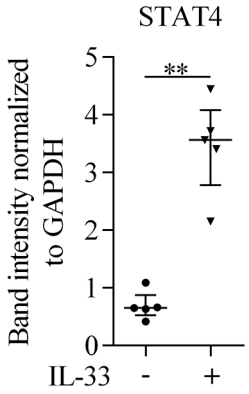

Figure 3.6: Administration of IL-33 significantly STAT4 protein in the lungs of mice. *Mice (n = 5 per group) were challenged with murine IL-33 in saline i.n., for five consecutive days. Protein was extracted from lung tissues of saline and IL-33 challenged mice. Western blot analysis of STAT4. Statistical analyses were performed using the Mann-Whitney U test (*p ≤ 0.05, **p ≤ 0.01).*

Comparative analyses of the multiplex MSD data with RNA-Seq dataset identified seven different cytokines that were significantly increased in response to IL-33, both at the transcript and protein level. *Il4*, *Il5*, *Il6*, *Il10*, *Ccl3* and *Cxcl10* were significantly upregulated at the mRNA level by 2- to 70- fold in response to IL-33, compared to naïve mice (Figure 3.7). Consistent with this, protein abundance of these cytokines was also significantly increased between 2.4 to 6102-fold in the lungs of the IL-33-challenged mice compared to naïve mice (Figure 3.7, Table 3.1). Moreover, cytokines that were not upregulated according to the RNA-Seq data i.e. the IL-17 family cytokines, IL-21, IL-22, IL-23, IL-30, IL-31, IFNγ and IL-12, were also not increased at the protein level in the lungs after IL-33 challenge (Table 3.1). These results indicate that specific cytokines (such as IL-4, IL-5, IL-6, IL-10, MIP1α and IP10) can serve as realiable signatures to assess response to IL-33, as these were increased both at the transcript and protein level in the lungs of IL-33-challenged mice compared to naïve.

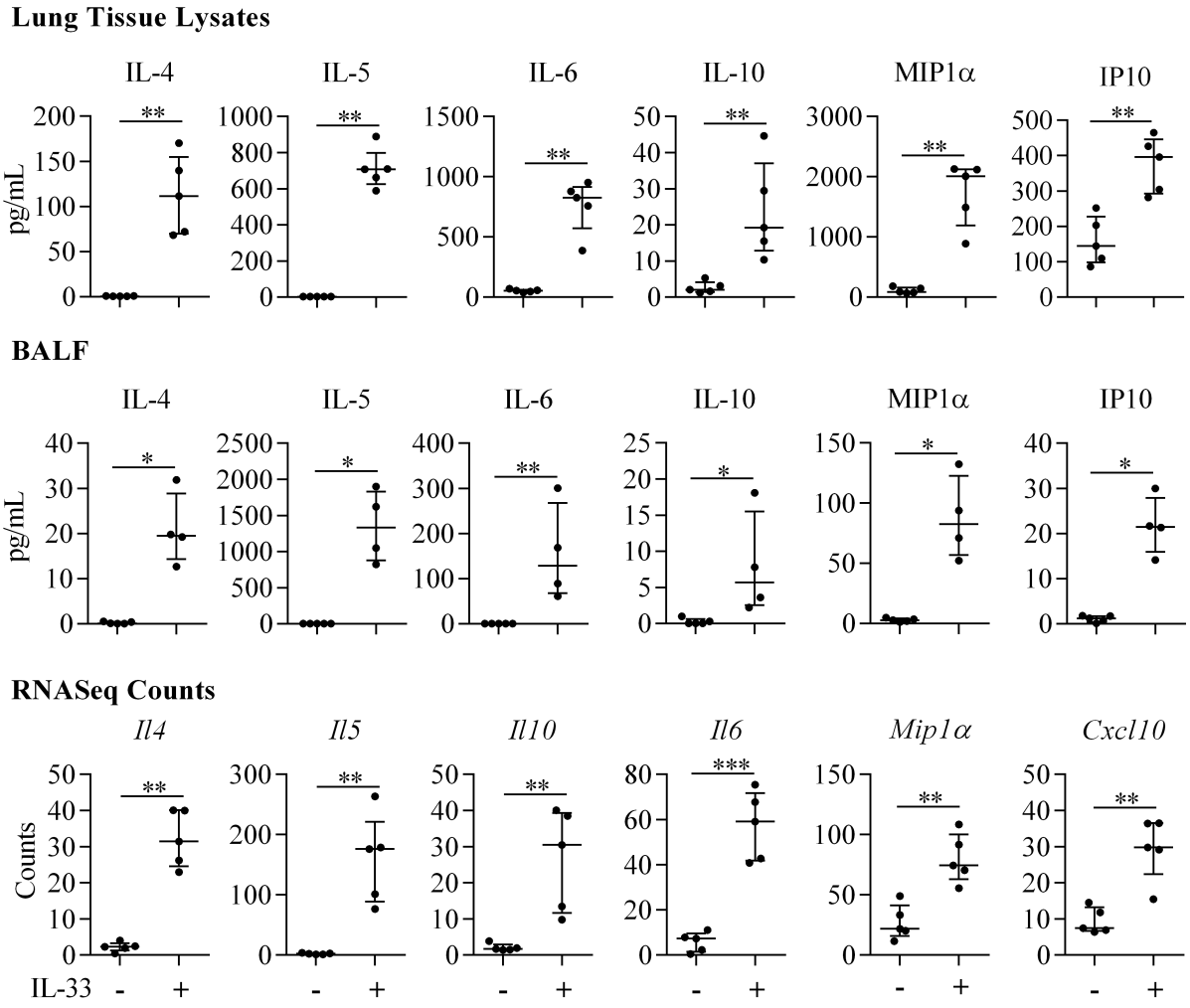

Figure 3.7: IL-33 induced cytokine found at the transcript and protein levels in lungs. *Mice were challenged with murine IL-33 in saline i.n., for five consecutive days. RNA was extracted from lung tissues of saline and IL-33 challenged mice. RNA (n=5 per group), Lung tissue lysates (n=5 per group), and BALF (Naïve n =5, IL-33 n=4) obtained from naïve and IL-33-challenged mice, 24 hr after the last IL-33 challenge. Cytokines, monitored by the multiplex MSD platform that were commonly increased by IL-33 in the* ***(A)*** *lung tissue and* ***(B)*** *BALF and* ***(C)*** *RNA-Seq dataset. Each dot represents individual mouse. Bar's show median and interquartile range. Statistical analyses were performed using the Mann-Whitney U test (*p ≤ 0.05, **p ≤ 0.01).*

3.3.4 Discussion and Conclusion

In this study, I evaluate the immunological and pathophysiological responses following IL-33 administration to the lungs of mice. The IL-33 challenge protocol used in this study resulted in AHR, increased accumulation of immune cells in the BALF and goblet cell hyperplasia, consistent with previous studies [275, 311, 312, 325, 327]. This study also defines a signature of cytokines that are significantly increased in the BALF and lung tissue following IL-33 challenge in mice. In addition, global transcriptional changes in murine lung tissue in response to inhaled IL-33-challenge is detailed in this study. The results of this study provide a comprehensive evaluation of IL-33-induced responses *in vivo*, and identify specific IL-33-induced molecular targets that can be used as outcomes in a murine model, for example in studies examining novel interventions to target downstream effects of IL-33.

IL-33 is strongly implicated in the pathophysiology of various inflammatory airway diseases including asthma and COPD [320, 333]. Epidemiological studies have linked the severity of disease to the levels of IL-33 which underscores the importance of studying the effect of IL-33 on the lungs [277, 305]. Therefore, examining the immunological and physiological effects of IL-33 is crucial in understanding the role and targeting IL-33 in airway diseases. Murine models of IL-33 provide a foundation to explore these questions. However, there are limited studies that have comprehensively investigated the effects of IL-33 on the lungs *in vivo* [306, 307]. This study directly addresses this gap in knowledge and provides a comprehensive analysis of the IL-33-induced responses in murine lungs.

In this study, I demonstrate a significant increase in total immune cells in the BALF of mice, with eosinophils and neutrophils accounting for the majority of the leukocyte infiltrates, followed

by macrophages and lymphocytes, in response to IL-33 challenge. Similar responses have been previously reported with allergens such as for HDM-induced airway inflammation in mice [280, 312]. The increase in leukocyte accumulation in the BALF may be a direct effect of IL-33 induced chemokines and chemokine receptors, as well as IL-33 directly acting as a chemoattractant [290, 323, 324]. Consistent with this, RNA-Seq analysis from this study showed that IL-33 significantly upregulates CC family chemokine receptors and associated ligands, known to induce migration of eosinophils, neutrophils, macrophages and lymphocytes. In addition, informatics interrogation of the IL-33-induced genes showed that the leukocyte extravasation pathway is a prominently induced biological pathway along with enrichment of leukocyte migration and chemokine-mediated signaling pathways in response to inhaled IL-33 in murine lungs, thus supporting the role of IL-33 as a chemoattractant for leukocytes

Biological network analysis of the top 50 IL-33-upregulated genes in this study clearly indicates that IL-33 administration results in pathways related to airway inflammation and respiratory disease. The transcriptomic profile in response to IL-33 reported here are consistent with, and expanded upon, previous studies indicating an association of IL-33 with the severity and pathogenesis of respiratory diseases characterized by airway inflammation such as allergic asthma [277, 305, 320]. In this study, I also demonstrate that IL-33 administration significantly induces the expression of neutrophil activation markers *Ly6g, Itgm* and *Cd63,* and markers of eosinophil activation such as *Epx, Ear2, Prg2,* and *Prg3*. In addition, IL-33 significantly increases both gene expression and protein production of IL-4 and IL-5. Both of these cytokines direct Th2 cell polarization and activation, as well as differentiation of eosinophils, thus contributing to airway inflammation, increased leukocyte accumulation into the lungs and subsequent tissue remodeling [266, 325, 334, 335]. It is worth noting that the IL-17-family of cytokines were not

detected to be upregulated in response to IL-33, based on either RNA-Seq data or MesoScale cytokine analyses of BALF or lung tissue lysates. Furthermore, Th1-cytokines such as IFNγ, IL-2 or TNF were also not significantly dysregulated in response to IL-33. This indicates that IL-33 predominantly drives a Th-2-skewed response in the lungs. Overall, in this study I provide a panel of specific molecular indicators associated with chemoattraction and activation of leukocytes in response to IL-33, in particular promoting eosinophil and neutrophil accumulation and consequent airway inflammation.

Chronic airway inflammation is often associated with lung fibrosis and tissue remodeling. A known downstream target of IL-33 is IL-13, which is a major contributing factor of Th2-skewed responses, goblet cell hyperplasia and airway remodeling in the lungs [336, 337]. Consistent with this, I show that gene expression of *Il13* and one of its receptor subunits *Il13ra2* are significantly upregulated in the lung tissues of IL-33-challenged mice (Supplementary Table 3.1). Furthermore, IL-33 administration increases chemokine *Ccl12* mRNA expression which encodes for macrophage chemokine MCP-5, known to play a critical role in inducing lung fibrosis primarily by attracting circulating fibrocytes in the lungs [338]. Consistent with this, IL-33 is known to directly induce lung fibrosis through alternatively activated macrophages [319]. . Alternative macrophage activation markers, Arg1 and IL4, were also was upregulated in response to IL-33, along with the chemokines CCL-3 (MIP1α), CCL20 (MIP3α), CXCL1 (KC) and CXCL3 (MIP1α). Interestingly, CCL12 and MCP1/CCL2, both induced by IL-33 administration, are potent chemoattractants for macrophages [339], suggesting that IL-33 might be orchestrating lung fibrosis, in part by inducing IL-13, IL-4, IL-5, CCL12 and CCL2 to attract, differentiate and activate macrophages. These results provide a further rationale for targeting IL-33 and/or IL-33-induced molecular mechanisms, as discussed above, for intervening in the process of lung fibrosis.

IL-33 also contributes to fibrosis and structural changes in the lungs by increasing airway epithelial basement membrane thickening in patients with severe steroid-resistant asthma [275]. Consistent with this, I confirmed that IL-33 administration in mice results in an increase in the thickening of the epithelial cells surrounding the airways, goblet cell hyperplasia in the upper airways, and an increase in the expression of mucin genes that are uniquely expressed by goblet cells in the lungs [340]; all of these mechanisms are known to contribute to blocking of the airways and increase in AHR. The physiological impact of IL-33 as seen by the increase in AHR was also confirmed in this study. However, known muscarinic receptors M2 and M3 that bind to bronchoconstrictors methacholine / acetylcholine during the lung function assessment were downregulated in response to IL-33 in this study, which is counterintuitive to the increase in AHR in response to IL-33. A possible explanation is that IL-33 engages mechanisms that might in part be independent of muscarinic receptor activity. As discussed above, narrowing of the airways could be due to an increase in mucus production and epithelial thickening induced by IL-33. In addition, the RNA-Seq data in this study showed that IL-33 significantly upregulates *Arg1* in the lungs of IL-33 treated mice. Arginase 1 is an alternative macrophage marker, which is increased in the lungs of HDM-challenged murine models, and in human asthma patients [341, 342]. Previous studies have demonstrated that arginase 1 competes with nitric oxide synthases (NOS) for arginine [341]. NOS converts arginine to NO which simulates inhibitory noradrenergic noncholinergic nerve (iNANC) resulting in airway relaxation [343]. Conversely, arginase 1 converts arginine to ornithine and urea, which results in a lower requirement for NO, thereby impairing airway relaxation. Thus, the increase of arginase 1 might be a critical pathway leading to increased AHR in response to IL-33. Overall, in this study I have defined several molecular indicators that contributed to IL-33-mediated structural changes and an increase in AHR in the

lungs, all of which were associated with narrowing of the airways and a decrease in breathing capacity.

TFBS analyses in this study predicted a PU.1 transcription binding site in 60 genes that were significantly altered in the lungs in mice following IL-33 challenge. PU.1 is known to positively regulate the ST2 promotor, which is the known receptor for IL-33 [344]. Interestingly, activation of NRF-2, also a predicted over-represented transcription factor in TFBS analysis, inhibits IL-33 release in epithelial cells [345]. This may possibly be an inhibition feedback mechanism to reduce endogenous release of IL-33 due to exogenous administration of IL-33. TFBS analysis also identified ETV4, E2F family and TEL-2A transcription factors to be involved in IL-33-induced responses. E2F family and TEL-2A is involved in proliferation, cell cycle regulation and cell differentiation processes, indicating a possible role for IL-33 in increased proliferation and differentiation of leukocytes. This is also consistent with the PANTHER Overrepresentation test showing 5 out of the top 15 biological processes predicted from the DE genes in response to IL-33 are those that are involved in cell proliferation [346, 347]. ETV4, also known as PEA3 or E1AF have been implicated in upregulation of matrix metalloproteinase (MMP) genes and associated with tumor progression [348-351] This is consistent with previous studies demonstrating that the IL-33/ST2 pathway is associated with MMP induction and contributing to tumor metastasis [352-355]. Consistent with this, the RNA-Seq data in this study revealed multiple MMPs to be significantly upregulated in response to IL-33. However, to my knowledge, E1AF previously has not been directly associated with IL-33-induced MMP induction, which provides an opportunity to further investigate IL-33/ST2/E1AF/MMP axis for molecular mechanisms involved in tumor metastasis.

Among the predicted upstream regulators of IL-33-target genes defined in this study were STAT6 and STAT4. Limited studies have indicated the involvement of STAT6 in IL-33-mediated airway inflammation. However, a study using STAT6-deficient mice showed that STAT6 is not required for IL-33-induced Th2 cytokines in the gut [356]. This is consistent with the independent validation reported in this study, where IL-33 challenge did not significantly increase the expression of STAT6 protein in IL-33-challenged mice compared to naïve. Conversely, STAT4 protein was significantly increased by more than 5-fold following IL-33 administration in the lungs. STAT4 is generally known to be involved in Th1 differentiation and IL-12-mediated IFNγ production [357]. A previous study has demonstrated the involvement of STAT4 through IL-33 in antiviral responses and the dependence of ST2 expression in Th1 cells on STAT4 [358, 359]. Therefore, the finding demonstrating increase in STAT4 expression in response to IL-33 in murine lungs in this study, where characterization of airway inflammation was predominantly Th2-skewed, is a novel finding. These results indicate a possible IL-33-driven association with STAT4 and ST2 receptor in the lungs. Thus, further investigation is warranted on the IL-33/STAT4 axis in chronic respiratory diseases that are characterized by airway inflammation and AHR, such as asthma and COPD.

In summary, this study provides a comprehensive analysis of the molecular responses that contribute to airway inflammation, fibrosis and AHR in the lungs following IL-33 challenge in a murine model, and further provides a baseline dataset that will enable deeper mechanistic interpretation as new insights into these phenomena unfold. I have defined IL-33-mediated transcriptomic changes in murine lungs, and identified potential novel pathways and transcription factors involved in IL-33-mediated pathobiology. In particular, this study demonstrates the upregulation of STAT4 transcription factor in response to IL-33 in the lungs. A limitation in this

study is the use of high concentration of IL-33 which may not represent the physiological levels of IL-33 in the airways. Nonetheless, results of this study will allow further systematic interrogation of IL-33-mediated molecular mechanisms and facilitate targeted intervention strategies to control IL-33 in respiratory diseases such as severe asthma.

In the above described results section 3.1 to 3.3, I have characterized the HDM-challenged and IL-33-challenged mice, and reported the beneficial effect of a synthetic IDR peptide, IDR-1002, on airway inflammation and lung function using the characterized murine models. Although I have reported the beneficial immunomodulatory functions of IDR-1002 in these models, the sequence/structure relationship to immunomodulatory activity of IDR-1002 is limited. Therefore, in the final results section, I examine the immunomodulatory effects of IDR-1002 with single amino acid substitutions HBEC-3KT cells *in vitro* and in the HDM-challenged murine model. The aim was to identify key amino acid residues of IDR-1002 that is responsible for its immunomodulatory biological activity.

3.4 Immunomodulatory activity of IDR-1002 is selectively altered by disrupting a central hydrophobic tryptophan.

This section contains text and figures from a collaborative project by **Hadeesha Piyadasa** in the Mookherjee research group along with Drs. Jason Kindrachuk and Oleg Krokhin. Kinomics was performed in Dr. Kindrachuck's laboratory and Dr. Krokhin collaborated for the biophysical prediction studies and retention time analyses of the peptides.

3.4.1 Abstract

Background: I have previously shown that IDR-1002 can improve AHR and airway inflammation in a HDM-challenged murine model of allergic asthma. However, there is still a limited understanding of the relationship between the specific sequence of IDR-1002 and the immunomodulatory activity mediated by the peptide in airway inflammation.

Objective: In this study, I used a series of single amino acid substitutions to disrupt specific residues of IDR-1002 and examined cytotoxicity and immunomodulatory effects of the peptides *in vitro* using HBEC-3KT cells, and the ability to mitigate allergen-challenged responses in an *in vivo* model.

Methods: 6 different IDR-1002-derived peptides with cationic, polar and large hydrophobic single amino acid substitutions in various segments of IDR-1002 that altered the predicted hydrophobicity and charge of the peptide were selected. IDR peptide experimental hydrophobicity was assessed using retention time on a C18 reverse-phase HPLC column. HBEC-3KT cells were stimulated with IDR-1002 and derivative peptides for 24 hr, cellular cytotoxicity was analyzed by LDH assay and cytokine production by western blots and ELISA. A Kinome array was used to

profile phosphoproteins involved in the bioactivity of IDR peptides using HBEC-3KT cell lysates following stimulation with peptides for 15 min. *In vivo* activity of IDR peptides was assessed by administration of the peptides (6 mg/Kg per mouse, s.c.) in HDM-challenged BALB/c mice. Lung function analysis was performed with increasing dose of methacholine by *flexi*Vent™ small animal ventilator, cell differentials in bronchoalveolar lavage performed by modified Wright-Giemsa staining, and cytokines monitored by MSD assay and ELISA.

Results: I show that a single amino acid substitution of IDR-1002 significantly alters cytotoxicity profile in HBEC-3KT cells. I also show that the tryptophan (W) at position 8 of IDR-1002 is critical for the immunomodulatory activity of the peptide, in particular its ability to induce anti-inflammatory cytokines IL-1RAand STC1, and chemokine MCP1 in HBEC-3KT cells. I further demonstrate that substituting the W8 residue to arginine (R) does not alter the stability or cellular uptake of IDR-1002. I demonstrate that W8 is essential for supressing the pro-inflammatory cytokine IL-33, immune cell accumulation, and altering the relative abundance of 27 cytokines in the lungs of allergen HDM-challenged mice *in vivo*. However, W8 residue of IDR-1002 is not essential for the ability of the peptide to improve AHR in a murine model. In addition, I characterize the effect of W8 substitution of IDR-1002 on cellular signalling molecules using kinome analysis.

Conclusion: This study demonstrates that W8 residue of IDR-1002 is critical for the immunomodulatory activity of the peptide, but not the ability to improve AHR. Therefore, the derivative peptide IDR-1002(W8/R) can be used to study specific molecular mechanisms involved in AHR independent of airway inflammation. Broadly, the results from the sequence/immunomodulatory function relationship from this study can be applied to design novel immunomodulatory peptides with targeted functions.

3.4.2 Rationale and Introduction

CHDP as discussed in chapter 1.2, exerts antimicrobial as well as a wide range of immunity-related functions. Consequently, synthetic IDR peptides can be designed for optimizing direct antimicrobial activity and/or modulating specific immune and inflammatory responses as discussed in chapter 1.2 and chapter 3.2 [67, 123, 286, 312, 360].

Although immunomodulatory functions of CHDP and IDR peptides have been extensively investigated [111, 130, 133, 134, 312], understanding of the sequence/structure relationship to biological activity have predominantly been limited to direct antimicrobial activity. For example a tryptophan next to an arginine in the sequence of CHDP is important for bacterial membrane interactions and also that the positive charge on the peptides results in interaction with negatively charged bacterial membrane thus facilitating direct antimicrobial action [361]. Similarly, other studies have also implicated that increasing positively charged residues combined with hydrophobic amino acids on the peptide facilitates increased membrane disruption activity and cell death related to CHDP-mediated direct antimicrobial activity [63, 362]. However, physical descriptors such as sequence, structure or hydrophobicity for antimicrobial activity do not strongly overlap with peptide-mediated immunomodulatory functions [127]. A recent study published by Haney *et al* examined the structure-activity relationship of two IDR peptides, including IDR-1002, in the context of anti-biofilm activity and examined the suppression of endotoxin LPS-induced IL-1β and induction of MCP1in blood-derived cells [96]. The study showed that the sequence characteristics for IDR peptide-mediated induction of MCP1 from PBMC was different from that required for optimal bacterial endotoxin-induced IL-1β suppression and anti-biofilm activity [96]. Haney *et al* also showed that the central hydrophobic region of IDR-1002 was important for anti-endotoxin and anti-biofilm activity, but did not identify key amino acid residues or patterns that

contributed to MCP1 induction [96]. The relationship between the specific sequence of IDR-1002 and the immunomodulatory activity mediated by the peptide in the context of airway inflammation has not been defined. Therefore, I examined the effects of peptides derived from single amino acid substitution of IDR-1002 in HBEC-3KT cells *in vitro* and in an *in vivo* model.

I have shown in chapter 3.2 that IDR-1002 can improve AHR and airway inflammation in an allergen HDM-challenged murine model of allergic asthma [312]. Therefore, in this study I used a series of second generation peptides derived from single amino acid substitutions of IDR-1002 and examined cytotoxicity and immunomodulatory effects *in vitro* using HBEC-3KT cells, and ability to mitigate allergen-challenged responses compared to IDR-1002 in an *in vivo* model [312]. The findings in this study demonstrate that the tryptophan at position 8 (W8) in the sequence of IDR-1002 is important for the immunomodulatory activity of IDR-1002. I showed that disrupting the hydrophobic W8 with an arginine (W8/R) does not alter the ability of the peptide to penetrate cellular membranes or the stability of the peptide, and yet mitigates immunomodulatory functions both *in vitro* and *in vivo* models. Interestingly, the disrupting W8 of IDR-1002 selectively altered the ability of the peptide to control airway inflammation, as the disruption did not alter its capacity to improve AHR in a HDM-challenged murine model. This suggests that disruption of a central W8 in the sequence of IDR-1002 selectively mitigates control of inflammation without altering ability to improve lung function in a murine model of allergic asthma. Therefore, IDR-1002(W8/R) can be used to study specific molecular mechanisms involved in AHR independent of airway inflammation. Broadly, the results from the sequence/immunomodulatory function relationship from this study can be applied to design novel immunomodulatory peptides with targeted functions.

3.4.3 Results

3.4.3.1 Retention times on a C18 reverse phase HPLC column of IDR-1002 and its derivatives: A previously published study by Haney *et al* showed that single amino acid substitutions of IDR-1002 altered MCP1 induction, LPS induced IL-1β production in PBMC, and anti-biofilm activity of the peptide in an infection model of Pseudomonas aeruginosa [96]. Based on this study, I selected 6 different IDR-1002-derived peptides with cationic, polar and large hydrophobic single amino acid substitutions in various segments of IDR-1002 that altered the predicted hydrophobicity and charge of the peptide (Table 4.1).

Reverse-phase HPLC is a powerful tool to measure the effects of single amino acid substitutions on the interaction of peptide to hydrophobic surfaces (e.g. phosphatidylcholine phospholipid bilayer). Therefore, the retention time (RT) of peptides on a reverse-phase column directly correlates with overall hydrophobicity of the peptides, which depends on amino acid composition and conformation of the peptide during the interaction with the hydrophobic membrane. Therefore, the RT of IDR-1002 and the IDR-1002 derivatives (Table 4.1 and Figure 4.1A) were examined on a C18(2) reverse phase HPLC column to measure the overall peptide hydrophobicity changes due to single amino acid substitutions of IDR-1002. IDR-1002.5(R11/W) had the longest RT whereas IDR-1002.2(W8/R) had the shortest RT on the reverse-phase column (Table 4.1 and Figure 4.1A). The RT for IDR-1002 was 16.27 min, placing IDR-1002 in the center of the RT assessments obtained from the 6 IDR-1002 derivatives (Table 4.1 and Figure 4.1A). The hydrophobic index **(**HI) was predicted for the peptides using SSRCalc [222], and the RT of the peptides significantly correlated (~80%) with HI (Table 4.1 and Figure 4.1B). This data shows that the single amino acid substitutions alters the overall hydrophobicity of IDR-1002-derived peptides.

Table 4.1: IDR peptide sequence information.

IDR Peptide ID	Sequence												Molecular weight (g/mol)	Charge	Hydrophobicity Index (HI)
	1	2	3	4	5	6	7	8	9	10	11	12			
1002	V	Q	R	W	L	I	V	W	R	I	R	K	1653.04	+4	12.36
1002.1	V	R	R	W	L	I	V	W	R	I	R	K	1681.09	+5	9.71
1002.2	V	Q	R	W	L	I	V	R	R	I	R	K	1623.01	+5	8.14
1002.3	V	Q	R	W	L	I	V	W	V	I	R	K	1595.98	+3	16.54
1002.4	V	L	R	W	L	I	V	W	R	I	R	K	1638.07	+4	13.39
1002.5	V	Q	R	W	L	I	V	W	R	I	W	K	1683.06	+3	17.04
1002.6	V	Q	R	W	L	I	V	I	R	I	R	K	1579.98	+4	11.88

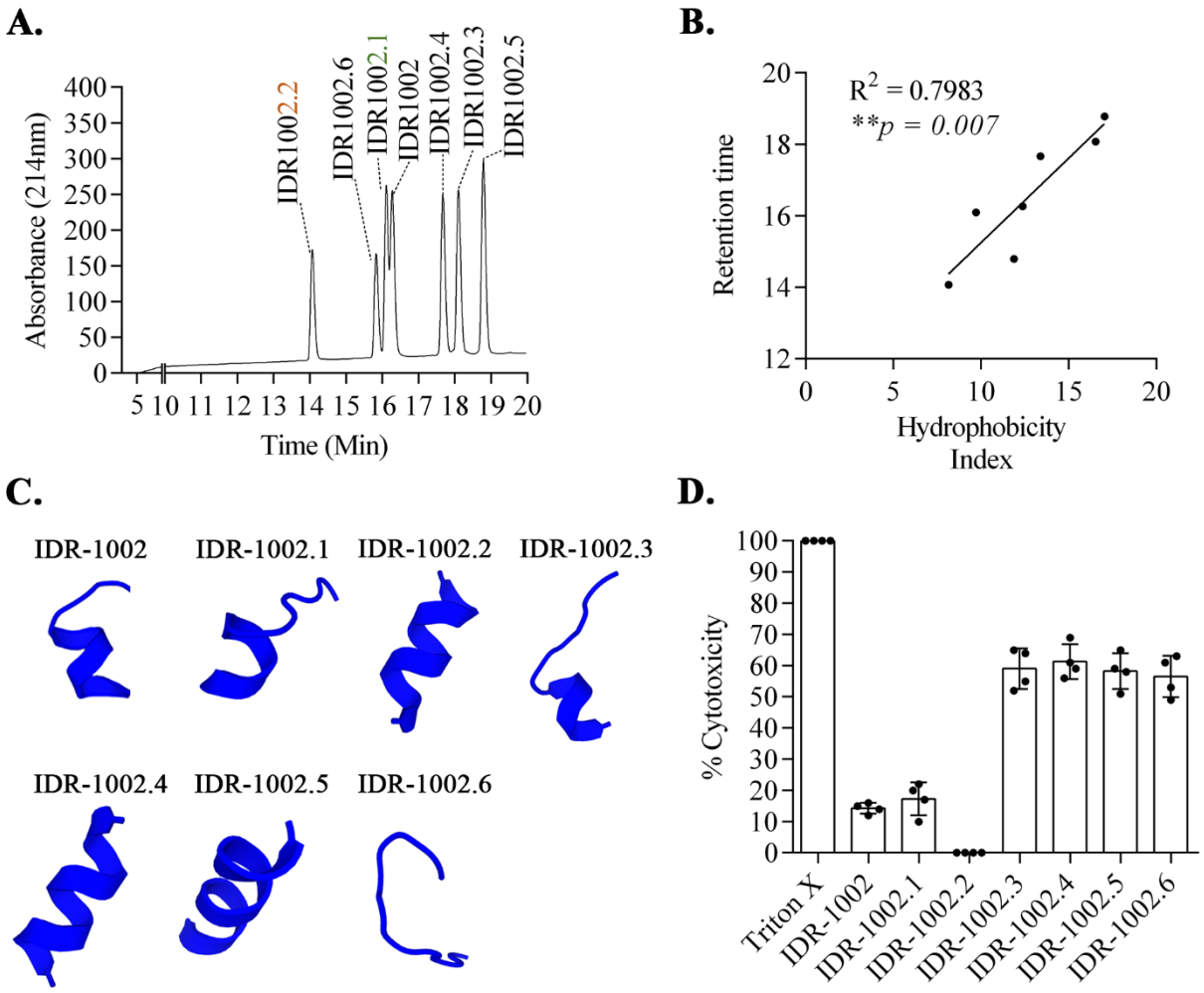

Figure 4.1: Single amino acid substitutions alter IDR-1002 peptide hydrophobicity and cellular cytotoxicity. ***(A)*** *Retention times for 2µg of IDR peptides were determined in a luna C18(2) 5 µm, Phenomenex, 1x100 mm column and were eluted using linear 2% water:acetonitrile gradient per mixture at a rate of 0.2 mL/min. Elution times were IDR-1002.2(W8/R) 14:04 min, IDR-1002.6(W8/I) 14:48 min, IDR-1002.1 (Q2/R) 16:06 min, IDR-1002 16:16 min, IDR-1002.4(Q8/L) 17:40 min, IDR-1002.3(R9/V) 18:05 min and IDR-1002.5(R11/W) 18:47 min.* ***(B)*** *Correlation analysis of HI vs peptide retention time on reverse phase HPLC column.* ***(C)*** *In-silico predictions of the secondary structures using PEP-FOLD.* ***(D)*** *LDH assay was performed to determine cellular cytotoxicity. All IDR peptides were used at 10 µM. Each dot represents individual replicate while column height corresponds to average percentage.*

3.4.3.2 *In silico* predictions and cellular cytotoxicity of IDR-1002 and its derivatives: PEP-FOLD *de novo* structure prediction algorithm was used to predict alterations of secondary structure of IDR-1002 and the derivative peptides. These *in silico* predictions showed that IDR-1002.3 and 1002.6 were largely linear/unfolded. IDR-1002.2, 1002.4 and 1002.5 were helical in structure. The parent peptide IDR-1002 and IDR-1002.1(Q2/R) were of mixed configuration showing partly helical and partly linear folds (Figure 4.1C).

HBEC-3KT cells were stimulated with the peptides and the effect of amino acid substitutions on cellular cytotoxicity was measured using LDH cytotoxicity assay after 24 hr. Peptides IDR-1002.3, 1002.4, 1002.5 and 1002.6 at 10uM concentration induced greater than 50% cytotoxicity (Figure 4.1D). Therefore, these peptides were excluded from further studies. IDR-1002 and IDR-1002.1(Q2/R) induced ~15% cytotoxicity whereas IDR-1002.2(W8/R) did not induce any detectable cytotoxicity. There was no significant correlation between cellular cytotoxicity with either the RT or *in silico* structure predictions. Based on the cellular cytotoxicity results, peptides IDR-1002, IDR-1002.1(Q2/R) and 1002.2(W8/R) were used in further studies.

3.4.3.3 Substitution of tryptophan (W8) with arginine (R) in IDR-1002 mitigates the immunomodulatory function of the peptide in bronchial epithelial cells: HBEC in the airways plays a pivotal role in innate immune responses and actively secrete various cytokines and chemokines as discussed in chapter 1.1 [38]. I have previously shown that IDR-1002 supresses IFNγ-induced pro-inflammatory cytokine IL-33 production in human PBEC [312]. Therefore, in this study I examined IFNγ-induced IL-33 in the HBEC-3KT cell line, in the presence and absence of IDR-1002, IDR-1002.1(Q2/R) and IDR-1002.2(W8/R). Consistent with our previous study [312], IDR-1002 supressed IFNγ-induced IL-33 by 85 ± 7% (Figure 4.2A). IDR-1002.1(Q2/R) suppressed IFNγ-induced IL-33 production by 70 ± 22%, however IDR-1002.2(W8/R) did not supress IFNγ-induced IL-33 production (Figure 4.2A).

IDR peptides have been shown to induce macrophage chemokines such as MCP1 in PBMC [135]. Therefore, I monitored the production of MCP1 and anti-inflammatory mediators IL-1RA and STC1 in HBEC-3KT cells. IFNγ-induced MCP1 was increased by both IDR-1002 (3.8 ± 0.35-fold) and IDR-1002.1(Q2/R) (2.9 ± 0.21-fold), but not by IDR-1002.2(W8/R) (Figure 4.2B). Similarly, release of anti-inflammatory mediators STC1 and IL1-RA were induced by IDR-1002 (4 ± 0.3 and 2.6 ± 0.4-fold respectively) and IDR-1002.1(Q2/R) (6 ± 0.35 and 2.6 ± 0.4-fold respectively), but not by IDR-1002.2(W8/R) compared to unstimulated cells (Figure 4.2C). Taken together, these results suggest that glutamine substituted with an arginine at position 2 (Q2/R) of IDR-1002 have minimal effects on immunomodulatory capacity of IDR-1002, whereas replacing the tryptophan at position 8 with arginine (W8/R) mitigates immunomodulatory functions of IDR-1002 in HBEC-3KT cells. Based on these results, I further compared the stability and cellular uptake of the peptides IDR-1002 and IDR-1002.2(W8/R) in HBEC-3KT cells, as well as the effects of the peptides in an allergen-challenged *in vivo* model.

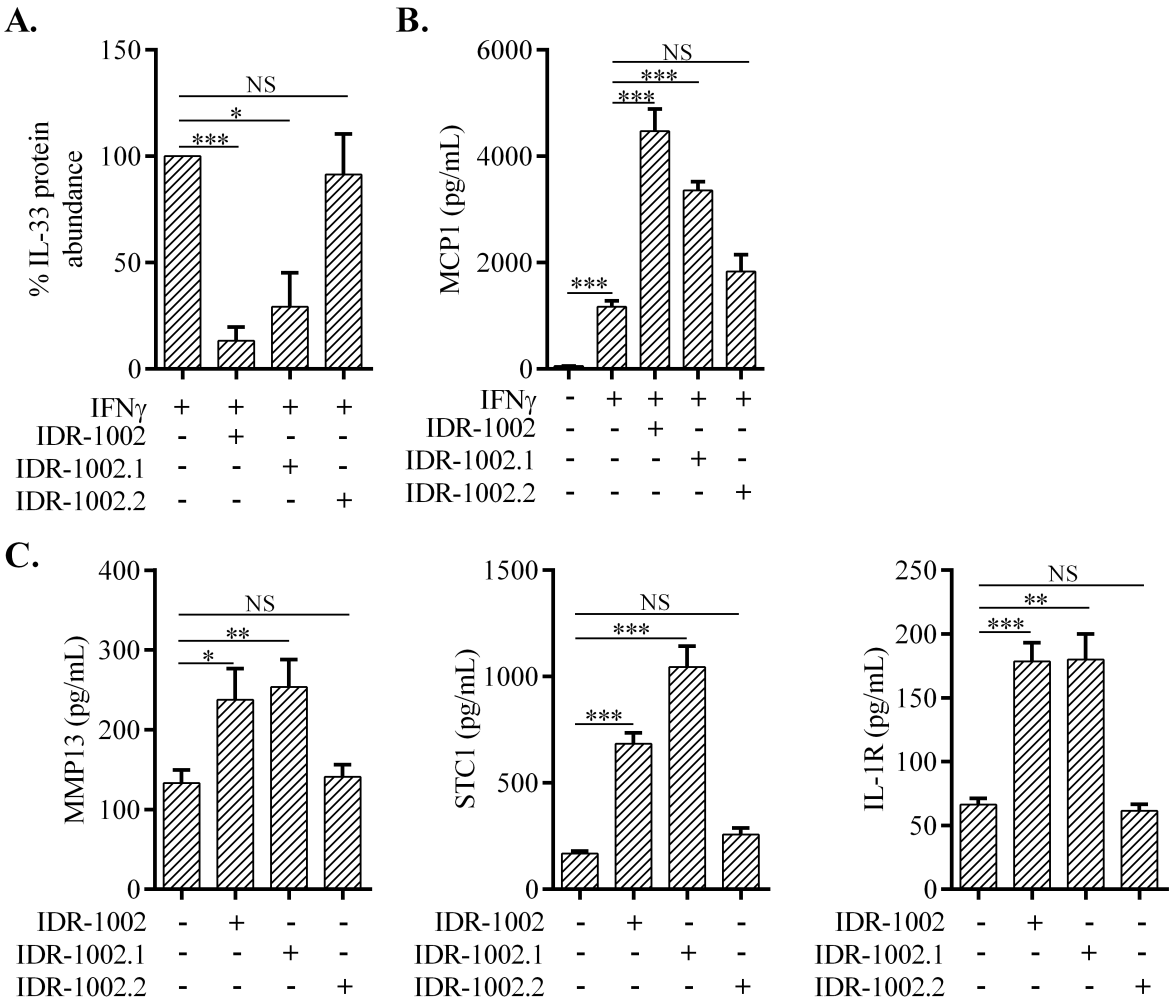

Figure 4.2: Immunomodulatory function of IDR-1002 in HBEC-3KT cells. *HBEC-3KT cells were stimulated with 10uM of IDR-1002 and IDR-1002.2(W8/R), in presence or absence of 30 ng/mL of IFNγ. Peptides were added 30 min prior to IFNγ stimulation. Supernatants and cell lysates were collected 24 hr post-stimulation.* ***(A)*** *IL-33 abundance in cell lysates was determined by western blots, the graph shows densitometry analysis for IL-33 (n=5) normalized using actin for protein loading control, shown as % protein abundance.* ***(B, C)*** *MCP1, STC1, and IL-1RA protein secretion levels were measured by ELISA. Column height represents mean and error bars show SEM. Statistical analysis was performed using one-way ANOVA with Dunnett's multiple corrections (*$p \leq 0.05$, **$p \leq 0.01$, ***$p \leq 0.001$).*

3.4.3.4 W8/R substitution of IDR-1002 does not alter peptide stability: As IDR-1002(W8/R) mitigated the immunomodulatory functions of the peptide *in vitro,* I examined if this substitution altered peptide stability. To measure peptide stability, a quencher was attached to the N-terminus of the 5FAM-tagged peptides and used for FRET assay. IDR peptides incubated with trypsin (1:50) to degrade the peptide, was used as positive control (Figure 4.3B). FRET assay demonstrated differences in degradation of the peptides, 2.3% of IDR-1002 and 1.9% IDR-1002.2(W8/R) were degraded in the presence of HBEC-3KT cells over 16 hr (Figure 4.3). Although, quantitatively the difference between degradation of the peptides were less than 1% over 16 hr, it was statistically significant. Taken together, this data shows that W8/R substitution does not significantly affect the stability of IDR-1002.

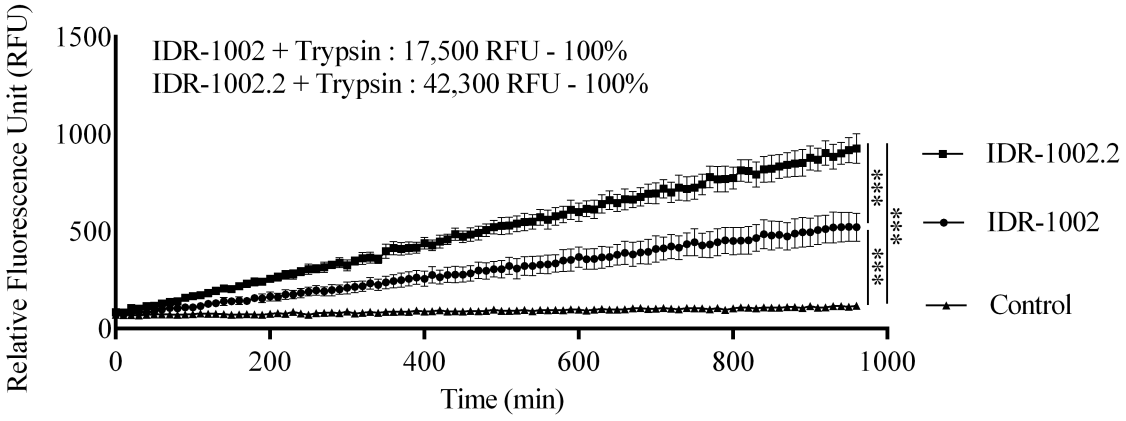

Figure 4.3: W8/R substitution does not alter internalization or stability of IDR-1002 in HBEC-3KT cells. *HBEC-3KT cells were stimulated with (CPQ)IDR-1002(5FAM) or (CPQ)IDR-1002.2(5FAM) and RFU was measured over 16 hr (n = 5). Statistical analysis was performed using one way repeated measures ANOVA with Tukey's multiple corrections (***p ≤ 0.001).*

3.4.3.5 Substitution of W8/R alters immunomodulatory function of IDR-1002 *in vivo*: I have previously shown that administration of IDR-1002 supresses airway inflammation (leukocyte accumulation and abundance of IL-33) in the lungs of allergen HDM-challenged mice [312]. Therefore, based on my previous study I examined the activity of IDR-1002.2(W8/R) in the HDM-challenged murine model in this study. Administration of IDR-1002.2(W8/R) did not supress allergen-induced IL-33, whereas IDR-1002 supressed IL-33 abundance in the lungs by 43 ± 36% (Figure 4.4A). Leukocyte accumulation, including eosinophils and neutrophils in the lungs of HDM-challenged mice were supressed by IDR-1002 (66 ± 23%, 63 ± 21%, and 60 ± 44% respectively) and not by IDR-1002.2(W8/R) (Figure 4.4B, 4.4C and 4.4D). Taken together, these results suggest that W8 of IDR-1002 is essential for the immunomodulatory function of the peptide *in vivo*.

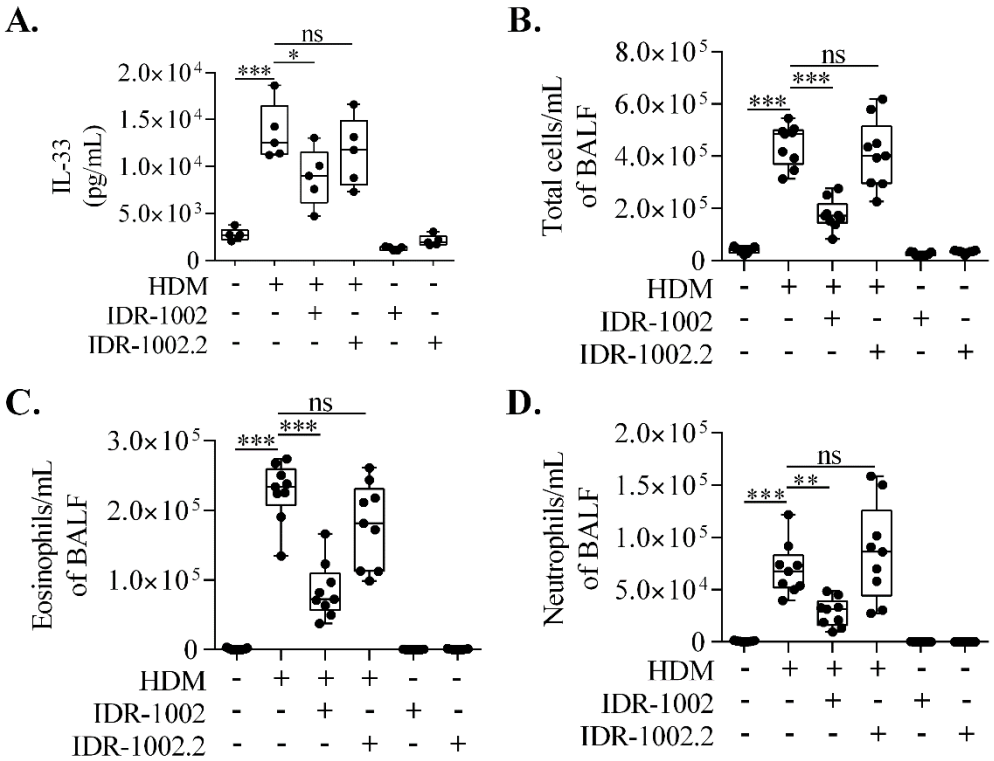

Figure 4.4: W8 is essential for immunomodulatory function of IDR-1002 *in vivo*. *Mice (n = 9 per group) were challenged by i.n. administration of whole HDM extract in saline, for 2 weeks (Figure VI). IDR peptides were administered s.c. 3 times a week (Figure VI). Lung tissue and BALF were collected 24 hr after last challenge.* ***(A)*** *IL-33 protein abundance measured in lung tissue lysates (n = 5 per group). Cell differentials measured in BALF for* ***(B)*** *Total cell,* ***(C)*** *eosinophil,* ***(D)*** *neutrophils. Statistical analysis was performed using one way repeated measures ANOVA with Tukey's multiple corrections (*p ≤ 0.05, **p ≤ 0.01, ***p ≤ 0.001).*

3.4.3.6 Cytokine production in the lungs and BALF monitors using multiplex MSD assay: The abundance of 27 cytokines in the lung tissue and BALF from mice was obtained using the MSD multiplex assay. Volcano plot analysis demonstrates the effects of peptide alone, in the absence of allergen change (Figure 4.5). IDR-1002 administration decreases the abundance of 12 pro-inflammatory cytokines, of which 8 were decreased between 2 and 5 fold compared to naïve (Figure 4.5). IDR102.2 administration decreased the abundance of only 5 cytokines, of none of which were less than 2-fold compared to naïve. IDR-1002 decreased IL-33, IL-17F, IL-1β, TNF, MIP2, MIP3α, and IP10 more than 2-fold in the lung tissues of naïve mice (Figure 4.5 and Supplementary Table 4.1). IDR-1002.2(W8/R) decreased IL-10 by more than 2-fold in the lung tissues of naïve mice (Figure 4.5 and Supplementary Table 4.1). In the BALF, both peptides significantly supressed TNF, while MIP2 was only supressed by IDR-1002 (Supplementary Table 4.2). This data suggest that IDR-1002 W8/R substitution abrogates the ability to supress multiple targets of IDR-1002 and uniquely gained the ability to supress IL-10 in the lungs of naïve mice.

Further examining the effects of the two peptides in allergen challenged mice showed that the peptides altered the profile of HDM-induced cytokines disparately. I examined the expression relationships between the 27 cytokines measured in the lung tissue lysates by the MSD platform using correlation analysis (ggcorr package in R). Although there was no significant change of the median abundance of any of the individual cytokines (Supplementary Figure 4.1, Supplementary Table 4.3), the correlation patterns showed a distinct profile in the cytokines induced by HDM-challenge compared to naïve mice (Figure 4.6A, 4.6B). This correlation pattern was disrupted by IDR-1002 (Figure 4.6C) and not by IDR-1002.2(W8/R) (Figure 4.6D). The disruption of the pattern by IDR-1002 is particularly apparent for IL-2, IL-4, IL-5, IL-6, KC, TNF, IL-17A, MCP1, IL-30, IL-15, MIP1α, IP-10 and MIP2, in HDM-challenged lung tissues. Taken together these data

suggest that disrupting the tryptophan at position 8 alters the immunomodulatory capacity of IDR-1002 in the lungs of naïve and allergen challenged mice.

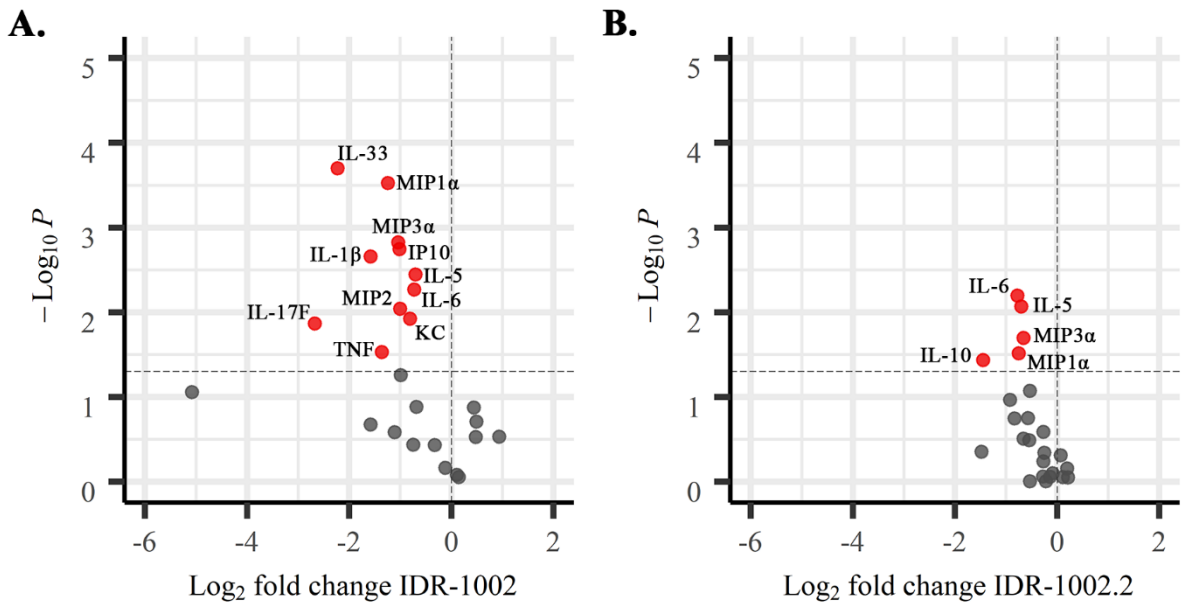

Figure 4.5: IDR peptides alter cytokines in the lung tissue. *IDR peptides (n = 9 per group) were administered s.c. 3 times a week (Figure VI). Lung tissue was collected 24 hr after last challenge. Volcano plot of cytokines altered by* ***(A)*** *IDR-1002* ***(B)*** *and IDR-1002.2(W8/R) in lung tissue lysates on mice. Significance score cut off was set at $p \leq 0.05$). Red dots represent significant altered cytokines.*

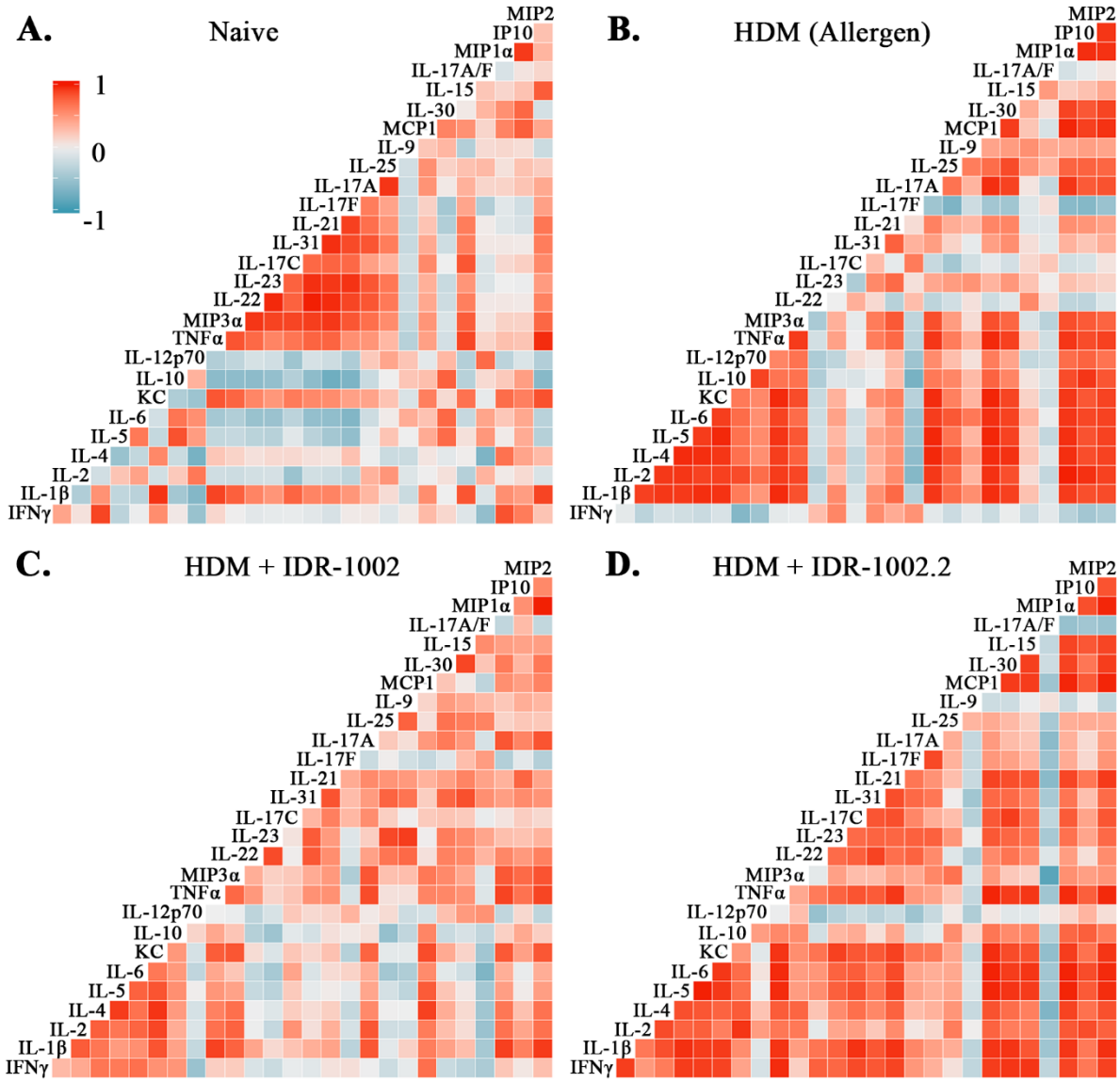

Figure 4.6: IDR peptides alter cytokines in the lung tissue. *Mice (n = 9 per group) were challenged by i.n. administration of whole HDM extract in saline, for 2 weeks (Figure VI). IDR peptides were administered s.c. 3 times a week (Figure VI). Lung tissue was collected 24 hr after last challenge. Correlation matrix generated using ggcorr package in R for* ***(A)*** *Naïve,* ***(B)*** *HDM (Allergen),* ***(C)*** *HDM + IDR-1002 and* ***(D)*** *HDM + IDR-1002.2(W8/R). Pearson correlation coefficient was used to measure strength of the linear relationships between cytokines.*

3.4.3.7 Both IDR-1002.2(W8/R) and IDR-1002 improves lung function of allergen challenged mice: I have previously shown that IDR-1002 improves AHR in HDM-challenged mice [312]. Therefore, I examined the importance of the W8 of IDR-1002 for improving AHR in the allergen-challenged murine model. Similar to IDR-1002, administration of IDR-1002.2(W8/R) significantly reduced maximum methacholine (50 mg/ml)-induced Newtonian resistance (Rn) tissue damping (G) and tissue elastance (H) (39 ± 24%, 64 ± 24%, and 63 ± 23% respectively) compared to HDM-challenged mice (Figure 4.7). Notably these effects were seen starting at low concentration of methacholine (12 mg/mL). Administration of both peptides alone had no observable effect on AHR of mice. Taken together, the results show that although W8 of IDR-1002 is critical for the immunomodulatory activity of the peptide, it is not essential for the ability of the peptide to improve lung function.

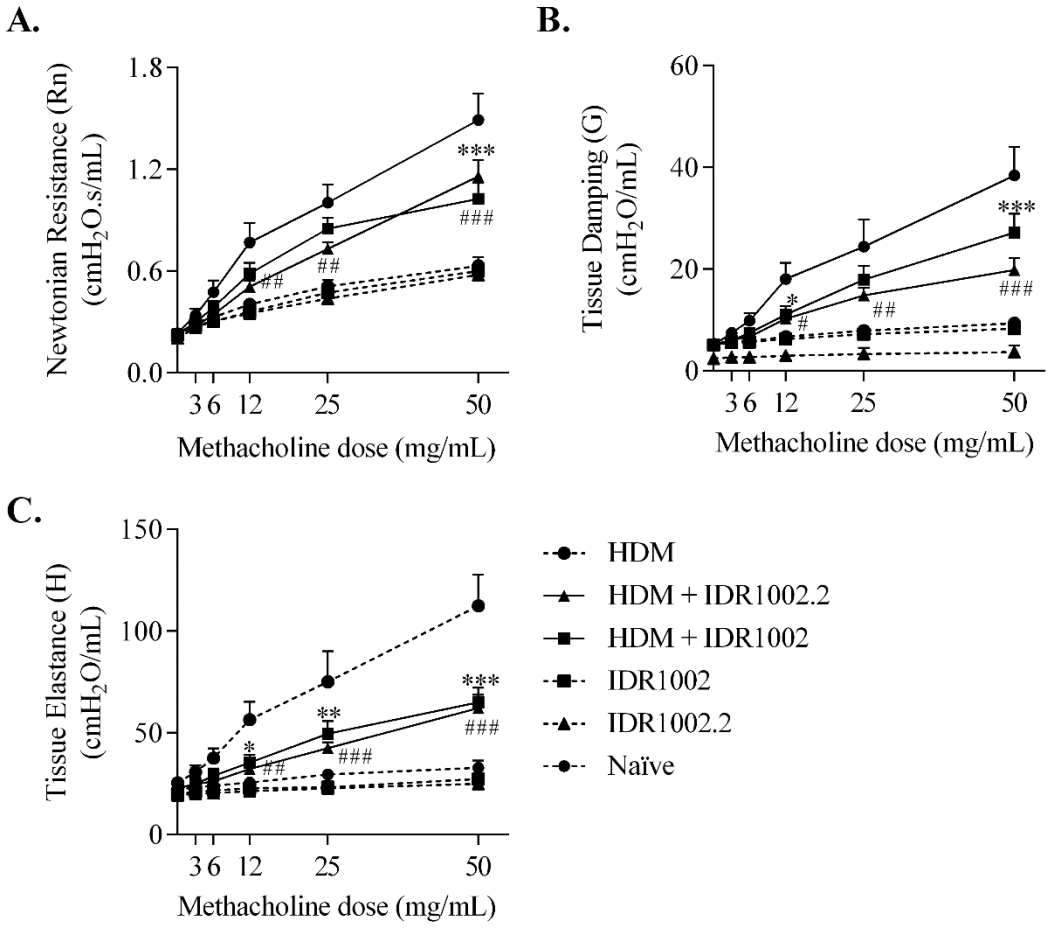

Figure 4.7: IDR peptides improve lung function in allergen-challenged mice. *Mice (n = 9 per group) were challenged by i.n. administration of whole HDM extract in saline, for 2 weeks (Figure VI). IDR peptides were administered s.c. 3 times a week (Figure VI). Lung mechanics were monitored 24 hr after the last HDM-challenge. Mice were exposed to nebulized saline (baseline measures) followed by increasing concentrations of nebulized methacholine (3-50 mg/mL) and changes in* ***(A)*** *Newtonian resistance (Rn),* ***(B)*** *tissue damping (G),* ***(C)*** *tissue elastance (H) was monitored. Statistical significance was determined using two-way repeated measures ANOVA with Tukey's multiple comparisons test ($p \leq 0.05$, $p \leq 0.01$, $p \leq 0.001$). * represent comparison between HDM and HDM + IDR-1002 group and # represent comparison between HDM and HDM + IDR-1002.2(W8/R) group.*

3.4.3.8 IDR-1002.2(W8/R) alters IDR-1002-mediated kinase profile: CHDP have been previously shown to alter kinase activity to intervene in cellular signalling pathways [58, 99]. Therefore, a kinase array was used to measure differences in phosphorylation profiles mediated by the peptides. HBEC-3KT cells lysates were collected post 15-minute exposure of IDR-1002 and IDR-1002.2(W8/R) to measure the phosphorylation of 282 unique phospho targets corresponding to 149 proteins. Both IDR peptides significantly mediated the phosphorylation of 94 common phospho targets, while IDR-1002 and IDR-1002.2(W8/R) uniquely mediated the phosphorylation of 28 and 18 protein targets respectively (Figure 4.8A). Further, out of the 94 commonly induced phospho targets by both IDR-1002 and IDR-1002.2(W8/R), phosphorylation levels of 11 targets were more than 2-fold different between IDR-1002 and IDR-1002.2(W8/R) (Figure 4.8B and Supplementary Table 4.5). For more stringent analysis, I applied a 2-fold change cut off to the differentially expressed 94 common phospho targets. This resulted in the identification of 17 common phospho targets induced by both peptides. IDR-1002 and IDR-1002.2(W8/R) uniquely altered 5 and 6 respectively (Figure 4.8C and Supplementary Table 4.6). The five phospho targets induced in response to IDR-1002 and not IDR1002.2 were STAT1-Y701, Rab5A-S123, Syk-Y525, TGFR1-T200, and TGFR1-T204, which may be involved in the anti-inflammatory responses mediated by IDR-1002. Taken together, kinome profile shows that IDR-1002 W8/R substitution results in altered kinase activation profile compared to IDR-1002.

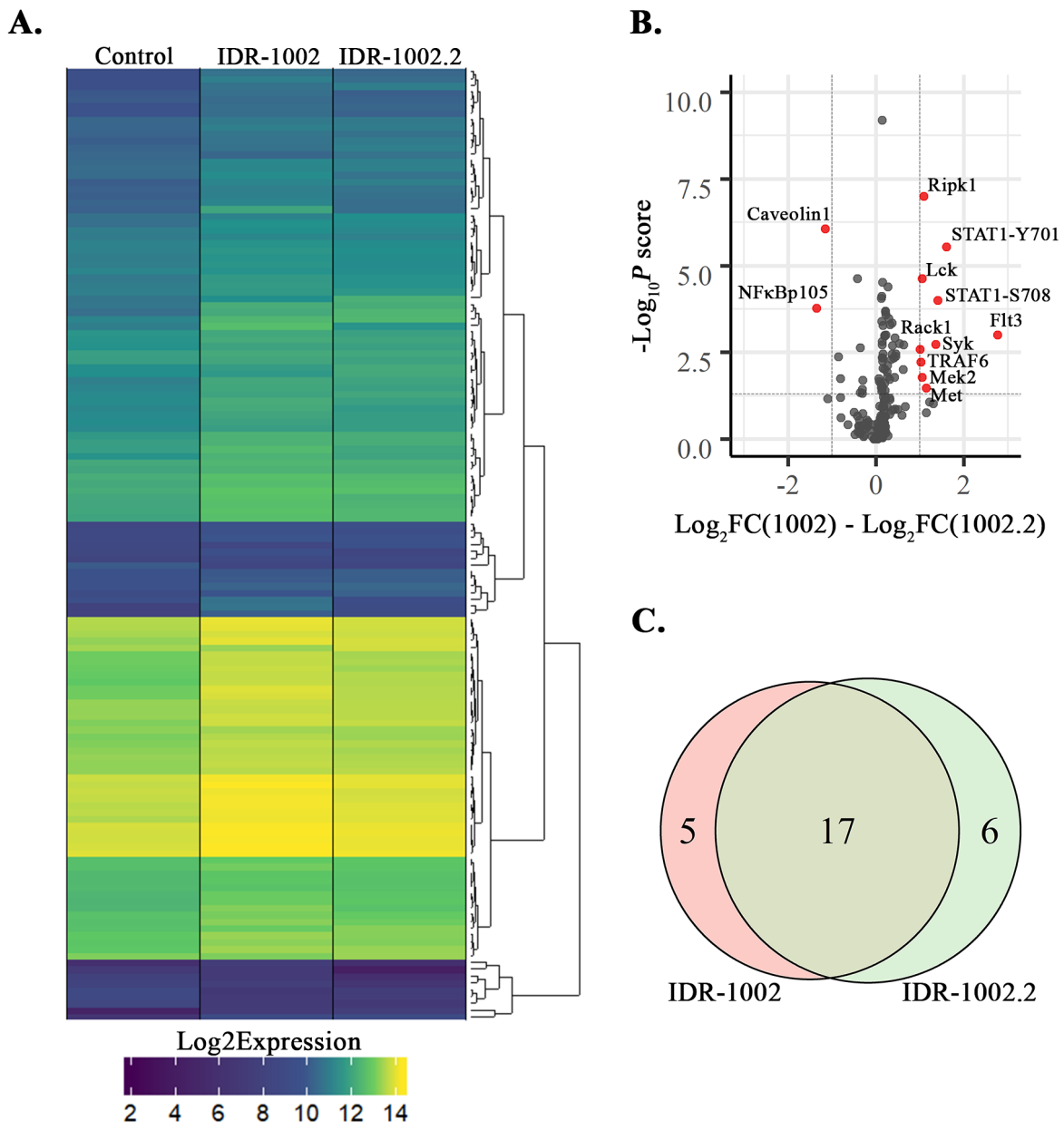

Figure 4.8: IDR peptide treatment enhances phosphorylation of proteins. *HBEC-3KT cells were stimulated with 10uM of IDR-1002 and IDR-1002.2(W8/R) and cell lysates were collected 15 min post stimulation. Kinase activity was measured using JPT Kinome peptide arrays.* ***(A)*** *Heat map of significantly altered phospho peptides (Log2 Expression values) by IDR peptides compared to unstimulated cells with kmeans clustering performed using superheat package in R.* ***(B)*** *Volcano plot of the 94 commonly altered phospho targets comparing IDR-1002 with IDR-1002.2(W8/R). Red dots show statistically significant (*$p \leq 0.05$) with 2-fold cut off.* ***(C)*** *Venn diagram of significantly altered phospho peptides by IDR peptides with 2-fold cut off, compared to unstimulated.*

3.4.4 Discussion and Conclusion

In this study, I evaluate the sequence and function relationship of IDR-1002. I show that a single amino acid substitution of IDR-1002 significantly alters cytotoxicity profile in HBEC-3KT cells. I also show that the tryptophan at position 8 (IDR-1002.2) substituted with arginine (R), and not the glutamine at position 2 (IDR-1002.1), is critical for IDR-1002 to induce anti-inflammatory mediators such as cytokines IL-1RA and STC1, and chemokine MCP1, in HBEC-3KT cells. I further demonstrate that substituting the W8 residue in IDR-1002 to R does not alter the stability or cellular uptake of IDR-1002. However, the W8 of IDR-1002 is essential for the immunomodulatory bioactivity, such as supressing the pro-inflammatory cytokine IL-33, disruption of the allergen-induced relative cytokine profile, and control of immune cell accumulation, in the lungs of allergen challenged mice. Interestingly, the W8 residue of IDR-1002 is not essential for improving allergen-mediated AHR by the peptide. In addition, I characterize the effect of W8 substitution of IDR-1002 on cellular signalling molecules using kinome analysis in HBEC-3KT cells, which provide the foundation for future studies to delineate the mechanisms underlying the immunomodulatory activity of IDR-1002.

The sequence/function relationship of CHDP have been extensively investigated in mechanistic studies for the direct antimicrobial functions of the peptides [63, 361-363]. However, the relationship between the sequence and immunomodulatory capacity of CHDP is still unclear [127]. I have previously shown that IDR-1002 improves airway inflammation and AHR in an allergen challenged murine model and that IDR-1002 could be used to develop alternative therapies for allergic asthma [312]. Therefore, it is critical to understand the relationship the sequence of IDR-1002 and its function to further develop IDR peptides as novel therapeutics for allergic asthma.

In this study, I showed that IDR-1002.1(Q2/R) retains the capability to induce anti-inflammatory mediators such as STC1 and IL-1RA. The negligible effect of the Q2/R substitution in IDR-1002 in the context of its immunomodulatory activity can be explained using blocks substitution matrices (BLOSUM) [364, 365]. BLOSUM matrices are commonly used to score sequence alignment for evolutionary divergent peptide sequences by calculating substitution probabilities of each amino acid [364, 365]. The higher the frequency that the amino acid substitution is found in evolutionary divergent sequences, the higher the BLOSUM score. According to the BLOSUM matrix on NCBI (https://www.ncbi.nlm.nih.gov /Class/Structure/aa/aa_explorer.cgi) arginine is the 3rd most frequently substituted amino acid for glutamine with a score of 2, suggesting similar functional roles for these amino acids within a sequence. Therefore, Q2/R substitution is unlikely to alter the molecular functions of IDR-1002, as demonstrated in this study.

However, it is difficult to explain the changes in cytotoxicity of IDR-1002-derivatives, using BLOSUM. For example, IDR-1002.2(W8/R) did not cause any cytotoxicity although W to R is the 15th most substituted amino acid in BLOSUM with a score of -4. However, the single amino acid substitutions that leads to increase cellular cytotoxicity (IDR-1002.3 to IDR-1002.6), were greater then 12th most substituted amino acid in BLOSUM, with scores higher than -4. Similarly, the hydrophobicity changes of peptide due to the single amino acid substitutions also did not correlate with cellular cytotoxicity. For example, IDR-1002.6(W8/I) showed similar hydrophobicity properties to IDR-1002 but induced greater than 50% cytotoxicity to HBEC-3KT cells. Overall the results of this study suggest that there is no correlation between the predicted 2D confirmations of the IDR peptides and peptide-mediated cellular cytotoxicity.

Interestingly, consistent with BLOSUM prediction (score of -4), IDR-1002.2 (W8/R) resulted in significantly compromising the immunomodulatory functions of IDR-1002 as IDR-1002.2(W8/R) did not induce anti-inflammatory mediators STC1 or IL-1RA, in contrast to IDR-1002 in HBEC-3KT cells.

I further observed that IDR-1002 and IDR-1002.2(W8/R) reduces a number of pro-inflammatory cytokines in the lung tissue lysates of naïve mice. However, IDR-1002.2(W8/R) only reduces 5 cytokines (IL-5, IL-6, IL-10, MIP3α and MIP1α) compared to 11 cytokines (IL-5, IL-6, IL-1β, KC, TNF, IL-17F, IL-33, IP10, MIP2, MIP3α and MIP1α) by IDR-1002. Notably both peptides seem to alter macrophage inflammatory proteins which suggest that W8 substitution still retains some immunomodulatory function of IDR-1002 *in vivo*. However, broadly examining the diversity of cytokines targeted by IDR-1002 compared to IDR-1002.2(W8/R) further confirms that disrupting the W8 residue of IDR-1002 significantly blunts the immunomodulatory function.

Various immunomodulatory activities of CHDP and IDR peptides have been shown to be dependent on the interaction with intracellular molecules including GPCRs, Sequestosome-1/p62 and GAPDH [56, 132]. As the hydrophobicity and charge are altered in IDR-1002.2(W8/R) compared to IDR-1002, I speculated that cellular uptake required to mediate signalling pathways effecting downstream cytokine and chemokine production may be compromised in IDR-1002.2(W8/R). Intracellular uptake of IDR-1002 has been demonstrated in structural cells such as fibroblasts [135]. However, using fluorescently-labelled peptides, I detected both IDR-1002 and IDR-1002.2(W8/R) in the cytoplasmic component in HBEC-3KT cells in this study (results shown in the chapter discussing future direction). This observation suggests that the peptides may be localized in the rough endoplasmic reticulum. However, more comprehensive studies are required to confirm the cellular localization of IDR peptides. In addition to cell membrane penetration,

IDR-1002.2(W8/R) substitution did not affect peptide stability as both IDR peptides showed less than 2.5% degradation over 16 hr in HBEC-3KT cells. The above discussed results suggest that W8 of IDR-1002 may be essential for association with a specific cellular target to exert the immunomodulatory function of IDR-1002 in HBEC-3KT cells. This was further evident from my in-depth kinase profiling where I demonstrate that IDR-1002 uniquely alters 5 phospho targets (greater than 2-fold) and induced significantly higher phosphorylation in commonly identified targets between IDR-1002 and IDR-1002.2(W8/R) as seen in Figure 4.4A and 4.4C.

In this study the kinome analyses showed that STAT1-Y701 was uniquely phosphorylated in the presence of IDR-1002. STAT1 phosphorylation at Y701 is involved in activating IFN pathways resulting in immune modulation and antiviral responses [366]. Further, activation of STAT1 at Y701 enhances the phosphorylation of STAT1(S708) site [367]. Consistent with this, the kinome analyses showed that STAT1-S708 was phosphorylated more than 6-fold in the presence of IDR-1002, whereas by 2-fold in the presence of IDR-1002.2(W8/R). Moreover, STAT1 phosphorylation is known to be involved in MCP1 production, which was induced by IDR-1002 and not by IDR-1002 in HBEC-3KT cells [368]. Inhibitor of NF-κB Kinase Subunit Epsilon (IκBkε) is responsible for phosphorylation of STAT1-S708, while MCP1 induction is blocked when IκBkε synthesis was supressed [369]. Therefore, it is likely that IDR-1002 activates IκBkε to induce MCP1 through STAT1 activation. The proposed mechanism underlying IDR-1002-mediated MCP-1 production needs to be investigated further.

Interestingly W8 disruption of IDR-1002 uniquely enhanced the phosphorylation in 2 kinase targets (Caveolin1 and NFκBp100) while significantly downregulating the phosphorylation of 4 kinase targets (Flt3, Met, NFAT2 and p53), compared to unstimulated cells. However, direct comparison of the kinase targets of the peptides IDR-1002 and IDR-1002.2(W8/R) showed only

Caveolin1 and NFκBp100 were statistically significant with a 2-fold change between the two peptides. These results suggest that these protein targets may be critical for the immunomodulatory activity of IDR-1002.

I also examined the importance of W8/R and Q2/R substitution of IDR-1002 in the presence of inflammatory stimuli both *in vitro* and *in vivo*. I demonstrate that in HBEC-3KT cells, IFNγ-induced MCP1 is enhanced by both IDR-1002 and IDR-1002.1(Q2/R), but not by IDR-1002.2(W8/R). I also show that IDR-1002.1(Q2/R) and IDR-1002 but not IDR-1002.2 (W8/R), supress IFNγ-induced IL-33. These results are aligned with a recent publication where IDR-1002.1(Q2/R) substitution had no effect on the anti-endotoxin activity of IDR-1002 to suppress LPS-induced IL-1β, and enhances the chemokine MCP1 production in human PBMC [96].

Furthermore, I demonstrated in the allergen-challenged mouse model that in contrast to IDR-1002, the key upstream inflammatory cytokine IL-33 was not supressed by IDR-1002.2(W8/R). I have previously shown that suppression of IL-33 production by IDR-1002 is essential for the ability of the peptide to reduce leukocyte accumulation in the lungs of allergen-challenged mice. Consistent with this, in this study I demonstrate that IDR-1002.2(W8/R) does not supress IL-33 production and does not reduce leukocyte accumulation in the lungs of HDM-challenged mice. The suppression of IL-33 in the murine lung by IDR-1002 and not by IDR-1002.2(W8/R) was consistent with the *in vitro* HBEC-3KT cells results discussed above. The specific mechanism of how IDR-1002 is capable of targeting the production of IL-33 remains elusive and is outside the scope of this chapter. However, I have performed foundational studies using kinome analysis to postulate possible mechanisms which is discussed in chapter 5.

In the allergen-challenged mice, IDR-1002 did not supress median levels of cytokines measured in the lung tissue. A more robust effect of IDR-1002 may be seen if the dose or frequency of IDR peptide administration was increased as IDR-1002 has been previously used as high as 200 mg/kg *in vivo* which is substantially higher than the dose used in this study [132]. Although the abundance of the allergen induced cytokines monitored did not change, I observed a distinct correlation pattern between allergen-induced cytokines that was disrupted in the IDR-1002 treated mice where the resulting correlation pattern was remarkably similar to the naïve mice. IDR-1002.2(W8/R) in contrast failed to disrupt correlations between cytokines induced by allergen challenge, resulting in a correlation profile that resembled the allergen-challenged mice. The correlation matrix is particularly interesting as CHDP and IDRs have long been discussed as molecules that help maintain immunological homeostasis [55, 56, 109, 134]. Representing relative cytokine abundance in a correlation matrix depicts how IDR-1002 alters relative cytokine levels to help maintain immunological homeostasis while IDR-1002.2(W8/R) does not. It is important to note that large amount of health and epidemiological studies heavily rely on correlation analysis for not only in research but also in policy making [370, 371]. However, unlike in large epidemiological studies, my study has a relatively small number of mice (n = 9) and therefore the correlation analysis should be viewed with caution. I also do not infer any direct causal relationships between any 2 compared cytokines but rather an association.

Although I show that W8 is important for immunomodulatory activity of IDR-1002, I also demonstrate that W8 is not essential for reducing AHR in allergen-challenged mice. IDR-1002 and IDR-1002.2(W8/R) both reduces resistance in the main and peripheral airways and reduces lung stiffness caused by allergen challenge. This highlights that W8 residue in IDR-1002 can be disrupted to alter a specific functional role i.e. immunomodulatory functions, without completely

mitigating all bioactivity of the peptide. This is consistent with recent studies that suggest that there is a disparate relationship between airway inflammation and AHR in humans [300]. Therefore, as IDR-1002.2(W8/R) has minimal immunomodulatory capability in response to allergen-challenge but improves AHR, this peptide could be used as a probe along with IDR-1002, to delineate mechanisms involved in AHR independent of airway inflammation. Signaling pathways uniquely mediated by IDR-1002.2(W8/R), but not by IDR-1002, may be involved in AHR independent of airway inflammation, which warrants further investigation.

In conclusion, in this study I have dissected the functional role of Q2 and W8 residues of IDR-1002, both in HBEC-3KT cells and in the mouse model of allergen-challenged airway inflammation. I identified a key residue W8, as being critical to the immunomodulatory function of IDR-1002, but not essential for reducing AHR. This study provides a probe (IDR-1002.2) to study molecular mechanisms of AHR independent of airway inflammation which is a critical in developing new therapies to treat the heterogeneous population of asthmatics. Broadly, the sequence/immunomodulatory function relationship from the study can further be applied to designing novel immunomodulatory peptide therapeutics.

Chapter 4: Overall Conclusions, Significance and Future Directions

The overall aim of this thesis was to investigate and establish the therapeutic potential of immunomodulatory IDR peptides in allergic asthma. Murine models play a key role in dissecting the pathogenesis of human diseases, including allergic asthma, yet the objective molecular readouts of the 2-week HDM-challenged murine model of allergic asthma had not been extensively characterized. To this end, I characterized immune responses and identified specific biomarkers that are altered in the lungs in a murine model of allergic asthma following two week of HDM-challenge [280].

I showed that HDM-challenge for two weeks results in significant AHR along with eosinophil and neutrophil accumulation in the lungs, as well as increased epithelial thickness and goblet cell hyperplasia 24 h after last HDM-challenge [280]. I identified a panel of cytokines elevated in lung tissue and BAL [280]. Using transcriptomics, I defined a network of 33 genes that are significantly upregulated in lung tissue in response to HDM in the murine model [280]. This study resulted in the establishment of a biosignature for HDM response. I used this biosignature subsequently to examine responses to the synthetic IDR peptide, IDR-1002, in the HDM-challenged murine model.

In HDM-challenged mice I showed that administration (s.c.) of IDR-1002 reduces eosinophil and neutrophil accumulation and AHR. I further showed that administration of IDR-1002 suppresses the production of IL-33 (a central node in the inflammatory network defined in the HDM-challenged mice) in lung tissues from HDM-challenged mice [312]. To confirm that the bioactivity of IDR-1002 targets IL-33, I performed experiments with exogenous administration of recombinant IL-33 in the HDM-challenged murine model. Administration of exogenous recombinant IL-33 abrogated the ability of the peptide to suppress leukocyte accumulation in the lungs [312]. These results suggest that the suppression of IL-33 accumulation is a key mechanism

associated with the control of airway inflammation by IDR-1002. However, IDR-1002 maintains the ability to reduce AHR in IL-33 and HDM co-challenged mice, suggesting that IDR-1002 lowers AHR by mechanisms either downstream or independent of IL-33. I further examined the effects of IDR-1002 administration in mice challenged with IL-33 alone. IL-33 by itself induced AHR and recruitment of eosinophils and neutrophils to the lungs. I showed that IDR-1002 significantly reduces IL-33-induced AHR, however the peptide is unable to suppress IL-33-mediated leukocyte accumulation in BAL [312]. These results suggest that IDR-1002 reduces IL-33 alone-induced AHR, but not airway inflammation.

IL-33 expression is increased in bronchial epithelial cells in asthma [277]. IFNγ is known to induce the production of IL-33 [281, 283, 372]. As IL-33 is a chromatin-associated cytokine that functions as an inflammatory mediator when released from the nucleus [308], I examined the abundance of IL-33 in cytoplasmic extracts of bronchial epithelial cells by Western blots. In these studies, I showed that IDR-1002 suppresses IFNγ-induced IL-33 production in a HBEC3-KT cell line and in hufman PBEC [312]. This study also shows that mechanisms associated with the activity of IDR-1002 in suppressing the production of IL-33 may be independent of the IFNγ-induced canonical pathway, as IDR-1002 did not suppress IFNγ-induced canonical targets such as IP-10, IRF1 [312]. I further confirmed that IFNγ-induced phosphorylation of STAT1 at Y701 and S727 sites which results in the homodimerization and activation of the STAT1 [373] were not altered by IDR-1002. However, IDR-1002 enhanced the phosphorylation of IFNγ-induced STAT1 at site S708. pSTAT1(S708) inhibits STAT1 homodimerization that is induced by pSTAT1(Y701 and S727) resulting in reduced activation of the GAF complex [374]. As the IL-33 promoter region contains binding sites to the GAF complex, this suggests that IDR-1002 may be supressing IL-33 by altering the GAF complex in HBEC-3KT cells. IL-33 is significantly increased in severe

asthmatics and plays a central role in mediating corticosteroid-resistant airway inflammation [275-278, 292, 293, 375], thus, IL-33 is considered an important therapeutic target for severe asthma. In addition, preclinical studies in mice, similar to the 5-day model used in this thesis, have confirmed that targeting IL-33 may be beneficial in treating airway inflammation [213, 303, 304].

There are limited studies that comprehensively characterize the inflammatory and physiological responses to IL-33 in the murine airways. Therefore, I systematically defined IL-33-induced responses in the lungs *in vivo* demonstrating a major Th2-skewed inflammatory response, airway wall, fibrosis, and AHR. I further defined IL-33-mediated transcriptomic changes in murine lungs, and identified potential novel pathways and transcription factors involved in IL-33-mediated pathobiology. This study provides a baseline dataset that will enable deeper mechanistic interpretation as new insights into IL-33 induced pathobiology are discovered.

Although IL-33 is a central mediator of airway inflammation, and IDR-1002 supresses eosinophil and neutrophil accumulation in HDM-challenged mice by targeting IL-33, it is important to emphasize that CHDP and IDR peptides are not merely immunosuppressive but rather immunomodulatory molecules that contribute to maintaining immunological homeostasis. IDR peptides have been administered in mice s.c. and intraperitoneally at substantial concentrations of over 150 mg/kg with minimal deleterious health effects [53, 124, 125]. Furthermore, pathways and molecules altered by IDR peptides during an infection or chronic inflammation, are often unaffected in control mice that received the peptide alone [132, 136, 270, 312]. In the event that IDR peptide treatment alters molecules in naïve mice, the balance between pro- and anti-inflammatory mediators is maintained. Moreover, IDR peptide-treated mice often mount an enhanced immune response to resolve a insult [125, 136].

The molecular mechanisms of immunomodulatory activity of IDR peptides are still under investigation. A major hurdle is the lack of peptide specific antibodies. In a therapeutic sense, this suggests that IDR peptides are non immunogenic. However, the difficulty of raising antibodies against IDR peptides also leads to difficulty in attempting to co-IP peptide bound proteins and identify direct interacting protein partners. Furthermore, CHDP are also though to transiently bind target proteins with low affinity, further increasing the difficulty in detecting direct binding partners [101]. This leads me to speculate that the mechanism of IDR peptide activity may be as a result of an inherent property of certain cellular proteins to interact positively charged peptides with low affinity based on certain physical characteristics. This interaction, thus results in a transient change in conformation that can either activate or deactivate the protein briefly, disrupting a signalling cascade. Additionally, in a resting state, signalling molecules and receptors are not expressed in high quantity and are not active and therefore the effect of IDR peptides in changing the protein conformation may have insignificantly consequences. However, when signalling proteins or receptors are upregulated or utilized (during inflammation), the effects of immunomodulatory peptides are amplified and translated to downstream alterations in function. However, this inherent attraction or binding of IDR peptides to "certain" cellular proteins and not all upregulated proteins remains under investigation. Inversely, there also seems to be certain physical characteristics of IDR peptides that play a role in determining the types of interacting proteins. For example, IG-19 (synthetic IDR peptide derived from LL-37) was previously shown to be effective at reducing the pathobiology of rheumatoid arthritis [287]. However, IG-19 administered in the HDM-challenged murine model shows negligible effects on airway inflammation and lung function. This indicates that the interacting partners of these peptides are likely different. As CHDP are conserved throughout evolution and are found in all multicellular

organisms, there may be a framework engrained in proteins that allow the interaction of small positively charged amphipathic peptides with matching physical characteristics to regulate activity.

This precise physical properties of the peptides that direct the common low affinity interacting sites on target proteins have not yet been identified. Future technological advancements and protein-protein-interaction modelling using artificial intelligence (AI) may shed light to the interface between CHDP and its binding partners. As an early foray into this area of research, in the final study of this thesis, I attempt to uncover the sequence function relationship of IDR-1002 to better understand the physical attributes of IDR-1002 that is important in its function. I showed that substituting a single amino acid, tryptophan (W8), with the basic and polar amino acid arginine results in blunted immunomodulatory function of IDR-1002; this substitution abrogates the ability of the peptide to reduce airway inflammation in the HDM-challenged murine model and ability to suppress IL-33 production in HBEC-3KT cell line. IDR-1002, apart from IL-33, did not supress the median or the mean of 28 additional cytokines measured in the lung tissue of HDM-challenged mice. However, by representing relative cytokine abundance in a correlation matrix, I show that IDR-1002, and not IDR-1002.2(W8/R), alters relative cytokine levels within each mouse to similar ratios seen in naïve mice. This correlation matrix highlights the capacity of IDR-1002 to help maintain immunological homeostasis by balancing pro an anti-inflammatory cytokines during an inflammatory response. Although IDR-1002.2(W8/R) showed blunted immunomodulatory activity, IDR-1002.2(W8/R) did not lose the ability to reduce AHR. This suggests that the physical properties of IDR-1002 that were required for improving AHR were not altered by disrupting the W8. These data further suggest that the peptide interacting partners for balancing inflammation may be different from reducing AHR. This study provides two peptides, IDR-1002 and IDR-

1002.2(W8/R), which can be used as probes for dissecting molecular mechanisms that are unique and common between airway inflammation and AHR, which is not yet well understood.

AHR is measured with an increasing dose of methacholine that bind GPCR Muscarinic Acetylcholine Receptors (mAChR) in ASM cells [205]. Although there are 5 isoforms of mAChR in mammals, M_2 and M_3 have been identified to be expressed in ASM cells [205]. M_3 upon activation, increases intracellular calcium resulting in ASM constriction. M_2 activation leads to the inhibition of β-adrenoreceptor agonists induced ASM relaxation, further contributing to AHR [205]. Interestingly, a recent publication from Wu *et al* showed that IDR-1002 can alter GPCR expression and downstream signalling [138]. Therefore, mAChR may be altered by IDR-1002. In addition, IDR-1002 may alter downstream signalling pathways to reduce intracellular calcium influx in ASM, resulting in reduced AHR. I also showed that IDR-1002 decreased goblet cells in the HDM-challenged mice [312]. Therefore, reduced goblet cells likely result in reduced mucus in the airways of HDM-challenged mice treated with IDR-1002 further contributing to decreased airway obstruction and reduced AHR.

The above discussed work establishes the foundation by generating fundamental understanding of IDR-1002 that can be used to further investigate IDR-1002 and its derivatives as potential therapeutics for airway inflammation and AHR. However, future work is still required to fully understand the molecular mechanisms and therapeutic potential of IDR peptides. There are several experiments that I have conducted to generate preliminary data (supplementary studies in appendix section) for possible future directions for this body of work. One particular direction that I am excited for is identifying the mechanism of IL-33 suppression by IDR-1002. Demonstrating this mechanism is significant as IL-33 plays a central role in airway inflammation. Several exciting potentials are that (i) identifying the molecular pathway of IL-33 induction can

lead to novel drug targets, and (ii) reveals possible binding targets and insight into structure function activity of IDR-1002. I also show IDR-1002 reduced goblet cell hyperplasia and AHR in the acute and chronic HDM-challenged murine mode. This opens another exciting avenue to study the effect of IDR-1002 on the physiological changes in the lung.

Overall, this thesis has contributed to the scientific literature by characterising two murine models of airway inflammation, an allergen-challenged and IL-33-challenged model. The objective molecular readouts provided in this thesis for these models can be used to further interrogate molecular mechanisms, and to predict new targets for intervention in chronic inflammatory airway diseases. Furthermore, my work advances the development of IDR-1002 therapeutics for asthma and shows the potential to be beneficial in the control of the steroid-refractory form of the disease. The scope of this project is broad, as the use of IDR-1002 can be expanded to other IDR peptides and other chronic diseases that exhibit overlapping symptoms with asthma such as COPD. As IDR peptides are immunomodulatory and not just immunosuppressive, as well as exhibit antimicrobial functions, the advantage of developing IDR peptide-based therapy for asthma is the potential to alleviate steroid refractory disease, without compromising the patients' ability to resolve infections.

Appendix

Supplementary studies

Investigate the mechanism involved in IDR-1002-mediated suppression of IL-33 production:

I have shown that IDR-1002 can supress IL-33 in HDM-challenged murine lungs. I have also demonstrated that IDR-1002 suppresses IFNγ-induced IL-33 production *in vitro* in human PBEC and in the HBEC-3KT cell line. In more recent studies, I have shown that IDR-1002 does not target the canonical IFNγ pathway as canonical IFNγ-induced targets such as IP10 and IRF1 were not supressed by IDR-1002. I further confirmed that IFNγ-induced phosphorylation of STAT1 at Y701 and S727 sites which results in the homodimerization and activation of the STAT1 [373] were not altered by IDR-1002 (Figure A1). Therefore, to investigate the molecular mechanism of IL-33 suppression by IDR-1002, it is necessary to 1) identify the non canonical IFNγ-induced pathway and 2) the modifying effect of IDR-1002 on this pathway that results in the suppression of IL-33 production. To generate preliminary data to address these questions for future peers in the Mookherjee lab, I performed a targeted kinome array as described in chapter 3.4. HBEC-3KT cells were stimulated with IFNγ, in the presence and absence of IDR-1002, for 15 minutes. IFNγ induced phosphorylation changes in 26 (11 upregulated and 15 downregulated) unique phospho targets (Figure A1). Of the 26 altered phospho targets by IFNγ, addition of IDR-1002 significantly altered PELI2(T290) and STAT1(S708) (Figure A1). PELI2 is an ubiquitin ligase known to be involved in IL-1 family signaling pathways [376]. Moreover, STAT1 phosphorylated at site S708 (by IKKε) inhibits STAT1 homodimerization that is induced by STAT1(Y701 and S727) phosphorylation resulting in reduced activation of the gamma activated factor (GAF) complex [374]. The GAF complex is comprised of STAT1 dimers, cytokine responsive transcription factors and signal transducers that bind to gamma interferon activation sites (GAS) [377]. The promoter region of IL-33 contains multiple GAS elements [378]. Taken

together, this data suggests that IDR-1002 maybe supressing IL-33 by altering the GAF complex in HBEC-3KT cells. Therefore, alterations in STAT phosphorylation sites and GAF complex by IDR-1002 should be further investigated to study the mechanisms of how IDR-1002 supresses IL-33.

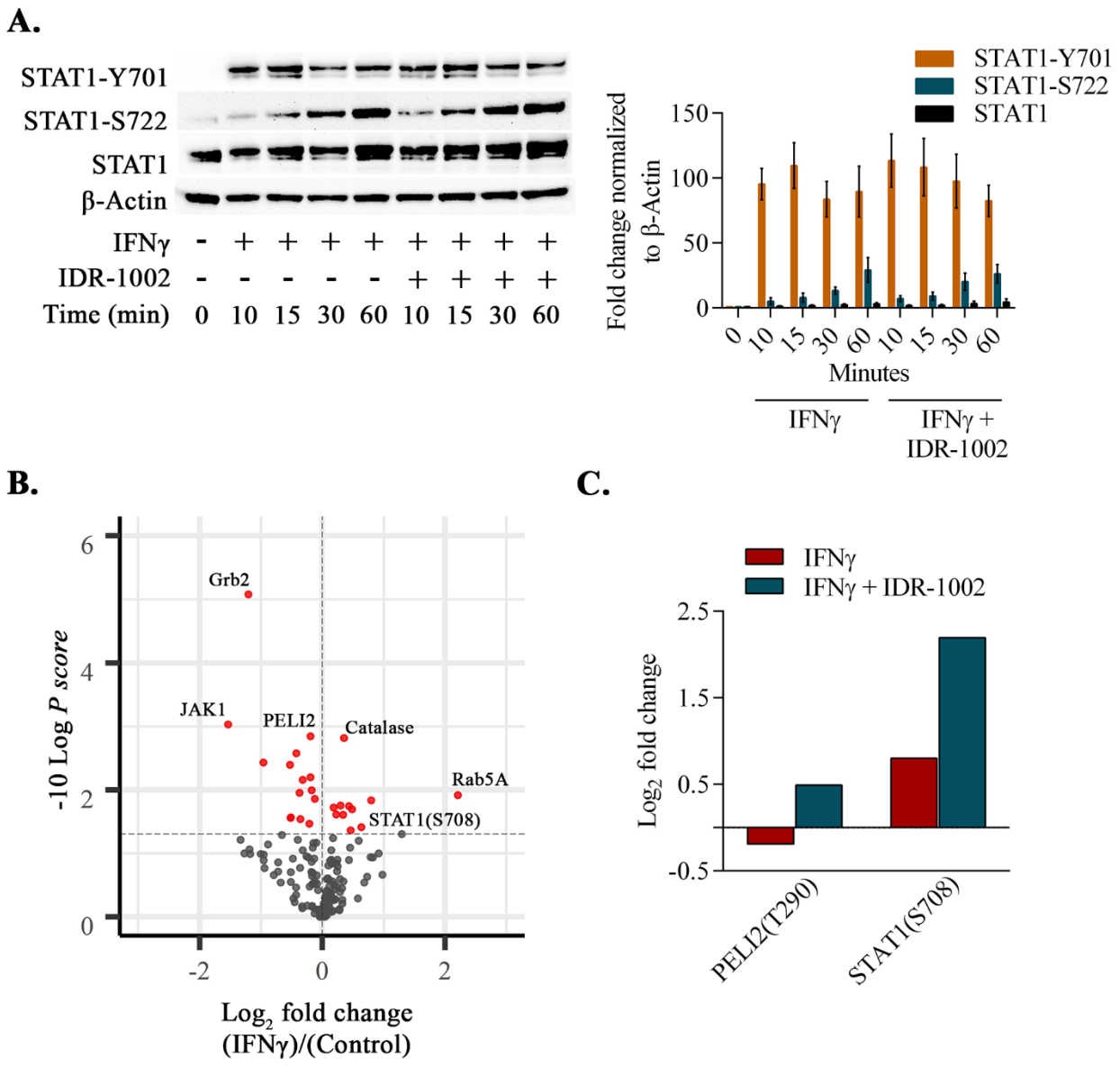

Figure A1: Phosphorylation and Kinome analysis in HBEC-3KT cells. *HBEC-3KT cells were stimulated with 30 ng/mL IFNγ ± 10uM of IDR-1002 and cell lysates were collected at multiple time points post-stimulation.* ***(A)*** *Representative western blot and fold changes (n = 5) calculated by densitometry analysis for STAT1* ***(B)*** *Kinase activity measured using JPT Kinome peptide arrays for IFNγ induced changes (n = 3) in 15 minutes* ***(C)*** *fold changes of PELI2 and STAT1.*

Investigate cellular localization and uptake of IDR peptides: Direct binding targets of IDR-1002 to date has not been identified. Determining these receptor(s) will be important to further probe molecular mechanisms of IDR-1002 activity. CHDP was shown to interact with intracellular receptors such as GAPDH and p62. Previous studies have demonstrated that IDR-1002 is taken up into synovial fibroblast cells within 15-30 min [135]. Therefore, I have performed a preliminary an experiment to measured intracellular uptake of the IDR peptides tagged with the fluorescent dye 5FAM at the C-terminal end. As IDR-1002(W8/R) mitigated the immunomodulatory functions of the peptide as discussed in chapter 3.4, I also examined if this substitution altered cellular uptake. Using fluorescent microscopy, I demonstrated that both IDR peptides (IDR-1002 and 1002.2) were in the cytoplasm in 12 hours and no notable differences in cellular uptake was observed (Figure A2). IDR peptides incubated with trypsin (1:50) for 1 hr at 37^0C and neutralized with soybean trypsin inhibitor was used as a negative control (Supplementary Figure 5.1). Preliminary analysis of Figure A1 shows accumulation of fluorescently tagged peptide around the nuclear membrane. This observation suggests that the peptides may be localized in the rough endoplasmic reticulum. This preliminary experiment facilitates future more comprehensive analysis with ER staining probes and co-localization studies by peers in the Mookherjee lab.

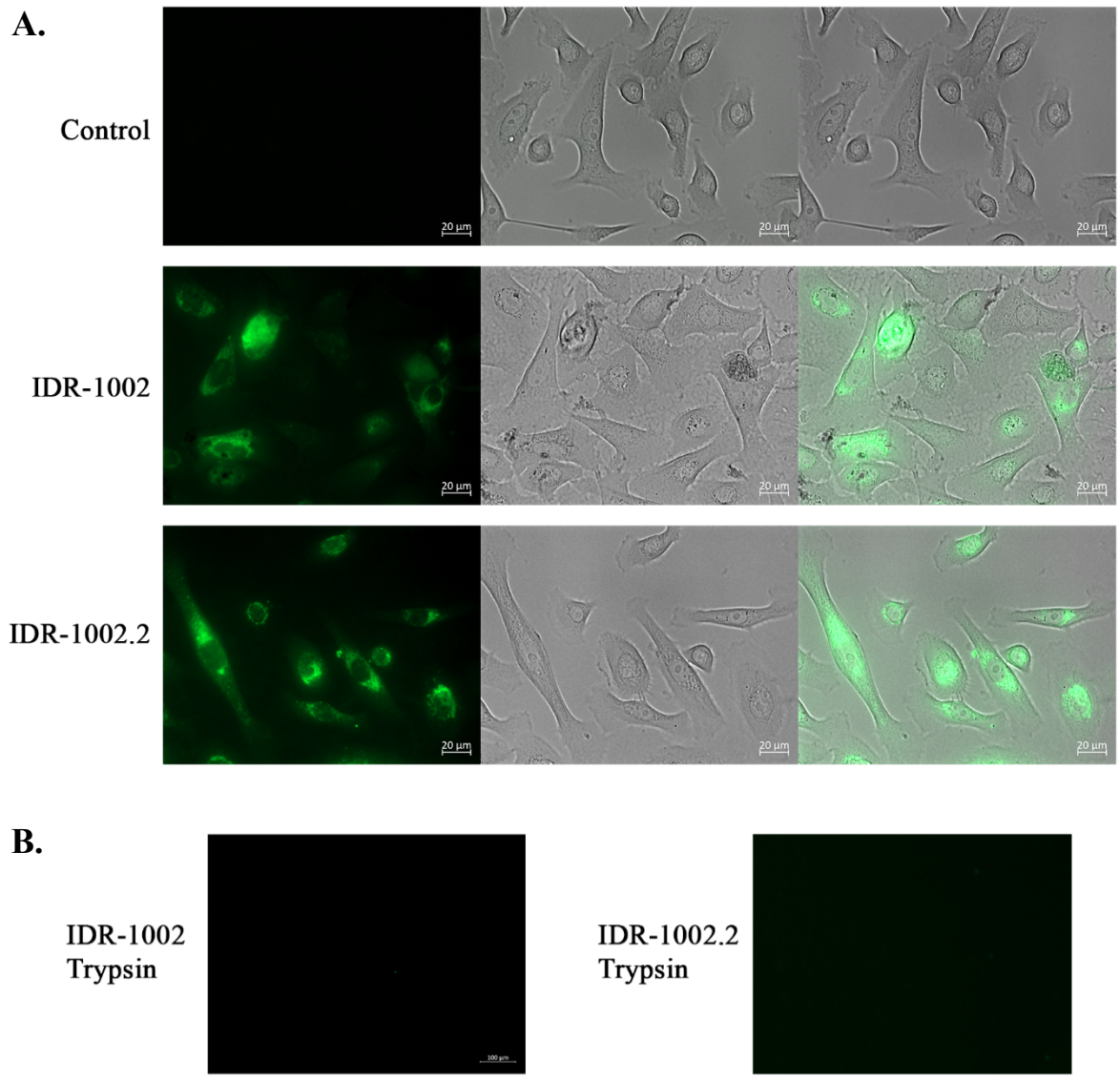

Figure A2: W8/R substitution does not alter internalization or stability of IDR-1002 in HBEC-3KT cells. *(A) Representative image of HBEC-3KT cells at 40X at 12 hr post stimulation with IDR-1002(5FAM) and IDR-1002.2(5FAM).* ***(B)*** *Representative image of HBEC-3KT cells at 40X at 12 hr post stimulation with IDR-1002(5FAM) incubated with trypsin at 37^0C for 30 min, neutralized with SBTI. Media was refreshed and imaged.*

Investigate the effects of IDR-1002 in influencing adaptive immunity: HDM-driven activation of immune cells, in particular mast cells, by HDM-specific antibodies play a central role in allergic asthma by triggering the release of activators such as histamine. To examine the effect of the peptide in HDM-mediated adaptive immune responses, I measured serum levels of total and HDM-specific IgE and IgG antibodies in the acute and chronic models of HDM-challenge, in the presence and absence of IDR-1002 administration. IDR-1002 peptide administration in the 2-week acute model did not alter the levels of HDM-specific or total IgE and IgG in the serum (Figure A3), thus suggesting that that the peptide may be intervening in allergen-specific antibody synthesis in later stage of the disease. In early preliminary studies, I have also examined the effect of IDR-1002 administration in the 5-week chronic model of HDM-challenge. Administration of the IDR-1002 lowered HDM-specific IgE antibodies (Figure A3). Therefore, future studies on the effects of IDR peptide on adaptive immune system, immunoglobulin production, B cell differentiation and activation is warranted. Further cells bridging the innate and adaptive immune systems such as ILC2, which is a downstream target of IL-33, may be altered with IDR peptide administration. Therefore, this body of work could be further expanded by investigating the effect of IDR peptides on all immune cells in the lungs that contribute to the initiation and pathogenesis of airway inflammation.

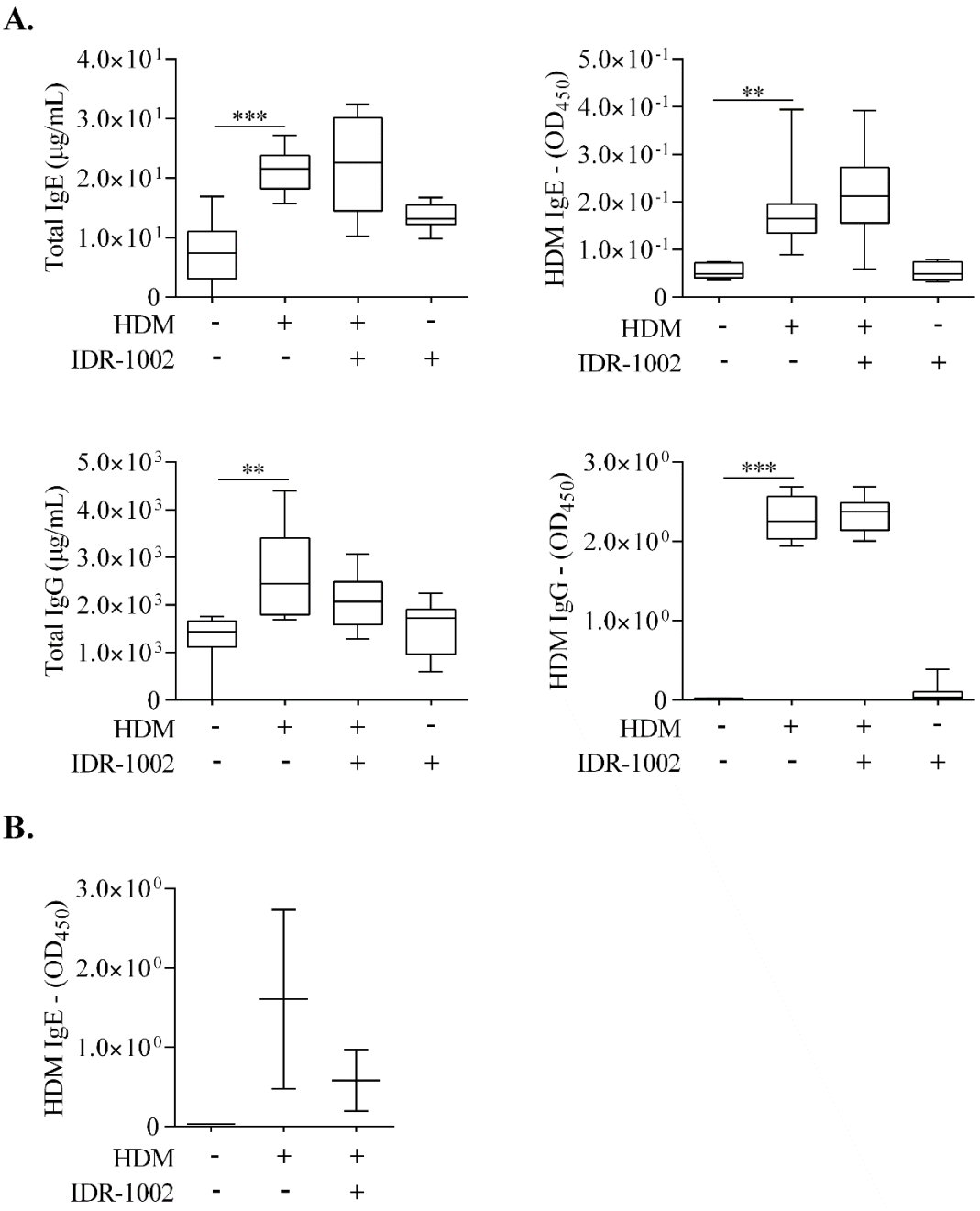

Figure A3: Immunoglobulin levels in acute and chronic HDM-challenged mice. *Mice were challenged by i.n. administration of 35 µl of whole HDM extract (0.7 mg/ml) in saline, for 2 weeks (acute) or 5 weeks (chronic). IDR-1002 was administered 3 times a week for both acute and chronic models. Immunoglobulin levels were monitored in serum from n = 8 for* ***(A)*** *acute and n = 2 for* ***(B)*** *chronic mice, 24 hr after the last HDM-challenge, by ELISA. Results are shown as box plots with median line, and statistical significance was determined using one-way ANOVA with Dunnett's multiple comparisons test (**p ≤ 0.01, ***p ≤ 0.001).*

Investigate the effects of IDR-1002 on the degranulation of eosinophils and neutrophils: Granulocytes contain a variety of granules that can be released when stimulated as discussed in chapter 1.1.4. The contents then contribute to asthma symptoms and pathogenesis. HDM-challenged in the murine model, resulted in a phenotypical "hole" like unstained portions in the granulocytes in the BALF cell H&E staining (Figure A4). As eosin potently stains basic proteins in the cytoplasm and in granules, this observation suggests possible degranulation event occurring in neutrophils and/or eosinophils following HDM-challenge. In contrast to HDM-challenged mice, the "hole" like unstained portions were predominantly absent from granulocytes of HDM-challenged mice treated with IDR-1002. Therefore, in preliminary studies, I measured granular contents specifically, mature MBP protein abundance by western blot and EPO enzyme activity in the BALF of HDM-challenged mice ± IDR-1002. I observed a complete absence of HDM induced MBP in the BALF of mice (n = 2) treated with IDR-1002 (Figure A4). Further, the EPO activity in BALF of HDM-challenged mice was significantly reduced with IDR-1002 administration (Figure A4). This suggests that there is less EPO present in the BALF or EPO activity is reduced in the presence of IDR-1002. Taken together, this preliminary data supports the hypothesis that IDR-1002 can alter degranulation of granulocytes. As such, future studies can be conducted by the Mookherjee lab to confirm these findings and investigate the mechanisms involved.

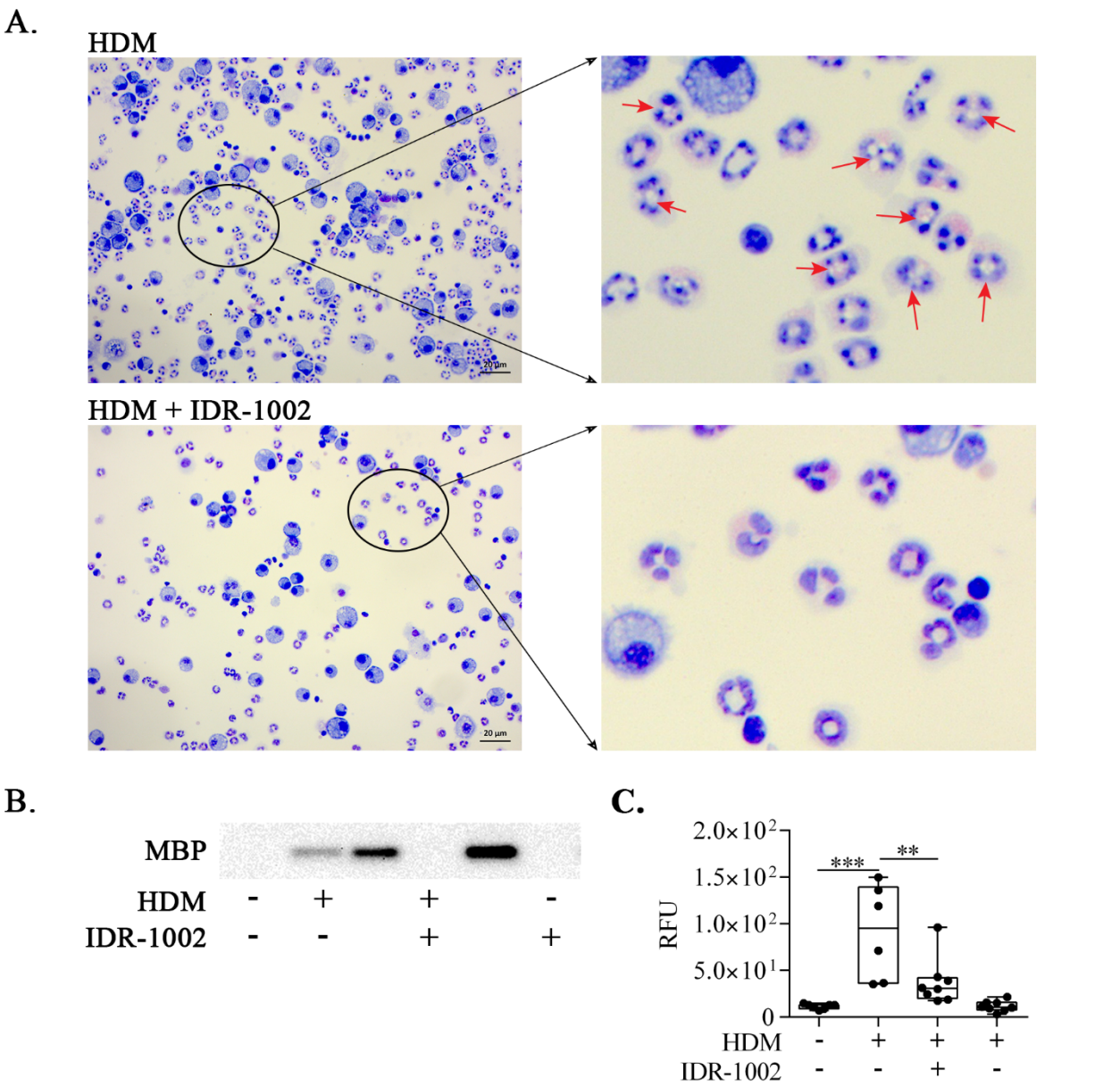

Figure A4: IDR-1002 reduces granule contents in the BALF of HDM-challenged mice. *Mice were challenged by i.n. administration of whole HDM extract in saline, for 2 weeks (Figure VI). IDR-1002 was administered s.c. 3 times a week (Figure VI). BALF was collected 24 hours after last HDM-challenge.* ***(A)*** *Representative image of H&E staining of BALF* ***(B)*** *Representative western blot image of MBP in the BALF* ***(C)*** *Relative Fluorescence Units (RFU) of EPO activity in the BALF. Results are shown as box plots with median line, and statistical significance was determined using one-way ANOVA with Dunnett's multiple comparisons test (**$p \leq 0.01$, ***$p \leq 0.001$).*

Investigate IDR-1002 in a chronic model of allergic asthma: Airway remodelling in asthma is seen after continuous and repetitive exposure to allergen. My thesis work has focused on the acute model, that precedes airway remodelling. To assess the effects of IDR-1002 on airway remodeling, a chronic HDM-challenged murine model could be used. Based on previous studies, 5-7 weeks of continuous HDM exposure have shown hallmarks of airway remodelling in asthma including, lung fibrosis, smooth muscle cell proliferation and collage deposition below the AEC basement membrane. I have performed a preliminary study to examine the effects of IDR-1002 in a chronic 5-week HDM-challenged model. BALB/c mice were challenged with (i.n.) HDM extract (0.7 mg/ml) in saline with five daily i.n administrations in week 1 and 2. The following week 3-5, HDM was administered on days 1,4, and 5. IDR-1002 (soluble in saline) was administered s.c. at 6 mg/kg per mouse (days 1, 3 and 5 per week). Assessment of lung mechanics showed that administration of IDR-1002 significantly reduced both maximum methacholine (50 mg/ml)-induced Newtonian resistance (Rn) by 89% (Figure A5), and decreased sensitivity to methacholine (amount required to double the baseline airway resistance (PC100)) by 3.5-fold in HDM-challenged mice. IDR-1002 reduced sensitivity to methacholine in HDM-challenged mice back to baseline levels as seen in naïve mice (Figure A5). I observed concomitant inhibition of HDM-challenge-induced maximum tissue damping (G) by 49% and tissue elastance (H) by 50% with IDR-1002 treatment (Figure A5), at maximal methacholine concentration. Notably, IDR-1002 fully abrogated the increase in Rn at all doses of methacholine due to HDM-challenge resulting in Rn similar to naïve mice. Taken together, these results indicate that the peptide exhibits the ability to decrease overall resistance of the airway tree (Rn), tissue resistance in the alveoli (G) and tissue elastance (H), demonstrating that the peptide have significant functional impact on airflow conductance of central, small and terminal bronchioles in a chronic HDM-challenged

murine model. This preliminary data provides the rationale for future studies to measure the impact of IDR-1002 on airway remodelling.

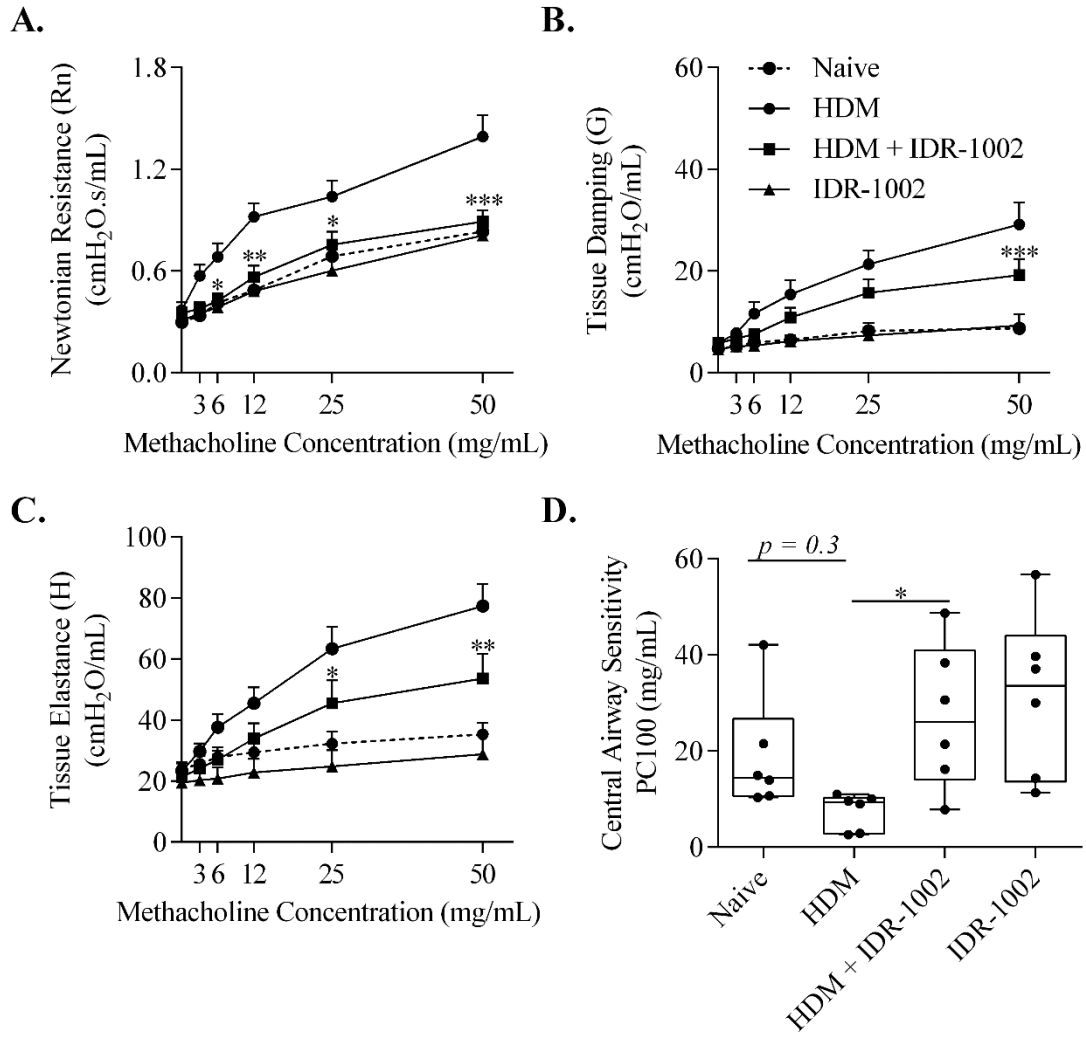

Figure A5: IDR peptides improve lung function in allergen challenged mice. *Mice (n = 6 per group) were challenged with 35 µl of whole HDM extract (0.7 mg/mL) in saline i.n., for 5 weeks. IDR-1002 was administered s.c. (6 mg/Kg) 3 times a week for 5 weeks. Lung mechanics were monitored, 24 hr after the last HDM-challenge. Mice were exposed to nebulized saline (baseline measures) followed by increasing concentrations of nebulized methacholine (3-50 mg/mL) and changes in* ***(A)*** *Newtonian resistance (Rn),* ***(B)*** *tissue damping (G),* ***(C)*** *tissue elastance (H) was monitored. Statistical significance was determined using two-way repeated measures ANOVA with Tukey's multiple comparisons test (*p ≤ 0.05, **p ≤ 0.01, ***p ≤ 0.001). * represent comparison between HDM and HDM + IDR-1002 group.*

Investigate the effects of IDR-1002 in steroid-resistant models of inflammation: Steroid insensitive asthma as detailed in chapter 1.3.4 is a major health care burden. I have shown that IDR-1002 supresses IL-33 in allergen-challenged murine lungs and in IFNγ-stimulated human bronchial cells. IL-33 is a key mediator associated with steroid resistant asthmatics as discussed in chapter 3.2. Therefore, my project may contribute to the development of novel therapies for steroid-refractory severe asthma. Future studies need to be conducted to further asses the effect of IDR-1002 administration in a steroid resistant murine model of asthma and cells obtained from severe asthmatic patients. These studies should also include combinatorial treatment with IDR-1002 and clinically used ICS that could lead to added benefit of lowering the effective dose of ICS.

Investigate IDR-1002 in a recall model of allergic asthma: I have shown that IDR-1002 reduces airway inflammation and AHR in an acute HDM-challenged murine model. Further studies need to be conducted to investigate the therapeutic window of IDR peptide administration. This includes administering IDR-1002 after the allergen sensitizing phase in an allergen-recall murine model. The recall model simulates the recall phenomenon to renewed allergen exposure in sensitized mice, following the development of immunological memory [229]. Therefore, by administering the peptide after sensitization phase, the ability of IDR-1002 as a therapeutic for allergic asthma can be effectively assessed.

In summary, I have discussed above multiple avenues to further explore the immunomodulatory and physiological functions of IDR-1002. I believe my research on uncovering regulatory mechanisms by which IDR peptides alter the airway inflammatory and structural phenotype will help to define pathways that are relevant to the therapeutic response in airway disease. Perhaps more importantly, my PhD project may unravel mechanisms that are at the core of steroid resistance. As such, I have provided preliminary studies outlined above, to

generate new hypotheses to evaluate the therapeutic potential of IDR-1002 and mechanisms of action in airway inflammatory diseases.

Supplementary figures

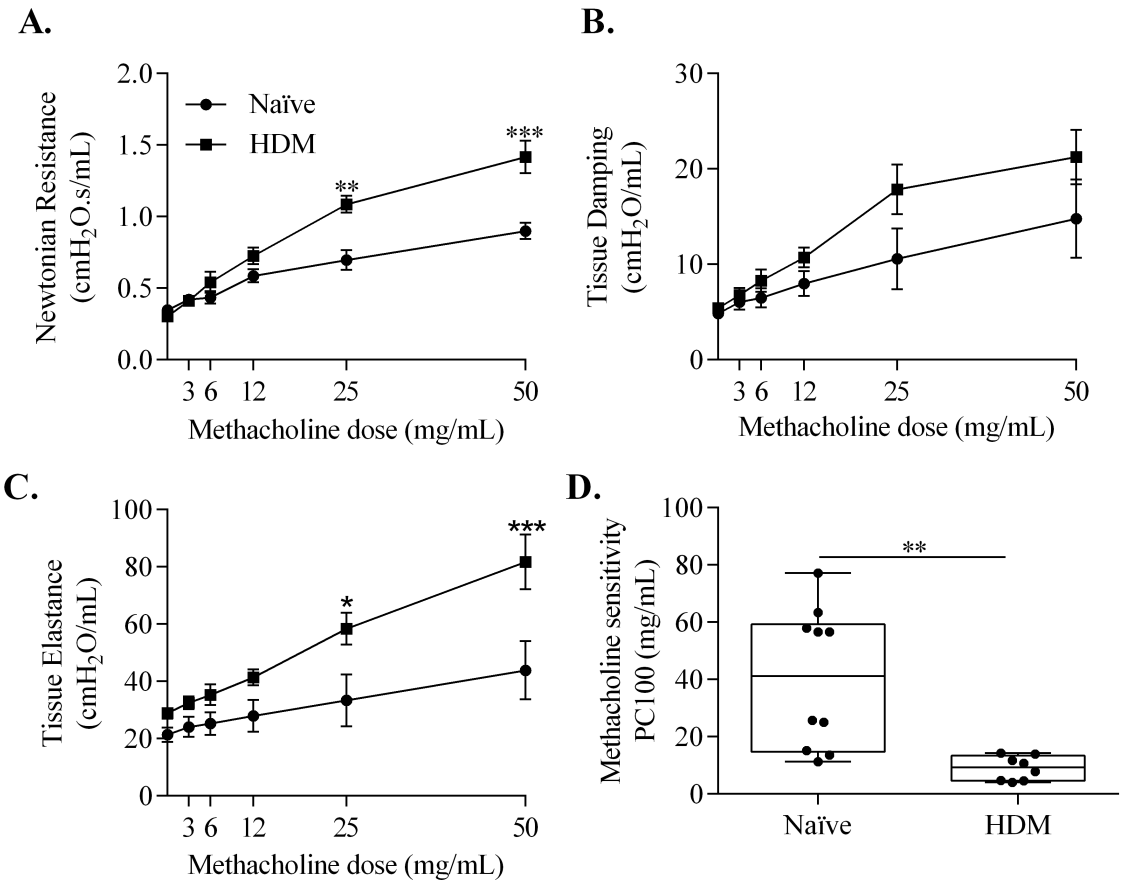

Supplementary Figure 1.1: Monitoring lung mechanics 8 hr after the last HDM-challenge. *Mice were challenged by i.n. administration of whole HDM extract in saline, for 2 weeks (Figure VI). Lung mechanics of naïve (n=10) and HDM-challenged (n=10) were monitored using a flexiVent™small animal ventilator, 8 hr after the last HDM-challenge. Baseline airway and tissue resistance and tissue elastance was calculated using saline. Mice were exposed to increasing dose of methacholine (3-50 mg/mL) and the change in airway and tissue resistance, and tissue elastance was monitored. Central airway sensitivity to methacholine was measured by calculating concentration of methacholine required to double baseline resistance (PC100). Mann-Whitney U test was used for statistical analyses (*p ≤ 0.05, **p ≤ 0.005, ***p ≤ 0.0005). Error bar shown represent SEM.*

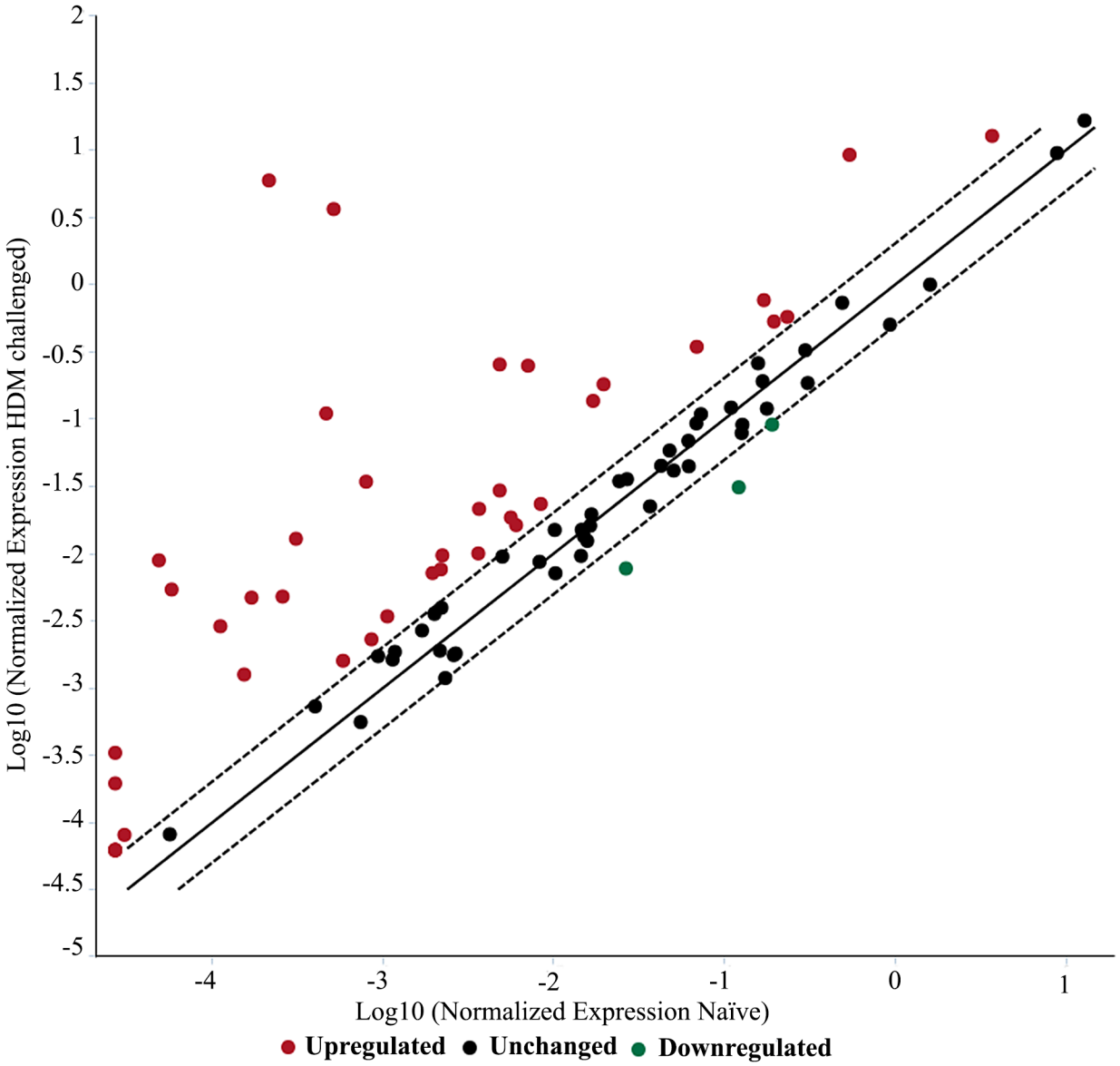

Supplementary Figure 1.2: Gene expression profile in the lung tissue lysates. *Mice were challenged by i.n. administration of whole HDM extract in saline, for 2 weeks (Figure VI). Lung tissues were collected in RNAlater® from HDM-challenged (n=3) and naïve mice (n=3), 24 hr after the last HDM-challenge. Total RNA was isolated from the tissues and the expressions of 84 murine genes (Mouse Allergy & Asthma PCR array) were monitored using a RT^2 Profiler™ PCR Array. Data quality control and relative fold changes were assessed using the RT^2 Profiler™ PCR Array data analysis software (Qiagen, data analysis center). The scatter plot shown represents normalized gene expression of HDM-challenged mice and allergen-naïve mice.*

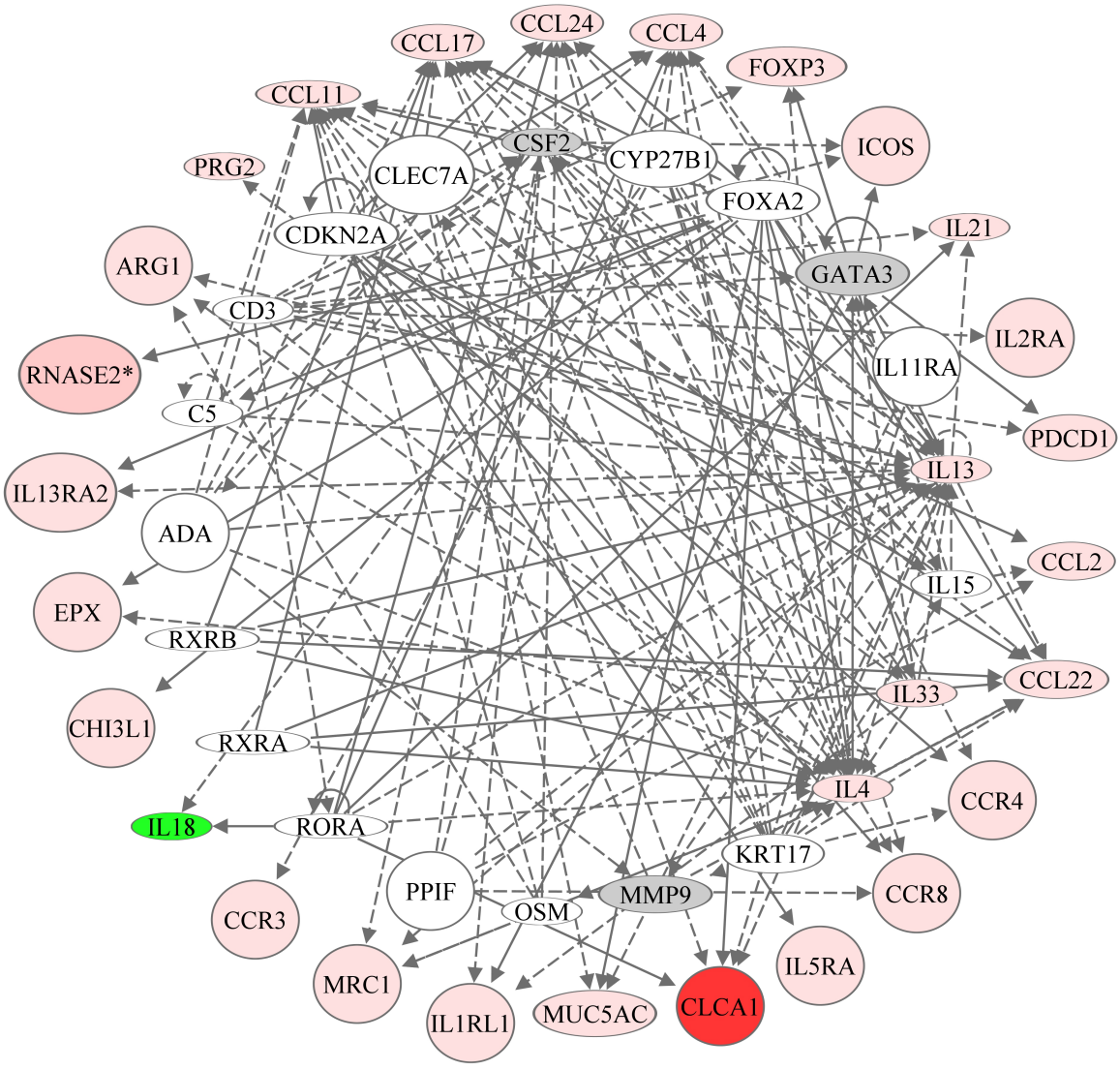

Supplementary Figure 1.3: Bioinformatics analyses of predicted upstream transcriptional regulators of the differentially expressed genes in response to allergen challenge. *Mice were challenged by i.n. administration of whole HDM extract in saline, for 2 weeks (Figure VI). Total RNA was isolated from the lung tissues and the expressions of 84 murine genes were monitored using a RT² Profiler™ PCR Array. Differentially expressed (DE) genes were defined as those that were either up- or down-regulated by ≥ 2-fold with associated p≤0.05, in HDM-challenged compared to naïve mice. 34 DE genes were identified in response to HDM (Supplementary Table 1.1).* ***(A)*** *shows the mRNA expression of some the predicted upstream regulators that were also identified to be DE in response to HDM. Red nodes = upregulated (intensity of color corresponds to the magnitude of fold change), green nodes = downregulated, orange nodes = upstream transcriptional regulators predicted to be activated, blue nodes = upstream transcriptional regulators predicted to be inhibited, solid lines = direct interactions and dotted lines = indirect interactions.*

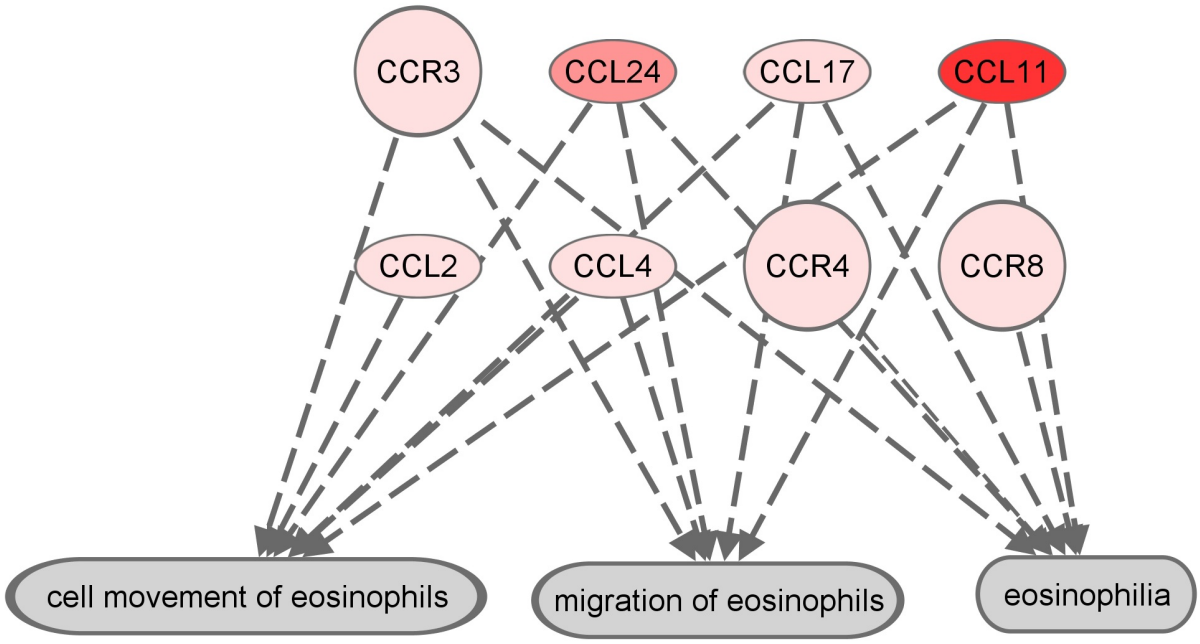

Supplementary Figure 1.4: Chemokines and chemokine receptors induced in response to HDM were predicted to be associated with eosinophil recruitment. *Of the 31 mRNAs induced in response to HDM-challenge, 5 out of the 6 chemokines upregulated and all three upregulated chemokine receptors were predicted to be associated with eosinophil migration, recruitment and eosinophilia using the Ingenuity® Pathway Analysis tool. Red nodes represent upregulated genes. The intensity of color corresponds to the magnitude of fold change in HDM-challenged lungs relative to that in allergen-naïve mice.*

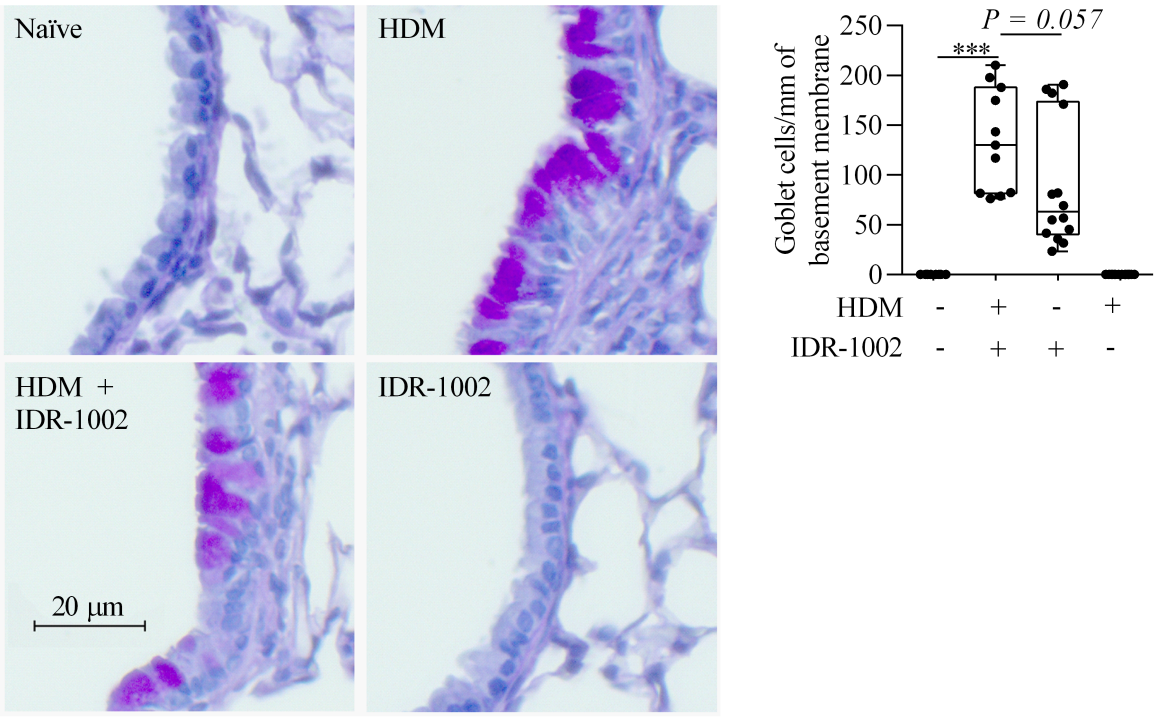

Supplementary Figure 2.1: Subcutaneous administration of IDR-1002 markedly decreases goblet cell hyperplasia. *Mice (n = 2-4 per group) were challenged by i.n. administration of whole HDM extract in saline, for 2 weeks (Figure VI). IDR-1002 was administered s.c. 3 times a week (Figure VI). Lung sections (6 µm) were stained with PAS staining.* ***(A)*** *Representative images of PAS staining of the lung tissue.* ***(B)*** *Number of goblet cells per mm of basement membrane length. Each dot represents individual airways. Statistical significance was determined by one-way ANOVA with Tukey's multiple comparisons test*

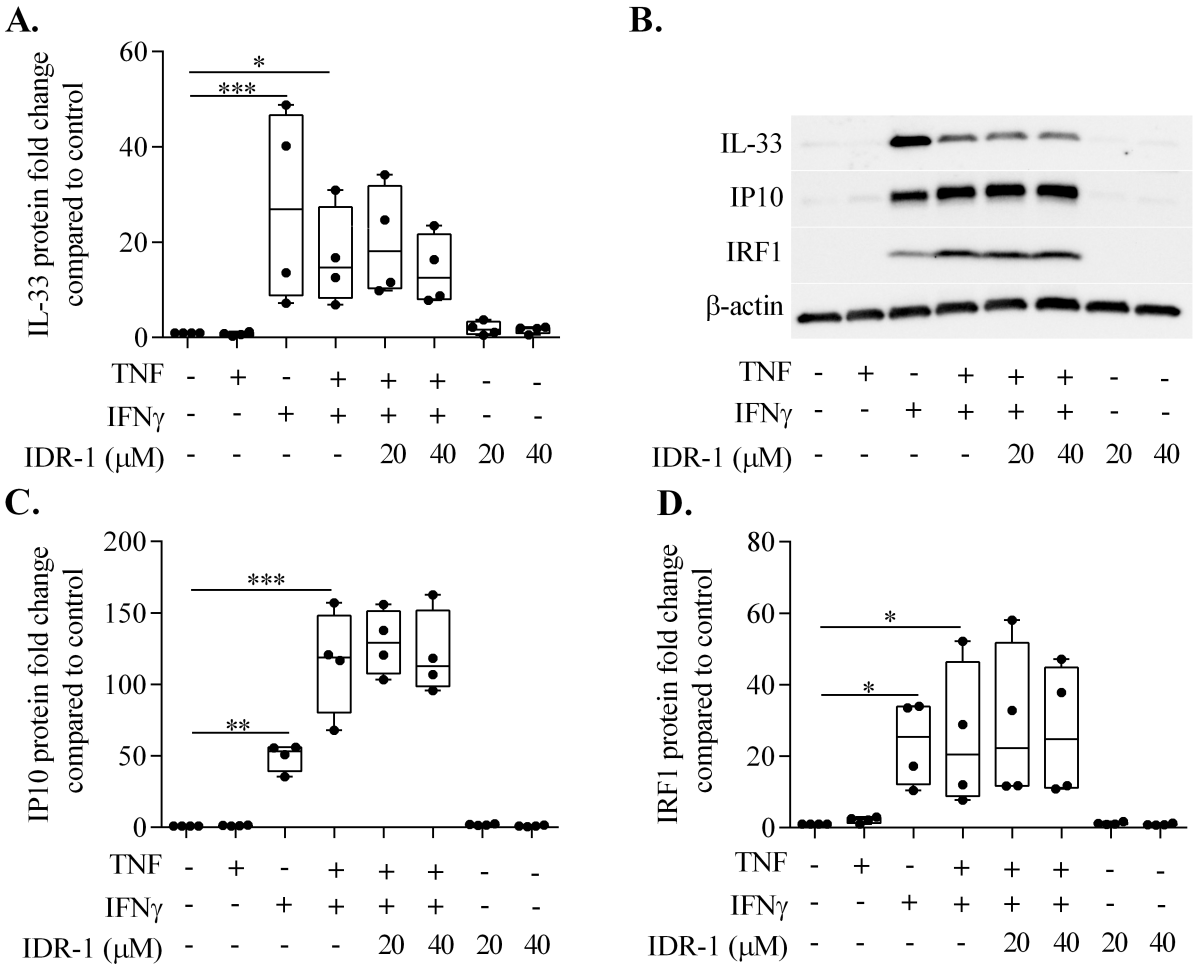

Supplementary Figure 2.2: IDR-1 does not alter IL-33 production in human PBEC. *Human PBEC obtained from 4 donors were stimulated with TNF (20 ng/mL) and IFNγ (30 ng/mL), in the presence and absence of IDR-1 (20 and 40 μM). IL-33, IRF1 and IP10 abundance was monitored in cytoplasmic fractions of the cell lysates by western blots, 24 hr post-stimulation. Protein abundance were quantified by densitometry.* ***(A)*** *A representative immunoblot for all proteins, and densitometry analyses (n=4) for* ***(B)*** *IL-33,* ***(C)*** *IRF1 and* ***(D)*** *IP-10 are shown. Protein fold change shown in the graphs represents relative band intensity compared to that in unstimulated cells normalized to 1, after normalization with β-actin for protein input. Each dot represents an individual donor, and bars show the median and interquartile range. RM one-way ANOVA with Fisher's LSD test was used for statistical analyses (*p ≤ 0.05, **p ≤ 0.01).*

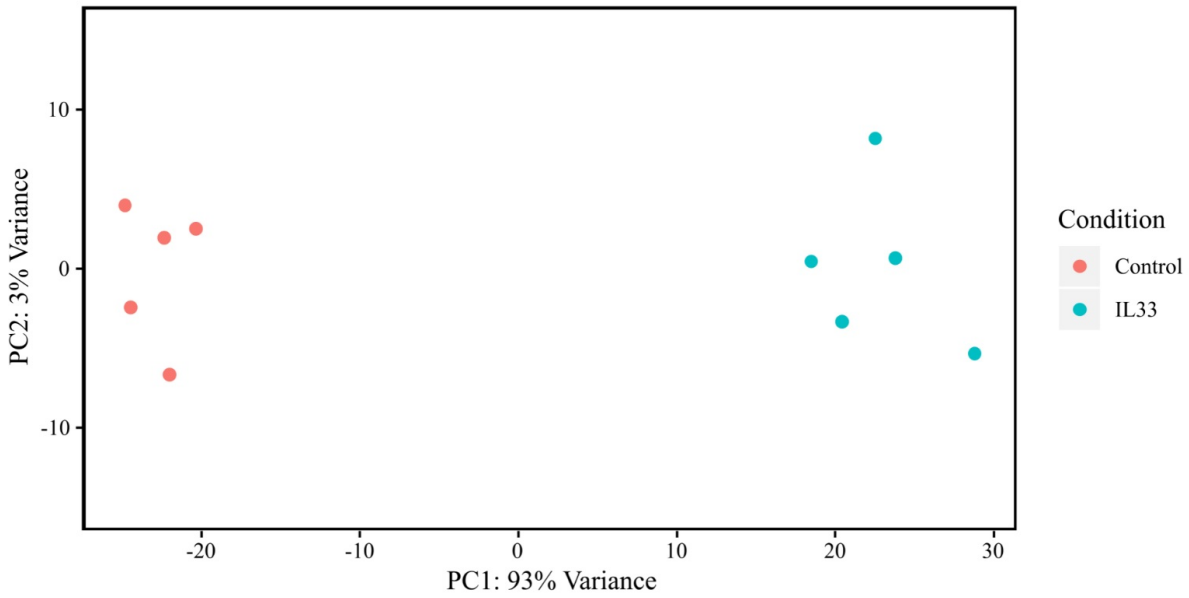

Supplementary Figure 3.1: PCA analysis of RNA-Seq data showing clustering of mice with IL-33 administration. *Mice were challenged with murine IL-33 in saline i.n., for five consecutive days. RNA was extracted from lung tissues of IL-33 challenged and saline mice (n=5). DEseq2 package in R was used to generate PCA plot.*

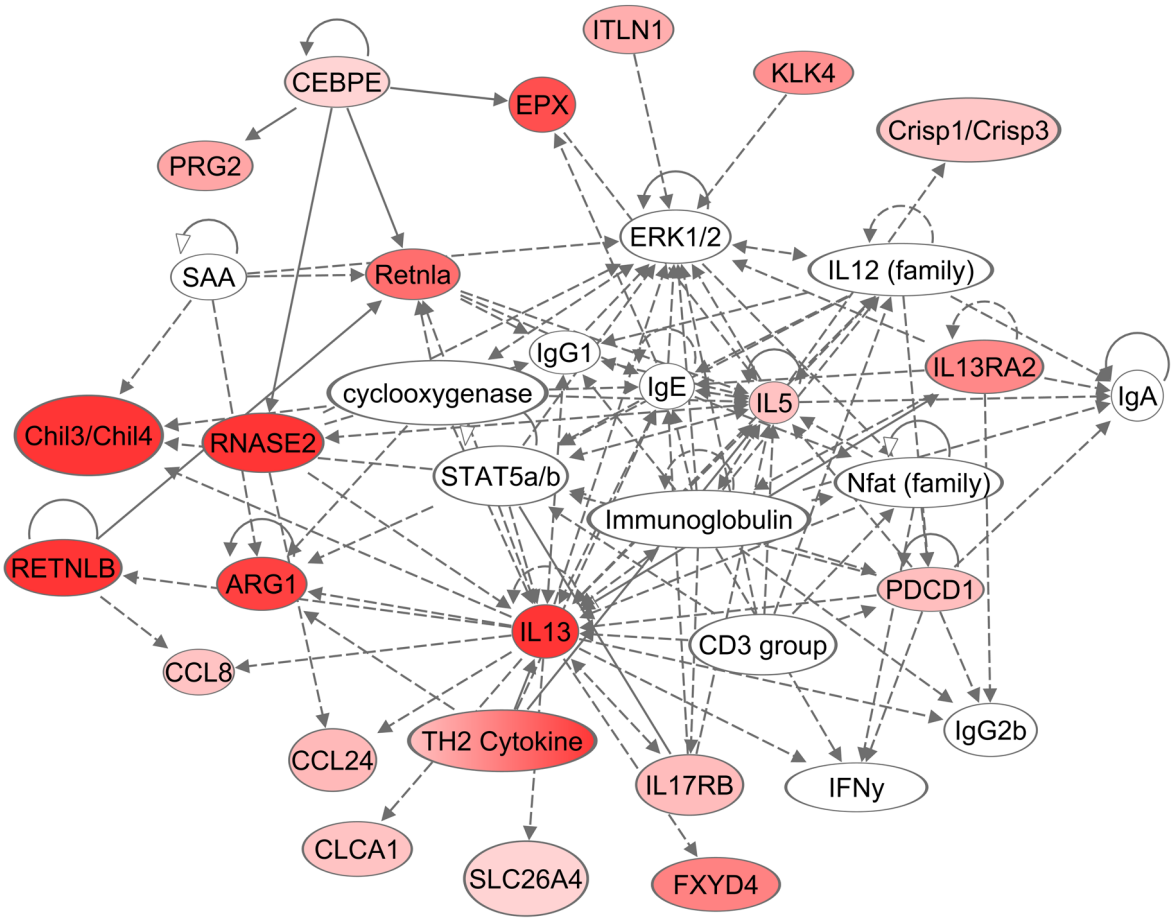

Supplementary Figure 3.2: Interaction network of genes altered by IL-33. *The top 50 genes upregulated by IL-33 using direct and indirect relationships formed a single biological network that contained 21 of the 50 upregulated genes. The intensity of red nodes depicts the degree of upregulation (darker = higher upregulation). Solid lines represent direct interactions, and dotted line represent indirect interactions.*

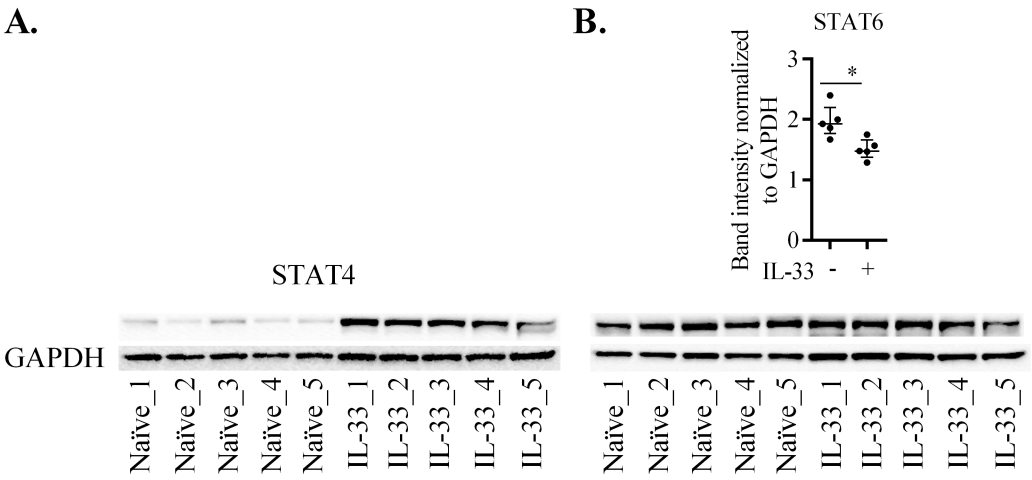

Supplementary Figure 3.3: Validation of biological network of predicted upstream regulators in response to IL-33. *Western blot analysis of **(A)** STAT4 (Densitometry shown in Figure 3.6) and **(B)** STAT6. Female BALB/c (8-10 wks) mice were challenged with 1µg of murine IL-33 in saline i.n., for five consecutive days. Lung tissue lysates were obtained from naïve and IL-33-challenged mice. Statistical analyses were performed using the Mann-Whitney U test (*p ≤ 0.05, **p ≤ 0.01).*

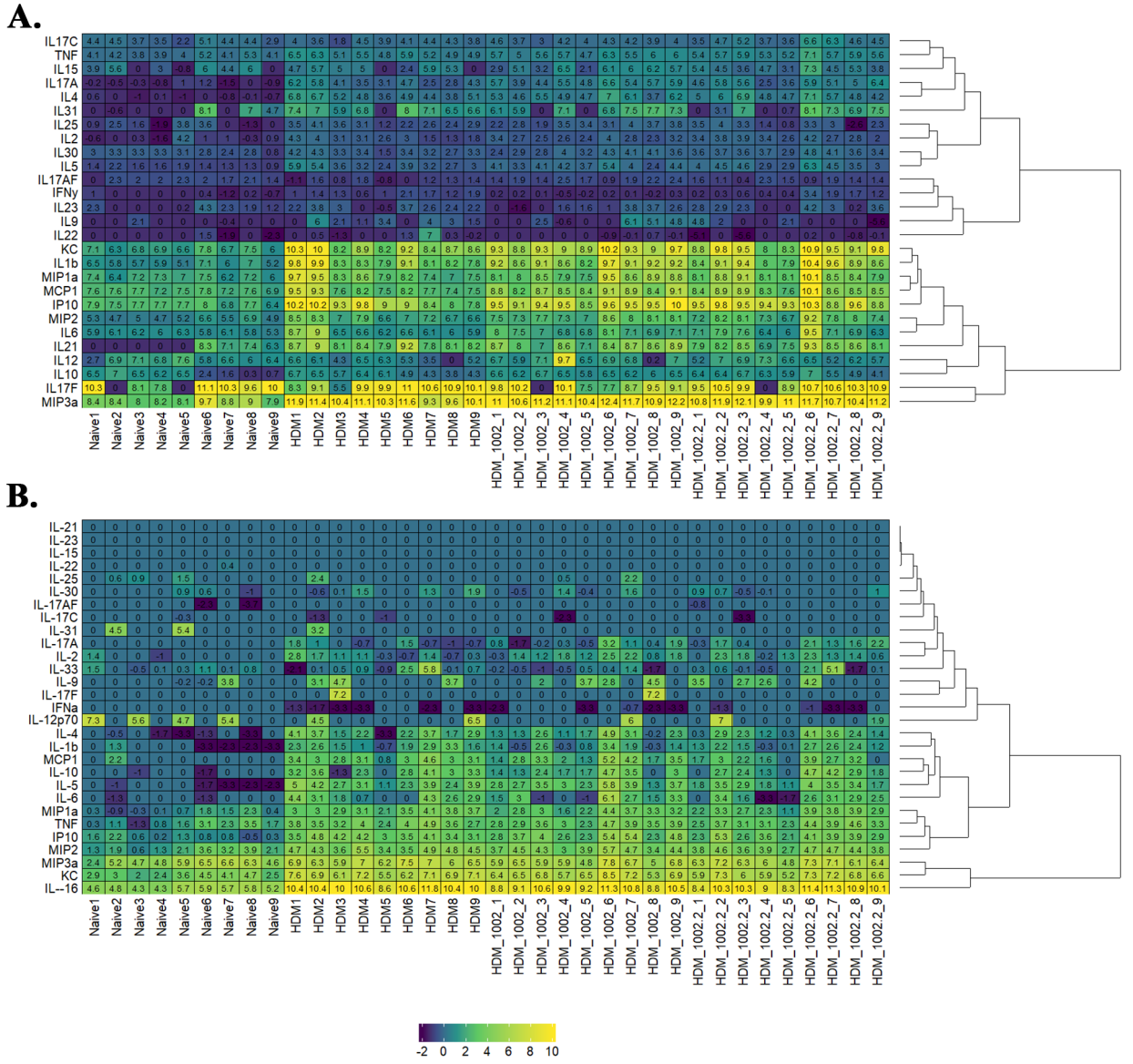

Supplementary Figure 4.1: Heat map of cytokine abundance in mice. *Mice (n = 9 per group) were challenged by i.n. administration of whole HDM extract in saline, for 2 weeks (Figure VI). IDR-1002 was administered s.c. 3 times a week (Figure VI). Lung tissue and BALF was collected 24 hr after last challenge. Figure shows heat map of normalized log2 expression values for cytokine abundance of individual mice in* ***(A)*** *lung tissue lysates and* ***(B)*** *BALF. Undetected outcomes were set as 0. Heat map and kmeans clustering was performed using superheat package in R.*

Supplementary tables

Supplementary Table 1.1: Fold change of mRNA expression of 84 genes monitored in lung tissues of HDM-challenged mice relative to allergen-naïve mice.

Gene	Gene Name	Fold Change	P-value
Clca3	Chloride Channel Calcium Activated 3	27508.69	<0.001
Ear11	Eosinophil-Associated, Ribonuclease A Family, Member 11	7032.07	<0.001
Muc5ac	Mucin 5, Subtypes A And C, Tracheobronchial/Gastric	235.58	<0.001
Epx	Eosinophil Peroxidase	181.60	<0.001
Il13ra2	Interleukin 13 Receptor, Alpha 2	93.09	0.01
Ccl11	Chemokine (C-C Motif) Ligand 11	52.70	<0.001
Prg2	Proteoglycan 2, Bone Marrow	42.88	<0.001
Il13	Interleukin 13	41.51	<0.001
Arg1	Arginase, Liver	35.16	0.03
Ccl24	Chemokine (C-C Motif) Ligand 24	27.59	0.01
Il10	Interleukin 10	25.70	0.08
Pdcd1	Programmed Cell Death 1	18.48	<0.001
Chia1	Chitinase, Acidic	17.06	<0.001
Il21	Interleukin 21	12.16	<0.001
Ccl17	Chemokine (C-C Motif) Ligand 17	9.24	<0.001
Tnfsf4	Tumor Necrosis Factor (Ligand) Superfamily, Member 4	8.17	0.03
Ccl12	Chemokine (C-C Motif) Ligand 12	8.00	<0.001
Il17a	Interleukin 17a	7.21	0.10
Ccl22	Chemokine (C-C Motif) Ligand 22	6.08	<0.001
Il4	Interleukin 4	5.86	0.01
Ccr3	Chemokine (C-C Motif) Receptor 3	4.99	0.01
Retnlg	Resistin Like Gamma	4.51	0.01
Ccr4	Chemokine (C-C Motif) Receptor 4	4.34	0.01
Ccr8	Chemokine (C-C Motif) Receptor 8	3.66	0.02
Il2ra	Interleukin 2 Receptor, Alpha Chain	3.49	0.01
Chil1	Chitinase 3-Like 1	3.45	<0.001
Ccl4	Chemokine (C-C Motif) Ligand 4	3.29	0.03
Il5ra	Interleukin 5 Receptor, Alpha	3.21	0.02
Il1rl1	Interleukin 1 Receptor-Like 1	2.78	0.04
Tnfrsf4	Tumor Necrosis Factor Receptor Superfamily, Member 4	2.77	0.06
Foxp3	Forkhead Box P3	2.73	0.01
Mrc1	Mannose Receptor, C Type 1	2.72	0.01
Icos	Inducible T-Cell Co-Stimulator	2.69	0.03
Il5	Interleukin 5	2.68	0.14
Ccl26	Chemokine (C-C Motif) Ligand 26	2.64	0.25
Il33	Interleukin 33	2.46	0.01
Adam33	A Disintegrin And Metallopeptidase Domain 33	2.31	0.41

Il25	Interleukin 25	2.31	0.41
Il3	Interleukin 3	2.31	0.41
Il9	Interleukin 9	2.31	0.41
Mgdc	Mouse Genomic Dna Contamination	2.31	0.25
Cpa3	Carboxypeptidase A3, Mast Cell	1.89	0.09
Tpsb2	Tryptase Beta 2	1.84	0.01
Pmch	Pro-Melanin-Concentrating Hormone	1.82	0.24
Cd40lg	Cd40 Ligand	1.80	0.06
Il17rb	Interleukin 17 Receptor B	1.78	0.01
Ifngr2	Interferon Gamma Receptor 2	1.65	<0.001
Fcer1a	Fc Receptor, Ige, High Affinity I, Alpha Polypeptide	1.58	0.14
Ifng	Interferon Gamma	1.58	0.19
Gapdh	Glyceraldehyde-3-Phosphate Dehydrogenase	1.50	0.12
Gusb	Glucuronidase, Beta	1.49	<0.001
Cma1	Chymase 1, Mast Cell	1.48	0.27
Ear5	Eosinophil-Associated, Ribonuclease A Family, Member 5	1.44	0.49
Il12b	Interleukin 12b	1.43	0.09
Stat5a	Signal Transducer And Activator Of Transcription 5a	1.42	0.04
Maf	Avian Musculoaponeurotic Fibrosarcoma (V-Maf) As42 Oncogene Homolog	1.36	0.03
Cysltr1	Cysteinyl Leukotriene Receptor 1	1.33	0.42
B2m	Beta-2 Microglobulin	1.29	0.34
Pparg	Peroxisome Proliferator Activated Receptor Gamma	1.22	0.21
Crlf2	Cytokine Receptor-Like Factor 2	1.17	0.44
Tgfb1	Transforming Growth Factor, Beta 1	1.14	0.58
Itga4	Integrin Alpha 4	1.12	0.87
Il13ra1	Interleukin 13 Receptor, Alpha 1	1.11	0.39
Postn	Periostin, Osteoblast Specific Factor	1.09	0.55
Actb	Actin, Beta	1.07	0.88
Csf3r	Colony Stimulating Factor 3 Receptor (Granulocyte)	1.06	0.98
Csf2	Colony Stimulating Factor 2 (Granulocyte-Macrophage)	1.05	0.62
Gata3	Gata Binding Protein 3	1.03	0.90
Mmp9	Matrix Metallopeptidase 9	-1.02	0.79
Alox5	Arachidonate 5-Lipoxygenase	-1.05	0.61
Ms4a2	Membrane-Spanning 4-Domains, Subfamily A, Member 2	-1.10	0.46
Bcl6	B-Cell Leukemia/Lymphoma 6	-1.12	0.24
Rorc	Rar-Related Orphan Receptor Gamma	-1.14	0.08
Ltb4r1	Leukotriene B4 Receptor 1	-1.21	0.29
Satb1	Special At-Rich Sequence Binding Protein 1	-1.22	0.19
Il4ra	Interleukin 4 Receptor, Alpha	-1.26	0.13
Il12a	Interleukin 12a	-1.33	0.36
Gpr44	G Protein-Coupled Receptor 44	-1.39	0.01
Il3ra	Interleukin 3 Receptor, Alpha Chain	-1.39	0.19

Kit	Kit Oncogene	-1.40	0.06
Stat6	Signal Transducer And Activator Of Transcription 6	-1.44	0.11
Ccl5	Chemokine (C-C Motif) Ligand 5	-1.47	0.24
Hsp90ab1	Heat Shock Protein 90 Alpha (Cytosolic), Class B Member 1	-1.48	0.13
Tslp	Thymic Stromal Lymphopoietin	-1.48	0.11
Ets1	E26 Avian Leukemia Oncogene 1, 5' Domain	-1.49	0.05
Kitl	Kit Ligand	-1.50	0.01
Tbx21	T-Box 21	-1.53	0.17
Adrb2	Adrenergic Receptor, Beta 2	-1.60	0.03
Areg	Amphiregulin	-1.60	0.01
Il18	Interleukin 18	-1.64	<0.001

Supplementary Table 1.2: Predicted upstream transcriptional regulators of genes identified to be differentially expressed in response to HDM-challenge.

Upstream Regulator	Predicted Activation State	Target molecules Activated by the Regulator & Upregulated in the dataset	Target molecules Activated by the Regulator & Downregulated in the dataset	Target molecules Inhibited by the Regulator & Upregulated in the dataset	Target molecules Affected by the Regulator (unknown activated or inhibited) & Upregulated in the dataset
IL33	Activated	*Epx, Il13, Il1rl1, Il4, Prg2*			
CLEC7A	Activated	*Ccl17, Ccl22, Clca1, Il33, Muc5ac*			
RORA	Activated	*Ccl24, Ccl4, Clca1, Il21*	*Il18*		
IL4	Activated	*Arg1, Ccl11, Ccl17, Ccl22, Ccl24, Ccl4, Ccr8*		*Foxp3*	*Il13, Il4, Mrc1*
CDKN2A	Activated	*Ccl11, Ccl2, Ccl22, Ccl24, Ccl4, Ccr4, Ccr8, Il5ra*			
CSF2	Activated	*Icos, Il13, Il1rl1, Il4, Mrc1*			
PPIF	Activated	*Ccl2, Ccl4, Ccr8, Il13*			
GATA3	Activated	*Foxp3, Icos, Il13, Il1Rl1, Il4, Pdcd1*			
IL13	Activated	*Arg1, Ccl11, Ccl17, Ccl22, Ccl24, Ccl4, Clca1, Il13, Il13Ra2, Il21, Il4, Mrc1*			
IL11RA	Activated	*Ccl11, Ccl17, Ccl4, Clca1, Muc5ac*			

IL15	Activated	*Ccl11, Ccl17, Ccl2, Foxp3, Il13*			
OSM	Activated	*Arg1, Ccl11, Ccl24, Il4, Mrc1*			
CD3	Inhibited			*Foxp3, Icos, Il13, Il21, Il2ra, Il4*	*Pdcd1*
RXRB	Inhibited			*Ccl17, Ccl22, Il13, Il4*	
MMP9	Inhibited			*Ccl11, Ccl22, Il13, Il4*	
RXRA	Inhibited			*Ccl17, Ccl22, Il13, Il4*	
FOXA2	Inhibited			*Ccl11, Ccl17, Ccl22, Ccl24, Clca1, Epx, Il13, Il13ra2, Il33, Il4, Muc5ac, Rnase2*	*Chi3l1*
ADA	Inhibited	*Ccl11, Ccl17, Ccl24, Il13, Il4*			
CYP27B1	Inhibited	*Ccl11, Ccl17, Ccl4, Ccr3, Ccr4, Ccr8, Il4*	*Il18*		
KRT17	Inhibited	*Ccl11, Ccl17, Ccl22, Ccl24, Ccl4, Ccr4, Il13, Il4*			

Supplementary Table 1.3: HDM-induced cytokine profile in Serum. *Serum obtained from naïve (n = 9) and HDM-challenged (n = 10) mice were monitored for production of a panel of cytokines using the multiplex MSD platform, 24 hr after the last HDM-challenge. Median values are reported. Statistical analyses were performed using the Mann-Whitney U test.*

Cytokine	Serum			
	Naïve (pg/mL)	HDM (pg/mL)	Fold Change	P value
IFNγ	0.62	0.54	0.87	0.191
IL-1β	6.29	5.46	0.87	0.529
IL-2	2.06	1.66	0.81	0.286
IL-4	0.36	0.51	1.41	0.262
IL-5	2.33	3.32	1.42	0.714
IL-6	253.00	448.00	1.77	0.826
KC	188.00	245.50	1.31	0.714
IL-10	97.10	108.40	1.12	1
IL-12	15.20	11.70	0.77	0.286
TNF	0.00	7.05	NA	1

Supplementary Table 2.1: Cytokine expression profile in lung homogenates of HDM-challenged mice, in the presence and absence of IDR-1002. *Lung tissue obtained from naïve (n = 9) and HDM-challenged (n = 10) mice were monitored for production of a panel of cytokines using the multiplex MSD platform, 24 hr after the last HDM-challenge. Median values are reported for each cytokine in pg/mL. Statistical analysis was performed using one-way ANOVA with Tukey's multiple corrections.*

Cytokine	Lung Tissue Lysates (pg/mL)				
	Naïve (Group 1)	HDM (Group 2)	HDM + IDR-1002 (Group 3)	IDR-1002 (Group 4)	P value (Group 2 vs 3)
IFNγ	0.32	0.89	0.72	0.43	0.98
IL-1β	4.69	25.24	27.40	7.64	0.79
IL-2	0.87	1.74	2.28	1.64	0.52
IL-4	0.62	10.02	8.81	1.00	0.98
IL-5	0.22	4.19	5.96	0.33	0.21
IL-6	12.11	50.08	60.16	21.09	0.92
KC	14.37	93.48	93.46	29.06	0.99
IL-10	2.69	8.61	9.91	4.11	1
IL-12	37.12	79.76	71.08	50.41	1
TNF	2.93	5.61	5.92	2.69	0.89
IL-13	171.80	333.00	297.30	249.70	0.99
IL-25	5.05	5.85	3.67	2.52	0.29
MDC	46.50	89.83	100.10	40.75	0.99
TARC	13.35	47.40	66.54	10.58	0.63
TSLP	6.98	7.40	5.95	4.64	0.33

Supplementary Table 3.1: Top 50 upregulated genes identified in the RNA-Seq dataset in response to IL-33 compared to naïve mice.

Gene Symbol	Gene Name	FC	Adjusted P value
Chil4	Chitinase-like 4	1481.2	4.34E-109
Sprr2a3	Small proline-rich protein 2A3	733.4	3.68E-27
Rnase2a	Ribonuclease, rnase A family, 2A	656.2	3.21E-212
Il13	Interleukin 13	624.1	2.48E-21
Tff1	Trefoil factor 1	620.1	1.23E-21
Retnlb	Resistin like beta	373.0	8.40E-37
Arg1	Arginase 1	279.1	0
Epx	Eosinophil peroxidase	258.1	7.97E-17
Gm15056	Predicted gene 15056(Gm15056)	224.4	2.64E-18
Msx3	Msh homeobox 3	224.1	1.10E-15
Retnla	Resistin like alpha	212.2	6.00E-79
Ear6	Eosinophil-associated, ribonuclease A family, member 6	185.0	9.39E-29
Fxyd4	FXYD domain-containing ion transport regulator 4	183.2	4.97E-51
Il13ra2	Interleukin 13 receptor, alpha 2	174.5	1.67E-14
Klk4	Kallikrein related-peptidase 4 (prostase, enamel matrix, prostate)	161.0	1.65E-13
Igkv4-74	Immunoglobulin kappa variable 4-74	153.8	3.55E-08
9230102O04Rik	RIKEN cDNA 9230102O04 gene	144.0	2.86E-13
Adgrg7	Adhesion G protein-coupled receptor G7	136.4	2.17E-13
Prg2	Proteoglycan 2, bone marrow	130.6	1.07E-37
Itln1	Intelectin 1 (galactofuranose binding)	118.1	2.47E-57
Serpina11	Serine (or cysteine) peptidase inhibitor, clade A (alpha-1 antiproteinase, antitrypsin), member 11	113.3	3.67E-11
Mucl1	Mucin-like 1	112.9	7.98E-65
Duoxa1	Dual oxidase maturation factor 1	112.1	1.02E-14
Ccl24	Chemokine (C-C motif) ligand 24	101.5	7.55E-129
Il17rb	Interleukin 17 receptor B	97.6	1.56E-259
Prg3	Proteoglycan 3	95.6	7.02E-11
Pdcd1	Programmed cell death 1	95.3	9.04E-79
Col6a5	Collagen, type VI, alpha 5	92.8	0.00E+00
AA467197	Expressed sequence AA467197	90.2	1.38E-61
Il5	Interleukin 5	89.7	1.91E-28
Krt83	Keratin 83	87.0	3.77E-19
Clca1	Chloride channel accessory 1	87.0	1.34E-08
Ccl8	Chemokine (C-C motif) ligand 8	86.9	1.52E-143
Gm49087	Predicted gene(Gm49087)	85.6	3.51E-19
A130023I24Rik	RIKEN cdna A130023I24 gene	83.1	8.25E-10
Capn9	Calpain 9	83.0	8.05E-25
Gm47615	Predicted gene(Gm47615)	82.6	2.93E-10
Crisp1	Cysteine-rich secretory protein 1	81.1	9.00E-10
Nxpe1-ps	Neurexophilin and PC-esterase domain family, member 1, pseudogene	73.5	6.49E-16
Ptgdr	Prostaglandin D receptor	73.1	6.55E-12
Gm9765	Predicted gene(Gm9765)	68.6	7.25E-11

Gm47050	Predicted gene(Gm47050)	64.8	1.14E-77
Kng1	Kininogen 1	64.4	2.57E-09
Slc26a4	Solute carrier family 26, member 4	64.0	2.83E-55
Cebpe	CCAAT/enhancer binding protein (C/EBP), epsilon	62.8	2.82E-17
Ocstamp	Osteoclast stimulatory transmembrane protein	62.6	5.08E-28
Alox15	Arachidonate 15-lipoxygenase	59.5	5.15E-257
Btbd17	BTB (POZ) domain containing 17	56.0	6.71E-09
Olfr60	Olfactory receptor 60	55.2	1.34E-17
Tcrg-C4	T cell receptor gamma, constant 4	52.5	5.00E-82

Supplementary Table 3.2: Top 15 enriched biological processes mediated by IL-33 using the PANTHER overrepresentation tool IL-33. *PANTHER Overrepresentation tool (Released 20190417) showed enrichment of 9 leukocyte migration and chemokine mediated signaling pathways in the top 15 enriched biological processes sorted by fold enrichment, in response to IL-33. Test type = Fisher, Correction = Bonferroni.*

GO Biological Process Complete	Fold Enrichment	P value
Kinetochore organization (go:0051383)	8.67	1.08E-02
Eosinophil migration (go:0072677)	**8.46**	**4.27E-03**
Eosinophil chemotaxis (go:0048245)	**8.19**	**1.63E-02**
DNA replication initiation (go:0006270)	7.66	9.43E-03
Lymphocyte chemotaxis (go:0048247)	**6.87**	**1.07E-05**
Monocyte chemotaxis (go:0002548)	**6.5**	**8.79E-04**
Chemokine-mediated signaling pathway (go:0070098)	**6.22**	**2.03E-07**
Mitotic spindle assembly (go:0090307)	5.91	5.67E-03
Positive t cell selection (go:0043368)	5.86	1.45E-02
Lymphocyte migration (go:0072676)	**5.85**	**3.20E-06**
Negative regulation of mitotic sister chromatid segregation (go:0033048)	5.62	4.90E-02
Mononuclear cell migration (go:0071674)	**5.5**	**5.24E-03**
Cellular response to chemokine (go:1990869)	**5.28**	**3.51E-06**
Response to chemokine (go:1990868)	**5.28**	**3.51E-06**
Regulation of mitotic metaphase/anaphase transition (go:0030071)	4.99	1.59E-03

Supplementary Table 3.3. Top 3 predicted biological pathways activated in response to IL-33 challenge in the lungs by IPA bioinformatics tool.

Ingenuity Canonical Pathways	-Log(P value)	Z-Score
EIF2 Signaling	1.65E+01	4.824
Th2 Pathway	1.29E+01	3.317
Leukocyte Extravasation Signaling	8.74E+00	1.82

Supplementary Table 4.1: Cytokines abundance in lung tissue lysates. *Lung tissue obtained from n = 9 mice per group were monitored for production of a panel of cytokines using the multiplex MSD platform, 24 hr after the last peptide administration. Median values are reported for each cytokine in pg/mL. Statistical analysis was performed using one-way ANOVA with Dunnett's multiple corrections (*p ≤ 0.05, **p ≤ 0.01, ***p ≤ 0.001).*

Cytokine	Lung Tissue Lysates (pg/mL)				
	Group 1 Naïve	Group 2 IDR-1002	P value (Group 1 vs 2)	Group 3 IDR-1002.2	P value (Group 1 vs 3)
IFNy	0.99	0.56	0.055	0.79	0.326
IL-1β	58.47	18.81	****0.0022**	63.68	0.258
IL-2	1.25	0.86	0.372	0.67	0.311
IL-4	0.63	0.66	0.688	0.49	0.458
IL-5	2.70	1.71	****0.0036**	1.48	****0.0086**
IL-6	66.12	39.17	****0.0054**	30.40	****0.0064**
KC	109.97	63.04	***0.0119**	108.86	0.577
IL-10	73.92	26.54	0.134	18.09	***0.0369**
IL-12p70	94.46	64.26	0.366	47.37	0.179
TNF	17.14	6.32	***0.0296**	15.51	0.870
MIP3α	341.30	163.81	****0.0015**	254.37	***0.0201**
IL-22	0.00	0.00	NA	0.00	NA
IL-23	2.22	0.00	0.088	0.00	0.700
IL-17C	20.67	7.74	0.263	18.36	0.992
IL-31	0.00	0.00	NA	0.00	NA
IL-21	0.00	0.00	NA	0.00	NA
IL-17F	773.20	326.62	***0.0136**	529.49	0.444
IL-17A	0.82	0.91	0.886	1.04	0.897
IL-25	1.83	1.22	0.213	3.07	0.802
IL-9	0.00	1.71	0.296	0.00	0.358
MCP1	188.14	114.67	0.131	140.16	0.991
IL-33	9029.77	1965.44	*****0.0002**	5064.32	0.108
IL-30	8.04	9.36	0.297	6.75	0.890
IL-15	14.73	36.95	0.197	27.03	0.490
IL-17A/F	3.95	4.52	0.832	3.68	0.877
MIP1α	143.06	49.18	*****0.0003**	78.60	***0.0307**
IP10	208.69	95.74	****0.0018**	149.59	0.179
MIP2	36.63	18.24	****0.0091**	28.78	0.085

Supplementary Table 4.2: Cytokines abundance in BALF. *BALF obtained from n = 9 mice per group were monitored for production of a panel of cytokines using the multiplex MSD platform, 24 hr after the last peptide administration. Median values are reported for each cytokine in pg/mL. Statistical analysis was performed using one-way ANOVA with Dunnett's multiple corrections (*p ≤ 0.05, **p ≤ 0.01, ***p ≤ 0.001).*

Cytokine	BALF (pg/mL)				
	Group 1 Naïve	Group 2 IDR-1002	P value (Group 1 vs 2)	Group 3 IDR-1002.2	P value (Group 1 vs 3)
IFNy	0.00	0.00	NA	0.00	NA
IL-1β	0.05	0.00	0.262	0.00	0.703
IL-2	0.00	0.00	0.616	0.20	0.999
IL-4	0.10	0.15	0.946	0.10	0.714
IL-5	0.05	0.05	0.594	0.20	0.850
IL-6	0.00	0.00	NA	0.00	NA
KC	7.85	5.65	0.060	8.20	0.289
IL-10	0.00	0.00	NA	0.00	NA
IL-12	0.00	0.00	NA	0.00	NA
TNF	2.80	0.70	***0.005**	0.90	***0.0103**
MIP3α	49.20	23.35	0.139	34.10	0.715
IL-22	0.00	0.00	NA	0.00	NA
IL-23	0.00	0.00	NA	0.00	NA
IL-17C	0.00	0.00	NA	0.00	NA
IL-31	0.00	0.00	NA	0.00	NA
IL-21	0.00	0.00	NA	0.00	NA
IL-17F	0.00	0.00	NA	0.00	NA
IL-16	41.55	38.00	0.862	39.50	0.999
IL-17A	0.00	0.00	NA	0.00	NA
IL-25	0.00	0.00	NA	0.00	NA
IL-9	0.00	0.00	NA	0.00	NA
MCP1	0.00	0.00	NA	0.00	NA
IL-33	1.09	0.54	0.565	0.30	0.113
IL-30	0.00	0.00	NA	0.00	NA
IL-15	0.00	0.00	NA	0.00	NA
IL-17A/F	0.00	0.00	NA	0.00	NA
MIP1α	1.44	1.29	0.194	1.64	0.757
IP10	1.60	1.06	0.211	0.89	0.491
MIP2	4.31	2.12	***0.0262**	2.76	0.066

Supplementary Table 4.3: Cytokines abundance in lung tissue of allergen challenged mice. *Lung tissue obtained from n = 9 mice per group were monitored for production of a panel of cytokines using the multiplex MSD platform, 24 hr after the last HDM-challenge. Median values are reported for each cytokine in pg/mL. Statistical analysis was performed using one-way ANOVA with Dunnett's multiple corrections (*p ≤ 0.05, **p ≤ 0.01, ***p ≤ 0.001).*

Cytokine	Lung Tissue Lysates (pg/mL)						
	Group 1 Naïve	Group 2 HDM	P Value Group 1 vs 2	Group 3 HDM + IDR-1002	P Value Group 2 vs 3	Group 4 HDM + IDR-1002.2	P Value Group 2 vs 4
IFNγ	0.99	2.46	***0.0338**	1.10	0.728	1.52	0.992
IL-1β	58.47	310.58	****0.0058**	538.40	0.909	484.13	0.726
IL-2	1.25	7.83	0.086	6.37	0.999	10.30	0.843
IL-4	0.63	30.38	***0.0487**	39.66	0.839	31.48	0.874
IL-5	2.70	9.47	0.160	16.63	0.990	16.55	0.961
IL-6	66.12	90.00	0.345	135.22	0.999	136.27	0.959
KC	109.97	424.22	***0.0242**	644.30	0.876	707.16	0.605
IL-10	73.92	52.46	0.991	87.53	0.264	79.72	0.756
IL-12p70	94.46	38.33	0.835	103.24	0.203	89.20	0.917
TNF	17.14	37.43	***0.0486**	50.35	0.994	51.13	0.734
MIP3α	341.30	1388.04	***0.0262**	1989.83	0.386	2035.46	0.698
IL-22	0.00	0.86	0.451	0.00	0.428	0.03	0.450
IL-23	2.22	5.17	0.999	2.04	0.934	7.01	0.999
IL-17C	20.67	16.12	0.983	16.20	1.000	23.57	0.060
IL-31	0.00	112.05	0.850	89.61	0.984	118.87	0.977
IL-21	0.00	293.21	0.284	337.62	0.961	286.09	0.933
IL-17F	773.20	941.55	0.882	707.96	0.685	1223.07	0.931
IL-17A	0.82	17.15	0.078	42.16	0.196	34.57	0.432
IL-25	1.83	7.26	0.560	8.78	0.932	8.01	0.952
IL-9	0.00	4.43	0.414	0.00	0.996	0.00	0.712
MCP1	188.14	203.82	0.331	427.92	0.467	371.58	0.370
IL-30	8.04	10.03	0.447	11.18	0.913	12.26	0.516
IL-15	14.73	31.13	1.000	34.22	0.719	22.94	0.882
IL-17AF	3.95	2.33	****0.003**	3.29	****0.0087**	2.70	0.359
MIP1α	143.06	294.53	0.068	352.13	0.998	346.86	0.844
IP10	208.69	512.13	****0.0012**	704.69	0.969	726.83	0.789
MIP2	36.63	124.23	***0.0349**	207.61	0.737	230.08	0.453

Supplementary Table 4.4: Cytokines abundance in BALF of allergen challenged mice. *BALF obtained from n = 9 mice per group were monitored for production of a panel of cytokines using the multiplex MSD platform, 24 hr after the last HDM-challenge. Median values are reported for each cytokine in pg/mL. Statistical analysis was performed using one-way ANOVA with Dunnett's multiple corrections (*p ≤ 0.05, **p ≤ 0.01, ***p ≤ 0.001).*

Cytokine	BALF (pg/mL)						
	Group 1 Naïve	Group 2 HDM	P value Group 1 vs 2	Group 3 HDM + IDR-1002	P value Group 2 vs 3	Group 4 HDM + IDR-1002.2	P value Group 2 vs 4
IFNγ	0.00	0.10	0.241	0.10	0.995	0.00	0.999
IL-1β	0.10	3.70	****0.0028**	2.60	0.753	2.90	0.829
IL-2	0.00	2.20	***0.041**	2.70	0.597	2.50	0.979
IL-4	0.10	4.70	0.176	3.20	0.915	5.00	0.982
IL-5	0.10	8.80	0.057	8.10	0.868	7.60	0.791
IL-6	0.00	6.00	0.477	2.80	0.917	5.50	0.945
KC	7.80	120.40	****0.0018**	90.70	0.981	95.70	0.932
IL-10	0.00	8.20	0.140	3.30	0.965	5.10	1.000
IL-12p70	0.00	0.00	0.826	0.00	0.984	0.00	0.999
TNF	3.10	12.40	****0.0084**	11.60	0.990	9.80	0.972
MIP3α	37.40	93.70	0.093	60.20	0.928	80.00	0.975
IL-22	0.00	0.00	0.546	0.00	1.000	0.00	1.000
IL-23	0.00	0.00	NA	0.00	NA	0.00	NA
IL-17C	0.00	0.00	0.994	0.00	0.724	0.00	0.672
IL-31	0.00	0.00	0.414	0.00	0.990	0.00	0.991
IL-21	0.00	0.00	NA	0.00	NA	0.00	NA
IL-17F	0.00	0.00	0.702	0.00	0.999	0.00	0.718
IL-16	36.80	1384.70	*****0.0009**	979.90	0.934	1260.20	0.974
IL-17A	0.00	0.60	0.364	1.30	0.548	2.40	0.699
IL-25	0.00	0.00	1.000	0.00	1.000	0.00	0.769
IL-9	0.00	0.00	0.898	0.00	0.997	0.00	0.998
MCP1	0.00	8.07	***0.0373**	6.86	0.885	4.53	0.639
IL-33	1.10	1.43	0.523	0.72	0.554	1.07	0.940
IL-30	0.00	0.65	0.389	0.00	0.956	0.72	0.870
IL-15	0.00	0.00	NA	0.00	NA	0.00	NA
IL-17AF	0.00	0.00	0.940	0.00	0.976	0.00	0.564
MIP1α	1.28	8.58	*****0.0006**	8.08	0.866	7.68	0.910
IP10	1.68	11.56	***0.0338**	13.43	0.728	11.84	0.992
MIP2	4.24	22.12	****0.0018**	20.29	0.970	14.81	0.611

Supplementary Table 4.5: Differences in log2 intensity between IDR-1002 and IDR-1002.2(W8/R). *HBEC-3KT cells were stimulated with 10uM of IDR-1002 and IDR-1002.2(W8/R) and cell lysates were collected 15 min post stimulation. Kinase activity was measured using JPT Kinome peptide arrays. Average log2 intensity shown. Greater than 2 fold changes reported. Statistical analysis was performed using Students t-test.*

Phospho Target	Log2Expression			
	Group 1 IDR-1002	Group 2 IDR-1002.2	Log2FC Group 1 vs 2	P value Group 1 vs 2
Flt3_P36888_Y842	7.01	4.25	2.76	1.01E-03
STAT1 _P42224_S708	10.68	9.07	1.61	2.89E-06
STAT1 _P42224_Y701	11.93	10.52	1.41	1.00E-04
Syk _P43405_Y525/6	10.59	9.23	1.36	1.88E-03
MK2_P16389_Y132	8.71	7.41	1.30	9.56E-02
p53 _P04637_S15	6.98	5.76	1.22	8.46E-02
Met _P08581_Y1003	7.55	6.40	1.15	3.35E-02
Jun _P05412_S73	9.14	7.99	1.15	1.75E-01
Ripk1_Q13546_Y694	12.59	11.50	1.09	1.01E-07
Mek2_P36507_S226	8.74	7.68	1.06	1.68E-02
Lck_P06239_Y192	10.30	9.24	1.05	2.34E-05
TRAF6_Q9Y4K3_Y353	9.37	8.35	1.02	5.99E-03
Rack1_P63244_Y194	10.08	9.08	1.00	2.62E-03
Caveolin1_Q03135_Y25	8.54	9.69	-1.16	8.76E-07
NFkBp105 _P19838_S907	9.01	10.35	-1.35	1.68E-04

Supplementary Table 4.6: Significantly altered phospho targets by IDR peptides compared to control. *HBEC-3KT cells were stimulated with 10uM of IDR-1002 and IDR-1002.2(W8/R) and cell lysates were collected 15 min post stimulation. Kinase activity was measured using JPT Kinome peptide arrays. Average log2 intensity shown. Statistical analysis was performed using Students t-test.*

Phospho Target	Log2Expression		Log2FC Group 1 vs 2	P value Group 1 vs 2	Log2 Expression	Log2FC Group 1 vs 3	P value Group 1 vs 3
	Group 1 Control	Group 2 IDR-1002			Group 3 IDR-1002.2		
Uniquely altered by IDR-1002 (*$p \leq 0.05$ and 2-fold cut off*)							
STAT1 _P42224 Y701	10.19	11.93	1.74	4.63E-10			
Rab5A_P20339 S123	5.89	7.34	1.45	1.06E-02			
Syk _P43405 Y525/6	9.39	10.59	1.21	4.83E-06			
TGFBR1_P36897 T200	10.00	8.35	-1.66	4.59E-02			
TGFBR1_P36897 T204	8.70	6.81	-1.88	1.21E-03			

Uniquely altered by IDR-1002.2 (*p ≤ 0.05 and 2-fold cut off)							
Caveolin1_Q03135 Y25	8.66				9.69	1.04	9.77E-05
Flt3_P36888 Y842	7.02				4.25	-2.77	1.44E-03
Met _P08581 Y1003	8.06				6.40	-1.66	2.27E-03
NFAT2 _O95644 S245	8.47				6.89	-1.58	2.60E-02
NFkBp100_Q00653 S108	10.70				12.23	1.53	1.02E-04
p53 _P04637 S15	7.90				5.76	-2.14	2.64E-04
Altered by IDR-1002 or IDR-1002.2 (*p ≤ 0.05 and 2-fold cut off)							
pyk2_Q14289 S213	4.61	7.20	2.59	6.95E-04	7.61	3.00	2.58E-05
PIK3R1 _P27986 Y556	6.53	9.10	2.57	3.99E-04	9.08	2.55	5.18E-04
STAT6 _P42226 T645	10.54	12.06	1.52	3.08E-03	12.36	1.81	6.79E-04
Grb2_P62993 Y209	9.48	10.62	1.14	3.77E-02	10.93	1.46	1.01E-02
Tgfbr2_P37173 Y336	10.73	12.15	1.42	8.51E-07	12.13	1.41	1.68E-06
STAT6 _P42226 Y641	11.12	12.40	1.28	9.92E-03	12.41	1.29	1.01E-02
Met _P08581 Y1234	9.07	9.83	0.77	2.63E-05	10.19	1.12	1.88E-07
STAT1 _P42224 S708	8.04	10.68	2.64	7.16E-10	9.07	1.04	9.37E-03
Keap1_Q14145 Y141	9.47	10.95	1.47	1.66E-05	10.49	1.02	1.90E-03
Rack1_P63244 Y194	8.18	10.08	1.91	1.21E-05	9.08	0.91	3.73E-02
Ripk1_Q13546 Y694	10.93	12.59	1.65	3.70E-21	11.50	0.57	1.97E-03
PKACa _P17612 S338	9.39	10.66	1.27	3.14E-06	10.34	0.95	5.66E-04
MAPK14_Q16539 Y322	8.53	9.60	1.07	2.95E-03	9.39	0.86	1.03E-02
NFkBp65 _Q04206 S536	10.06	11.11	1.04	1.50E-06	10.97	0.91	1.63E-05
PLCG2_P16885 Y759	8.82	9.83	1.01	4.07E-06	9.63	0.81	1.97E-04
LSD1_O60341 S131	10.99	12.00	1.01	2.98E-04	11.92	0.93	7.98E-04
JAK1_P23458 Y220	8.80	6.96	-1.84	1.59E-02	7.32	-1.48	8.05E-03

References

1. Freire, M.O. and T.E. Van Dyke, Natural resolution of inflammation. *Periodontol 2000*, 2013. 63(1): p. 149-64.

2. Nicholson, L.B., The immune system. *Essays Biochem*, 2016. 60(3): p. 275-301.

3. Villani, A.C., S. Sarkizova, and N. Hacohen, Systems immunology: Learning the rules of the immune system. *Annu Rev Immunol*, 2018. 36(1): p. 813-42.

4. Abbas, A.K., Lichtman, Andrew H, Pillai, Shiv,, *Basic immunology : functions and disorders of the immune system*. 5th ed. 2016, St. Louis, Missouri: Elsevier.

5. Chaplin, D.D., Overview of the immune response. *J Allergy Clin Immunol*, 2010. 125(2 Suppl 2): p. S3-23.

6. Perdue, S.S. *Immune system*. 2019 [cited 2019 April 11].

7. Crimeen-Irwin, B., et al., Failure of immune homeostasis - the consequences of under and over reactivity. *Curr Drug Targets Immune Endocr Metabol Disord*, 2005. 5(4): p. 413-22.

8. Iwasaki, A. and R. Medzhitov, Control of adaptive immunity by the innate immune system. *Nat Immunol*, 2015. 16(4): p. 343-53.

9. Takeuchi, O. and S. Akira, Pattern recognition receptors and inflammation. *Cell*, 2010. 140(6): p. 805-20.

10. Souza-Fonseca-Guimaraes, F., M. Adib-Conquy, and J.M. Cavaillon, Natural killer (NK) cells in antibacterial innate immunity: angels or devils? *Mol Med*, 2012. 18: p. 270-85.

11. Bratton, D.L. and P.M. Henson, Neutrophil clearance: when the party is over, clean-up begins. *Trends Immunol*, 2011. 32(8): p. 350-7.

12. Commins, S.P., L. Borish, and J.W. Steinke, Immunologic messenger molecules: cytokines, interferons, and chemokines. *J Allergy Clin Immunol*, 2010. 125(2 Suppl 2): p. S53-72.

13. Justiz Vaillant, A.A. and A. Qurie, *Interleukin*, in *StatPearls*. 2019: Treasure Island (FL).

14. Chung, K.F., *Chapter 27 - Cytokines*, in *Asthma and COPD (Second Edition)*, P.J. Barnes, et al., Editors. 2009, Academic Press: Oxford. p. 327-41.

15. Atamas, S.P., S.P. Chapoval, and A.D. Keegan, Cytokines in chronic respiratory diseases. *F1000 Biol Rep*, 2013. 5: p. 3.

16. Gohy, S.T., et al., Chronic inflammatory airway diseases: the central role of the epithelium revisited. *Clin Exp Allergy*, 2016. 46(4): p. 529-42.

17. Opal, S.M. and V.A. DePalo, Anti-inflammatory cytokines. *Chest*, 2000. 117(4): p. 1162-72.

18. Murray, P.J., Understanding and exploiting the endogenous interleukin-10/STAT3-mediated anti-inflammatory response. *Curr Opin Pharmacol*, 2006. 6(4): p. 379-86.

19. Turner, M.D., et al., Cytokines and chemokines: At the crossroads of cell signalling and inflammatory disease. *Biochim Biophys Acta*, 2014. 1843(11): p. 2563-82.

20. Roy, I., D.B. Evans, and M.B. Dwinell, Chemokines and chemokine receptors: update on utility and challenges for the clinician. *Surgery*, 2014. 155(6): p. 961-73.

21. Hughes, C.E. and R.J.B. Nibbs, A guide to chemokines and their receptors. *FEBS J*, 2018.

22. *How your lungs get the job done*. 2017 [cited 2019 April 11th]; Available from: https://www.lung.org/about-us/blog/2017/07/how-your-lungs-work.html.

23. Frohlich, E., et al., Measurements of deposition, lung surface area and lung fluid for simulation of inhaled compounds. *Front Pharmacol*, 2016. 7: p. 181.

24. Weiskopf, K., et al., Myeloid cell origins, differentiation, and clinical implications. *Microbiol Spectr*, 2016. 4(5): p. 31.

25. Rosales, C., et al., Neutrophils: Their role in innate and adaptive immunity. *J Immunol Res*, 2017. 2017: p. 9748345.

26. Selders, G.S., et al., An overview of the role of neutrophils in innate immunity, inflammation and host-biomaterial integration. *Regen Biomater*, 2017. 4(1): p. 55-68.

27. Petri, B. and M.J. Sanz, Neutrophil chemotaxis. *Cell Tissue Res*, 2018. 371(3): p. 425-36.

28. Liu, J., et al., Advanced role of neutrophils in common respiratory diseases. *J Immunol Res*, 2017. 2017: p. 6710278.

29. Holtzman, M.J., et al., The role of airway epithelial cells and innate immune cells in chronic respiratory disease. *Nat Rev Immunol*, 2014. 14(10): p. 686-98.

30. McBrien, C.N. and A. Menzies-Gow, The biology of eosinophils and their role in asthma. *Front Med (Lausanne)*, 2017. 4: p. 93.

31. Bandeira-Melo, C. and P.F. Weller, Mechanisms of eosinophil cytokine release. *Mem Inst Oswaldo Cruz*, 2005. 100 Suppl 1: p. 73-81.

32. Klion, A.D. and T.B. Nutman, The role of eosinophils in host defense against helminth parasites. *J Allergy Clin Immunol*, 2004. 113(1): p. 30-7.

33. Mosser, D.M. and J.P. Edwards, Exploring the full spectrum of macrophage activation. *Nat Rev Immunol*, 2008. 8(12): p. 958-69.

34. Varol, C., A. Mildner, and S. Jung, Macrophages: development and tissue specialization. *Annu Rev Immunol*, 2015. 33: p. 643-75.

35. Davies, L.C., et al., Tissue-resident macrophages. *Nat Immunol*, 2013. 14(10): p. 986-95.

36. Hussell, T. and T.J. Bell, Alveolar macrophages: plasticity in a tissue-specific context. *Nat Rev Immunol*, 2014. 14(2): p. 81-93.

37. Shi, C. and E.G. Pamer, Monocyte recruitment during infection and inflammation. *Nat Rev Immunol*, 2011. 11(11): p. 762-74.

38. Hiemstra, P.S., P.B. McCray, Jr., and R. Bals, The innate immune function of airway epithelial cells in inflammatory lung disease. *Eur Respir J*, 2015. 45(4): p. 1150-62.

39. Davies, D.E., Epithelial barrier function and immunity in asthma. *Ann Am Thorac Soc*, 2014. 11 Suppl 5: p. S244-51.

40. Crystal, R.G., et al., Airway epithelial cells: current concepts and challenges. *Proc Am Thorac Soc*, 2008. 5(7): p. 772-7.

41. Soleas, J.P., et al., Engineering airway epithelium. *J Biomed Biotechnol*, 2012. 2012: p. 982971.

42. Gon, Y. and S. Hashimoto, Role of airway epithelial barrier dysfunction in pathogenesis of asthma. *Allergol Int*, 2018. 67(1): p. 12-17.

43. Ridley, C. and D.J. Thornton, Mucins: the frontline defence of the lung. *Biochem Soc Trans*, 2018. 46(5): p. 1099-106.

44. Thornton, D.J., K. Rousseau, and M.A. McGuckin, Structure and function of the polymeric mucins in airways mucus. *Annu Rev Physiol*, 2008. 70: p. 459-86.

45. Lillehoj, E.P., et al., Cellular and molecular biology of airway mucins. *Int Rev Cell Mol Biol*, 2013. 303: p. 139-202.

46. Thornton, D.J. and J.K. Sheehan, From mucins to mucus: toward a more coherent understanding of this essential barrier. *Proc Am Thorac Soc*, 2004. 1(1): p. 54-61.

47. Livraghi-Butrico, A., et al., Contribution of mucus concentration and secreted mucins Muc5ac and Muc5b to the pathogenesis of muco-obstructive lung disease. *Mucosal Immunol*, 2017. 10(3): p. 829.

48. Felgentreff, K., et al., The antimicrobial peptide cathelicidin interacts with airway mucus. *Peptides*, 2006. 27(12): p. 3100-6.

49. Mall, M.A. and D. Hartl, CFTR: cystic fibrosis and beyond. *Eur Respir J*, 2014. 44(4): p. 1042-54.

50. Joo, N.S., et al., Marked increases in mucociliary clearance produced by synergistic secretory agonists or inhibition of the epithelial sodium channel. *Sci Rep*, 2016. 6: p. 36806.

51. Kato, A. and R.P. Schleimer, Beyond inflammation: airway epithelial cells are at the interface of innate and adaptive immunity. *Curr Opin Immunol*, 2007. 19(6): p. 711-20.

52. Denney, L. and L.P. Ho, The role of respiratory epithelium in host defence against influenza virus infection. *Biomed J*, 2018. 41(4): p. 218-33.

53. Choi, K.Y., L.N. Chow, and N. Mookherjee, Cationic host defence peptides: multifaceted role in immune modulation and inflammation. *J Innate Immun*, 2012. 4(4): p. 361-70.

54. Hancock, R.E. and G. Diamond, The role of cationic antimicrobial peptides in innate host defences. *Trends Microbiol*, 2000. 8(9): p. 402-10.

55. Hancock, R.E., E.F. Haney, and E.E. Gill, The immunology of host defence peptides: beyond antimicrobial activity. *Nat Rev Immunol*, 2016. 16(5): p. 321-34.

56. Haney, E.F., S.K. Straus, and R.E.W. Hancock, Reassessing the host defense peptide landscape. *Front Chem*, 2019. 7: p. 43.

57. Gupta, S., et al., Host defense peptides: An insight into the antimicrobial world. *J Oral Maxillofac Pathol*, 2018. 22(2): p. 239-44.

58. Hemshekhar, M., V. Anaparti, and N. Mookherjee, Functions of cationic host defense peptides in immunity. *Pharmaceuticals (Basel)*, 2016. 9(3): p. 40.

59. Mansour, S.C., O.M. Pena, and R.E. Hancock, Host defense peptides: front-line immunomodulators. *Trends Immunol*, 2014. 35(9): p. 443-50.

60. Springer, K. and E. Kaiser, On the action of the skin secretion of the orange-speckled toad (Bombina variegata l.) on cultures of human fibroblasts. *Wien Klin Wochenschr*, 1964. 76(1): p. 638-9.

61. Le, C.F., C.M. Fang, and S.D. Sekaran, Intracellular targeting mechanisms by antimicrobial peptides. *Antimicrob Agents Chemother*, 2017. 61(4): p. 73-89.

62. Hultmark, D., et al., Insect immunity. Purification and properties of three inducible bactericidal proteins from hemolymph of immunized pupae of Hyalophora cecropia. *Eur J Biochem*, 1980. 106(1): p. 7-16.

63. Lee, T.H., K.N. Hall, and M.I. Aguilar, Antimicrobial peptide structure and mechanism of action: A focus on the role of membrane structure. *Curr Top Med Chem*, 2016. 16(1): p. 25-39.

64. Lee, H.T., et al., A large-scale structural classification of antimicrobial peptides. *Biomed Res Int*, 2015. 2015: p. 475062.

65. Nijnik, A. and R. Hancock, Host defence peptides: antimicrobial and immunomodulatory activity and potential applications for tackling antibiotic-resistant infections. *Emerg Health Threats J*, 2009. 2: p. e1.

66. Wang, G., X. Li, and Z. Wang, APD3: the antimicrobial peptide database as a tool for research and education. *Nucleic Acids Res*, 2016. 44(D1): p. D1087-93.

67. Choi, K.Y., S. Napper, and N. Mookherjee, Human cathelicidin LL-37 and its derivative IG-19 regulate interleukin-32-induced inflammation. *Immunology*, 2014. 143(1): p. 68-80.

68. Mookherjee, N., et al., Modulation of the TLR-mediated inflammatory response by the endogenous human host defense peptide LL-37. *J Immunol*, 2006. 176(4): p. 2455-64.

69. Davidson, D.J., et al., The cationic antimicrobial peptide LL-37 modulates dendritic cell differentiation and dendritic cell-induced T cell polarization. *J Immunol*, 2004. 172(2): p. 1146-56.

70. Scott, M.G., et al., The human antimicrobial peptide LL-37 is a multifunctional modulator of innate immune responses. *J Immunol*, 2002. 169(7): p. 3883-91.

71. Hilchie, A.L., K. Wuerth, and R.E. Hancock, Immune modulation by multifaceted cationic host defense (antimicrobial) peptides. *Nat Chem Biol*, 2013. 9(12): p. 761-8.

72. Bals, R., Epithelial antimicrobial peptides in host defense against infection. *Respir Res*, 2000. 1(3): p. 141-50.

73. McPhee, J.B., M.G. Scott, and R.E. Hancock, Design of host defence peptides for antimicrobial and immunity enhancing activities. *Comb Chem High Throughput Screen*, 2005. 8(3): p. 257-72.

74. Conibear, A.C. and D.J. Craik, The chemistry and biology of theta defensins. *Angew Chem Int Ed Engl*, 2014. 53(40): p. 10612-23.

75. Seiler, F., R. Bals, and C. Beisswenger, *Function of antimicrobial peptides in lung innate immunity*, in *Antimicrobial Peptides: Role in Human Health and Disease*, J. Harder and J.-M. Schröder, Editors. 2016, Springer International Publishing: Cham. p. 33-52.

76. Silva, O.N., et al., Exploring the pharmacological potential of promiscuous host-defense peptides: from natural screenings to biotechnological applications. *Front Microbiol*, 2011. 2: p. 232.

77. Doss, M., et al., Human defensins and LL-37 in mucosal immunity. *J Leukoc Biol*, 2010. 87(1): p. 79-92.

78. Yamasaki, K. and R.L. Gallo, Antimicrobial peptides in human skin disease. *Eur J Dermatol*, 2008. 18(1): p. 11-21.

79. Kuroda, K., et al., The human cathelicidin antimicrobial peptide LL-37 and mimics are potential anticancer drugs. *Front Oncol*, 2015. 5: p. 144.

80. Tomasinsig, L. and M. Zanetti, The cathelicidins--structure, function and evolution. *Curr Protein Pept Sci*, 2005. 6(1): p. 23-34.

81. Sorensen, O.E., et al., Human cathelicidin, hCAP-18, is processed to the antimicrobial peptide LL-37 by extracellular cleavage with proteinase 3. *Blood*, 2001. 97(12): p. 3951-9.

82. Sorensen, O.E., et al., Processing of seminal plasma hCAP-18 to ALL-38 by gastricsin: a novel mechanism of generating antimicrobial peptides in vagina. *J Biol Chem*, 2003. 278(31): p. 28540-6.

83. Murakami, M., et al., Postsecretory processing generates multiple cathelicidins for enhanced topical antimicrobial defense. *J Immunol*, 2004. 172(5): p. 3070-7.

84. Pestonjamasp, V.K., K.H. Huttner, and R.L. Gallo, Processing site and gene structure for the murine antimicrobial peptide CRAMP. *Peptides*, 2001. 22(10): p. 1643-50.

85. Valore, E.V. and T. Ganz, Posttranslational processing of defensins in immature human myeloid cells. *Blood*, 1992. 79(6): p. 1538-44.

86. Gallo, R.L., Sounding the alarm: multiple functions of host defense peptides. *J Invest Dermatol*, 2008. 128(1): p. 5-6.

87. Diamond, G., et al., The roles of antimicrobial peptides in innate host defense. *Curr Pharm Des*, 2009. 15(21): p. 2377-92.

88. Zasloff, M., Sunlight, vitamin D, and the innate immune defenses of the human skin. *J Invest Dermatol*, 2005. 125(5): p. xvi-xvii.

89. Hiemstra, P.S., et al., Antimicrobial peptides and innate lung defenses: Role in infectious and noninfectious lung diseases and therapeutic applications. *Chest*, 2016. 149(2): p. 545-51.

90. Lecaille, F., G. Lalmanach, and P.M. Andrault, Antimicrobial proteins and peptides in human lung diseases: A friend and foe partnership with host proteases. *Biochimie*, 2016. 122: p. 151-68.

91. Diamond, G., N. Beckloff, and L.K. Ryan, Host defense peptides in the oral cavity and the lung: similarities and differences. *J Dent Res*, 2008. 87(10): p. 915-27.

92. Lemaitre, B., et al., Pillars article: the dorsoventral regulatory gene cassette spatzle/Toll/cactus controls the potent antifungal response in Drosophila adults. Cell. 1996. 86: 973-983. *J Immunol*, 2012. 188(11): p. 5210-20.

93. Raquil, M.A., et al., Blockade of antimicrobial proteins S100A8 and S100A9 inhibits phagocyte migration to the alveoli in streptococcal pneumonia. *J Immunol*, 2008. 180(5): p. 3366-74.

94. Guilhelmelli, F., et al., Antibiotic development challenges: the various mechanisms of action of antimicrobial peptides and of bacterial resistance. *Front Microbiol*, 2013. 4: p. 353.

95. Faust, J.E., P.Y. Yang, and H.W. Huang, Action of antimicrobial peptides on bacterial and lipid membranes: A direct comparison. *Biophys J*, 2017. 112(8): p. 1663-72.

96. Haney, E.F., et al., High throughput screening methods for assessing antibiofilm and immunomodulatory activities of synthetic peptides. *Peptides*, 2015. 71: p. 276-85.

97. Jorge, P., A. Lourenco, and M.O. Pereira, New trends in peptide-based anti-biofilm strategies: a review of recent achievements and bioinformatic approaches. *Biofouling*, 2012. 28(10): p. 1033-61.

98. Benincasa, M., et al., Activity of antimicrobial peptides in the presence of polysaccharides produced by pulmonary pathogens. *J Pept Sci*, 2009. 15(9): p. 595-600.

99. Bowdish, D.M., et al., The human cationic peptide LL-37 induces activation of the extracellular signal-regulated kinase and p38 kinase pathways in primary human monocytes. *J Immunol*, 2004. 172(6): p. 3758-65.

100. Hiemstra, P.S., Antimicrobial peptides in the real world: implications for cystic fibrosis. *Eur Respir J*, 2007. 29(4): p. 617-8.

101. Mookherjee, N., et al., Intracellular receptor for human host defense peptide LL-37 in monocytes. *J Immunol*, 2009. 183(4): p. 2688-96.

102. Yang, Y.M., et al., Antimicrobial peptide LL-37 circulating levels in chronic obstructive pulmonary disease patients with high risk of frequent exacerbations. *J Thorac Dis*, 2015. 7(4): p. 740-5.

103. Barlow, P.G., et al., The human cathelicidin LL-37 preferentially promotes apoptosis of infected airway epithelium. *Am J Respir Cell Mol Biol*, 2010. 43(6): p. 692-702.

104. Nagaoka, I., H. Tamura, and M. Hirata, An antimicrobial cathelicidin peptide, human CAP18/LL-37, suppresses neutrophil apoptosis via the activation of formyl-peptide receptor-like 1 and P2X7. *J Immunol*, 2006. 176(5): p. 3044-52.

105. Soehnlein, O., et al., Neutrophil primary granule proteins HBP and HNP1-3 boost bacterial phagocytosis by human and murine macrophages. *J Clin Invest*, 2008. 118(10): p. 3491-502.

106. Jo, E.K., Innate immunity to mycobacteria: vitamin D and autophagy. *Cell Microbiol*, 2010. 12(8): p. 1026-35.

107. Allaker, R.P., Host defence peptides-a bridge between the innate and adaptive immune responses. *Trans R Soc Trop Med Hyg*, 2008. 102(1): p. 3-4.

108. Mookherjee, N., L.M. Rehaume, and R.E. Hancock, Cathelicidins and functional analogues as antisepsis molecules. *Expert Opin Ther Targets*, 2007. 11(8): p. 993-1004.

109. Choi, K.Y. and N. Mookherjee, Multiple immune-modulatory functions of cathelicidin host defense peptides. *Front Immunol*, 2012. 3: p. 149.

110. van der Does, A.M., P.S. Hiemstra, and N. Mookherjee, Antimicrobial host defence peptides: Immunomodulatory functions and translational prospects. *Adv Exp Med Biol*, 2019. 1117: p. 149-71.

111. Hemshekhar, M., K.G. Choi, and N. Mookherjee, Host defense peptide LL-37-mediated chemoattractant properties, but not anti-inflammatory cytokine IL-1RA production, is selectively controlled by cdc42 rho GTPase via G protein-coupled receptors and jnk mitogen-activated protein kinase. *Front Immunol*, 2018. 9: p. 1871.

112. Putsep, K., et al., Deficiency of antibacterial peptides in patients with morbus Kostmann: an observation study. *Lancet*, 2002. 360(9340): p. 1144-9.

113. Ganz, T., et al., Microbicidal/cytotoxic proteins of neutrophils are deficient in two disorders: Chediak-Higashi syndrome and "specific" granule deficiency. *J Clin Invest*, 1988. 82(2): p. 552-6.

114. Lande, R., et al., Neutrophils activate plasmacytoid dendritic cells by releasing self-DNA-peptide complexes in systemic lupus erythematosus. *Sci Transl Med*, 2011. 3(73): p. 73ra19.

115. Kanda, N., et al., Increased serum leucine, leucine-37 levels in psoriasis: positive and negative feedback loops of leucine, leucine-37 and pro- or anti-inflammatory cytokines. *Hum Immunol*, 2010. 71(12): p. 1161-71.

116. Dombrowski, Y., et al., Cytosolic DNA triggers inflammasome activation in keratinocytes in psoriatic lesions. *Sci Transl Med*, 2011. 3(82): p. 82ra38.

117. Lim, R., et al., Investigation of human cationic antimicrobial protein-18 (hCAP-18), lactoferrin and CD163 as potential biomarkers for ovarian cancer. *J Ovarian Res*, 2013. 6(1): p. 5.

118. Chow, J.Y., et al., Cathelicidin a potential therapeutic peptide for gastrointestinal inflammation and cancer. *World J Gastroenterol*, 2013. 19(18): p. 2731-5.

119. Beisswenger, C., et al., Allergic airway inflammation inhibits pulmonary antibacterial host defense. *J Immunol*, 2006. 177(3): p. 1833-7.

120. Wang, P., et al., Budesonide suppresses pulmonary antibacterial host defense by down-regulating cathelicidin-related antimicrobial peptide in allergic inflammation mice and in lung epithelial cells. *BMC Immunol*, 2013. 14: p. 7.

121. Golec, M., et al., Cathelicidin LL-37 in bronchoalveolar lavage and epithelial lining fluids from COPD patients and healthy individuals. *J Biol Regul Homeost Agents*, 2012. 26(4): p. 617-25.

122. Droin, N., et al., Human defensins as cancer biomarkers and antitumour molecules. *J Proteomics*, 2009. 72(6): p. 918-27.

123. Scott, M.G., et al., An anti-infective peptide that selectively modulates the innate immune response. *Nat Biotechnol*, 2007. 25(4): p. 465-72.

124. Ab Naafs, M., The antimicrobial peptides: Ready for clinical trials? *Biomedical Journal of Scientific & Technical Research*, 2018. 7(4): p. 6038-42.

125. Hancock, R.E., A. Nijnik, and D.J. Philpott, Modulating immunity as a therapy for bacterial infections. *Nat Rev Microbiol*, 2012. 10(4): p. 243-54.

126. Jenssen, H., et al., QSAR modeling and computer-aided design of antimicrobial peptides. *J Pept Sci*, 2008. 14(1): p. 110-4.

127. Haney, E.F. and R.E. Hancock, Peptide design for antimicrobial and immunomodulatory applications. *Biopolymers*, 2013. 100(6): p. 572-83.

128. Achtman, A.H., et al., Effective adjunctive therapy by an innate defense regulatory Peptide in a preclinical model of severe malaria. *Sci Transl Med*, 2012. 4(135): p. 135ra64.

129. Steinstraesser, L., et al., Innate defense regulator peptide 1018 in wound healing and wound infection. *PLoS One*, 2012. 7(8): p. e39373.

130. Pena, O.M., et al., Synthetic cationic peptide IDR-1018 modulates human macrophage differentiation. *PLoS One*, 2013. 8(1): p. e52449.

131. Wieczorek, M., et al., Structural studies of a peptide with immune modulating and direct antimicrobial activity. *Chem Biol*, 2010. 17(9): p. 970-80.

132. Nijnik, A., et al., Synthetic cationic peptide IDR-1002 provides protection against bacterial infections through chemokine induction and enhanced leukocyte recruitment. *J Immunol*, 2010. 184(5): p. 2539-50.

133. Madera, L. and R.E. Hancock, Anti-infective peptide IDR-1002 augments monocyte chemotaxis towards CCR5 chemokines. *Biochem Biophys Res Commun*, 2015. 464(3): p. 800-6.

134. Madera, L. and R.E. Hancock, Synthetic immunomodulatory peptide IDR-1002 enhances monocyte migration and adhesion on fibronectin. *J Innate Immun*, 2012. 4(5-6): p. 553-68.

135. Turner-Brannen, E., et al., Modulation of interleukin-1beta-induced inflammatory responses by a synthetic cationic innate defence regulator peptide, IDR-1002, in synovial fibroblasts. *Arthritis Res Ther*, 2011. 13(4): p. R129.

136. Wuerth, K.C., R. Falsafi, and R.E.W. Hancock, Synthetic host defense peptide IDR-1002 reduces inflammation in Pseudomonas aeruginosa lung infection. *PLoS One*, 2017. 12(11): p. e0187565.

137. Wuerth, K., et al., Characterization of host responses during pseudomonas aeruginosa acute infection in the lungs and blood and after treatment with the synthetic immunomodulatory peptide iDR-1002. *Infect Immun*, 2019. 87(1): p. 661-18.

138. Wu, B.C., A.H. Lee, and R.E.W. Hancock, Mechanisms of the innate defense regulator peptide-1002 anti-inflammatory activity in a sterile inflammation mouse model. *J Immunol*, 2017. 199(10): p. 3592-603.

139. Wasan, E.K., et al., A lipidic delivery system of a triple vaccine adjuvant enhances mucosal immunity following nasal administration in mice. *Vaccine*, 2019. 37(11): p. 1503-15.

140. Prysliak, T. and J. Perez-Casal, Immune responses to Mycoplasma bovis proteins formulated with different adjuvants. *Can J Microbiol*, 2016. 62(6): p. 492-504.

141. Garlapati, S., et al., Immunization with PCEP microparticles containing pertussis toxoid, CpG ODN and a synthetic innate defense regulator peptide induces protective immunity against pertussis. *Vaccine*, 2011. 29(38): p. 6540-8.

142. Garlapati, S., et al., Enhanced immune responses and protection by vaccination with respiratory syncytial virus fusion protein formulated with CpG oligodeoxynucleotide and innate defense regulator peptide in polyphosphazene microparticles. *Vaccine*, 2012. 30(35): p. 5206-14.

143. Papi, A., et al., Asthma. *Lancet*, 2018. 391(10122): p. 783-800.

144. Nunes, C., A.M. Pereira, and M. Morais-Almeida, Asthma costs and social impact. *Asthma Res Pract*, 2017. 3: p. 1.

145. Leynaert, B., et al., Gender differences in prevalence, diagnosis and incidence of allergic and non-allergic asthma: a population-based cohort. *Thorax*, 2012. 67(7): p. 625-31.

146. Carr, T.F. and E. Bleecker, Asthma heterogeneity and severity. *World Allergy Organ J*, 2016. 9(1): p. 41.

147. Siroux, V., et al., Genetic heterogeneity of asthma phenotypes identified by a clustering approach. *Eur Respir J*, 2014. 43(2): p. 439-52.

148. Irvin, C.G. *Pulmonary function testing in asthma*. 2019 [cited 2019 April 19]; Available from: https://www.uptodate.com/contents/pulmonary-function-testing-in-asthma.

149. Stephen Peters, J.W.M. *Treatment of moderate persistent asthma in adolescents and adults*. 2018 [cited 2019 April 19]; Available from: https://www.uptodate.com/contents/treatment-of-moderate-persistent-asthma-in-adolescents-and-adults.

150. Meurs, H., R. Gosens, and J. Zaagsma, Airway hyperresponsiveness in asthma: lessons from in vitro model systems and animal models. *Eur Respir J*, 2008. 32(2): p. 487-502.

151. Holgate, S.T., et al., Asthma. *Nat Rev Dis Primers*, 2015. 1: p. 15025.

152. Franks, T.J., et al., Resident cellular components of the human lung: current knowledge and goals for research on cell phenotyping and function. *Proc Am Thorac Soc*, 2008. 5(7): p. 763-6.

153. Schittny, J.C., Development of the lung. *Cell Tissue Res*, 2017. 367(3): p. 427-44.

154. Effros, R.M., Anatomy, development, and physiology of the lungs. *GI Motil. Online (Part 1)*, 2006.

155. Howat, W.J., et al., Basement membrane pores in human bronchial epithelium: a conduit for infiltrating cells? *Am J Pathol*, 2001. 158(2): p. 673-80.

156. OpenStax, *Anatomy and physiology*, ed. B.O.T. project. 2013: OpenStax.

157. Irvin, C.G. and J.H. Bates, Measuring the lung function in the mouse: the challenge of size. *Respir Res*, 2003. 4: p. 4.

158. Darrah, R.J., et al., Ventilatory pattern and energy expenditure are altered in cystic fibrosis mice. *J Cyst Fibros*, 2013. 12(4): p. 345-51.

159. Wielgosz, J., et al., Long-term mindfulness training is associated with reliable differences in resting respiration rate. *Sci Rep*, 2016. 6: p. 27533.

160. Portelli, M.A., E. Hodge, and I. Sayers, Genetic risk factors for the development of allergic disease identified by genome-wide association. *Clin Exp Allergy*, 2015. 45(1): p. 21-31.

161. Galli, S.J., M. Tsai, and A.M. Piliponsky, The development of allergic inflammation. *Nature*, 2008. 454(7203): p. 445-54.

162. Lambrecht, B.N. and H. Hammad, The immunology of asthma. *Nat Immunol*, 2015. 16(1): p. 45-56.

163. Cianferoni, A. and J. Spergel, The importance of TSLP in allergic disease and its role as a potential therapeutic target. *Expert Rev Clin Immunol*, 2014. 10(11): p. 1463-74.

164. Huang, L., et al., OX40L induces helper T cell differentiation during cell immunity of asthma through PI3K/AKT and P38 MAPK signaling pathway. *J Transl Med*, 2018. 16(1): p. 74.

165. Tangye, S.G., et al., The good, the bad and the ugly - TFH cells in human health and disease. *Nat Rev Immunol*, 2013. 13(6): p. 412-26.

166. Krystel-Whittemore, M., K.N. Dileepan, and J.G. Wood, Mast cell: A multi-functional master cell. *Front Immunol*, 2015. 6: p. 620.

167. *Chapter 6 - Eosinophil trafficking*, in *Eosinophils in Health and Disease*, J.J. Lee and H.F. Rosenberg, Editors. 2013, Academic Press: Boston. p. 121-66.

168. Walford, H.H. and T.A. Doherty, Diagnosis and management of eosinophilic asthma: a US perspective. *J Asthma Allergy*, 2014. 7: p. 53-65.

169. Ciepiela, O., M. Ostafin, and U. Demkow, Neutrophils in asthma - A review. *Respir Physiol Neurobiol*, 2015. 209: p. 13-6.

170. Gounni, A.S., et al., Human neutrophils express the high-affinity receptor for immunoglobulin E (Fc epsilon RI): role in asthma. *FASEB J*, 2001. 15(6): p. 940-9.

171. Possa, S.S., et al., Eosinophilic inflammation in allergic asthma. *Front Pharmacol*, 2013. 4: p. 46.

172. Halwani, R., et al., Eosinophils induce airway smooth muscle cell proliferation. *J Clin Immunol*, 2013. 33(3): p. 595-604.

173. Lommatzsch, M., Airway hyperresponsiveness: new insights into the pathogenesis. *Semin Respir Crit Care Med*, 2012. 33(6): p. 579-87.

174. Matsumoto, H., et al., Interleukin-13 enhanced Ca2+ oscillations in airway smooth muscle cells. *Cytokine*, 2012. 57(1): p. 19-24.

175. Porsbjerg, C.M., et al., Relationship between airway pathophysiology and airway inflammation in older asthmatics. *Respirology*, 2013. 18(7): p. 1128-34.

176. Kirby, J.G., et al., Bronchoalveolar cell profiles of asthmatic and nonasthmatic subjects. *Am Rev Respir Dis*, 1987. 136(2): p. 379-83.

177. Walker, J.K., M. Kraft, and J.T. Fisher, Assessment of murine lung mechanics outcome measures: alignment with those made in asthmatics. *Front Physiol*, 2012. 3: p. 491.

178. Loutfi Sami Aboussouan, J.K.S. *Flow-volume loops*. Asthma 2019 Feb 22, 2019 [cited 2019 April 19]; Available from: https://www.uptodate.com/contents/flow-volume-loops.

179. Irvin, C.G. and J.H. Bates, Physiologic dysfunction of the asthmatic lung: what's going on down there, anyway? *Proc Am Thorac Soc*, 2009. 6(3): p. 306-11.

180. Bailey, K.L., The importance of the assessment of pulmonary function in COPD. *Med Clin North Am*, 2012. 96(4): p. 745-52.

181. Hantos, Z., et al., Input impedance and peripheral inhomogeneity of dog lungs. *J Appl Physiol (1985)*, 1992. 72(1): p. 168-78.

182. Schuessler, T.F. and J.H. Bates, A computer-controlled research ventilator for small animals: design and evaluation. *IEEE Trans Biomed Eng*, 1995. 42(9): p. 860-6.

183. Hildebrandt, J., Pressure-volume data of cat lung interpreted by a plastoelastic, linear viscoelastic model. *J Appl Physiol*, 1970. 28(3): p. 365-72.

184. Bates, J.H., et al., Oscillation mechanics of the respiratory system. *Compr Physiol*, 2011. 1(3): p. 1233-72.

185. Irvin, C.G. *Bronchoprovocation testing*. 2018 [cited 2019 April 19]; Available from: https://www.uptodate.com/contents/bronchoprovocation-testing.

186. Shalaby, K.H., et al., Combined forced oscillation and forced expiration measurements in mice for the assessment of airway hyperresponsiveness. *Respir Res*, 2010. 11: p. 82.

187. Chapman, D.G. and C.G. Irvin, Mechanisms of airway hyper-responsiveness in asthma: the past, present and yet to come. *Clin Exp Allergy*, 2015. 45(4): p. 706-19.

188. Leckie, M.J., et al., Effects of an interleukin-5 blocking monoclonal antibody on eosinophils, airway hyper-responsiveness, and the late asthmatic response. *Lancet*, 2000. 356(9248): p. 2144-8.

189. Kariyawasam, H.H., et al., Remodeling and airway hyperresponsiveness but not cellular inflammation persist after allergen challenge in asthma. *Am J Respir Crit Care Med*, 2007. 175(9): p. 896-904.

190. Haldar, P., et al., Mepolizumab and exacerbations of refractory eosinophilic asthma. *N Engl J Med*, 2009. 360(10): p. 973-84.

191. James, A., et al., Airway smooth muscle hypertrophy and hyperplasia in asthma. *Am J Respir Crit Care Med*, 2012. 186(6): p. 568-9.

192. Grainge, C.L., et al., Effect of bronchoconstriction on airway remodeling in asthma. *N Engl J Med*, 2011. 364(21): p. 2006-15.

193. Busse, W.W., Biological treatments for severe asthma: A major advance in asthma care. *Allergol Int*, 2019. 68(2): p. 158-66.

194. Larsson, K., et al., Prevalence and management of severe asthma in primary care: an observational cohort study in Sweden (PACEHR). *Respir Res*, 2018. 19(1): p. 12.

195. Backman, H., et al., Severe asthma among adults: Prevalence and clinical characteristics. *European Respiratory Journal*, 2018. 52(suppl 62): p. PA3918.

196. Hekking, P.P., et al., The prevalence of severe refractory asthma. *J Allergy Clin Immunol*, 2015. 135(4): p. 896-902.

197. Lefebvre, P., et al., Acute and chronic systemic corticosteroid-related complications in patients with severe asthma. *J Allergy Clin Immunol*, 2015. 136(6): p. 1488-95.

198. Hall, I.P. and I. Sayers, Pharmacogenetics and asthma: false hope or new dawn? *Eur Respir J*, 2007. 29(6): p. 1239-45.

199. Engelkes, M., et al., Medication adherence and the risk of severe asthma exacerbations: a systematic review. *Eur Respir J*, 2015. 45(2): p. 396-407.

200. FitzGerald, J.M., et al., Recognition and management of severe asthma: A canadian thoracic society position statement. *Canadian Journal of Respiratory, Critical Care, and Sleep Medicine*, 2017. 1(4): p. 199-221.

201. Dweik, R.A. *Role of anticholinergic therapy in COPD*. 2018 [cited 2019 April 19]; Available from: https://www.uptodate.com/contents/role-of-anticholinergic-therapy-in-copd.

202. Wenzel, S. *Treatment of severe asthma in adolescents and adults*. 2019 [cited 2019 April 19]; Available from: https://www.uptodate.com/contents/treatment-of-severe-asthma-in-adolescents-and-adults.

203. Cazzola, M., et al., beta2-agonist therapy in lung disease. *Am J Respir Crit Care Med*, 2013. 187(7): p. 690-6.

204. Barnes, P.J., Inhaled corticosteroids. *Pharmaceuticals (Basel)*, 2010. 3(3): p. 514-40.

205. Buels, K.S. and A.D. Fryer, Muscarinic receptor antagonists: effects on pulmonary function. *Handb Exp Pharmacol*, 2012. 1(208): p. 317-41.

206. Theron, A.J., et al., Cysteinyl leukotriene receptor-1 antagonists as modulators of innate immune cell function. *J Immunol Res*, 2014. 2014: p. 608930.

207. Ismaila, A.S., et al., Clinical, economic, and humanistic burden of asthma in Canada: a systematic review. *BMC Pulm Med*, 2013. 13: p. 70.

208. Giovannini-Chami, L., et al., New insights into the treatment of severe asthma in children. *Paediatr Respir Rev*, 2015. 16(3): p. 167-73.

209. Wener, R.R. and E.H. Bel, Severe refractory asthma: an update. *Eur Respir Rev*, 2013. 22(129): p. 227-35.

210. Zhang, L., et al., Inhaled corticosteroids increase the risk of oropharyngeal colonization by Streptococcus pneumoniae in children with asthma. *Respirology*, 2013. 18(2): p. 272-7.

211. Beckmann, J.D., et al., Controls of EGF-induced morphological transformation of human bronchial epithelial cells. *J Cell Physiol*, 2001. 189(2): p. 171-8.

212. Kilkenny, C., et al., Improving bioscience research reporting: the ARRIVE guidelines for reporting animal research. *PLoS Biol*, 2010. 8(6): p. e1000412.

213. Salmond, R.J., et al., IL-33 induces innate lymphoid cell-mediated airway inflammation by activating mammalian target of rapamycin. *J Allergy Clin Immunol*, 2012. 130(5): p. 1159-66.

214. Ryu, M.H., et al., Chronic exposure to perfluorinated compounds: Impact on airway hyperresponsiveness and inflammation. *Am J Physiol Lung Cell Mol Physiol*, 2014. 307(10): p. L765-74.

215. Jha, A., et al., Prophylactic benefits of systemically delivered simvastatin treatment in a house dust mite challenged murine model of allergic asthma. *Br J Pharmacol*, 2018. 175(7): p. 1004-16.

216. Zhu, M., et al., Role of Rho kinase isoforms in murine allergic airway responses. *Eur Respir J*, 2011. 38(4): p. 841-50.

217. Zarcone, M.C., et al., Cellular response of mucociliary differentiated primary bronchial epithelial cells to diesel exhaust. *Am J Physiol Lung Cell Mol Physiol*, 2016. 311(1): p. L111-23.

218. Love, M.I., W. Huber, and S. Anders, Moderated estimation of fold change and dispersion for RNA-seq data with DESeq2. *Genome Biol*, 2014. 15(12): p. 550.

219. Breuer, K., et al., InnateDB: systems biology of innate immunity and beyond--recent updates and continuing curation. *Nucleic Acids Res*, 2013. 41: p. 1228-33.

220. Thevenet, P., et al., PEP-FOLD: an updated de novo structure prediction server for both linear and disulfide bonded cyclic peptides. *Nucleic Acids Res*, 2012. 40(Web Server issue): p. W288-93.

221. Shen, Y., et al., Improved PEP-FOLD Approach for Peptide and Miniprotein Structure Prediction. *J Chem Theory Comput*, 2014. 10(10): p. 4745-58.

222. Krokhin, O.V. and V. Spicer, Predicting peptide retention times for proteomics. *Curr Protoc Bioinformatics*, 2010. Chapter 13: p. 13-14.

223. Nickol, M.E., et al., Characterization of host and bacterial contributions to lung barrier dysfunction following co-infection with 2009 pandemic influenza and methicillin resistant staphylococcus aureus. *Viruses*, 2019. 11(2): p. E116.

224. Kindrachuk, J., et al., Antiviral potential of ERK/MAPK and PI3K/AKT/mTOR signaling modulation for Middle East respiratory syndrome coronavirus infection as identified by temporal kinome analysis. *Antimicrob Agents Chemother*, 2015. 59(2): p. 1088-99.

225. Gandhi, V.D., et al., House dust mite interactions with airway epithelium: role in allergic airway inflammation. *Curr Allergy Asthma Rep*, 2013. 13(3): p. 262-70.

226. Gregory, L.G. and C.M. Lloyd, Orchestrating house dust mite-associated allergy in the lung. *Trends Immunol*, 2011. 32(9): p. 402-11.

227. Stevenson, C.S. and M.A. Birrell, Moving towards a new generation of animal models for asthma and COPD with improved clinical relevance. *Pharmacol Ther*, 2011. 130(2): p. 93-105.

228. Cates, E.C., et al., Modeling responses to respiratory house dust mite exposure. *Contrib Microbiol*, 2007. 14: p. 42-67.

229. Cates, E.C., et al., Intranasal exposure of mice to house dust mite elicits allergic airway inflammation via a GM-CSF-mediated mechanism. *J Immunol*, 2004. 173(10): p. 6384-92.

230. Johnson, J.R., et al., Continuous exposure to house dust mite elicits chronic airway inflammation and structural remodeling. *Am J Respir Crit Care Med*, 2004. 169(3): p. 378-85.

231. Locke, N.R., et al., Comparison of airway remodeling in acute, subacute, and chronic models of allergic airways disease. *Am J Respir Cell Mol Biol*, 2007. 36(5): p. 625-32.

232. Al Heialy, S., T.K. McGovern, and J.G. Martin, Insights into asthmatic airway remodelling through murine models. *Respirology*, 2011. 16(4): p. 589-97.

233. Monteseirin, J., Neutrophils and asthma. *J Investig Allergol Clin Immunol*, 2009. 19(5): p. 340-54.

234. De Alba, J., et al., House dust mite induces direct airway inflammation in vivo: implications for future disease therapy? *Eur Respir J*, 2010. 35(6): p. 1377-87.

235. Ho, W.E., et al., Metabolomics reveals inflammatory-linked pulmonary metabolic alterations in a murine model of house dust mite-induced allergic asthma. *J Proteome Res*, 2014. 13(8): p. 3771-82.

236. Koyama, D., et al., Myeloid differentiation-2 is a potential biomarker for the amplification process of allergic airway sensitization in mice. *Allergol Int*, 2015. 64 Suppl: p. S37-45.

237. Saglani, S., et al., Pathophysiological features of asthma develop in parallel in house dust mite-exposed neonatal mice. *Am J Respir Cell Mol Biol*, 2009. 41(3): p. 281-9.

238. Lewkowich, I.P., et al., Allergen uptake, activation, and IL-23 production by pulmonary myeloid DCs drives airway hyperresponsiveness in asthma-susceptible mice. *PLoS One*, 2008. 3(12): p. e3879.

239. van der Velden, J.L., et al., Absence of c-Jun NH2-terminal kinase 1 protects against house dust mite-induced pulmonary remodeling but not airway hyperresponsiveness and inflammation. *Am J Physiol Lung Cell Mol Physiol*, 2014. 306(9): p. L866-75.

240. Vignola, A.M., et al., Airway remodeling in the pathogenesis of asthma. *Curr Allergy Asthma Rep*, 2001. 1(2): p. 108-15.

241. Platts-Mills, T.A., The role of immunoglobulin E in allergy and asthma. *Am J Respir Crit Care Med*, 2001. 164(8 Pt 2): p. S1-5.

242. Woo, L.N., et al., A 4-Week Model of House Dust Mite (HDM) Induced Allergic Airways Inflammation with Airway Remodeling. *Sci Rep*, 2018. 8(1): p. 6925.

243. Park, S.G., et al., Genome-wide profiling of antigen-induced time course expression using murine models for acute and chronic asthma. *Int Arch Allergy Immunol*, 2008. 146(1): p. 44-56.

244. Laprise, C., et al., Functional classes of bronchial mucosa genes that are differentially expressed in asthma. *BMC Genomics*, 2004. 5(1): p. 21.

245. Woodruff, P.G., et al., Genome-wide profiling identifies epithelial cell genes associated with asthma and with treatment response to corticosteroids. *Proc Natl Acad Sci U S A*, 2007. 104(40): p. 15858-63.

246. Louten, J., et al., Biomarkers of disease and treatment in murine and cynomolgus models of chronic asthma. *Biomark Insights*, 2012. 7: p. 87-104.

247. Zhu, J., Transcriptional regulation of Th2 cell differentiation. *Immunol Cell Biol*, 2010. 88(3): p. 244-9.

248. Lloyd, C.M. and E.M. Hessel, Functions of T cells in asthma: more than just T(H)2 cells. *Nat Rev Immunol*, 2010. 10(12): p. 838-48.

249. Hyde, E.J., et al., Similar immune mechanisms control experimental airway eosinophilia elicited by different allergens and treatment protocols. *BMC Immunol*, 2019. 20(1): p. 18.

250. Melgert, B.N., et al., Female mice are more susceptible to the development of allergic airway inflammation than male mice. *Clin Exp Allergy*, 2005. 35(11): p. 1496-503.

251. Blacquiere, M.J., et al., Airway inflammation and remodeling in two mouse models of asthma: comparison of males and females. *Int Arch Allergy Immunol*, 2010. 153(2): p. 173-81.

252. Canada, P.H.A.o., *To promote and protect the health of canadians through leadership, partnership, innovation and action in public health*. 2018, Canada.

253. Crotty Alexander, L.E., et al., Myeloid cell HIF-1alpha regulates asthma airway resistance and eosinophil function. *J Mol Med (Berl)*, 2013. 91(5): p. 637-44.

254. Foster, P.S., et al., Targeting eosinophils in asthma. *Curr Mol Med*, 2008. 8(6): p. 585-90.

255. Tournoy, K.G., et al., Airway eosinophilia is not a requirement for allergen-induced airway hyperresponsiveness. *Clin Exp Allergy*, 2000. 30(1): p. 79-85.

256. Lu, M., et al., Therapeutic induction of tolerance by IL-10-differentiated dendritic cells in a mouse model of house dust mite-asthma. *Allergy*, 2011. 66(5): p. 612-20.

257. Schulman, E.S. and C. Pohlig, Rationale for specific allergen testing of patients with asthma in the clinical pulmonary office setting. *Chest*, 2015. 147(1): p. 251-8.

258. Bush, A., How early do airway inflammation and remodeling occur? *Allergol Int*, 2008. 57(1): p. 11-9.

259. Jeffery, P.K., Remodeling in asthma and chronic obstructive lung disease. *Am J Respir Crit Care Med*, 2001. 164(10 Pt 2): p. S28-38.

260. Thai, P., et al., Differential regulation of MUC5AC/Muc5ac and hCLCA-1/mGob-5 expression in airway epithelium. *Am J Respir Cell Mol Biol*, 2005. 33(6): p. 523-30.

261. Kulkarni, N.S., et al., Eosinophil protein in airway macrophages: a novel biomarker of eosinophilic inflammation in patients with asthma. *J Allergy Clin Immunol*, 2010. 126(1): p. 61-9 e3.

262. Bhakta, N.R., et al., A qPCR-based metric of Th2 airway inflammation in asthma. *Clin Transl Allergy*, 2013. 3(1): p. 24.

263. Grotenboer, N.S., et al., Decoding asthma: translating genetic variation in IL33 and IL1RL1 into disease pathophysiology. *J Allergy Clin Immunol*, 2013. 131(3): p. 856-65.

264. Scanlon, S.T. and A.N. McKenzie, Type 2 innate lymphoid cells: new players in asthma and allergy. *Curr Opin Immunol*, 2012. 24(6): p. 707-12.

265. Seki, N., et al., IL-4-induced GATA-3 expression is a time-restricted instruction switch for Th2 cell differentiation. *J Immunol*, 2004. 172(10): p. 6158-66.

266. Gour, N. and M. Wills-Karp, IL-4 and IL-13 signaling in allergic airway disease. *Cytokine*, 2015. 75(1): p. 68-78.

267. Mestas, J. and C.C. Hughes, Of mice and not men: differences between mouse and human immunology. *J Immunol*, 2004. 172(5): p. 2731-8.

268. Shanks, N., R. Greek, and J. Greek, Are animal models predictive for humans? *Philos Ethics Humanit Med*, 2009. 4: p. 2.

269. Rivas-Santiago, B., et al., Ability of Innate Defence Regulator Peptides IDR-1002, IDR-HH2 and IDR-1018 to Protect against Mycobacterium tuberculosis Infections in Animal Models. *PLoS One*, 2013. 8(3): p. e59119.

270. Hou, M., et al., Antimicrobial peptide LL-37 and IDR-1 ameliorate MRSA pneumonia in vivo. *Cell Physiol Biochem*, 2013. 32(3): p. 614-23.

271. Dahl, R., Systemic side effects of inhaled corticosteroids in patients with asthma. *Respir Med*, 2006. 100(8): p. 1307-17.

272. McKeever, T., et al., Inhaled corticosteroids and the risk of pneumonia in people with asthma: a case-control study. *Chest*, 2013. 144(6): p. 1788-1794.

273. Caramori, G., et al., New drugs targeting Th2 lymphocytes in asthma. *J Occup Med Toxicol*, 2008. 3: p. S6.

274. Mayer, M.L., et al., Rescue of dysfunctional autophagy attenuates hyperinflammatory responses from cystic fibrosis cells. *J Immunol*, 2012. 190: p. 1227-1238.

275. Saglani, S., et al., IL-33 promotes airway remodeling in pediatric patients with severe steroid-resistant asthma. *J Allergy Clin Immunol*, 2013. 132(3): p. 676-685 e13.

276. Prefontaine, D., et al., Increased expression of IL-33 in severe asthma: evidence of expression by airway smooth muscle cells. *J Immunol*, 2009. 183(8): p. 5094-103.

277. Prefontaine, D., et al., Increased IL-33 expression by epithelial cells in bronchial asthma. *J Allergy Clin Immunol*, 2010. 125(3): p. 752-4.

278. Castanhinha, S., et al., Pediatric severe asthma with fungal sensitization is mediated by steroid-resistant IL-33. *J Allergy Clin Immunol*, 2015. 136(2): p. 312-22 e7.

279. Johnson, J.R., et al., Chronic respiratory aeroallergen exposure in mice induces epithelial-mesenchymal transition in the large airways. *PLoS One*, 2011. 6(1): p. e16175.

280. Piyadasa, H., et al., Biosignature for airway inflammation in a house dust mite-challenged murine model of allergic asthma. *Biol Open*, 2016. 5(2): p. 112-21.

281. Shan, J., et al., Interferon gamma-Induced Nuclear Interleukin-33 Potentiates the Release of Esophageal Epithelial Derived Cytokines. *PLoS One*, 2016. 11(3): p. e0151701.

282. Taniguchi, K., et al., Interleukin 33 is induced by tumor necrosis factor alpha and interferon gamma in keratinocytes and contributes to allergic contact dermatitis. *J Investig Allergol Clin Immunol*, 2013. 23(6): p. 428-34.

283. Meephansan, J., et al., Regulation of IL-33 expression by IFN-gamma and tumor necrosis factor-alpha in normal human epidermal keratinocytes. *J Invest Dermatol*, 2012. 132(11): p. 2593-600.

284. Platanias, L.C., Mechanisms of type-I- and type-II-interferon-mediated signalling. *Nat Rev Immunol*, 2005. 5(5): p. 375-86.

285. Domalaon, R., et al., Structure-activity relationships in ultrashort cationic lipopeptides: the effects of amino acid ring constraint on antibacterial activity. *Amino Acids*, 2014. 46(11): p. 2517-30.

286. Niyonsaba, F., et al., The innate defense regulator peptides IDR-HH2, IDR-1002, and IDR-1018 modulate human neutrophil functions. *J Leukoc Biol*, 2013. 94(1): p. 159-70.

287. Chow, L.N., et al., Human cathelicidin LL-37-derived peptide IG-19 confers protection in a murine model of collagen-induced arthritis. *Mol Immunol*, 2013. 57(2): p. 86-92.

288. Yeung, A.T., S.L. Gellatly, and R.E. Hancock, Multifunctional cationic host defence peptides and their clinical applications. *Cell Mol Life Sci*, 2011. 68(13): p. 2161-76.

289. Cherkasov, A., et al., Use of artificial intelligence in the design of small peptide antibiotics effective against a broad spectrum of highly antibiotic-resistant superbugs. *ACS Chem Biol*, 2009. 4(1): p. 65-74.

290. Verri, W.A., Jr., et al., IL-33 induces neutrophil migration in rheumatoid arthritis and is a target of anti-TNF therapy. *Ann Rheum Dis*, 2010. 69(9): p. 1697-703.

291. Borish, L. and J.W. Steinke, Interleukin-33 in asthma: how big of a role does it play? *Curr Allergy Asthma Rep*, 2011. 11(1): p. 7-11.

292. Besnard, A.G., et al., IL-33-activated dendritic cells are critical for allergic airway inflammation. *Eur J Immunol*, 2011. 41(6): p. 1675-86.

293. Murakami-Satsutani, N., et al., IL-33 promotes the induction and maintenance of Th2 immune responses by enhancing the function of OX40 ligand. *Allergol Int*, 2014. 63(3): p. 443-55.

294. Olson, T.S. and K. Ley, Chemokines and chemokine receptors in leukocyte trafficking. *Am J Physiol Regul Integr Comp Physiol*, 2002. 283(1): p. R7-28.

295. Hueber, A.J., et al., IL-33 induces skin inflammation with mast cell and neutrophil activation. *Eur J Immunol*, 2011. 41(8): p. 2229-37.

296. Chambers, E.S., et al., Distinct endotypes of steroid-resistant asthma characterized by IL-17A(high) and IFN-gamma(high) immunophenotypes: Potential benefits of calcitriol. *J Allergy Clin Immunol*, 2015. 136(3): p. 628-637 e4.

297. Bao, Y., et al., Identification of IFN-gamma-producing innate B cells. *Cell Res*, 2014. 24(2): p. 161-76.

298. Janssen-Heininger, Y.M., et al., Airway hyperresponsiveness and inflammation: Causation, correlation, or no relation? *J Allergy Ther*, 2012. 2012(1): p. 008.

299. Bates, J.H., et al., The synergistic interactions of allergic lung inflammation and intratracheal cationic protein. *Am J Respir Crit Care Med*, 2008. 177(3): p. 261-8.

300. Brusasco, V., E. Crimi, and R. Pellegrino, Airway hyperresponsiveness in asthma: not just a matter of airway inflammation. *Thorax*, 1998. 53(11): p. 992-8.

301. Lynch, J.P., et al., Aeroallergen-induced IL-33 predisposes to respiratory virus-induced asthma by dampening antiviral immunity. *J Allergy Clin Immunol*, 2016. 138(5): p. 1326-1337.

302. Sandrock, C.E. and A. Norris, Infection in severe asthma exacerbations and critical asthma syndrome. *Clin Rev Allergy Immunol*, 2015. 48(1): p. 104-13.

303. Zhao, J. and Y. Zhao, Interleukin-33 and its Receptor in Pulmonary Inflammatory Diseases. *Crit Rev Immunol*, 2015. 35(6): p. 451-61.

304. Kaur, D., et al., IL-33 drives airway hyper-responsiveness through IL-13-mediated mast cell: airway smooth muscle crosstalk. *Allergy*, 2015. 70(5): p. 556-67.

305. Hamzaoui, A., et al., Induced sputum levels of IL-33 and soluble ST2 in young asthmatic children. *J Asthma*, 2013. 50(8): p. 803-9.

306. Seehus, C.R., et al., Alternative activation generates IL-10 producing type 2 innate lymphoid cells. *Nat Commun*, 2017. 8(1): p. 1900.

307. Yamamoto, T., et al., DUSP10 constrains innate IL-33-mediated cytokine production in ST2(hi) memory-type pathogenic Th2 cells. *Nat Commun*, 2018. 9(1): p. 4231.

308. Di Salvo, E., et al., IL-33/IL-31 axis: A potential inflammatory pathway. *Mediators Inflamm*, 2018. 2018: p. 3858032.

309. Liew, F.Y., J.P. Girard, and H.R. Turnquist, Interleukin-33 in health and disease. *Nat Rev Immunol*, 2016. 16(11): p. 676-89.

310. Cayrol, C. and J.P. Girard, Interleukin-33 (IL-33): A nuclear cytokine from the IL-1 family. *Immunol Rev*, 2018. 281(1): p. 154-168.

311. Drake, L.Y. and H. Kita, IL-33: biological properties, functions, and roles in airway disease. *Immunol Rev*, 2017. 278(1): p. 173-84.

312. Piyadasa, H., et al., Immunomodulatory innate defence regulator (IDR) peptide alleviates airway inflammation and hyper-responsiveness. *Thorax*, 2018. 73(10): p. 908-17.

313. Michaudel, C., et al., Ozone exposure induces respiratory barrier biphasic injury and inflammation controlled by IL-33. *J Allergy Clin Immunol*, 2018. 142(3): p. 942-58.

314. Takatori, H., et al., Regulatory mechanisms of IL-33-ST2-mediated allergic inflammation. *Front Immunol*, 2018. 9: p. 2004.

315. Zoltowska, A.M., et al., The interleukin-33 receptor ST2 is important for the development of peripheral airway hyperresponsiveness and inflammation in a house dust mite mouse model of asthma. *Clin Exp Allergy*, 2016. 46(3): p. 479-90.

316. Lei, Y., et al., Vaccination against IL-33 inhibits airway hyperresponsiveness and inflammation in a house dust mite model of asthma. *PLoS One*, 2015. 10(7): p. e0133774.

317. Oboki, K., et al., IL-33 is a crucial amplifier of innate rather than acquired immunity. *Proc Natl Acad Sci U S A*, 2010. 107(43): p. 18581-6.

318. Byers, D.E., et al., Long-term IL-33-producing epithelial progenitor cells in chronic obstructive lung disease. *J Clin Invest*, 2013. 123(9): p. 3967-82.

319. Li, D., et al., IL-33 promotes ST2-dependent lung fibrosis by the induction of alternatively activated macrophages and innate lymphoid cells in mice. *J Allergy Clin Immunol*, 2014. 134(6): p. 1422-1432 e11.

320. Iijima, K., et al., IL-33 and thymic stromal lymphopoietin mediate immune pathology in response to chronic airborne allergen exposure. *J Immunol*, 2014. 193(4): p. 1549-59.

321. Moffatt, M.F., et al., A large-scale, consortium-based genomewide association study of asthma. *N Engl J Med*, 2010. 363(13): p. 1211-21.

322. Morikawa, T., et al., Activation of group 2 innate lymphoid cells exacerbates and confers corticosteroid resistance to mouse nasal type 2 inflammation. *Int Immunol*, 2017. 29(5): p. 221-33.

323. Stolarski, B., et al., IL-33 exacerbates eosinophil-mediated airway inflammation. *J Immunol*, 2010. 185(6): p. 3472-80.

324. Kim, J., et al., IL-33-induced hematopoietic stem and progenitor cell mobilization depends upon CCR2. *J Immunol*, 2014. 193(7): p. 3792-802.

325. Kondo, Y., et al., Administration of IL-33 induces airway hyperresponsiveness and goblet cell hyperplasia in the lungs in the absence of adaptive immune system. *Int Immunol*, 2008. 20(6): p. 791-800.

326. Zhang, Y., et al., [IL-33 promotes airway remodeling in a mouse model of asthma via ERK1/2 signaling pathway]. *Xi Bao Yu Fen Zi Mian Yi Xue Za Zhi*, 2016. 32(5): p. 590-4.

327. Guo, Z., et al., IL-33 promotes airway remodeling and is a marker of asthma disease severity. *J Asthma*, 2014. 51(8): p. 863-9.

328. Kingwell, K., Seeing the potential of targeting CCR3. *Nature Reviews Drug Discovery*, 2009. 8: p. 614.

329. Barmania, F. and M.S. Pepper, C-C chemokine receptor type five (CCR5): An emerging target for the control of HIV infection. *Appl Transl Genom*, 2013. 2: p. 3-16.

330. Barsheshet, Y., et al., CCR8(+)FOXp3(+) Treg cells as master drivers of immune regulation. *Proc Natl Acad Sci U S A*, 2017. 114(23): p. 6086-91.

331. White, G.E., A.J. Iqbal, and D.R. Greaves, CC chemokine receptors and chronic inflammation--therapeutic opportunities and pharmacological challenges. *Pharmacol Rev*, 2013. 65(1): p. 47-89.

332. Gilliland, C.T., et al., The chemokine receptor CCR1 is constitutively active, which leads to G protein-independent, beta-arrestin-mediated internalization. *J Biol Chem*, 2013. 288(45): p. 32194-210.

333. Gorska, K., et al., Comparative study of IL-33 and IL-6 levels in different respiratory samples in mild-to-moderate asthma and COPD. *COPD*, 2018. 15(1): p. 36-45.

334. Kouro, T. and K. Takatsu, IL-5- and eosinophil-mediated inflammation: from discovery to therapy. *Int Immunol*, 2009. 21(12): p. 1303-9.

335. Xu, J., et al., IL33-mediated ILC2 activation and neutrophil IL5 production in the lung response after severe trauma: A reverse translation study from a human cohort to a mouse trauma model. *PLoS Med*, 2017. 14(7): p. e1002365.

336. Blease, K., et al., Therapeutic effect of IL-13 immunoneutralization during chronic experimental fungal asthma. *J Immunol*, 2001. 166(8): p. 5219-24.

337. Nagashima, H., et al., Effect of genetic variation of IL-13 on airway remodeling in bronchial asthma. *Allergol Int*, 2011. 60(3): p. 291-8.

338. Moore, B.B., et al., The role of CCL12 in the recruitment of fibrocytes and lung fibrosis. *Am J Respir Cell Mol Biol*, 2006. 35(2): p. 175-81.

339. DeLeon-Pennell, K.Y., et al., Periodontal-induced chronic inflammation triggers macrophage secretion of Ccl12 to inhibit fibroblast-mediated cardiac wound healing. *JCI Insight*, 2017. 2(18): p. 94207.

340. Ishinaga, H., et al., Interleukin-33 induces mucin gene expression and goblet cell hyperplasia in human nasal epithelial cells. *Cytokine*, 2017. 90: p. 60-65.

341. Zimmermann, N., et al., Dissection of experimental asthma with DNA microarray analysis identifies arginase in asthma pathogenesis. *J Clin Invest*, 2003. 111(12): p. 1863-74.

342. Morris, C.R., et al., Decreased arginine bioavailability and increased serum arginase activity in asthma. *Am J Respir Crit Care Med*, 2004. 170(2): p. 148-53.

343. Maarsingh, H., et al., Arginase strongly impairs neuronal nitric oxide-mediated airway smooth muscle relaxation in allergic asthma. *Respir Res*, 2006. 7: p. 6.

344. Baba, Y., et al., Involvement of PU.1 in mast cell/basophil-specific function of the human IL1RL1/ST2 promoter. *Allergol Int*, 2012. 61(3): p. 461-7.

345. Uchida, M., et al., Oxidative stress serves as a key checkpoint for IL-33 release by airway epithelium. *Allergy*, 2017. 72(10): p. 1521-31.

346. Attwooll, C., E. Lazzerini Denchi, and K. Helin, The E2F family: specific functions and overlapping interests. *EMBO J*, 2004. 23(24): p. 4709-16.

347. Gu, X., et al., Tel-2 is a novel transcriptional repressor related to the Ets factor Tel/ETV-6. *J Biol Chem*, 2001. 276(12): p. 9421-36.

348. Izumiyama, Y., et al., E1AF expression is closely correlated with malignant phenotype of tongue squamous cell carcinoma through activation of MT1-MMP gene promoters. *Oncol Rep*, 2005. 13(4): p. 715-20.

349. Shindoh, M., F. Higashino, and T. Kohgo, E1AF, an ets-oncogene family transcription factor. *Cancer Lett*, 2004. 216(1): p. 1-8.

350. Maruta, S., et al., E1AF expression is associated with extra-prostatic growth and matrix metalloproteinase-7 expression in prostate cancer. *APMIS*, 2009. 117(11): p. 791-6.

351. Horiuchi, S., et al., Association of ets-related transcriptional factor E1AF expression with tumour progression and overexpression of MMP-1 and matrilysin in human colorectal cancer. *J Pathol*, 2003. 200(5): p. 568-76.

352. Yu, X.X., et al., IL-33 promotes gastric cancer cell invasion and migration via ST2-ERK1/2 pathway. *Dig Dis Sci*, 2015. 60(5): p. 1265-72.

353. Yang, Z.P., et al., The association of serum IL-33 and SST2 with breast cancer. *Dis Markers*, 2015. 2015: p. 516895.

354. Larsen, K.M., et al., The role of IL-33/ST2 pathway in tumorigenesis. *Int J Mol Sci*, 2018. 19(9): p. 2676.

355. Andersson, P., et al., Molecular mechanisms of IL-33-mediated stromal interactions in cancer metastasis. *JCI Insight*, 2018. 3(20): p. 122375.

356. Yang, Z., et al., IL-33-induced alterations in murine intestinal function and cytokine responses are MyD88, STAT6, and IL-13 dependent. *Am J Physiol Gastrointest Liver Physiol*, 2013. 304(4): p. G381-9.

357. Dulek, D.E., et al., STAT4 deficiency fails to induce lung Th2 or Th17 immunity following primary or secondary respiratory syncytial virus (RSV) challenge but enhances the lung RSV-specific CD8+ T cell immune response to secondary challenge. *J Virol*, 2014. 88(17): p. 9655-72.

358. Peine, M., R.M. Marek, and M. Lohning, IL-33 in T Cell Differentiation, Function, and Immune Homeostasis. *Trends Immunol*, 2016. 37(5): p. 321-333.

359. Baumann, C., et al., T-bet- and STAT4-dependent IL-33 receptor expression directly promotes antiviral Th1 cell responses. *Proc Natl Acad Sci U S A*, 2015. 112(13): p. 4056-61.

360. Chow, L.N., et al., Human cathelicidin LL-37-derived peptide IG-19 confers protection in a murine model of collagen-induced arthritis. *Mol Immunol*, 2014. 57(2): p. 86-92.

361. Li, J., et al., Membrane active antimicrobial peptides: Translating mechanistic insights to design. *Front Neurosci*, 2017. 11: p. 73.

362. Yang, M., et al., Structure-function analysis of Avian beta-defensin-6 and beta-defensin-12: role of charge and disulfide bridges. *BMC Microbiol*, 2016. 16: p. 210.

363. Li, P., et al., Perturbation of lipopolysaccharide (LPS) micelles by sushi 3 (S3) antimicrobial peptide. The importance of an intermolecular disulfide bond in S3 dimer for binding, disruption, and neutralization of LPS. *J Biol Chem*, 2004. 279(48): p. 50150-6.

364. Pearson, W.R., An introduction to sequence similarity ("homology") searching. *Curr Protoc Bioinformatics*, 2013. Chapter 3: p. 1.

365. Henikoff, S. and J.G. Henikoff, Performance evaluation of amino acid substitution matrices. *Proteins*, 1993. 17(1): p. 49-61.

366. Wei, J., et al., Parafibromin Is a component of IFN-gamma-triggered signaling pathways that facilitates JAK1/2-mediated tyrosine phosphorylation of STAT1. *J Immunol*, 2015. 195(6): p. 2870-8.

367. Khodarev, N.N., B. Roizman, and R.R. Weichselbaum, Molecular pathways: interferon/stat1 pathway: role in the tumor resistance to genotoxic stress and aggressive growth. *Clin Cancer Res*, 2012. 18(11): p. 3015-21.

368. Rauch, I., M. Muller, and T. Decker, The regulation of inflammation by interferons and their STATs. *JAKSTAT*, 2013. 2(1): p. e23820.

369. Bauer, D., et al., Apigenin inhibits TNFalpha/IL-1alpha-induced CCL2 release through IKBK-epsilon signaling in MDA-MB-231 human breast cancer cells. *PLoS One*, 2017. 12(4): p. e0175558.

370. Kraemer, H.C., Correlation coefficients in medical research: from product moment correlation to the odds ratio. *Stat Methods Med Res*, 2006. 15(6): p. 525-45.

371. Hung, M., J. Bounsanga, and M.W. Voss, Interpretation of correlations in clinical research. *Postgrad Med*, 2017. 129(8): p. 902-6.

372. Du, H.Y., et al., The Expression and Regulation of Interleukin-33 in Human Epidermal Keratinocytes: A New Mediator of Atopic Dermatitis and Its Possible Signaling Pathway. *J Interferon Cytokine Res*, 2016. 36(9): p. 552-62.

373. Kramer, O.H., et al., A phosphorylation-acetylation switch regulates STAT1 signaling. *Genes Dev*, 2009. 23(2): p. 223-35.

374. Ng, S.L., et al., IkappaB kinase epsilon (IKK(epsilon)) regulates the balance between type I and type II interferon responses. *Proc Natl Acad Sci U S A*, 2011. 108(52): p. 21170-5.

375. Zeng, S., et al., IL-33 Receptor (ST2) Signalling is Important for Regulation of Th2-Mediated Airway Inflammation in a Murine Model of Acute Respiratory Syncytial Virus Infection. *Scand J Immunol*, 2015. 81(6): p. 494-501.

376. Butler, M.P., J.A. Hanly, and P.N. Moynagh, Kinase-active interleukin-1 receptor-associated kinases promote polyubiquitination and degradation of the Pellino family: direct evidence for PELLINO proteins being ubiquitin-protein isopeptide ligases. *J Biol Chem*, 2007. 282(41): p. 29729-37.

377. Decker, T., P. Kovarik, and A. Meinke, GAS elements: a few nucleotides with a major impact on cytokine-induced gene expression. *J Interferon Cytokine Res*, 1997. 17(3): p. 121-34.

378. Cayrol, C. and J.-P. Girard, Interleukin-33 (IL-33): A nuclear cytokine from the IL-1 family. *Immunological Reviews*, 2018. 281(1): p. 154-168.